ISSN 2307-8960 (online)

World Journal of *Clinical Cases*

Thrice Monthly Volume 13 Number 18 June 26, 2025



Published by Baishideng Publishing Group Inc

World Journal of Clinical Cases

Contents

Thrice Monthly Volume 13 Number 18 June 26, 2025

EDITORIAL

Ait Addi R. Rates of p16 and p53 expression in head and neck cutaneous squamous cell carcinoma vary according to human papillomavirus status. *World J Clin Cases* 2025; 13(18): 104313 [DOI: 10.12998/wjcc.v13.i18.104313]

CASE REPORT

Abed M, Bradley A, Ghazanfar A. Use of OviTex 1S, reinforced tissue matrix, for the repair of post renal transplant incisional hernias: Four case reports. *World J Clin Cases* 2025; 13(18): 99749 [DOI: 10.12998/wjcc.v13.i18.99749]

Li MZ, Deng J. Birt-Hogg-Dubé syndrome - a rare genetic disorder complicated by pneumothorax: A case report. *World J Clin Cases* 2025; 13(18): 100610 [DOI: 10.12998/wjcc.v13.i18.100610]

Song YL, Wang CF. Temporary bilateral uterine artery occlusion in the control of hemorrhage: A case report and review of literature. *World J Clin Cases* 2025; 13(18): 101309 [DOI: 10.12998/wjcc.v13.i18.101309]

Wójcik-Niklewska B, Filipek E. Luscan-Lumish syndrome: A case report. *World J Clin Cases* 2025; 13(18): 101471 [DOI: 10.12998/wjcc.v13.i18.101471]

Chang YHS, Chen YH, Yu JH. Improved superelastic Ni–Ti alloy wire for treating skeletal class III malocclusion combined with anterior crossbite: A case report. *World J Clin Cases* 2025; 13(18): 101545 [DOI: 10.12998/wjcc.v13.i18.101545]

Ma L, Wang KP, Jin C. Abdominal tuberculosis with pancreatic head involvement mimicking pancreatic malignancy in a young man: A case report. *World J Clin Cases* 2025; 13(18): 101612 [DOI: 10.12998/wjcc.v13.i18.101612]

Wei L, Tian Z, Wang ZY, Liu WJ, Li HB, Zhang Y. Concurrent invasive ductal carcinoma and ductal carcinoma *in situ* arising inside and outside a breast hamartoma: A case report. *World J Clin Cases* 2025; 13(18): 101882 [DOI: 10.12998/wjcc.v13.i18.101882]

Nigro A. Misdiagnosis of psoriatic arthritis in a patient with paronychia confirmed by dermatological examination: A case report. *World J Clin Cases* 2025; 13(18): 102194 [DOI: 10.12998/wjcc.v13.i18.102194]

Lee MR, Jang KY, Yang JD. Primary mucosa associated lymphoid tissue lymphoma of the gallbladder: A case report and review of literature. *World J Clin Cases* 2025; 13(18): 103055 [DOI: 10.12998/wjcc.v13.i18.103055]

Iwamuro M, Yoshikawa T, Kamio T, Hirata S, Matsueda K, Kametaka D, Otsuka M. Temporal changes in computed tomography findings of a persimmon bezoar: A case report. *World J Clin Cases* 2025; 13(18): 103426 [DOI: 10.12998/wjcc.v13.i18.103426]

Martínez-Hincapie CI, González-Arroyave D, Ardila CM. Rectal abscess secondary to foreign body insertion: A case report. *World J Clin Cases* 2025; 13(18): 103438 [DOI: 10.12998/wjcc.v13.i18.103438]

Lin YT, Hong ZJ, Liao GS, Dai MS, Chao TK, Tsai WC, Sung YK, Chiu CH, Chang CK, Yu JC. Unexpected contralateral axillary lymph node metastasis without ipsilateral involvement in triple-negative breast cancer: A case report and review of literature. *World J Clin Cases* 2025; 13(18): 103571 [DOI: 10.12998/wjcc.v13.i18.103571]

Contents

Liu AN, Yang JY, Chen XY, Wu SS, Ji Zhi SN, Zheng SM. Refractory Crohn's disease complicated with Guillain-Barré syndrome: A case report. *World J Clin Cases* 2025; 13(18): 103618 [DOI: 10.12998/wjcc.v13.i18.103618]

Hu WT, Zhang ZY, Qu J, Piao CD. New surgical approach for distal clavicle fractures: A case report. *World J Clin Cases* 2025; 13(18): 103777 [DOI: 10.12998/wjcc.v13.i18.103777]

ABOUT COVER

Peer Reviewer of *World Journal of Clinical Cases*, Raktim Swarnakar, MD, Chief Physician, Department of Physical Medicine and Rehabilitation, R. G. Kar Medical College and Hospital, Kolkata 700064, India. raktimswarnakar@hotmail.com

AIMS AND SCOPE

The primary aim of *World Journal of Clinical Cases* (*WJCC*, *World J Clin Cases*) is to provide scholars and readers from various fields of clinical medicine with a platform to publish high-quality clinical research articles and communicate their research findings online.

WJCC mainly publishes articles reporting research results and findings obtained in the field of clinical medicine and covering a wide range of topics, including case control studies, retrospective cohort studies, retrospective studies, clinical trials studies, observational studies, prospective studies, randomized controlled trials, randomized clinical trials, systematic reviews, meta-analysis, and case reports.

INDEXING/ABSTRACTING

The *WJCC* is now abstracted and indexed in PubMed, PubMed Central, *Reference Citation Analysis*, China Science and Technology Journal Database, and Superstar Journals Database. The 2024 Edition of Journal Citation Reports® cites the 2023 journal impact factor (JIF) for *WJCC* as 1.0; JIF without journal self cites: 0.9; 5-year JIF: 1.1; JIF Rank: 170/329 in medicine, general and internal; JIF Quartile: Q3; and 5-year JIF Quartile: Q3.

RESPONSIBLE EDITORS FOR THIS ISSUE

Production Editor: *Lei Zhang*; **Production Department Director:** *Xiang Li*; **Cover Editor:** *Jin-Lei Wang*.

NAME OF JOURNAL
World Journal of Clinical Cases

ISSN
ISSN 2307-8960 (online)

LAUNCH DATE
April 16, 2013

FREQUENCY
Thrice Monthly

EDITORS-IN-CHIEF
Bao-Gan Peng, Salim Surani

EDITORIAL BOARD MEMBERS
https://www.wjgnet.com/2307-8960/editorialboard.htm

PUBLICATION DATE
June 26, 2025

COPYRIGHT
© 2025 Baishideng Publishing Group Inc

INSTRUCTIONS TO AUTHORS
https://www.wjgnet.com/bpg/gerinfo/204

GUIDELINES FOR ETHICS DOCUMENTS
https://www.wjgnet.com/bpg/GerInfo/287

GUIDELINES FOR NON-NATIVE SPEAKERS OF ENGLISH
https://www.wjgnet.com/bpg/gerinfo/240

PUBLICATION ETHICS
https://www.wjgnet.com/bpg/GerInfo/288

PUBLICATION MISCONDUCT
https://www.wjgnet.com/bpg/gerinfo/208

ARTICLE PROCESSING CHARGE
https://www.wjgnet.com/bpg/gerinfo/242

STEPS FOR SUBMITTING MANUSCRIPTS
https://www.wjgnet.com/bpg/GerInfo/239

ONLINE SUBMISSION
https://www.f6publishing.com

© 2025 Baishideng Publishing Group Inc. All rights reserved. 7041 Koll Center Parkway, Suite 160, Pleasanton, CA 94566, USA
E-mail: office@baishideng.com https://www.wjgnet.com

World Journal of Clinical Cases

Submit a Manuscript: https://www.f6publishing.com

World J Clin Cases 2025 June 26; 13(18): 104313

DOI: 10.12998/wjcc.v13.i18.104313

ISSN 2307-8960 (online)

EDITORIAL

Rates of p16 and p53 expression in head and neck cutaneous squamous cell carcinoma vary according to human papillomavirus status

Rachid Ait Addi

Specialty type: Medicine, research and experimental

Provenance and peer review: Invited article; Externally peer reviewed.

Peer-review model: Single blind

Peer-review report's classification

Scientific Quality: Grade C, Grade C, Grade E

Novelty: Grade B, Grade C, Grade D

Creativity or Innovation: Grade B, Grade C, Grade D

Scientific Significance: Grade B, Grade C, Grade D

P-Reviewer: Bu YX; Kanda T; Lu H

Received: December 17, 2024

Revised: January 27, 2025

Accepted: February 8, 2025

Published online: June 26, 2025

Processing time: 72 Days and 12.8 Hours

Rachid Ait Addi, Department of Biology, Independent Senior Researcher, Marrakesh 41020, Morocco

Corresponding author: Rachid Ait Addi, PhD, Assistant Professor, Senior Researcher, Department of Biology, Independent Senior Researcher, 1368 Rte Essaouira, N 03, Marrakesh 41020, Morocco. dr.rachid.aitaddi@gmail.com

Abstract

The strong association between human papillomavirus (HPV) infection and oropharyngeal squamous cell carcinoma (SCC) is well-documented, with p16 expression serving as a reliable predictor of HPV involvement. HPV-related tumors are characterized by distinct mechanisms affecting p16 and p53 protein pathways. However, the prevalence of HPV and the combined predictive utility of p16 and p53 expression in head and neck cutaneous SCC remain less explored, necessitating further research to understand their role in this subset of SCC. HPV, p16, and p53 statuses were determined using immunohistochemistry staining methods rather than more sensitive techniques such as polymerase chain reaction or HPV genotyping, limiting the ability to assess specific area HPV types potentially associated with prognosis. Further studies assessing multiple molecular markers in head and neck cutaneous patients will better predict the diverse outcomes and potentially the type of treatment targeted to those markers.

Key Words: Squamous cell carcinoma; Oropharyngeal; Non-oropharyngeal; Human papillomavirus; p16; p53

©The Author(s) 2025. Published by Baishideng Publishing Group Inc. All rights reserved.

Core Tip: In this editorial, we comment on a retrospective cohort study published in the recent issue of the *World Journal of Clinical Cases*. The authors of this article aimed to highlight that p16, commonly used as a surrogate marker for human papillomavirus in oropharyngeal squamous cell carcinoma (SCC), is not a reliable indicator in head and neck cutaneous SCC. This finding offers important insights for future research focusing on Asian populations.

Citation: Ait Addi R. Rates of p16 and p53 expression in head and neck cutaneous squamous cell carcinoma vary according to human papillomavirus status. *World J Clin Cases* 2025; 13(18): 104313
URL: https://www.wjgnet.com/2307-8960/full/v13/i18/104313.htm
DOI: https://dx.doi.org/10.12998/wjcc.v13.i18.104313

INTRODUCTION

Squamous cell carcinoma (SCC) is the second most common skin cancer after basal cell carcinoma, with a tendency to develop from premalignant lesions, particularly in areas that are frequently exposed to sunlight like the head and neck. Major underlying causes for SCC include ultraviolet (UV) radiation, exposure to chemical carcinogens, genetic factors, immune dysfunction, specific medications, and pathogenic viral conditions[1,2]. SCC ranks as the second most prevalent form of non-melanoma skin cancer, comprising around 40.2% of every head and neck malignancies. Several risk factors for the advancement of head and neck SCC (HNSCC) have been recognized, comprising tobacco use, alcohol intake, nutritional influences, and human papillomavirus (HPV) contamination[3].

Like many other oncogenic viruses, HPV integration disrupts cellular immune surveillance and homeostasis by altering gene expression and inducing epigenetic modifications[4]. This process initially enhances cellular proliferation, creating a favorable environment for viral replication and persistence[5]. The key contributors to this mechanism are the HPV oncoproteins E6 and E7, which target and inhibit various cellular proteins. E6 promotes the rapid degradation of p53, disrupting cell cycle checkpoints and driving re-entry into the S-phase[6]. Meanwhile, E7 binds to the retinoblastoma protein (pRb) and triggers its degradation, leading to the upregulation of the cyclin-dependent kinase inhibitor p16[7].

The role of HPV in SCC development is widely recognized, particularly in cases associated with epidermodysplasia verruciformis (EV)[2]. EV is an autosomal recessive inherited skin disorder and significantly increases the risk of SCC development and shows high susceptibility to infection by beta-type HPV, particularly HPV-5 and HPV-8. In EV, SCC often arises in skin with long-term infection with HPV, especially in areas frequently uncovered from sunlight[8].

p53 is a key driver mutation in SCC, functioning as a tumor suppressor to protect against damage caused by UV radiation. Meanwhile, p16 serves as a substitute biomarker for HPV, demonstrating a high accuracy in predicting positive outcomes in oropharyngeal SCC (OPSCC) and being linked to an encouraging clinical outcome[9].

Several studies have investigated the prevalence and role of HPV infections in OPSCC and their correlation with a favorable prognosis[10-12].

This is linked to HPV's ability to upregulate p16 expression, a commonly used surrogate marker for HPV infection that is also associated with better treatment outcomes in these cancers[13].

P16 AND P53 EXPRESSION IN NECK CUTANEOUS SCC

The overexpression of the p16 protein, combined with the loss of function of the p53 tumor suppressor gene, enhance responsiveness to radiotherapy and chemotherapy, leading to improved therapeutic responses and higher overall survival outcomes among patients with HPV-positive OPSCC[9,14].

HPV's role in oral and oropharyngeal carcinogenesis was first identified by Syrjänen[15] in 1983. Following that, extensive research has explored HPV's role in HNSCC, especially in OPSCC. The prevalence of HPV positivity in OPSCC fluctuates significantly, between 40% and 80%, contingent upon the detection method's sensitivity and specificity[9,16].

OPSCC associated to HPV is more commonly seen in locations like the United States than in Asia or Europe, perhaps as a result of variations in sexual activity and cultural customs, as well as HPV immunization rate[17]. Also, OPSCC associated to HPV is more commonly observed in younger individuals and those having several sexual partners in the past and increased oral-genital contact[18].

Moreover, HPV-positive OPSCC generally displays characteristics of a solitary, confined tumor within the oropharynx, primarily found in the tonsils or at the lingual base, it typically presents with a reduced initial tumor and a decreased incidence of lymphatic spread compared to tumors with no links with HPV[19-21]. Furthermore, OPSCC associated to HPV has a reduced association with smoking and alcohol intake. Subjects often have less comorbid conditions and exhibit greater overall health and physical condition at the time of diagnosis[22,23].

There is evidence suggesting that HPV infection may worsen UV-induced damage and could potentially play a role in the development of SCC. Multiple studies have reported HPV positivity rates in head and neck cutaneous SCC (HNCSCC) ranging from 5% to 20%. However, the role of HPV in the pathogenesis of HNCSCC remains uncertain[24,25].

In the study by Nam *et al*[1], the HPV detection rate using immunohistochemistry (IHC) for HNCSCC was 8.06%, with 5 out of 62 cases testing positive[1]. This rate was lower than the 21.8% HPV positivity observed in a prior study utilizing the polymerase chain reaction (PCR) technique among North American participants[26]. The difference in testing procedures is believed to be one explanation for this finding. PCR is the most sensitive method for detecting HPV and may yield an increased positivity occurrence compared to the IHC technique applied in this investigation[1,27]. Also, in the study by Nam *et al*[1], the sample size was relatively modest, consisting of only 62 subjects and featuring a restricted set of HPV-positive cases which may contribute to the observed variation in HPV positivity rates. These constraints underscore the necessity for bigger, multi-site investigations with longer follow-up periods to more thoroughly elucidate the prognostic impact of HPV, p16, and p53 activity in head and HNCSCC.

Moreover, the survey by Nam *et al*[1] suggests that the expression of p16 and p53, parallel with HPV infection, may serve as poor prognostic indicators in head and HNCSCC, revealing an increased risk of return and metastasis.

P53 is the most frequently mutated gene in SCC, observed in as much as 90% of SCC cases. Once mutated, tumor cells escape programmed cell death and bypass cell cycle arrest, facilitating uncontrolled proliferation and clonal expansion. UV-induced mutations in p53 are implicated in SCC development[28]. The differing functions of p16 and p53 in OPSCC opposed to head and HNCSCC highlight the multifaceted connection between HPV contamination, exposure to UV radiation, and specific molecular shifts associated with head and HNCSCC.

Additionally, the frequency of p53 mutations caused by UV damage in the study by Nam *et al*[1] was found to be lower than that reported in previous studies involving Caucasian individuals[29]. The same study found no statistically significant relationship between p16 expression and tumor location, suggesting that p16 is not correlated with a favorable prognosis in HNCSCC. These results indicates that the interconnection linking p16 expression and HPV stage can very among OPSCC and HNCSCC. It underscores the requirement for additional studies to clarify the role of p16 in HNCSCC disease mechanism and to evaluate its ability to act as a prognostic tool[1].

On the other hand, Wang *et al*[30] observed that p16 and p53 serve as important prognostic markers for HNSCC. High levels of p16 and p53 expression are often linked to a more favorable prognosis.

On the whole, the differing positivity rates of p16 in OPSCC and HNCSCC emphasize the multifaceted interaction linking HPV contamination, UV radiation exposure, and other pathogenic influences that contribute to the development of head and neck cancer.

CONCLUSION

HPV-positive OPSCC frequently may be different between geographical regions due to variations in sexual behavior, cultural practices, and HPV vaccination rates. The presence of p16 and p53 expression, in combination with HPV infection, may act as unfavorable forecasts of recovery in head and HNCSCC, suggesting a higher likelihood of reappearance and distant spread.

Further studies evaluating various molecular markers in head and neck cutaneous patients can enhance the prediction of diverse outcomes and help tailor treatments specifically to those markers.

FOOTNOTES

Author contributions: Ait Addi R was responsible for drafting and revision of the manuscript, read and approved the final version of the manuscript to be published.

Conflict-of-interest statement: All authors declare no conflict of interest in publishing the manuscript.

Open Access: This article is an open-access article that was selected by an in-house editor and fully peer-reviewed by external reviewers. It is distributed in accordance with the Creative Commons Attribution NonCommercial (CC BY-NC 4.0) license, which permits others to distribute, remix, adapt, build upon this work non-commercially, and license their derivative works on different terms, provided the original work is properly cited and the use is non-commercial. See: https://creativecommons.org/Licenses/by-nc/4.0/

Country of origin: Morocco

ORCID number: Rachid Ait Addi 0000-0001-8825-4133.

S-Editor: Luo ML
L-Editor: A
P-Editor: Zhang L

REFERENCES

1 **Nam H**, Ryu H, Lee D, Byeon JY, Kim JH, Lee JH, Lim S, Choi HJ. Expression rates of p16, p53 in head and neck cutaneous squamous cell carcinoma based on human-papillomavirus positivity. *World J Clin Cases* 2025; **13** [DOI: 10.12998/wjcc.v13.i9.99463]

2 **Feller L**, Khammissa RAG, Kramer B, Altini M, Lemmer J. Basal cell carcinoma, squamous cell carcinoma and melanoma of the head and face. *Head Face Med* 2016; **12**: 11 [PMID: 26850723 DOI: 10.1186/s13005-016-0106-0]

3 **Barsouk A**, Aluru JS, Rawla P, Saginala K, Barsouk A. Epidemiology, Risk Factors, and Prevention of Head and Neck Squamous Cell Carcinoma. *Med Sci (Basel)* 2023; **11**: 42 [PMID: 37367741 DOI: 10.3390/medsci11020042]

4 **Tomaić V**. Functional Roles of E6 and E7 Oncoproteins in HPV-Induced Malignancies at Diverse Anatomical Sites. *Cancers (Basel)* 2016; **8**: 95 [PMID: 27775564 DOI: 10.3390/cancers8100095]

5 **Hoppe-Seyler K**, Bossler F, Braun JA, Herrmann AL, Hoppe-Seyler F. The HPV E6/E7 Oncogenes: Key Factors for Viral Carcinogenesis and Therapeutic Targets. *Trends Microbiol* 2018; **26**: 158-168 [PMID: 28823569 DOI: 10.1016/j.tim.2017.07.007]

6 **Kim Y**, Joo YH, Kim MS, Lee YS. Prevalence of high-risk human papillomavirus and its genotype distribution in head and neck squamous cell carcinomas. *J Pathol Transl Med* 2020; **54**: 411-418 [PMID: 32683856 DOI: 10.4132/jptm.2020.06.22]

7 **Wang S**, Zhuang X, Gao C, Qiao T. Expression of p16, p53, and TLR9 in HPV-Associated Head and Neck Squamous Cell Carcinoma: Clinicopathological Correlations and Potential Prognostic Significance. *Onco Targets Ther* 2021; **14**: 867-877 [PMID: 33574680 DOI: 10.2147/OTT.S293163]

8 **da Cruz Silva LL**, de Oliveira WRP, Sotto MN. Epidermodysplasia verruciformis: revision of a model of carcinogenic disease. *Surg Exp Pathol* 2019; **2**: 20 [DOI: 10.1186/s42047-019-0046-7]

9 **Lifsics A**, Cistjakovs M, Sokolovska L, Deksnis R, Murovska M, Groma V. The Role of the p16 and p53 Tumor Suppressor Proteins and Viral HPV16 E6 and E7 Oncoproteins in the Assessment of Survival in Patients with Head and Neck Cancers Associated with Human Papillomavirus Infections. *Cancers (Basel)* 2023; **15**: 2722 [PMID: 37345059 DOI: 10.3390/cancers15102722]

10 **Lechner M**, Liu J, Masterson L, Fenton TR. HPV-associated oropharyngeal cancer: epidemiology, molecular biology and clinical management. *Nat Rev Clin Oncol* 2022; **19**: 306-327 [PMID: 35105976 DOI: 10.1038/s41571-022-00603-7]

11 **Khoo A**, Boyer M, Jafri Z, Makeham T, Pham T, Khachigian LM, Floros P, Dowling E, Fedder K, Shonka D Jr, Garneau J, O'Meara CH. Human Papilloma Virus Positive Oropharyngeal Squamous Cell Carcinoma and the Immune System: Pathogenesis, Immunotherapy and Future Perspectives. *Int J Mol Sci* 2024; **25**: 2798 [PMID: 38474047 DOI: 10.3390/ijms25052798]

12 **Argirion I**, Zarins KR, McHugh J, Cantley RL, Teeramatwanich W, Laohasiriwong S, Kasemsiri P, Naruikon J, Srimanta P, Chinn SB, Vatanasapt P, Rozek LS. Increasing prevalence of HPV in oropharyngeal carcinoma suggests adaptation of p16 screening in Southeast Asia. *J Clin Virol* 2020; **132**: 104637 [PMID: 32932151 DOI: 10.1016/j.jcv.2020.104637]

13 **da Mata S**, Ferreira J, Nicolás I, Esteves S, Esteves G, Lérias S, Silva F, Saco A, Cochicho D, Cunha M, Del Pino M, Ordi J, Félix A. P16 and HPV Genotype Significance in HPV-Associated Cervical Cancer-A Large Cohort of Two Tertiary Referral Centers. *Int J Mol Sci* 2021; **22**: 2294 [PMID: 33669021 DOI: 10.3390/ijms22052294]

14 **Alsahafi EN**, Thavaraj S, Sarvestani N, Novoplansky O, Elkabets M, Ayaz B, Tavassoli M, Legends MF. EGFR overexpression increases radiotherapy response in HPV-positive head and neck cancer through inhibition of DNA damage repair and HPV E6 downregulation. *Cancer Lett* 2021; **498**: 80-97 [PMID: 33137407 DOI: 10.1016/j.canlet.2020.10.035]

15 **Syrjänen S**. Human papillomavirus (HPV) in head and neck cancer. *J Clin Virol* 2005; **32** Suppl 1: S59-S66 [PMID: 15753013 DOI: 10.1016/j.jcv.2004.11.017]

16 **Krsek A**, Baticic L, Sotosek V, Braut T. The Role of Biomarkers in HPV-Positive Head and Neck Squamous Cell Carcinoma: Towards Precision Medicine. *Diagnostics (Basel)* 2024; **14**: 1448 [PMID: 39001338 DOI: 10.3390/diagnostics14131448]

17 **Ndon S**, Singh A, Ha PK, Aswani J, Chan JY, Xu MJ. Human Papillomavirus-Associated Oropharyngeal Cancer: Global Epidemiology and Public Policy Implications. *Cancers (Basel)* 2023; **15**: 4080 [PMID: 37627108 DOI: 10.3390/cancers15164080]

18 **Johnson DE**, Burtness B, Leemans CR, Lui VWY, Bauman JE, Grandis JR. Head and neck squamous cell carcinoma. *Nat Rev Dis Primers* 2020; **6**: 92 [PMID: 33243986 DOI: 10.1038/s41572-020-00224-3]

19 **Lim YX**, D'Silva NJ. HPV-associated oropharyngeal cancer: in search of surrogate biomarkers for early lesions. *Oncogene* 2024; **43**: 543-554 [PMID: 38191674 DOI: 10.1038/s41388-023-02927-9]

20 **Margalit DN**, Anker CJ, Aristophanous M, Awan M, Bajaj GK, Bradfield L, Califano J, Caudell JJ, Chapman CH, Garden AS, Harari PM, Helms A, Lin A, Maghami E, Mehra R, Parker L, Shnayder Y, Spencer S, Swiecicki PL, Tsai JC, Sher DJ. Radiation Therapy for HPV-Positive Oropharyngeal Squamous Cell Carcinoma: An ASTRO Clinical Practice Guideline. *Pract Radiat Oncol* 2024; **14**: 398-425 [PMID: 39078350 DOI: 10.1016/j.prro.2024.05.007]

21 **Manoharan M**, Kalman NS, Rabinowits G. Head and Neck Squamous Cell Carcinoma of Unknown Primary: A Diagnostic Work-Up. *Oncologist* 2024; **29**: 192-199 [PMID: 37995312 DOI: 10.1093/oncolo/oyad311]

22 **Korsten LHA**, Jansen F, Lissenberg-Witte BI, Vergeer M, Brakenhoff RH, Leemans CR, Verdonck-de Leeuw IM. The course of health-related quality of life from diagnosis to two years follow-up in patients with oropharyngeal cancer: does HPV status matter? *Support Care Cancer* 2021; **29**: 4473-4483 [PMID: 33454834 DOI: 10.1007/s00520-020-05932-w]

23 **Nishikawa D**, Hanai N, Ozawa T, Kitahara T, Hasegawa Y. Role of Human Papilloma Virus and Lifestyle Factors in Overall Survival of Patients with Oropharyngeal Squamous Cell Carcinoma. *Medicina (Kaunas)* 2022; **58**: 557 [PMID: 35454395 DOI: 10.3390/medicina58040557]

24 **Karimi A**, Mohebbi E, Mckay-Chopin S, Rashidian H, Hadji M, Peyghambari V, Marzban M, Naghibzadeh-Tahami A, Gholipour M, Kamangar F, Tommasino M, Gheit T, Zendehdel K. Human Papillomavirus and Risk of Head and Neck Squamous Cell Carcinoma in Iran. *Microbiol Spectr* 2022; **10**: e0011722 [PMID: 35708339 DOI: 10.1128/spectrum.00117-22]

25 **Brennan S**, Baird AM, O'Regan E, Sheils O. The Role of Human Papilloma Virus in Dictating Outcomes in Head and Neck Squamous Cell Carcinoma. *Front Mol Biosci* 2021; **8**: 677900 [PMID: 34250016 DOI: 10.3389/fmolb.2021.677900]

26 **Sias C**, Salichos L, Lapa D, Del Nonno F, Baiocchini A, Capobianchi MR, Garbuglia AR. Alpha, Beta, gamma human PapillomaViruses (HPV) detection with a different sets of primers in oropharyngeal swabs, anal and cervical samples. *Virol J* 2019; **16**: 27 [PMID: 30832688 DOI: 10.1186/s12985-019-1132-x]

27 **Simoens C**, Gheit T, Ridder R, Gorbaslieva I, Holzinger D, Lucas E, Rehm S, Vermeulen P, Lammens M, Vanderveken OM, Kumar RV, Gangane N, Caniglia A, Maffini F, Rubio MBL, Anantharaman D, Chiocca S, Brennan P, Pillai MR, Sankaranarayanan R, Bogers J, Pawlita M, Tommasino M, Arbyn M; HPV-AHEAD study group. Accuracy of high-risk HPV DNA PCR, p16((INK4a)) immunohistochemistry or the combination of both to diagnose HPV-driven oropharyngeal cancer. *BMC Infect Dis* 2022; **22**: 676 [PMID: 35933382 DOI: 10.1186/s12879-022-07654-2]

28 **Piipponen M**, Riihilä P, Nissinen L, Kähäri VM. The Role of p53 in Progression of Cutaneous Squamous Cell Carcinoma. *Cancers (Basel)* 2021; **13**: 4507 [PMID: 34572732 DOI: 10.3390/cancers13184507]

29 **Wang H**, Guo M, Wei H, Chen Y. Targeting p53 pathways: mechanisms, structures, and advances in therapy. *Signal Transduct Target Ther* 2023; **8**: 92 [PMID: 36859359 DOI: 10.1038/s41392-023-01347-1]

30 **Wang Y**, Wang F, Wang S, Zhang L, Fu H, Sun L, Wang W, Liu C, Ren W, Gao L, Xing G, Ma X. p16 and p53 can Serve as Prognostic Markers for Head and Neck Squamous Cell Carcinoma. *Int Dent J* 2024; **74**: 543-552 [PMID: 38105167 DOI: 10.1016/j.identj.2023.11.007]

World Journal of Clinical Cases

Submit a Manuscript: https://www.f6publishing.com

World J Clin Cases 2025 June 26; 13(18): 99749

DOI: 10.12998/wjcc.v13.i18.99749

ISSN 2307-8960 (online)

CASE REPORT

Use of OviTex 1S, reinforced tissue matrix, for the repair of post renal transplant incisional hernias: Four case reports

Mariam Abed, Angus Bradley, Abbas Ghazanfar

Specialty type: Medicine, research and experimental

Provenance and peer review: Unsolicited article; Externally peer reviewed.

Peer-review model: Single blind

Peer-review report's classification

Scientific Quality: Grade D

Novelty: Grade B

Creativity or Innovation: Grade B

Scientific Significance: Grade D

P-Reviewer: Ferreira GSA

Received: July 29, 2024

Revised: November 5, 2024

Accepted: February 14, 2025

Published online: June 26, 2025

Processing time: 212 Days and 19.8 Hours

Mariam Abed, Angus Bradley, Department of Renal Transplantation, St George's University Hospital, London SW17 0QT, United Kingdom

Abbas Ghazanfar, Renal and Transplant Unit, St Georges University Hospitals NHS Foundation Trust, London SW17 0QT, United Kingdom

Co-first authors: Mariam Abed and Angus Bradley.

Corresponding author: Abbas Ghazanfar, Renal and Transplant Unit, St Georges University Hospitals NHS Foundation Trust, Blackshaw Road, Tooting, London SW17 0QT, United Kingdom. a.ghazanfar@nhs.net

Abstract

BACKGROUND

Incisional hernia is one of the known complications of renal transplant surgery, with a reported incidence between 1.1% to 3.8%. Depending on the site and extent of incisional hernia, it may require surgery particularly if it contains the transplanted kidney either partially or completely. The current common clinical practice is to repair incisional hernias using polypropylene meshes, which have their own risks and benefits. Biological meshes, which are made from human or animal-derived connective tissue, are also in use and have a less inflammatory response. Recently, hybrid meshes have been developed. These are composed of both biological and synthetic products. One such example is OviTex 1S permanent, which is a sterile reinforced tissue matrix composed of ovine (sheep) derived extracellular matrix and monofilament polypropylene. In this case report, we are sharing our experience with the use of OviTex 1S in the repair of post-renal transplant incisional hernias.

CASE SUMMARY

We report four cases of post-renal transplant incisional hernia with a median time of 27 months post-surgery. The median size of the defect was 15 cm long. There was no post-operative complication. One patient required renal transplant biopsy after mesh repair, which was easily performed compared with polypropylene meshes repaired hernias in the past.

CONCLUSION

The OviTex 1S mesh provides benefits in hernial repairs pKTx, but cost is an issue, and their long-term viability is unclear. Continued use and reporting will help build a more informed picture.

Key Words: Incisional hernia; Kidney transplantation; Surgical mesh; Hybrid mesh; End stage renal failure; Case report

©The Author(s) 2025. Published by Baishideng Publishing Group Inc. All rights reserved.

Core Tip: An incisional hernia is one of the known complications of renal transplant surgery and, depending on the site and extent of the hernia, may require surgery. The repair of incisional hernias post kidney transplantation (pRTx) has traditionally used synthetic mesh. However, they are associated with complications. Hybrid meshes, such as OviTex 1S, are a new type of mesh combining both synthetic and biological mesh properties in an attempt to improve post-operative outcomes. This case series reports 4 cases where OviTex 1S permanent mesh is used in the repair of pRTx incisional hernias.

Citation: Abed M, Bradley A, Ghazanfar A. Use of OviTex 1S, reinforced tissue matrix, for the repair of post renal transplant incisional hernias: Four case reports. *World J Clin Cases* 2025; 13(18): 99749
URL: https://www.wjgnet.com/2307-8960/full/v13/i18/99749.htm
DOI: https://dx.doi.org/10.12998/wjcc.v13.i18.99749

INTRODUCTION

Incisional hernia is one of the known complications of renal transplant surgery, with the reported incidence between 1.1% to 3.8%[1]. It commonly presents within 3 months of surgery[1]. Post kidney transplantation (pRTx) incisional hernia has multi-factorial risk factors. Amongst others, these include incision type, recipient age, smoking history, body mass index (BMI), and wound infection[2]. Obesity has been found to be a strong predictor for incisional hernias[3]. This is due to the increased intra-abdominal pressure on the incision, causing mechanical stress. Immunosuppressive regime, long-term dialysis and associated co-morbidities such as adult polycystic kidney disease are other risk factors[3,4]. Depending on the site and extent of the incisional hernia, it may require surgery if it contains the transplanted kidney either partially or completely.

The current common clinical practice is to repair incisional hernias using polypropylene meshes. Although affordable and strong, these are associated with complications, including increased risk of infection, chronic inflammation, fistula formation and bowel obstruction[5]. They can also become brittle, reduce in size over time and can be difficult to remove [5]. Biological meshes made from human or animal-derived connective tissue are also in use. They have the advantage of reduced inflammatory response and can be left in situ during infection[6]. To date, their use has been limited due to high costs and some reports of high recurrence rates and increased laxity[7]. Recently, hybrid meshes have been developed. These are composed of both biological and synthetic products. One such example is OviTex 1S permanent, which is a sterile reinforced tissue matrix composed of ovine (sheep) derived extracellular matrix and monofilament polypropylene. It has been shown to produce a reduced inflammatory response, promote better wound healing and reduce hernia recurrence[8,9]. To date, there is limited data available for the use of OviTex 1S in pRTx incisional hernia repairs.

In this current case series, we report 4 cases where we used OviTex 1S permanent mesh for the repair of pRTx incisional hernias.

CASE PRESENTATION

Chief complaints

Case 1: A 67-year-old male patient with end-stage renal failure (ESRF) secondary to hypertensive nephropathy received a living donor renal transplant in 2021. His relevant history included a BMI of 25.6, more than 2 years of haemodialysis and a 10-year history of smoking. As per our unit's protocol, he received 20 mg of Basiliximab at induction and day 4 post renal transplant. He was started on triple immunosuppression therapy, including Tacrolimus, Mycophenolate Mofetil and Prednisolone 20 mg. Prednisolone was stopped after day 7 due to primary graft function.

His renal allograft functions stabilised with a mean estimated glomerular filtration rate (eGFR) of 47 to 50 mL/min/1.73 m^2 at 1-year post-transplant. He was maintained on Tacrolimus and Mycophenolate Mofetil. Fourteen months following his renal transplant, he noticed a swelling over the upper part of his right iliac fossa (RIF) incision. A screening Ultrasound (US) confirmed a fascial defect, and a computer tomography (CT) scan confirmed an approximately 16cm to 8cm wide incisional hernia. The hernia contained small bowel loops and the upper 2/3 of the transplanted kidney. The hernial defect was repaired with OviTex 1S mesh using sublay pre-peritoneal technique. The surgery was uneventful, with no post-operative complications. He was discharged three days post-operatively. A repeat CT confirmed intact repair after 3 months. The patient required an US of the kidney transplant after 6 months of surgery due to raised creatinine and later had a renal transplant biopsy. The US images had better depth and quality as compared with polypropylene mesh. The biopsy was also more controlled and less forceful as compared to polypropylene mesh repairs. There has been no recurrence until a recent follow-up 18 months after hernia repair.

Case 2: A 45-year-old male patient with ESRF secondary to an unknown cause received a donation after a circulatory death (DCD) renal transplant in 2015. He had a past medical history of ulcerative colitis and thyroid cancer, was a non-smoker and had a BMI of 34. As per our unit's protocol, he received 20 mg of Basiliximab at induction and day 4 post renal transplant. He was started on triple immunosuppression therapy, including Tacrolimus, Mycophenolate Mofetil and Prednisolone 20 mg. The patient was reviewed in the surgical clinic 7 years following the transplant with a failed transplant and an associated long-standing reducible incisional hernia. The cause of allograft failure was chronic allograft nephropathy on renal transplant biopsy. At the time of presentation for incisional hernia, he was on low-dose Tacrolimus and Mycophenolate Mofetil. The CT scan confirmed a significant defect, approximately 14 cm to 7 cm (Figure 1). The patient underwent simultaneous transplant nephrectomy and incisional hernia repair with OviTex 1S using sublay technique (Figures 2 and 3) and was discharged 4 days later. The operation and initial post-operative period proceeded without complication. The most recent follow-up, 14 months after surgery, did not show any recurrence.

Case 3: A 55-year-old female patient with ESRF secondary to polycystic kidney disease received a DCD renal transplant in 2014. As per our unit's protocol, she received 20 mg of Basiliximab at induction and day 4 post renal transplant. She was started on triple immunosuppression therapy, including Tacrolimus, Mycophenolate Mofetil and Prednisolone 20 mg.

She developed an incisional hernia three years after transplant surgery, which was repaired using polypropylene mesh. She presented with recurrent incisional hernia in 2021, with tenderness over the RIF surgical site. At the time of presentation for incisional hernia, she was on Tacrolimus and Mycophenolate Mofetil. She had good renal allograft function with eGFR of 48 mL/min/1.73 m^2. CT scan confirmed a loop of bowel herniating into the right inguinal canal and involving the lower half of the transplant incision. She had a BMI of 24.5 and was a non-smoker. The recurrent dual inguinal incisional hernia was repaired with OviTex 1S mesh using sublay technique. There were no intra-operative or post-operative complications. She was discharged after 1 day and has had no reported re-occurrence 13 months following the surgery.

Case 4: A 62-year-old male patient with ESRF secondary to focal segmental glomerulosclerosis (FSGS). He had a previous history of significant diverticular disease with multiple surgeries in the past, resulting in colectomy and ileostomy. His BMI was 32 at the time of surgery. He received an end-of-chain live donor kidney transplant in 2022. As per our unit's protocol, he received 20 mg of Basiliximab at induction and day 4 post renal transplant. He was started on triple immunosuppression therapy, including Tacrolimus, Mycophenolate Mofetil and Prednisolone 20 mg. He had good renal allograft function with eGFR of 63 mL/min/1.73 m^2. The patient developed a post-transplant incisional hernia six months after his transplant. At the time of presentation for incisional hernia, he was Tacrolimus and Mycophenolate Mofetil. His hernia was repaired with OviTex1S mesh using sublay technique. He had an uneventful recovery and was discharged 24 hours after his surgery. No recurrence was reported in a recent follow-up 6 months after surgery.

History of present illness

With regards to most of the cases, the patients presented with a non-tender swelling over the surgical incisional site. In case 3, the patient presented with tenderness over the RIF surgical site where she had a previous incisional hernia repair following her renal transplant.

History of past illness

The patients in this case report developed ESRF due to a variety of reasons. Case 1 developed hypertensive nephropathy, case 3 had a history of polycystic kidney disease, and case 4 developed FSGS. The cause for case 2 is unknown.

Personal and family history

With regard to developing recurrent incisional hernia, there was no relevant family or personal history.

Physical examination

Examination revealed non-obstructed reducible swelling in all cases.

Laboratory examinations

The eGFR in cases 1, 3 and 4 were 47, 48 and 63 mL/min/1.73 m^2, respectively. Case 2 was on established haemodialysis.

Imaging examinations

All cases had a US scan as screening text followed by a CT scan to confirm and measure the defect size for surgical planning.

FINAL DIAGNOSIS

As with all our patients, they were thoroughly investigated, and CT imaging confirmed post-renal transplant incisional hernia with defects as large as 16 cm × 8 cm. In case 3, a loop of large bowel was found to be herniated through the incision site. However, there were no signs of strangulation or incarceration.

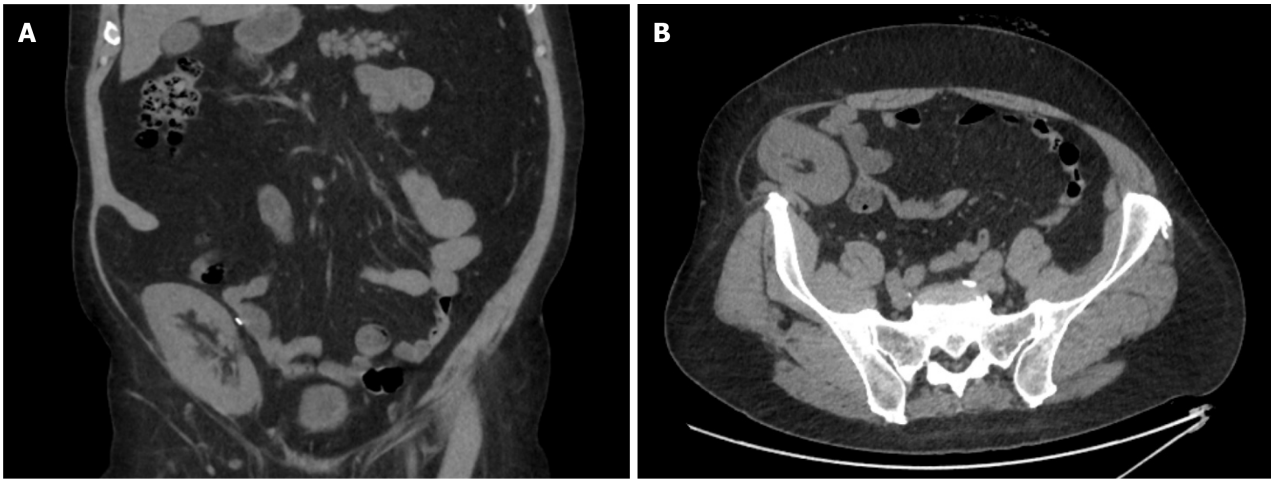


Figure 1 Computed tomography images showing an incisional hernia containing transplanted kidney. A: Coronal computed tomography (CT) image; B: Axial CT image.

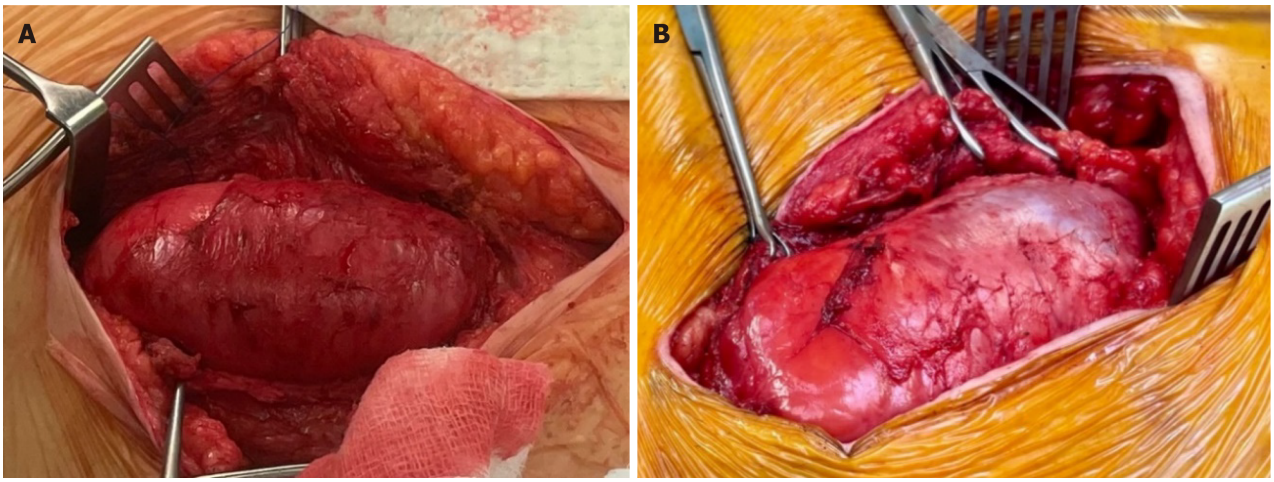


Figure 2 Operative findings of the transplanted kidney within the incisional hernia. A: Transverse view; B: Oblique view.

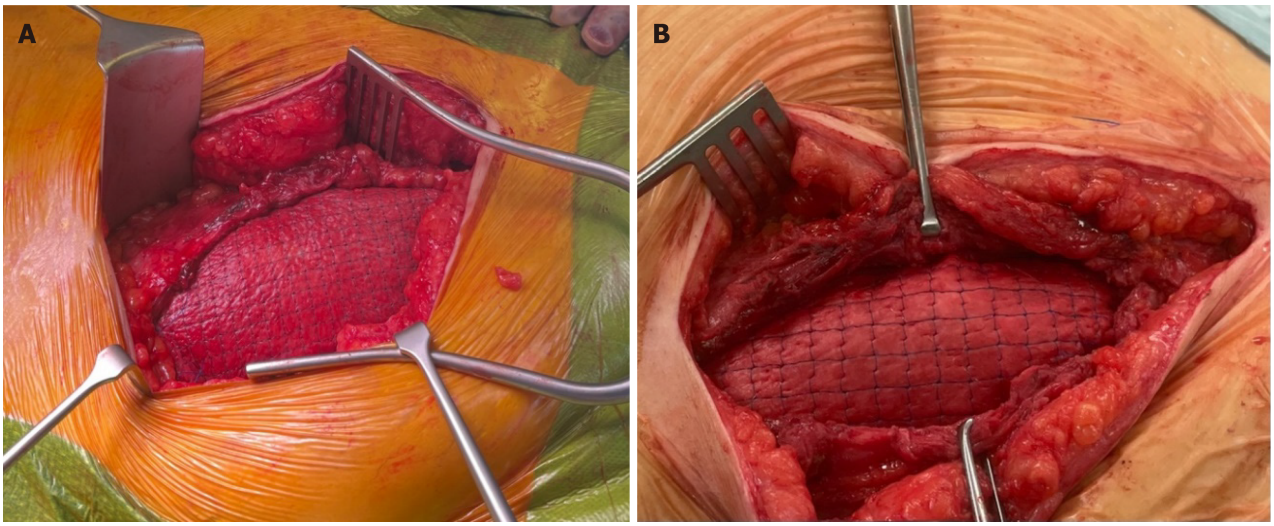


Figure 3 Operative repair of transplanted kidney within the incisional hernia using OviTex 1S mesh. A: Oblique view; B: Transverse view.

TREATMENT

With a confirmed diagnosis of a recurrent incisional hernia, the patients underwent incisional hernia repair with OviTex1S mesh using a sublay technique. Post-operative recovery was uneventful, and patients were discharged within a few days of hospital admission.

OUTCOME AND FOLLOW-UP

The patients have been regularly followed up in the clinic following their repairs, and there has been no recurrence with follow-up up to 18 months post-operative. They will continue to be followed up regularly.

DISCUSSION

The above-described cases provide useful information for the use of OviTex 1S meshes in the repair of hernias pKTx.

A clear conundrum exists between synthetic and biological meshes; synthetics provide good strength, structure, and affordability but they do not integrate into the host tissue as well as biologics and are associated with a higher infection risk. Biologics, on the other hand, have been shown to lose their structural integrity quickly and are more expensive. Hybrid meshes such as the OviTex 1S have been developed with the aim of preserving the benefits of both components whilst negating their downsides. Benefits include greater strength and better integration into the host, as well as a reduced inflammatory response, improved wound healing, and reduced hernia recurrence[6]. In contrast to synthetic meshes, which create a pro-inflammatory response in the host, OviTex 1S has been shown to have limited foreign body response with earlier infiltration, earlier functional vasculature establishment and a decreased risk of bacterial colonisation and infection[9].

Kidney transplant patients are a unique group who require close follow-up. Throughout the life of an allograft, it is not uncommon to have an US and transplant biopsy due to allograft dysfunction. The type of mesh used and how it integrates into the host tissue can influence the effectiveness of these investigations. The cases showed that OviTex 1S produced better depth and quality US images when compared to polypropylene mesh and allowed for a more controlled, less forceful transplant biopsy. This provides more accurate imaging results, reduces the risk of damage to the kidney and improves precision in biopsy. Other potential benefits may include an easier nephrectomy following the use of OviTex 1S mesh. Reduced scar tissue production and better integration into the host provide an easier operating field.

There has been no reported hernial recurrence in the cases presented above, and all patients made a quick recovery with no associated complications. The current reported 12-month recurrence rate of hernias repaired with OviTex 1S use is approximately 2.6%[6]. This is significantly lower than the re-occurrence rate in synthetic meshes of approximately 10% [10].

CONCLUSION

The OviTex 1S mesh provides benefits in hernial repairs pKTx, but cost is an issue, and the long-term viability of them is unclear. Continued use and reporting will help build a more informed picture.

FOOTNOTES

Author contributions: Abed M was responsible for data collection, data analysis and wrote the paper; Bradley A was responsible for data analysis, wrote the paper; Ghazanfar A conceived and designed the analysis, contributed data or analysis tools, and advisor; Abed M and Bradley A contribute equally to this study as co-first authors.

Informed consent statement: Patient details kept confidential with no identifiable information used.

Conflict-of-interest statement: The authors have nothing to disclose.

CARE Checklist (2016) statement: The authors have read the CARE Checklist (2016), and the manuscript was prepared and revised according to the CARE Checklist (2016).

Open Access: This article is an open-access article that was selected by an in-house editor and fully peer-reviewed by external reviewers. It is distributed in accordance with the Creative Commons Attribution NonCommercial (CC BY-NC 4.0) license, which permits others to distribute, remix, adapt, build upon this work non-commercially, and license their derivative works on different terms, provided the original work is properly cited and the use is non-commercial. See: https://creativecommons.org/Licenses/by-nc/4.0/

Country of origin: United Kingdom

ORCID number: Mariam Abed 0009-0002-0313-3573; Abbas Ghazanfar 0000-0003-0084-5057.

S-Editor: Lin C
L-Editor: A
P-Editor: Zhang L

REFERENCES

1 **Ooms LS**, Verhelst J, Jeekel J, Ijzermans JN, Lange JF, Terkivatan T. Incidence, risk factors, and treatment of incisional hernia after kidney transplantation: An analysis of 1,564 consecutive patients. *Surgery* 2016; **159**: 1407-1411 [PMID: 26775222 DOI: 10.1016/j.surg.2015.11.017]
2 **Mazzucchi E**, Nahas WC, Antonopoulos I, Ianhez LE, Arap S. Incisional hernia and its repair with polypropylene mesh in renal transplant recipients. *J Urol* 2001; **166**: 816-819 [PMID: 11490225 DOI: 10.1097/00005392-200109000-00005]
3 **Simson N**, Parker S, Stonier T, Halligan S, Windsor A. Incisional Hernia in Renal Transplant Recipients: A Systematic Review. *Am Surg* 2018; **84**: 930-937 [PMID: 29981627 DOI: 10.1177/000313481808400644]
4 **Costa L**, Martin D, Zingg T, Venetz JP, Demartines N, Golshayan D, Matter M. Incidence, Risk Factors, and Management of Incisional Hernias After Kidney Transplant: A 20-Year Single Center Experience. *Transplant Proc* 2023; **55**: 337-341 [PMID: 36813692 DOI: 10.1016/j.transproceed.2023.01.020]
5 **Burger JW**, Luijendijk RW, Hop WC, Halm JA, Verdaasdonk EG, Jeekel J. Long-term follow-up of a randomized controlled trial of suture versus mesh repair of incisional hernia. *Ann Surg* 2004; **240**: 578-83; discussion 583 [PMID: 15383785 DOI: 10.1097/01.sla.0000141193.08524.e7]
6 **DeNoto G 3rd**, Ceppa EP, Pacella SJ, Sawyer M, Slayden G, Takata M, Tuma G, Yunis J. A Prospective, Single Arm, Multi-Center Study Evaluating the Clinical Outcomes of Ventral Hernias Treated with OviTex(®) 1S Permanent Reinforced Tissue Matrix: The BRAVO Study 12-Month Analysis. *J Clin Med* 2021; **10** [PMID: 34768516 DOI: 10.3390/jcm10214998]
7 **Cavallaro A**, Lo Menzo E, Di Vita M, Zanghì A, Cavallaro V, Veroux PF, Cappellani A. Use of biological meshes for abdominal wall reconstruction in highly contaminated fields. *World J Gastroenterol* 2010; **16**: 1928-1933 [PMID: 20397274 DOI: 10.3748/wjg.v16.i15.1928]
8 **Klinge U**, Klosterhalfen B, Müller M, Schumpelick V. Foreign body reaction to meshes used for the repair of abdominal wall hernias. *Eur J Surg* 1999; **165**: 665-673 [PMID: 10452261 DOI: 10.1080/11024159950189726]
9 **Overbeck N**, Nagvajara GM, Ferzoco S, May BCH, Beierschmitt A, Qi S. In-vivo evaluation of a reinforced ovine biologic: a comparative study to available hernia mesh repair materials. *Hernia* 2020; **24**: 1293-1306 [PMID: 32006122 DOI: 10.1007/s10029-019-02119-z]
10 **Langer C**, Neufang T, Kley C, Liersch T, Becker H. Central mesh recurrence after incisional hernia repair with Marlex--are the meshes strong enough? *Hernia* 2001; **5**: 164-167 [PMID: 11759806 DOI: 10.1007/s100290100023]

World Journal of Clinical Cases

Submit a Manuscript: https://www.f6publishing.com

World J Clin Cases 2025 June 26; 13(18): 100610

DOI: 10.12998/wjcc.v13.i18.100610

ISSN 2307-8960 (online)

CASE REPORT

Birt-Hogg-Dubé syndrome - a rare genetic disorder complicated by pneumothorax: A case report

Meng-Zhen Li, Jun Deng

Specialty type: Medicine, research and experimental

Provenance and peer review: Unsolicited article; Externally peer reviewed.

Peer-review model: Single blind

Peer-review report's classification

Scientific Quality: Grade B, Grade D

Novelty: Grade B, Grade B

Creativity or Innovation: Grade B, Grade B

Scientific Significance: Grade A, Grade B

P-Reviewer: Namata TT

Received: August 21, 2024

Revised: October 10, 2024

Accepted: January 24, 2025

Published online: June 26, 2025

Processing time: 190 Days and 2 Hours

Meng-Zhen Li, Department of Orthopedics, The First People's Hospital of Kunshan, Jiangsu University, Kunshan 215300, Jiangsu Province, China

Jun Deng, Department of Emergency Surgery, The First People's Hospital of Kunshan, Jiangsu University, Kunshan 215300, Jiangsu Province, China

Corresponding author: Jun Deng, PhD, Affiliate Associate Professor, Surgeon, Department of Emergency Surgery, The First People's Hospital of Kunshan, Jiangsu University, No. 566 Qianjin East Road, Kunshan 215300, Jiangsu Province, China. yaya850830@126.com

Abstract

BACKGROUND

Birt-Hogg-Dubé (BHD) syndrome is a rare genetic disorder associated with mutations in the *BHD* gene, which can manifest symptoms at any age, including dermatological and pulmonary complications, as well as renal tumors. This study presents a case of a BHD patient who experienced spontaneous pneumothorax, aiming to enhance the understanding of this syndrome.

CASE SUMMARY

A 42-year-old female patient presented with left-sided chest pain and tightness lasting three days. Chest computed tomography scans revealed left-sided pneumothorax and multiple pulmonary bullae. Physical examination indicated decreased vocal fremitus and tympanic percussion on the left side. A thorough family history revealed a pattern of pulmonary disorders, including emphysema, spontaneous pneumothorax, and lung cancer among relatives. Genetic testing identified a heterozygous frameshift mutation in the *FLCN* gene at the 17p11.2 locus. Based on the clinical presentation, imaging findings, family history, and genetic results, the patient was suspected to have BHD syndrome.

CONCLUSION

We present a case of a heterozygous mutation in the *FLCN* gene in a patient with BHD syndrome, aiming to review the associated clinical characteristics and genetic mechanisms of this condition. This case serves as a reference point to offer insights into the diagnosis of multiple pulmonary cysts and spontaneous pneumothorax of unknown etiology in clinical practice.

Key Words: Birt-Hogg-Dubé syndrome; Spontaneous pneumothorax; Genetic disorder; *FLCN* gene; Folliculin; Case report

©The Author(s) 2025. Published by Baishideng Publishing Group Inc. All rights reserved.

Core Tip: Birt-Hogg-Dubé (BHD) syndrome is a rare autosomal dominant genetic disorder. The non-specific nature of its symptoms often results in frequent misdiagnoses and overlooked cases. In this report, we describe a patient with BHD syndrome who presented solely with multiple pulmonary bullae and pneumothorax. This case serves as a focal point for an in-depth discussion regarding the diagnosis, clinical presentation, prognosis, and management strategies for BHD syndrome.

Citation: Li MZ, Deng J. Birt-Hogg-Dubé syndrome - a rare genetic disorder complicated by pneumothorax: A case report. *World J Clin Cases* 2025; 13(18): 100610
URL: https://www.wjgnet.com/2307-8960/full/v13/i18/100610.htm
DOI: https://dx.doi.org/10.12998/wjcc.v13.i18.100610

INTRODUCTION

Birt-Hogg-Dubé (BHD) syndrome is an uncommon genetic disorder initially documented by Birt, Hogg, and Dubé in 1977[1,2]. It is primarily attributed to mutations in the *BHD* gene (folliculin gene), which is located on chromosome 17 and is responsible for encoding the folliculin protein[3,4]. Although the precise role of this protein within cells has not been fully elucidated, it is recognized for its pivotal involvement in cell proliferation, differentiation, and metabolic regulation. The inheritance pattern of BHD syndrome follows an autosomal dominant trait, indicating that the presence of a single mutated *BHD* gene is adequate for disease manifestation. Consequently, individuals with BHD syndrome are 50% likely to transmit this mutated gene to their offspring. Research indicates[1,4,5] that approximately 80% of patients have a familial history of the disorder, whereas 20% of cases arise from spontaneous mutations.

The prevalence of BHD syndrome varies between 1 in 200000 and 1 in 300000 individuals on the basis of geographical data[1,4,6,7]. Onset age displays considerable diversity, with symptoms potentially emerging from infancy to advanced age. Notable features of the syndrome include skin and lung abnormalities, which are frequently accompanied by the emergence of kidney tumours. Spontaneous pneumothorax represents a prevalent complication of BHD syndrome, but the precise underlying mechanisms remain unclear.

This manuscript presents a clinical case study of a confirmed BHD syndrome patient encountering spontaneous pneumothorax, with the intention of enriching comprehension of this condition.

CASE PRESENTATION

Chief complaints

The patient had left-sided chest pain and tightness persisting for 3 days.

History of present illness

The patient is a 42-year-old female who presented with left-sided chest pain and tightness that has lasted for three days. She reported no history of trauma, previous similar episodes, or recent strenuous physical activity. An emergency electrocardiogram (ECG) indicated sinus bradycardia and low voltage in the left precordial leads. Vital signs showed a heart rate of 56 beats per minute, a respiratory rate of 18 breaths per minute, blood pressure of 124/84 mmHg, and oxygen saturation of 98%. Acute myocardial infarction was ruled out based on these findings.

History of past illness

The patient has no significant past medical history, including no history of cardiovascular disease, cerebrovascular disease, or substance use (tobacco or alcohol).

Personal and family history

The patient has a significant family history of pulmonary disorders: (1) Grandmother: Emphysema, which led to her death; (2) Mother: Experienced unilateral spontaneous pneumothorax requiring surgical intervention; (3) One aunt: Developed pulmonary nodules that progressed to lung cancer; (4) Another aunt: Had numerous untreated pulmonary cysts; and (5) Sister: Experienced bilateral spontaneous pneumothorax on separate occasions, each managed surgically.

Physical examination

Physical examination revealed decreased vocal fremitus and tympanic percussion on the left side of the chest. No notable changes were observed in the skin of the face or anterior chest.

Laboratory examinations

Genetic testing revealed a heterozygous *FLCN* gene variant, specifically a frameshift mutation at the 17p11.2 locus of the *FLCN* gene (Table 1).

Imaging examinations

Emergency chest computed tomography (CT; Figures 1 and 2) scans showed left-sided pneumothorax and multiple pulmonary bullae in both lungs.

MULTIDISCIPLINARY EXPERT CONSULTATION

In light of the patient's complex clinical presentation, a multidisciplinary team was assembled, comprising specialists in pulmonology, genetics, and cardiology. The pulmonologist assessed the chest CT findings, confirming the presence of left-sided pneumothorax and multiple pulmonary bullae, and discussed potential management strategies for these pulmonary complications. The geneticist reviewed the patient's family history of pulmonary disorders and the results of genetic testing, highlighting the significance of the identified heterozygous *FLCN* gene variant. The cardiologist evaluated the ECG findings, which indicated sinus bradycardia and low voltage, ensuring that any cardiac issues were appropriately managed and did not contribute to the patient's respiratory symptoms. This collaborative approach aimed to formulate a comprehensive management plan that addressed both the immediate respiratory concerns and the underlying genetic condition.

FINAL DIAGNOSIS

Based on the patient's clinical presentation, imaging studies, family medical history, and genetic test results, the final diagnosis was confirmed as BHD syndrome, inherited through her maternal lineage (Figure 3). This diagnosis explains the patient's left-sided pneumothorax, the presence of multiple pulmonary bullae, and the notable family history of associated pulmonary disorders.

TREATMENT

We recommended surgical intervention for the patient, thoroughly explaining the associated risks and prognosis, and obtained her informed consent for the procedure. Routine preoperative examinations were performed, revealing that the patient tested positive for Treponema pallidum antibodies. A complete blood count, along with liver and kidney function tests, C-reactive protein, and erythrocyte sedimentation rate, were all within normal ranges, and no respiratory pathogens were cultured from sputum over a two-day period.

After comprehensive preoperative preparation, the patient underwent video-assisted thoracoscopic bullectomy and pleurodesis. Intraoperatively, a roughly 1.0 cm-long observation orifice was established at the 7th intercostal space along the left midaxillary line for the thoracoscope. An incision measuring 2 cm at the 4th intercostal space along the left anterior axillary line was designated as the operative port. Exploration unveiled approximately 80 mL of pale yellow turbid fluid within the pleural cavity devoid of adhesions. Various bullae were identified in distinct locations, including the left lung apex, the anterior segment of the left upper lobe, in proximity to the left upper lobe oblique fissure, and adjacent to the mediastinum beside the left lower lobe ligament, manifesting as clustered bubble-like structures (Figure 4). Among them, the largest bulla measured approximately 3.0 cm × 3.0 cm. The bullae were completely excised, and following suction and reinflation of the lung, no significant air leakage was noted. Closure of the pleural cavity was conducted along each intercostal space, and a 24 French chest tube was placed through the observation port. Histological evaluation of the excised tissue during the surgical intervention substantiated findings consistent with a pulmonary bulla (Figure 5).

OUTCOME AND FOLLOW-UP

Upon emergence from anesthesia, the patient expressed incisional pain; however, her vital signs remained stable, and she reported no other significant discomfort. Symptomatic management, including analgesia and fluid supplementation, was initiated. On the first postoperative day, the chest tube drained 150 mL of serosanguineous fluid, which increased to 180 mL on the second day, decreased to 100 mL on the third day, and further to 80 mL on the fourth day. During this timeframe, there was no significant air leakage noted in the chest drainage bottle, and the water column fluctuated appropriately. The patient did not report any specific discomfort aside from wound pain, leading to the removal of the chest tube on the fifth postoperative day.

The patient's postoperative incision exhibited primary intention healing. A follow-up examination conducted one month after the surgery indicated a well-healed thoracic cage, as assessed by chest X-ray (Figure 6), with the patient reporting no symptoms of chest pain, tightness, or dyspnea. Additionally, no significant complications were observed.

Table 1 Patient family genetic testing results

	Gene	Chromosomal location	Reference transcript	Location	cDNA level	Protein level	Status	Mutation classification
A	*FLCN*	17p11.2	NM-144997.6	Exon11	c.1285delC	p.(His429fs)	Hybrid	Pathogenic mutation
B	*FLCN*	17p11.2	NM-144997.6	Exon11	c.1285delC	p.(His429fs)	Hybrid	Pathogenic mutation
C	*FLCN*	17p11.2	NM-144997.6	Exon11	c.1285delC	p.(His429fs)	Hybrid	Pathogenic mutation

Project name: Family testing for genetic diseases through whole exome sequencing (Trio). A: Patient; B: Mother; C: Sister.

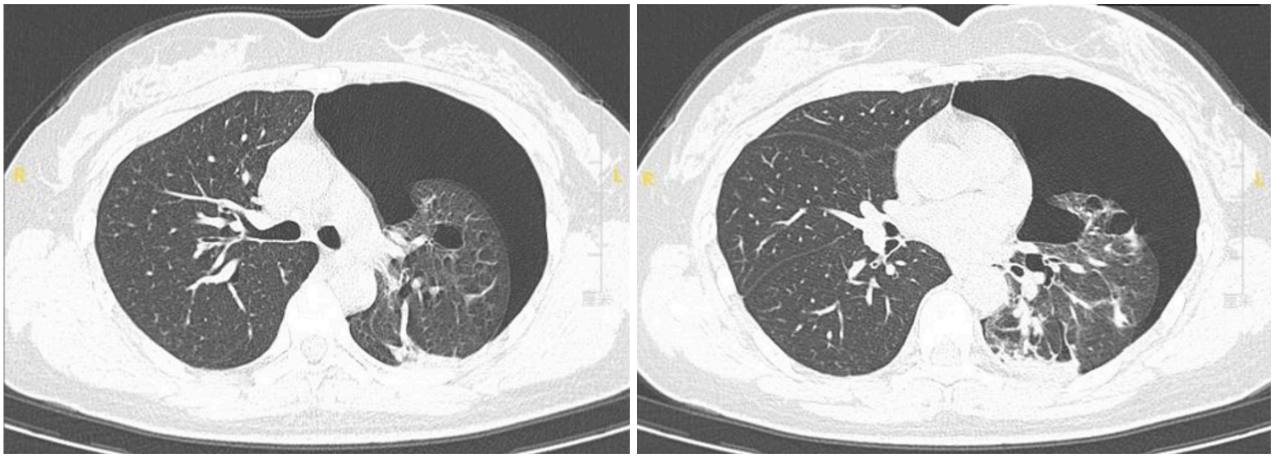


Figure 1 A chest computed tomography scan revealing left-sided pneumothorax and multiple thin-walled cysts.

DISCUSSION

BHD syndrome, a rare genetic autosomal dominant condition stemming from germline mutations in the tumor suppressor gene *FLCN* responsible for encoding folliculin. Notably, 90% of documented BHD cases originate from Europe and the United States, with limited recognition in Southeast Asia, particularly in China. In the Western regions, 82% to 92% of BHD instances prominently feature distinctive skin manifestations, whereas in Asian cohorts, these manifestations are observed in only 20% to 29% of cases, potentially contributing to underdiagnosis. Asian individuals with BHD frequently present pulmonary cysts and spontaneous pneumothorax, occurring at a rate of approximately 58%. Consequently, a family history of pneumothorax in Asian populations can serve as a pivotal diagnostic indicator for BHD syndrome[8,9]. Thus, a comprehensive exploration of the clinical presentations, genetic underpinnings, and therapeutic approaches of BHD syndrome is crucial to deepen comprehension of the disorder and enhance diagnostic accuracy.

Diagnosis of BHD

BHD syndrome, while relatively uncommon in clinical settings, is frequently subject to misdiagnosis or delayed diagnosis owing to its varied clinical manifestations. The identification of BHD syndrome hinges predominantly on clinical symptoms and germline mutations within the *FLCN* gene. Thus, when suspicion of BHD arises, a thorough exploration of the individual's and family's medical history concerning skin lesions, pneumothorax, pulmonary cysts, and renal tumors is advised, as these serve as pivotal diagnostic indicators for the syndrome. The current diagnostic criteria proposed are delineated in the subsequent table (Table 1)[6,8-12], albeit necessitating formal validation.

For individuals fulfilling the clinical diagnostic criteria for BHD, the option of *FLCN* sequence analysis can be pursued. In instances where sequence analysis fails to reveal any pathogenic variants, alternative methodologies like multiplex ligation-dependent probe amplification should be contemplated to identify deletions or duplications. It is crucial to emphasize that a non-detectable result in *FLCN* gene testing does not definitively rule out the diagnosis[6,9].

Clinical picture

Cutaneous manifestations: The predominant clinical presentation of BHD syndrome manifests as skin lesions, observed in roughly 80%-90% of cases in Europe and the United States, featuring distinctive skin alterations. Conversely, among Asian individuals, skin manifestations are less prevalent and less distinctive[6,9,13]. The characteristic skin manifestations in BHD patients encompass multiple, smooth, asymptomatic round or oval papules, commonly situated on the face, neck, and upper chest[2,7,14-16], appearing as fibrofolliculomas, trichodiscomas, and angiofibromas. While skin tumors in BHD syndrome are predominantly benign, instances of malignant melanoma have been documented[6,9]. Studies by Sattler *et al*[17] revealed an overall melanoma incidence of 6.0% in BHD patients, markedly surpassing the general population's 1.8%. Nonetheless, further investigations are imperative to ascertain whether *FLCN* gene mutations elevate

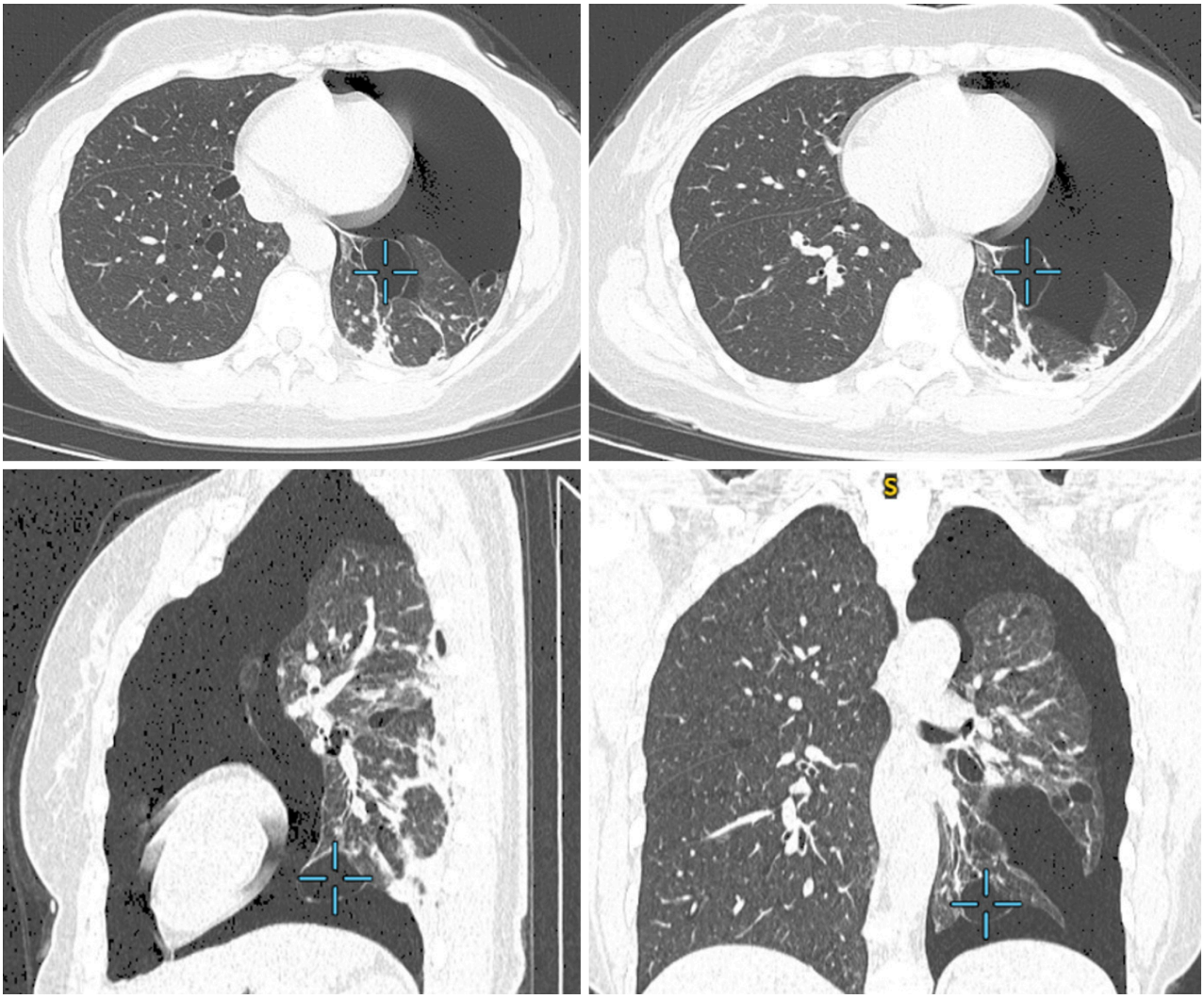


Figure 2 Chest computed tomography volume reconstruction showing pneumothorax and multiple pulmonary cysts.

the susceptibility to malignant skin neoplasms. Notably, the identification of skin fibromas during dermatological assessments should trigger suspicion of BHD syndrome, prompting comprehensive evaluations encompassing pulmonary and renal assessments.

Pulmonary manifestations: Another distinctive clinical feature observed in individuals with BHD syndrome is the occurrence of lung cysts[18] and recurrent pneumothorax. Imaging studies reveal that over 80% of BHD patients exhibit multiple lung cysts. Characteristic chest CT findings include bilateral multiple thin-walled cysts with well-defined borders[7], often presenting as oval, round, or irregular shapes ranging in size from a few millimeters to several centimeters[14,19]. However, the pulmonary manifestations of BHD syndrome can be mistaken for lymphangioleiomyomatosis (LAM) due to shared clinical features involving the skin, lungs, and kidneys[2,13,20]. LAM cysts typically display a diffuse round morphology. In contrast to BHD, LAM cysts are smaller, rounder, more uniformly distributed, and possess thinner and smoother walls[19,20]. Lung cysts in BHD patients are commonly situated in the lung bases and mediastinal regions[2,6,9,13,18,20]. The lung parenchyma between these lesions typically appears normal, and patients often remain asymptomatic or may only experience mild coughing or exertional dyspnea[2,6,7,9,19].

Data indicates that 90% of Asian individuals with BHD experience recurrent pneumothorax, a rate 60% higher than in Western populations[13], with recurrence rates reaching 40%-75%[2,7]. Although lung involvement typically represents the initial manifestation in patients, the triad phenotype of BHD (involving the skin, lungs, and kidneys) demonstrates clinical variability among affected individuals, with some presenting solely with pneumothorax[10,20]. In a study involving 12 families[21], at least two first-degree relatives in each family exhibited spontaneous pneumothorax, without concurrent renal or skin manifestations in genetically affected individuals.

The current BHD syndrome patient under our care presents solely with unexplained spontaneous pneumothorax, devoid of skin or renal symptoms. Several family members have a history of spontaneous pneumothorax or lung cysts. Therefore, when confronted with a patient displaying unexplained multiple lung cysts or recurrent pneumothorax, particularly in the context of familial occurrences, maintaining a high index of suspicion for BHD syndrome is crucial to avert misdiagnosis or oversight.

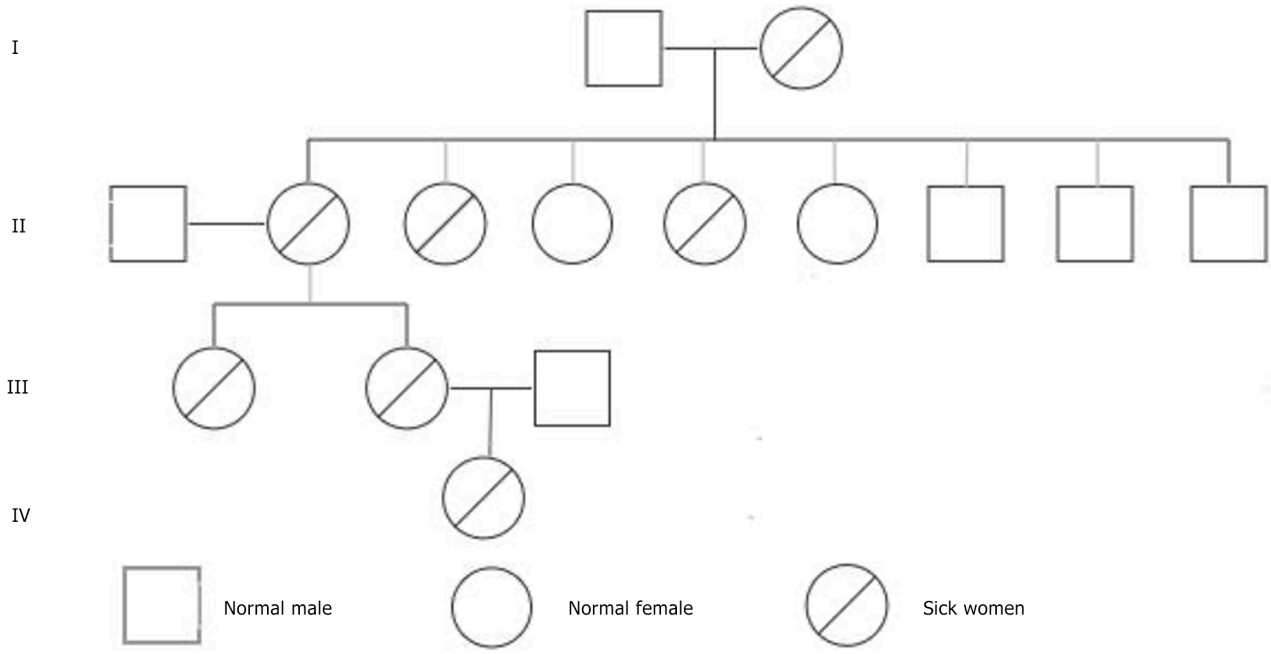


Figure 3 Medical conditions of the patient's family members.

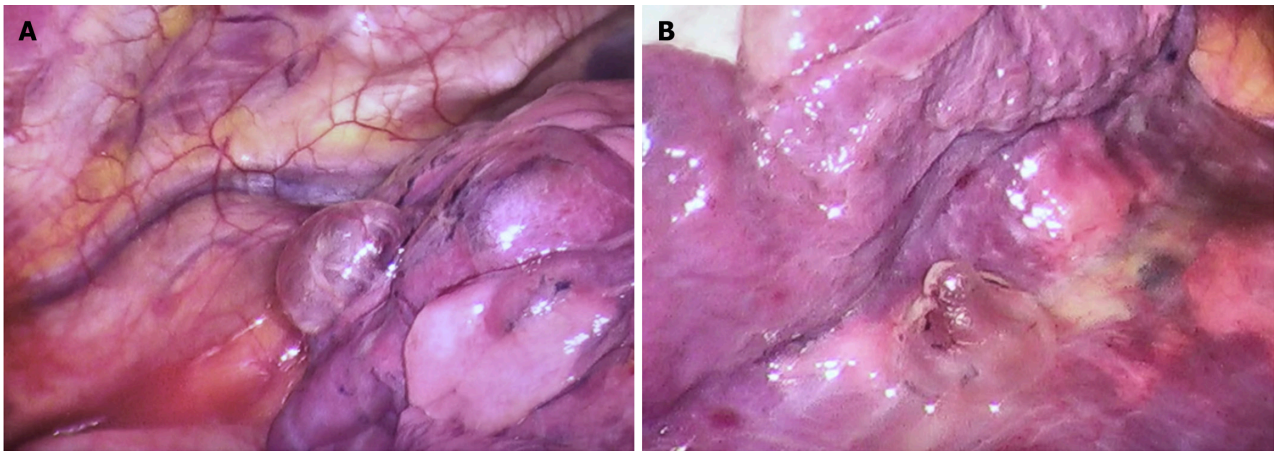


Figure 4 Multiple bullae in the thoracic cavity were observed under intraoperative thoracoscopy. A: Multiple bullae in the apical segment of the left upper lobe, presenting as fish bubble-like structures; B: Bullae near the diaphragmatic surface of the left lower lobe, exhibiting a fish hook-shaped appearance.

Renal manifestations: Renal tumors stand out as the most critical characteristic manifestation in individuals diagnosed with BHD syndrome[6,9,18], with an estimated incidence rate ranging from 12% to 34%[6,9,14,16]. Research indicates[12] that the average age at which BHD patients develop renal tumors is 50.4 years, with the earliest diagnosis of BHD-related renal tumors reported at 20 years of age[6,9,14]. In a risk evaluation involving BHD family members, those affected by the syndrome presented a sevenfold increased of developing renal tumors compared to genetically unaffected relatives, and a fiftyfold increased risk of experiencing spontaneous pneumothorax[6,9,14,19]. The predominant histological subtype of BHD renal tumors is the hybrid oncocytic tumor, which constitute approximately half of all cases. Furthermore, these tumors can manifest as chromophobe renal cell carcinoma, papillary tumors, and clear cell renal cell carcinoma[2,7,14,19]. Prognosis primarily hinges on the prevalence of renal cell carcinoma and the histological classification of the renal tumor. Hence, early detection through imaging studies or familial screening plays a pivotal role in determining the optimal timing of surgical intervention for patients, as well as in evaluating postoperative renal function and overall prognosis.

Genetics

Folliculin serves as a tumour suppressor, with *FLCN* representing the gene encoding folliculin, which is recognized as a tumour suppressor gene[6,9]. Deletion or functional mutations in *FLCN* are linked to increased susceptibility to BHD-related tumours[6,8,9]. Recent investigations[3,4,14,22] have highlighted the involvement of *FLCN* in diverse metabolic pathways, encompassing the regulation of the mTOR pathway, the modulation of PGC1α and mitochondrial biogenesis,

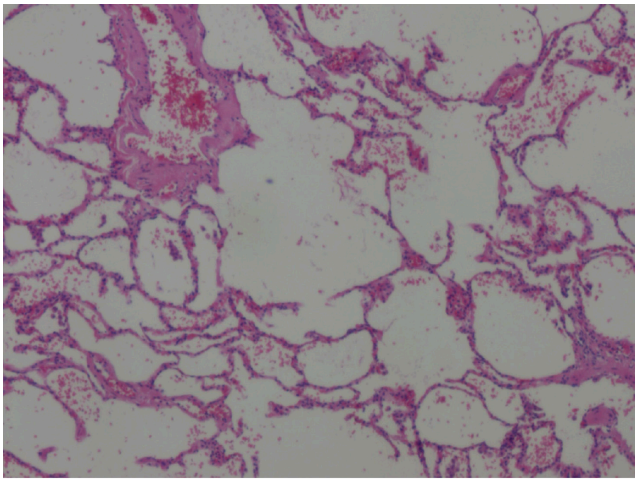


Figure 5 Postoperative pathological findings.

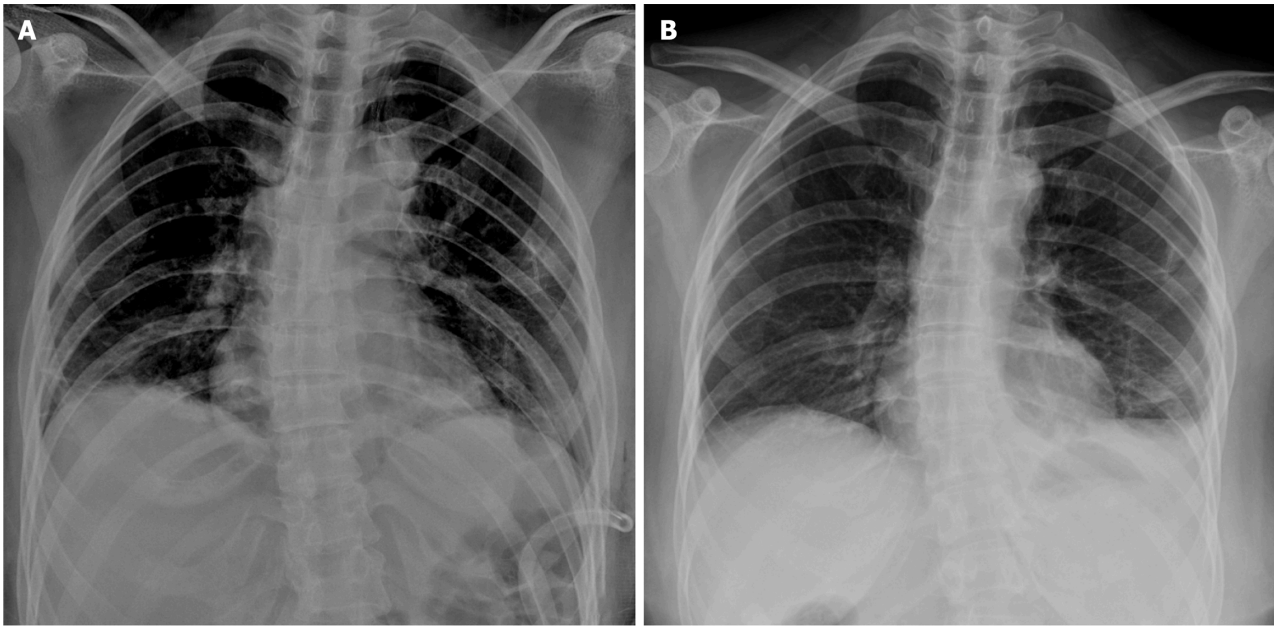


Figure 6 Postoperative review results of the patient. A: The first day after the surgery; B: One month after the surgery.

the control of TFE3/TFEB transcriptional activity, and the management of cellular autophagy[3,23]. It has been proposed that through these signalling and metabolic pathways, *FLCN* may impact the balance between cell proliferation and apoptosis, culminating in disease progression.

To date, two folliculin-interacting proteins, FNIP1 and FNIP2, have been identified[3,24]. FNIP1 interacts with the carboxyl terminus of *FLCN* and AMPK, while FNIP2 shares 49% homology with FNIP1[4,15,24]. Consequently, FNIP1, FNIP2, and *FLCN* collaborate synergistically or independently to form a *FLCN* complex that interacts with AMPK, thereby modulating mTOR signalling. Studies utilizing *FLCN* knockout mouse models have demonstrated that *FLCN* deficiency triggers mTORC1 activation[3,5]. Moreover, as a suppressor of AMPK, *FLCN* loss induces the phosphorylation of the autophagy proteins ULK-1, VPS34, and BECN1, promoting cellular autophagy. Investigations have revealed[3,4,23] that *FLCN* loss-induced AMPK activation leads to the upregulation of PGC1α. When the expression of PGC1α, a transcription factor in BHD tumours, is elevated, it enhances oxidative phosphorylation in cancer cells, resulting in the accumulation of reactive oxygen species, subsequently activating HIF1α and fostering aerobic glycolysis.

Furthermore, *FLCN* has been identified as a negative regulator of another MiTF family member, TFE3[4,5,24]. In the absence of *FLCN* in cells and tissues, mTORC1 activation enables TFE3 to evade mTORC1 phosphorylation, facilitating its nuclear translocation and transcriptional activity[22]. The transcriptional activity of TFE3 contributes to the development of aggressive renal cell carcinoma. In lung cyst cells, researchers[18] have detected the positive expression of mTOR and S6, alongside the identification of hypoxia-inducible factor 1α and VEGF. It is postulated that *FLCN* activates mTOR signalling, thereby governing downstream molecules such as the S6 protein and VEGF and promoting cyst formation (Figure 7).

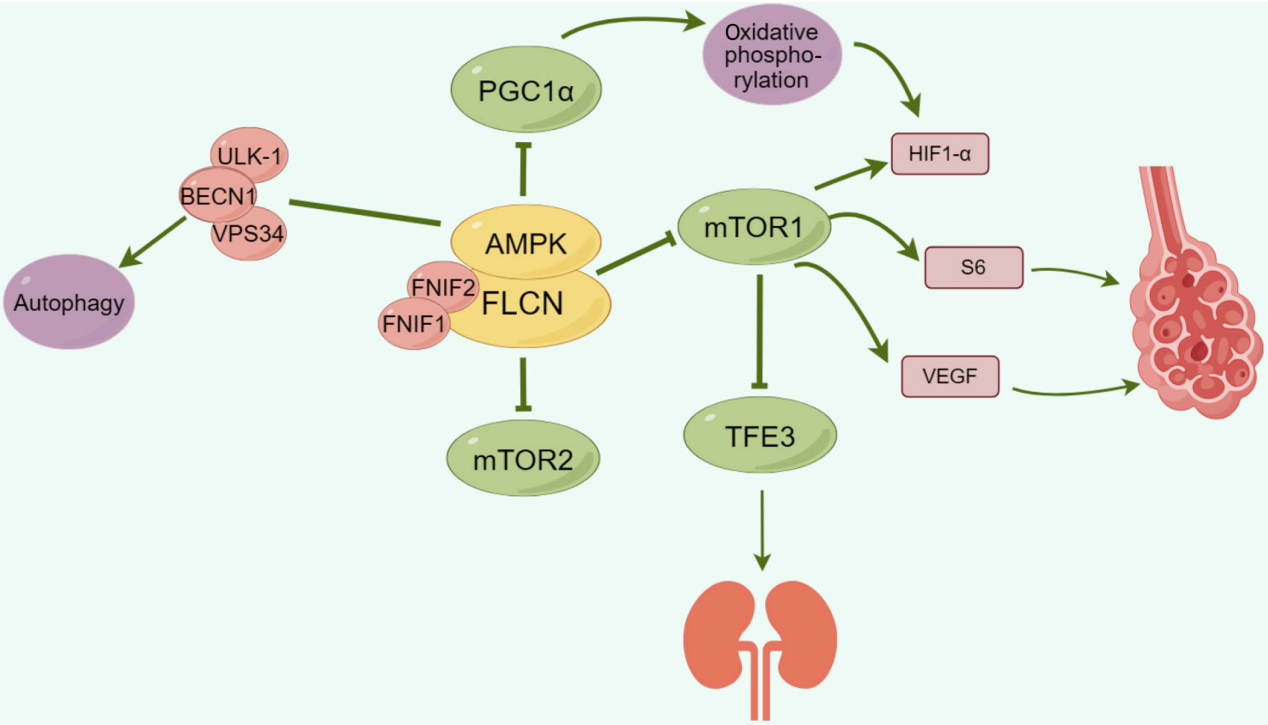


Figure 7 FLCN-associated pathways.

Management and prognosis

Treatment options for BHD syndrome are currently limited and are primarily centred on symptom alleviation. For example, addressing skin fibrofolliculomas may involve surgical excision or laser therapy. The management of renal lesions necessitates the regular monitoring of kidney function and tumour screening. Pulmonary lesions can be conservatively managed or require surgical intervention, contingent upon the patient's clinical status. Given the notable recurrence rate of pneumothorax in BHD patients, surgical resection and pleurectomy are commonly recommended[6,10], with studies demonstrating a markedly reduced recurrence rate postsurgery compared with conservative approaches [6,11].

Conversely, pulmonary care in BHD individuals involves considerations regarding air travel or diving activities. Fluctuations in atmospheric pressure during these pursuits may heighten the risk of pneumothorax. Guidelines from the British Thoracic Society caution that individuals with lung cysts or bullae face a risk of barotrauma while diving, with lung cysts serving as a contraindication for diving[10,11]. With respect to air travel, existing evidence does not indicate significant risks associated with this mode of transportation. Generally, most BHD patients should be able to safely engage in air travel. Nonetheless, patients with persistent or recent pneumothorax episodes are advised to refrain from air travel. If they experience unexplained chest tightness, chest pain, or breathing difficulties before boarding, they should postpone their travel plans. Additionally, patients should be informed that BHD cystic lung disease typically has a minimal impact on lung function. Nevertheless, individuals with compromised lung function or extensive pulmonary cystic changes should undergo routine lung function assessments and adhere to timely physician follow-up.

For individuals diagnosed with BHD, diligent screening for renal involvement is imperative. It is recommended that all BHD patients commence renal tumour screening around the age of 20, with subsequent screening every 3-4 years to facilitate early detection and intervention. Screening modalities primarily include renal ultrasound, CT, and magnetic resonance imaging (MRI), although ultrasound may lack sensitivity in detecting small renal lesions. Research indicates [11] that for renal lesions measuring 1.5-2.0 cm, the detection rate with ultrasound is merely 58%. Given the lifelong need for renal surveillance in BHD patients and to mitigate excessive radiation exposure from CT scans, renal MRI is presently the preferred modality. In the event of a renal tumour diagnosis during screening, subsequent diagnostic and treatment strategies should be tailored on the basis of factors such as tumour size and quantity. Treatment modalities typically encompass surgical excision, radiofrequency ablation, and cryotherapy. Presently, the recommended surgical threshold is a renal lesion size of 3 cm, with lesions smaller than 3 cm warranting preservation techniques such as radiofrequency ablation or cryotherapy to safeguard kidney function and avert metastatic spread.

As the majority of skin lesions in BHD patients are benign and pose a low risk of malignant transformation, specific pharmacological treatments for skin lesions are generally unnecessary. Nevertheless, for cosmetic purposes, certain patients may opt for surgical interventions such as excision, volume reduction, ablative laser therapy (CO_2 or Erb-Yag laser), or electrocautery. Notably, skin lesions also carry a risk of recurrence.

CONCLUSION

On the basis of our experiential insights and pertinent literature, upon establishing that a patient's pulmonary symptoms, such as multiple pulmonary bullae complicated by pneumothorax, stem from BHD syndrome, we advocate proactive consideration of additional surgical measures. The rationale is delineated as follows: (1) Surgical intervention, coupled with pleural space closure, notably reduces the probability of postoperative pneumothorax recurrence; (2) The prevailing trend towards minimally invasive surgical approaches has advantages such as reduced trauma and expedited recovery; and (3) After surgery, the patient's quality of life will considerably improve, with a reduction in psychological distress.

FOOTNOTES

Author contributions: Li MZ was responsible for writing the main manuscript text and overseeing the production of Figures 3 and 7; Figures 1, 2 and 4-6 of this article were provided by Deng J, who also served as the chief surgeon for the patient; the manuscript was thoroughly reviewed by all authors.

Informed consent statement: Informed consent from the patients was provided.

Conflict-of-interest statement: Both authors declare no conflict of interests.

CARE Checklist (2016) statement: The authors have read the CARE Checklist (2016), and the manuscript was prepared and revised according to the CARE Checklist (2016).

Open Access: This article is an open-access article that was selected by an in-house editor and fully peer-reviewed by external reviewers. It is distributed in accordance with the Creative Commons Attribution NonCommercial (CC BY-NC 4.0) license, which permits others to distribute, remix, adapt, build upon this work non-commercially, and license their derivative works on different terms, provided the original work is properly cited and the use is non-commercial. See: https://creativecommons.org/Licenses/by-nc/4.0/

Country of origin: China

ORCID number: Meng-Zhen Li 0009-0006-0950-037X; Jun Deng 0009-0009-1527-9642.

S-Editor: Lin C
L-Editor: A
P-Editor: Zhang XD

REFERENCES

1 **Ghosh S**, Farver CF. Birt-Hogg-Dubé Syndrome. *Radiology* 2022; **302**: 514 [PMID: 34846202 DOI: 10.1148/radiol.2021211972]
2 **Lu YR**, Yuan Q, Liu J, Han X, Liu M, Liu QQ, Wang YG. A rare occurrence of a hereditary Birt-Hogg-Dubé syndrome: A case report. *World J Clin Cases* 2021; **9**: 7123-7132 [PMID: 34540968 DOI: 10.12998/wjcc.v9.i24.7123]
3 **Ramirez Reyes JMJ**, Cuesta R, Pause A. Folliculin: A Regulator of Transcription Through AMPK and mTOR Signaling Pathways. *Front Cell Dev Biol* 2021; **9**: 667311 [PMID: 33981707 DOI: 10.3389/fcell.2021.667311]
4 **Schmidt LS**, Linehan WM. FLCN: The causative gene for Birt-Hogg-Dubé syndrome. *Gene* 2018; **640**: 28-42 [PMID: 28970150 DOI: 10.1016/j.gene.2017.09.044]
5 **Marziali V**, Geropoulos G, Frasca L, Longo F, Patrini D, Panagiotopoulos N, Crucitti P. Focus on the pulmonary involvement and genetic patterns in Birt-Hogg-Dubè syndrome: Literature review. *Respir Med* 2020; **168**: 105995 [PMID: 32469710 DOI: 10.1016/j.rmed.2020.105995]
6 **Daccord C**, Good JM, Morren MA, Bonny O, Hohl D, Lazor R. Birt-Hogg-Dubé syndrome. *Eur Respir Rev* 2020; **29** [PMID: 32943413 DOI: 10.1183/16000617.0042-2020]
7 **Boone PM**, Scott RM, Marciniak SJ, Henske EP, Raby BA. The Genetics of Pneumothorax. *Am J Respir Crit Care Med* 2019; **199**: 1344-1357 [PMID: 30681372 DOI: 10.1164/rccm.201807-1212CI]
8 **Yukawa T**, Fukazawa T, Yoshida M, Morita I, Kato K, Monobe Y, Furuya M, Naomoto Y. A Case of Birt-Hogg-Dubé (BHD) Syndrome Harboring a Novel Folliculin (FLCN) Gene Mutation. *Am J Case Rep* 2016; **17**: 788-792 [PMID: 27780965 DOI: 10.12659/ajcr.899407]
9 **Garg A**, Herts BR. Birt-Hogg-Dube syndrome. *J Urol* 2012; **188**: 1343-1344 [PMID: 22906666 DOI: 10.1016/j.juro.2012.06.125]
10 **Dal Sasso AA**, Belém LC, Zanetti G, Souza CA, Escuissato DL, Irion KL, Guimarães MD, Marchiori E. Birt-Hogg-Dubé syndrome. State-of-the-art review with emphasis on pulmonary involvement. *Respir Med* 2015; **109**: 289-296 [PMID: 25519092 DOI: 10.1016/j.rmed.2014.11.008]
11 **Gupta N**, Seyama K, McCormack FX. Pulmonary manifestations of Birt-Hogg-Dubé syndrome. *Fam Cancer* 2013; **12**: 387-396 [PMID: 23715758 DOI: 10.1007/s10689-013-9660-9]
12 **Menko FH**, van Steensel MA, Giraud S, Friis-Hansen L, Richard S, Ungari S, Nordenskjöld M, Hansen TV, Solly J, Maher ER; European BHD Consortium. Birt-Hogg-Dubé syndrome: diagnosis and management. *Lancet Oncol* 2009; **10**: 1199-1206 [PMID: 19959076 DOI: 10.1016/S1470-2045(09)70188-3]
13 **Hao S**, Long F, Sun F, Liu T, Li D, Jiang S. Birt-Hogg-Dubé syndrome: a literature review and case study of a Chinese woman presenting a novel FLCN mutation. *BMC Pulm Med* 2017; **17**: 43 [PMID: 28222720 DOI: 10.1186/s12890-017-0383-9]
14 **Schmidt LS**, Linehan WM. Molecular genetics and clinical features of Birt-Hogg-Dubé syndrome. *Nat Rev Urol* 2015; **12**: 558-569 [PMID:

26334087 DOI: 10.1038/nrurol.2015.206]

15 **Kunogi M**, Kurihara M, Ikegami TS, Kobayashi T, Shindo N, Kumasaka T, Gunji Y, Kikkawa M, Iwakami S, Hino O, Takahashi K, Seyama K. Clinical and genetic spectrum of Birt-Hogg-Dube syndrome patients in whom pneumothorax and/or multiple lung cysts are the presenting feature. *J Med Genet* 2010; **47**: 281-287 [PMID: 20413710 DOI: 10.1136/jmg.2009.070565]

16 **Toro JR**, Pautler SE, Stewart L, Glenn GM, Weinreich M, Toure O, Wei MH, Schmidt LS, Davis L, Zbar B, Choyke P, Steinberg SM, Nguyen DM, Linehan WM. Lung cysts, spontaneous pneumothorax, and genetic associations in 89 families with Birt-Hogg-Dubé syndrome. *Am J Respir Crit Care Med* 2007; **175**: 1044-1053 [PMID: 17322109 DOI: 10.1164/rccm.200610-1483OC]

17 **Sattler EC**, Ertl-Wagner B, Pellegrini C, Peris K, Reithmair M, Schädle N, Ruzicka T, Steinlein OK. Cutaneous melanoma in Birt-Hogg-Dubé syndrome: part of the clinical spectrum? *Br J Dermatol* 2018; **178**: e132-e133 [PMID: 28869776 DOI: 10.1111/bjd.15937]

18 **Furuya M**, Nakatani Y. Birt-Hogg-Dube syndrome: clinicopathological features of the lung. *J Clin Pathol* 2013; **66**: 178-186 [PMID: 23223565 DOI: 10.1136/jclinpath-2012-201200]

19 **Lee JE**, Cha YK, Kim JS, Choi JH. Birt-Hogg-Dubé syndrome: characteristic CT findings differentiating it from other diffuse cystic lung diseases. *Diagn Interv Radiol* 2017; **23**: 354-359 [PMID: 28830849 DOI: 10.5152/dir.2017.16606]

20 **Gunji Y**, Akiyoshi T, Sato T, Kurihara M, Tominaga S, Takahashi K, Seyama K. Mutations of the Birt Hogg Dube gene in patients with multiple lung cysts and recurrent pneumothorax. *J Med Genet* 2007; **44**: 588-593 [PMID: 17496196 DOI: 10.1136/jmg.2007.049874]

21 **Kumar K**, Ross C. Birt-Hogg-Dubé syndrome presenting with spontaneous pneumothorax and extensive pulmonary cysts in the absence of skin lesions or renal pathology. *BMJ Case Rep* 2019; **12** [PMID: 31494588 DOI: 10.1136/bcr-2019-231039]

22 **Kobayashi K**. Incidental detection of asymptomatic pneumothorax resulting in a diagnosis of Birt-Hogg-Dubé syndrome. *BMJ Case Rep* 2019; **12** [PMID: 30696655 DOI: 10.1136/bcr-2018-228939]

23 **Napolitano G**, Di Malta C, Esposito A, de Araujo MEG, Pece S, Bertalot G, Matarese M, Benedetti V, Zampelli A, Stasyk T, Siciliano D, Venuta A, Cesana M, Vilardo C, Nusco E, Monfregola J, Calcagnì A, Di Fiore PP, Huber LA, Ballabio A. A substrate-specific mTORC1 pathway underlies Birt-Hogg-Dubé syndrome. *Nature* 2020; **585**: 597-602 [PMID: 32612235 DOI: 10.1038/s41586-020-2444-0]

24 **Min H**, Ma D, Zou W, Wu Y, Ding Y, Zhu C, Lin A, Song S, Liang Q, Chen B, Zhang B, Wan Y, Ye M, Pan Y, Wen Y, Yi L, Gao Q. FLCN-regulated miRNAs suppressed reparative response in cells and pulmonary lesions of Birt-Hogg-Dubé syndrome. *Thorax* 2020; **75**: 476-485 [PMID: 32184379 DOI: 10.1136/thoraxjnl-2019-213225]

World Journal of Clinical Cases

Submit a Manuscript: https://www.f6publishing.com

World J Clin Cases 2025 June 26; 13(18): 101309

DOI: 10.12998/wjcc.v13.i18.101309

ISSN 2307-8960 (online)

CASE REPORT

Temporary bilateral uterine artery occlusion in the control of hemorrhage: A case report and review of literature

Yu-Liang Song, Chun-Feng Wang

Specialty type: Medicine, research and experimental

Provenance and peer review: Unsolicited article; Externally peer reviewed.

Peer-review model: Single blind

Peer-review report's classification

Scientific Quality: Grade D

Novelty: Grade B

Creativity or Innovation: Grade B

Scientific Significance: Grade B

P-Reviewer: Perelmuter S

Received: September 10, 2024

Revised: November 1, 2024

Accepted: December 5, 2024

Published online: June 26, 2025

Processing time: 169 Days and 18.5 Hours

Yu-Liang Song, Chun-Feng Wang, Department of Gynecology, Zhejiang Hospital, Hangzhou 310030, Zhejiang Province, China

Corresponding author: Chun-Feng Wang, Deputy Chief Doctor, Surgeon, Department of Gynecology, Zhejiang Hospital, No. 1229 Gudun Road, West Lake District, Hangzhou 310030, Zhejiang Province, China. chunfengwang123sdu@163.com

Abstract

BACKGROUND

Intramural pregnancy is rare, with an unclear etiology and pathophysiology. Surgical, medical, and expectant management options are available for this condition. However, most reported cases are managed surgically. Despite the risks of massive intraoperative bleeding and acute and long-term complications, uterine artery embolization is often selected. Temporary occlusion of the bilateral uterine arteries during surgery is associated with fewer complications.

CASE SUMMARY

We reported the case of a patient who was diagnosed with intramural pregnancy approximately one month after medical abortion. We performed laparoscopic resection with hysteroscopy. Since the lesion had abundant blood flow, we temporarily blocked the bilateral uterine arteries to prevent massive intraoperative bleeding. The surgical process went smoothly. The postoperative course was uneventful.

CONCLUSION

Temporary occlusion of the bilateral uterine arteries in the treatment of intramural pregnancy may prevent excessive uterine bleeding during surgery.

Key Words: Intramural pregnancy; Hysteroscopy; Laparoscopic surgery; Uterine artery temporary occlusion; Case report

©The Author(s) 2025. Published by Baishideng Publishing Group Inc. All rights reserved.

Core Tip: Intramural pregnancy is rare. There are few reports on temporary uterine artery occlusion for the treatment of intramural pregnancy. Here, we review studies on intramural pregnancy and report bilateral uterine artery occlusion during laparoscopic surgery and hysteroscopy for intramural pregnancy. The surgical process and postoperative course were uneventful.

Citation: Song YL, Wang CF. Temporary bilateral uterine artery occlusion in the control of hemorrhage: A case report and review of literature. *World J Clin Cases* 2025; 13(18): 101309
URL: https://www.wjgnet.com/2307-8960/full/v13/i18/101309.htm
DOI: https://dx.doi.org/10.12998/wjcc.v13.i18.101309

INTRODUCTION

Intramural pregnancy is rare and represents less than 1% of all ectopic pregnancies[1,2]. Intramural pregnancy is characterized by the presence of the gestational sac in the uterine myometrium without any connection to the uterine cavity[3]. In intramural pregnancy, uterine rupture is potentially fatal, as it can lead to severe hemorrhage and hysterectomy. Early diagnosis of intramural pregnancy is very important. Surgical, including uterine artery embolization (UAE), medical, and expectant management options are available for this condition, and the optimal method depends on the size and location of the gestational sac, gestational age, and the patient's desire for future fertility. Here, we report laparoscopic surgery and hysteroscopy for intramural pregnancy after medical abortion. The bilateral uterine arteries were temporarily blocked during surgery.

CASE PRESENTATION

Chief complaints

A 41-year-old patient, gravidity 3, parity 1, artificial abortion 2, was admitted to the hospital because of a small amount of vaginal bleeding for approximately half a month after medical abortion.

History of present illness

The patient underwent medical abortion on December 13, 2021. The gestational sac was successfully discharged. After medical abortion, a small amount of vaginal bleeding persisted for one week. Approximately one month later, on January 27, 2022, the patient experienced vaginal bleeding again, which initially appeared to be a normal amount of menstruation. Afterward, a small amount of intermittent vaginal bleeding persisted.

History of past illness

She was healthy without internal medical disease and had no history of surgery.

Personal and family history

She denied any family history of inherited disease or malignant tumors.

Physical examination

Physical examination revealed a normal sized uterus with no tenderness and no abnormalities in the uterine cervix or abdomen. There was a small amount of vaginal bleeding.

Laboratory examinations

On February 9, 2022, her serum β-human chorionic gonadotropin (β-hCG) level was 2649.00 mIU/mL.

Imaging examinations

Three-dimensional transvaginal examination revealed an abnormal echo approximately 1.0 cm × 0.5 cm × 0.4 cm in size in the uterus cavity near the left uterine corner, and the echo extended to the myometrium of the uterus fundus. Color Doppler ultrasound revealed abundant blood flow around it (the "ring of fire" "sign"; Figure 1). Doppler ultrasound also revealed highly vascular tissue approximately 1.7 cm × 1.6 cm × 1.3 cm in size in the left bottom muscle layer, with detectable arterial and venous abnormalities, low resistance and high-speed blood flow, suggesting an arteriovenous fistula. T1 and T2 images on pelvic magnetic resonance imaging revealed a nodule approximately 1.5 cm in diameter with equal shadows and signals within the myometrium in the left wall of the uterus and no significant limitation in diffusion.

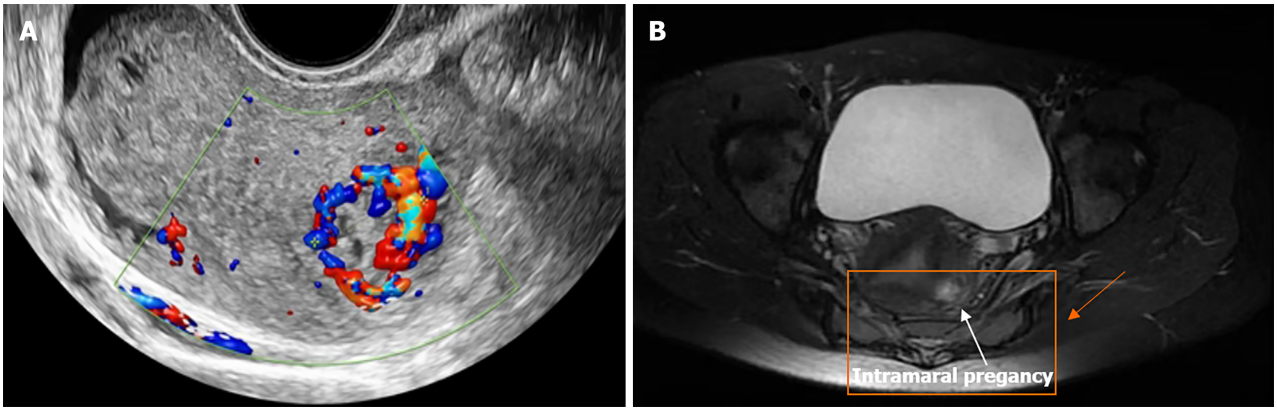


Figure 1 Imaging examinations. A: Color Doppler ultrasound image showing abundant blood flow around it (the "ring of fire" sign); B: Pelvic magnetic resonance imaging showed a nodular measuring approximately 1.5 cm within the myometrium in the left wall of the uterus.

MULTIDISCIPLINARY EXPERT CONSULTATION

The diagnosis was unsure, maybe intrauterine residue, cornual pregnancy, gestational trophoblastic disease or intramural pregnancy.

FINAL DIAGNOSIS

Intramural pregnancy was diagnosed *via* surgical and pathological examinations.

TREATMENT

We performed hysteroscopy under general anesthesia, and although no apparent pregnant tissue was found, a membrane-like substance was observed in the uterine cavity near the left uterine horn and tubal ostia. We performed uterine curettage and scraped out a small amount of endometrial tissue.

We subsequently performed laparoscopic surgery and found no apparent adhesion or blood in the pelvic cavity. The uterus was average in size and positioned posterior, with no obvious myoma on the surface or protrusions in the bilateral uterine horns. We considered the possibility of intraoperative hemorrhage and decided to temporarily block the bilateral uterine arteries with titanium clamps. This step was essential. First, we exposed the uterine arteries by separating the anterior leaf of the broad ligament, dissecting the internal iliac artery and locating the uterine artery originating from the internal iliac artery. We then used titanium clips to block the bilateral uterine arteries intuitively. On the basis of the preoperative imaging examination, unipolar electrocoagulation was performed to cut the serous membrane layer of the left posterior wall near the uterine corner approximately 2 cm deep, where villous tissue with a diameter of approximately 1 cm was visible (Figure 2). The tissue was removed entirely. An enlarged excision measuring 0.5 cm was made in the myometrium along the outer edge of the villous tissue. Bipolar electrocoagulation was performed to stop the bleeding on the wound surface, and 1/0 absorbable sutures were used to close the uterine wound layer by layer, restoring the typical anatomical structure of the uterus. The titanium clips were removed from the bilateral uterine arteries. The surgical process went smoothly.

OUTCOME AND FOLLOW-UP

The postoperative course was uneventful. The patient was discharged on the 7th postoperative day. Pathological examination confirmed the diagnosis of intramural pregnancy. The serum β-hCG level was normal one week after surgery. Until July 2024, the patient was healthy. She had no desire to become pregnant again.

DISCUSSION

Intramural pregnancy is rare and represents less than 1% of all ectopic pregnancies[1,2]. Intramural pregnancy is characterized by the presence of the gestational sac in the uterine myometrium without any connection to the uterine cavity[3]. Considering that intramural ectopic pregnancy is not common, there is a lack of information on the clinical features, available treatments, and long-term reproductive outcomes of patients, as most information is conveyed in case reports.

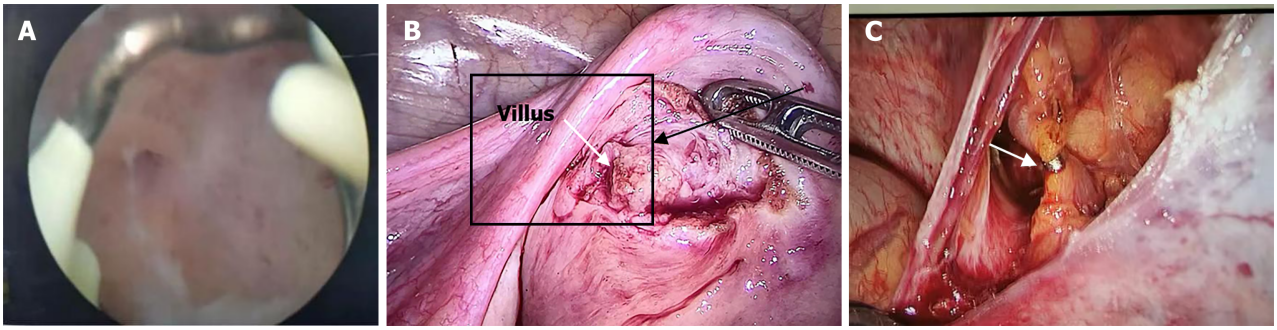


Figure 2 Surgical images. A: Hysteroscopy showing no apparent pregnant tissue but rather a membrane-like substance measuring approximately 1 cm × 1 cm near the left uterine horn; B: We cut the serous membrane layer near the left uterine corner approximately 2 cm deep, where villous tissue measuring approximately 1 cm in diameter was visible; C: The uterine artery was occluded with titanium clamps.

We reviewed publications on intramural pregnancy from August 2017 to August 2024 and studied and reviewed 12 articles (Table 1). The cause and pathophysiology of intramural pregnancy are unclear. Adenomyosis, infertility, uterine curettage, cesarean section, myomectomy, and pelvic infection are among the potential reasons[4]. Nearly every prior procedure mentioned in the 12 studies retrieved during the search for relevant literature involved in the uterine cavity[5-16]. One possible risk factor for the case we reported here was the patient's history of medical abortions. However, there are also two cases in which there has not been a uterine cavity operation, pregnancy or any other remarkable history of gynecological diseases[5,6]. Thus, in-depth study of the causes and factors contributing to intramural pregnancy is still necessary.

Researchers believe that intramural pregnancies should be managed individually[17]. Owing to the rarity of intramural pregnancy, there are no established guidelines for treatment at present. Various factors, such as the patient's state, conception location, gestational age, and desire to preserve fertility, influence the treatment selected for intramural pregnancy. A range of management strategies, including methotrexate treatment, laparoscopic surgery, laparotomy surgery, and expectant management, have been attempted. Methotrexate is administered systemically *via* a local injection and has been used successfully to arrest pregnancy development in cases of intramural pregnancy[18-20]. Katano *et al*[20] managed intramural pregnancy in the 8th week of gestation, as evidenced by an hCG level of 4000 IU/L, with laparoscopic and transvaginal local injections of methotrexate and reported that such an approach is an effective way to preserve reproductive potential. Memtsa *et al*[21] described a case in which the hCG level was 1159 IU/L and was managed with an injection of methotrexate. The hCG test was negative 6 weeks thereafter. The patient experienced transient severe lower abdominal pain. The major disadvantages of medical treatment for ectopic pregnancy are the need for prolonged follow-up and uncertainty about the effects on future fertility and pregnancies[22]. In our case, intramural pregnancy is difficult to diagnose *via* imaging examination and requires intraoperative and pathological examination for diagnosis; however, the patient refused treatment with methotrexate. Therefore, we adopted conservative surgical management.

Expectant management was occasionally applied in a case report in which the serum β-hCG level was 9.5 mIU/mL [23]. After a literature review, most of the case reports involved conservative surgical management, such as laparoscopic surgery[15], hysteroscopic surgery[24], and UAE [25]. Shen *et al*[26] reported that 10 of the 17 cases reported were successfully managed with laparoscopic surgery, indicating that laparoscopic surgery was more widely performed than other methods were for treating early intramural pregnancy; moreover, 8/12 cases reported were also treated with laparoscopic surgery. However, it is important to note that patients in mid- or late-term pregnancy should consider a cesarean section as their first option since they may experience excessive bleeding and their uterus may not be able to tolerate laparoscopic surgery. Auer-Schmidt *et al*[24] successfully managed intramural pregnancy with hysteroscopic surgery using a resectoscope loop to resect the sac through a visualized false tract. However, most of the time, hysteroscopy is used to examine the uterine cavity during laparoscopic surgery.

Once we perform conservative laparoscopic surgery, we should consider the situation of intraoperative bleeding and avoid emergency hysterectomy due to excessive bleeding during surgery. Clinical doctors evaluate intraoperative bleeding *via* examinations to determine the richness of blood flow signals, lesion size, and hCG values, similar to the treatment of caesarean scar pregnancy. Taking massive intraoperative bleeding into account, some researchers have implemented UAE[27] to help maintain fertility. UAE plays a vital role in decreasing bleeding and has been widely used in postpartum hemorrhage, symptomatic uterine fibroids, adenomyosis, and caesarean scar pregnancy. As UAE has become widely performed, concerns about complications have increased. Acute complications include fever, pain, nausea, vomiting, and lower limb vascular embolism. The long-term complications of UAE can include endometrial ischemic necrosis, uterine intrauterine adhesions, ovarian failure, and subsequent infertility[28]. Homer and Saridogan [29] reported that UAE is associated with an increased risk of miscarriage. Another report[30] revealed a decrease in fertility in patients who previously underwent UAE.

Compared with UAE, temporary occlusion of the uterine artery is a promising new approach that causes less postoperative pain[31] and fewer unfavorable pregnancy outcomes[32], reduces intraoperative bleeding without increasing the operative time[33] and does not influence the function of the ovary[34] since uterine artery occlusion is temporary. Li *et al*[35] managed intramural ectopic pregnancy with temporary aortic balloon occlusion *via* the femoral

Table 1 Summary of the findings reported in the studies identified by the literature search

	Ref.	Reproductive history	Previous uterine surgery	Other medical history	Location of pregnancy	Treatment	Intraoperative blood loss (mL)	Gestational age (week)
1	Guo *et al*[5], 2023	G3P2	No	Primary dysmenorrhea	Inside the myometrium below the right uterine horn	Hysteroscopy combined with laparoscopy, used pituitrin to help find the gestational sac	Approximately 10	-
2	Aouragh *et al*[6], 2024	G0P0	No	No	In the right side closely located to the cornua	Laparotomy	-	6
3	Kubo *et al*[7], 2024	G2P0	Two dilatation and curettage procedures	No	In the anterior muscular layer of the uterus	Total laparoscopic wedge resection using intraoperative ultrasonography	45	6
4	Truong *et al*[8], 2022	G2P1	Laparoscopic surgery for an ectopic pregnancy	No	In the myometrium layer close to the uterine fundus	Laparotomy, hysterectomy	Under 100	-
5	Xie *et al*[9], 2022	G1P0	Laparoscopic salpingotomy, laparoscopic bilateral salpingectomy for bilateral tubal pregnancy, hysteroscopy three times	Secondary infertility	In the left side of the anterior uterus	Laparoscopic surgery, with methotrexate injected into the myometrium	-	7
6	Hlinecká *et al*[10], 2022	G1P0	Cesarean section, hysteroscopic resection of retained products of conception	No	-	Laparoscopic artery occlusion and removal of pregnancy	-	7
7	Song *et al*[11], 2020	G6P2	Uterine curettage twice	No	In the posterior wall of the uterus	Diagnostic chemotherapy with (Etoposide+Methotrexate+Actinomycin D+cyclophosphamide), but false.	-	-
8	Nees *et al*[12], 2020	G1P0	Cesarean section	No	Near the left tubal os	Laparotomy with uterine wedge resection	-	-
9	Liu and Wu[13], 2020	G2P1	Ectopic pregnancy, IVF treatment and had 2 implantation failures in the first cycle of IVF.	No	In the right side of the posterior uterine	Exploratory laparoscopy, hysteroscopy and conservative surgical excision	100	7
10	Zhang *et al*[14], 2019	G1P1	Cesarean section	No	In the posterior wall below the left horn of the uterus	Laparoscopic surgery, with methotrexate injected into the myometrium	-	-
11	Vagg *et al*[15], 2018	G2P2	Open myomectomy	No	In the right uterine horn	A midline laparotomy, total abdominal hysterectomy, and bilateral salpingectomy	-	12
12	Mahmoud and Mahmoud[16], 2017	G8P7	Cesarean section	No	Anterior myometrium of the lower uterine segment, cesarean scar pregnancy	Exploratory laparotomy	-	8

artery during cesarean delivery, decreasing hemorrhage, preventing blood transfusion, and maintaining fertility. Preoperative endovascular balloon occlusion can successfully prevent heavy bleeding. However, serious complications may occur, such as thrombosis, arterial pseudoaneurysms, acute lower extremity ischemia, and arterial rupture[36]. There is currently no research published on the use of uterine artery occlusion with titanium clips in the treatment of intramural pregnancy. Titanium surgical clips were first used in combination with an injection of vasopressin by Shao *et al*[37] to decrease uterine vascularization during the surgical excision of cesarean scar ectopic pregnancies. After that, more cases involved temporary occlusion of the bilateral uterine arteries. In another case, researchers demonstrated that a

transvaginal laparoscopic procedure with temporary occlusion of the bilateral uterine arteries could terminate the cervical pregnancy[38]. Temporary occlusion of the uterine arteries is an effective strategy to avoid serious intraoperative bleeding from conditions such as uterine fibroids, uterine adenomyosis, tubal interstitial pregnancy, and cornual pregnancy. Shen *et al*[26] described 8 cases of intramural pregnancy treated with laparoscopic surgery or hysteroscopic surgery without preoperative intervention and reported that, in most cases, the intraoperative bleeding volume was greater than 100 mL, up to 400 mL. In our case, we temporarily occluded the bilateral uterine arteries during laparoscopic surgery to reduce intraoperative bleeding (intraoperative bleeding was approximately 20 mL) and successfully halt the progression of the pregnancy. Here, we recommend temporary occlusion of the uterine artery when the patient is at risk of excessive uterine bleeding during surgery.

Attention is needed here. Temporary occlusion of the uterine artery with titanium clips must be performed by experienced operators who are familiar with the anatomy of the pelvic organs and pelvic vessels. The operators should carefully expose the uterine artery, which is concealed and sometimes difficult to expose. By dissecting the internal iliac artery and locating the uterine artery originating from the internal iliac artery, operators can free and temporarily block the uterine artery. All operators should pay attention to the ureter and important pelvic vessels. In situations in which the uterine artery cannot be identified, causing occlusion to fail, uterine artery tears or heavy bleeding can occur, and temporarily occlusion of the internal iliac artery can be a remedial measure. There are several serious complications, including thromboembolism, lower organ ischemia and reperfusion injury, and aortic damage. The contraindications include dissecting aneurysms, substantial aortic meandering, and calcification.

Unfortunately, long-term follow-up, especially of fertility status, has not been performed in most investigations. This is also a limitation in our case. We recommend large case series studies to ascertain long-term outcomes.

Significant challenges are associated with managing intramural pregnancy. When selecting strategies for treatment, it is important to consider individual differences, particularly expectations for fertility and quality of life. Once patients with intramural pregnancy are managed, a thorough and unbiased evaluation of the benefits and drawbacks of each treatment option is essential.

CONCLUSION

We reported a case of intramural pregnancy approximately one month after medical abortion. We performed hysteroscopy and temporarily occluded the bilateral uterine arteries during laparoscopic surgery. The postoperative course was uneventful. We recommend temporary occlusion of the uterine arteries in patients at risk of excessive uterine bleeding during surgery.

ACKNOWLEDGEMENTS

We want to express our thanks to the patients, doctors, nurses, and other medical staff at Zhejiang Hospital for agreeing to participate in this study.

FOOTNOTES

Author contributions: Song YL helped collect data and images and wrote the manuscript; Wang CF helped review and edit the manuscript; all the authors helped revise the manuscript; all the authors read and approved the final manuscript.

Informed consent statement: All procedures involving human participants were performed in accordance with the ethical standards of the institutional research committee. The patient provided consent for the publication of this case report and accompanying images.

Conflict-of-interest statement: The authors declare that they have no conflicts of interest.

CARE Checklist (2016) statement: The authors have read the CARE Checklist (2016), and the manuscript was prepared and revised according to the CARE Checklist (2016).

Open Access: This article is an open-access article that was selected by an in-house editor and fully peer-reviewed by external reviewers. It is distributed in accordance with the Creative Commons Attribution NonCommercial (CC BY-NC 4.0) license, which permits others to distribute, remix, adapt, build upon this work non-commercially, and license their derivative works on different terms, provided the original work is properly cited and the use is non-commercial. See: https://creativecommons.org/Licenses/by-nc/4.0/

Country of origin: China

ORCID number: Yu-Liang Song 0009-0003-9249-692X; Chun-Feng Wang 0009-0007-1442-7047.

S-Editor: Lin C
L-Editor: A
P-Editor: Yu HG

REFERENCES

1 **Fadhlaoui A**, Khrouf M, Nouira K, Chaker A, Zhioua F. Ruptured intramural pregnancy with myometrial invasion treated conservatively. *Case Rep Obstet Gynecol* 2011; **2011**: 965910 [PMID: 22567521 DOI: 10.1155/2011/965910]

2 **Ko HS**, Lee Y, Lee HJ, Park IY, Chung DY, Kim SP, Park TC, Shin JC. Sonographic and MR findings in 2 cases of intramural pregnancy treated conservatively. *J Clin Ultrasound* 2006; **34**: 356-360 [PMID: 16869015 DOI: 10.1002/jcu.20245]

3 **Ginsburg KA**, Quereshi F, Thomas M, Snowman B. Intramural ectopic pregnancy implanting in adenomyosis. *Fertil Steril* 1989; **51**: 354-356 [PMID: 2912784 DOI: 10.1016/s0015-0282(16)60506-x]

4 **Chen X**, Gao L, Yu H, Liu M, Kong S, Li S. Intramural Ectopic Pregnancy: Clinical Characteristics, Risk Factors for Uterine Rupture and Hysterectomy. *Front Med (Lausanne)* 2021; **8**: 769627 [PMID: 34778327 DOI: 10.3389/fmed.2021.769627]

5 **Guo Y**, Feng T, Du X. A detective of intramural ectopic pregnancy: The use of pituitrin under hysteroscopy combined with laparoscopy. *Medicine (Baltimore)* 2023; **102**: e33379 [PMID: 36961158 DOI: 10.1097/MD.0000000000033379]

6 **Aouragh A**, Boukroute M, Aloua YE, Regragui A, Bellajdel I, Taheri H, Saadi H, Mimouni A. Intramural pregnancy at 6 and 8 weeks gestation with no predisposing factors: As two uncommon case reports. *Radiol Case Rep* 2024; **19**: 2390-2394 [PMID: 38572273 DOI: 10.1016/j.radcr.2024.02.092]

7 **Kubo K**, Fujikawa A, Mitoma T, Mishima S, Ohira A, Kirino S, Maki J, Eto E, Masuyama H. Total laparoscopic wedge resection for an intramural ectopic pregnancy using an intraoperative ultrasound system: A case report. *Asian J Endosc Surg* 2024; **17**: e13303 [PMID: 38488404 DOI: 10.1111/ases.13303]

8 **Truong DP**, Pham TH, Nguyen PN, Ho QN. Misdiagnosis of intramural ectopic pregnancy and invasive gestational trophoblastic disease on ultrasound: A challenging case at Tu Du Hospital in Vietnam in COVID-19 pandemic peak and mini-review of literature. *Radiol Case Rep* 2022; **17**: 4821-4827 [PMID: 36238215 DOI: 10.1016/j.radcr.2022.09.034]

9 **Xie QJ**, Li X, Ni DY, Ji H, Zhao C, Ling XF. Intramural pregnancy after in vitro fertilization and embryo transfer: A case report. *World J Clin Cases* 2022; **10**: 2871-2877 [PMID: 35434105 DOI: 10.12998/wjcc.v10.i9.2871]

10 **Hlinecká Kristýna**, Lisá Zdeňka, Richtárová Adéla, Kužel David. Intramyometrial pregnancy after hysteroscopic resection of retained products of conception - a case report. *Ceska Gynekol* 2022; **87**: 35-39 [PMID: 35240834 DOI: 10.48095/cccg202235]

11 **Song QY**, Yang F, Luo H. A Case of Intramural Pregnancy: Differential Diagnosis for Distinguishing from Retained Products of Conception and Gestational Trophoblastic Disease. *Gynecol Minim Invasive Ther* 2020; **9**: 231-233 [PMID: 33312868 DOI: 10.4103/GMIT.GMIT_39_19]

12 **Nees J**, Faigle-Krehl G, Brucker J, Leucht D, Platzer LK, Flechtenmacher C, Sohn C, Wallwiener M. Intramural pregnancy: A case report. *Case Rep Womens Health* 2020; **27**: e00215 [PMID: 32695612 DOI: 10.1016/j.crwh.2020.e00215]

13 **Liu Y**, Wu Y. Intramyometrial pregnancy after cryopreserved embryo transfer: a case report. *BMC Pregnancy Childbirth* 2020; **20**: 90 [PMID: 32041575 DOI: 10.1186/s12884-020-2784-7]

14 **Zhang Q**, Xing X, Liu S, Xie X, Liu X, Qian F, Liu Y. Intramural ectopic pregnancy following pelvic adhesion: case report and literature review. *Arch Gynecol Obstet* 2019; **300**: 1507-1520 [PMID: 31729562 DOI: 10.1007/s00404-019-05379-3]

15 **Vagg D**, Arsala L, Kathurusinghe S, Ang WC. Intramural Ectopic Pregnancy Following Myomectomy. *J Investig Med High Impact Case Rep* 2018; **6**: 2324709618790605 [PMID: 30046624 DOI: 10.1177/2324709618790605]

16 **Mahmoud OA**, Mahmoud MZ. A rare case of ectopic pregnancy in a caesarean section scar: a case report. *BJR Case Rep* 2017; **3**: 20170010 [PMID: 30363216 DOI: 10.1259/bjrcr.20170010]

17 **Ntafam CN**, Sanusi-Musa I, Harris RD. Intramural ectopic pregnancy: An individual patient data systematic review. *Eur J Obstet Gynecol Reprod Biol X* 2024; **21**: 100272 [PMID: 38269031 DOI: 10.1016/j.eurox.2023.100272]

18 **Ong C**, Su LL, Chia D, Choolani M, Biswas A. Sonographic diagnosis and successful medical management of an intramural ectopic pregnancy. *J Clin Ultrasound* 2010; **38**: 320-324 [PMID: 20544869 DOI: 10.1002/jcu.20703]

19 **Peng Y**, Dai Y, Yu G, Jin P. High-intensity focused ultrasound ablation combined with systemic methotrexate treatment of intramural ectopic pregnancy: A case report. *Medicine (Baltimore)* 2022; **101**: e31615 [PMID: 36401379 DOI: 10.1097/MD.0000000000031615]

20 **Katano K**, Ikuta K, Matsubara H, Oya N, Nishio M, Suzumori K. A case of successful conservative chemotherapy for intramural pregnancy. *Fertil Steril* 1999; **72**: 744-746 [PMID: 10521123 DOI: 10.1016/s0015-0282(99)00330-1]

21 **Memtsa M**, Jamil A, Sebire N, Jauniaux E, Jurkovic D. Diagnosis and management of intramural ectopic pregnancy. *Ultrasound Obstet Gynecol* 2013; **42**: 359-362 [PMID: 23417903 DOI: 10.1002/uog.12437]

22 **Hafner T**, Aslam N, Ross JA, Zosmer N, Jurkovic D. The effectiveness of non-surgical management of early interstitial pregnancy: a report of ten cases and review of the literature. *Ultrasound Obstet Gynecol* 1999; **13**: 131-136 [PMID: 10079493 DOI: 10.1046/j.1469-0705.1999.13020131.x]

23 **Bernstein HB**, Thrall MM, Clark WB. Expectant management of intramural ectopic pregnancy. *Obstet Gynecol* 2001; **97**: 826-827 [PMID: 11336768 DOI: 10.1016/s0029-7844(01)01126-7]

24 **Auer-Schmidt MM**, Rahimi G, Wahba AH, Schmidt T. Hysteroscopic management of intramural ectopic pregnancy. *BMJ Case Rep* 2021; **14** [PMID: 34728506 DOI: 10.1136/bcr-2021-244514]

25 **Wang S**, Dong Y, Meng X. Intramural ectopic pregnancy: treatment using uterine artery embolization. *J Minim Invasive Gynecol* 2013; **20**: 241-243 [PMID: 23465260 DOI: 10.1016/j.jmig.2012.10.005]

26 **Shen Z**, Liu C, Zhao L, Xu L, Peng B, Chen Z, Li X, Zhou J. Minimally-invasive management of intramural ectopic pregnancy: an eight-case series and literature review. *Eur J Obstet Gynecol Reprod Biol* 2020; **253**: 180-186 [PMID: 32871441 DOI: 10.1016/j.ejogrb.2020.08.021]

27 **Niu X**, Tang Y, Li S, Ni S, Zheng W, Huang L. The feasibility of laparoscopically assisted, hysteroscopic removal of interstitial pregnancies: A case series. *J Obstet Gynaecol Res* 2021; **47**: 3447-3455 [PMID: 34227727 DOI: 10.1111/jog.14924]

28 **Qi F**, Zhou W, Wang MF, Chai ZY, Zheng LZ. Uterine artery embolization with and without local methotrexate infusion for the treatment of cesarean scar pregnancy. *Taiwan J Obstet Gynecol* 2015; **54**: 376-380 [PMID: 26384053 DOI: 10.1016/j.tjog.2015.01.003]

29 **Homer H**, Saridogan E. Uterine artery embolization for fibroids is associated with an increased risk of miscarriage. *Fertil Steril* 2010; **94**: 324-330 [PMID: 19361799 DOI: 10.1016/j.fertnstert.2009.02.069]

30 **Serres-Cousine O**, Kuijper FM, Curis E, Atashroo D. Clinical investigation of fertility after uterine artery embolization. *Am J Obstet Gynecol* 2021; **225**: 403.e1-403.e22 [PMID: 34058169 DOI: 10.1016/j.ajog.2021.05.033]

31 **Hald K**, Langebrekke A, Kløw NE, Noreng HJ, Berge AB, Istre O. Laparoscopic occlusion of uterine vessels for the treatment of symptomatic fibroids: Initial experience and comparison to uterine artery embolization. *Am J Obstet Gynecol* 2004; **190**: 37-43 [PMID: 14749632 DOI:

10.1016/s0002-9378(03)00910-4]

32 **Holub Z**, Mara M, Kuzel D, Jabor A, Maskova J, Eim J. Pregnancy outcomes after uterine artery occlusion: prospective multicentric study. *Fertil Steril* 2008; **90**: 1886-1891 [PMID: 18155701 DOI: 10.1016/j.fertnstert.2007.08.033]

33 **Istre O**. Uterine artery occlusion for the treatment of symptomatic fibroids: endoscopic, radiological and vaginal approach. *Minim Invasive Ther Allied Technol* 2005; **14**: 167-174 [PMID: 16754159 DOI: 10.1080/13645700510033976]

34 **Liu L**, Li Y, Xu H, Chen Y, Zhang G, Liang Z. Laparoscopic transient uterine artery occlusion and myomectomy for symptomatic uterine myoma. *Fertil Steril* 2011; **95**: 254-258 [PMID: 21168582 DOI: 10.1016/j.fertnstert.2010.05.006]

35 **Li S**, Liu H, Li X, Liu Z, Li Y, Li N. Transfemoral temporary aortic balloon occlusion in surgical treatment of second trimester intramural ectopic pregnancy. *J Obstet Gynaecol Res* 2016; **42**: 716-718 [PMID: 26989891 DOI: 10.1111/jog.12968]

36 **Xu W**, Liu Z, Ren Q, Dai C, Wang B, Peng Y, Gao L. Treatment of infected placenta accreta in the uterine horn by transabdominal temporary occlusion of internal iliac arteries: A case report and literature review. *Medicine (Baltimore)* 2023; **102**: e34525 [PMID: 37565879 DOI: 10.1097/MD.0000000000034525]

37 **Shao MJ**, Hu MX, Hu M. Temporary bilateral uterine artery occlusion combined with vasopressin in control of hemorrhage during laparoscopic management of cesarean scar pregnancies. *J Minim Invasive Gynecol* 2013; **20**: 205-208 [PMID: 23403088 DOI: 10.1016/j.jmig.2012.10.018]

38 **Jin L**, Ji L, Shao M, Hu M. Laparoscopic temporary bilateral uterine artery occlusion - a successful pregnancy outcome of heterotopic intrauterine and cervical pregnancy. *J Obstet Gynaecol* 2021; **41**: 668-670 [PMID: 32314618 DOI: 10.1080/01443615.2020.1733949]

World Journal of Clinical Cases

Submit a Manuscript: https://www.f6publishing.com

World J Clin Cases 2025 June 26; 13(18): 101471

DOI: 10.12998/wjcc.v13.i18.101471

ISSN 2307-8960 (online)

CASE REPORT

Luscan-Lumish syndrome: A case report

Bogumiła Wójcik-Niklewska, Erita Filipek

Specialty type: Medicine, research and experimental

Provenance and peer review: Unsolicited article; Externally peer reviewed.

Peer-review model: Single blind

Peer-review report's classification

Scientific Quality: Grade D

Novelty: Grade C

Creativity or Innovation: Grade C

Scientific Significance: Grade B

P-Reviewer: Wang X

Received: September 15, 2024

Revised: January 25, 2025

Accepted: February 18, 2025

Published online: June 26, 2025

Processing time: 164 Days and 21.3 Hours

Bogumiła Wójcik-Niklewska, Erita Filipek, Department of Pediatric Ophtalmology, Faculty of Medical Sciences in Katowice, Medical University of Silesia in Katowice, Katowice 40-514, Silesia, Poland

Bogumiła Wójcik-Niklewska, Kornel Gibiński University Clinical Centre, Medical University of Silesia in Katowice, Katowice 40-514, Silesia, Poland

Corresponding author: Bogumiła Wójcik-Niklewska, MD, PhD, Doctor, Department of Pediatric Ophtalmology, Faculty of Medical Sciences in Katowice, Medical University of Silesia in Katowice, Ceglana 35, Katowice 40-514, Silesia, Poland.
bogumila_wojcik_niklewska@op.pl

Abstract

BACKGROUND

Luscan-Lumish syndrome (LLS) is a rare genetic congenital anomaly syndrome characterised by neurodevelopmental disorders, including delayed psychomotor development, behavioral difficulties, relative or true macrocephaly and, in individual cases, ocular abnormalities. This paper aims to present the case of a child with ocular abnormalities associated with LLS.

CASE SUMMARY

A 10-year-old girl born at 40 weeks gestation with features of dysmorphia, neurodevelopmental disorders, genetically confirmed LLS, convergent strabismus and suspected congenital glaucoma. Eye examination, ultrasound, optical coherence tomography (OCT), perimetry and electrophysiological study [pattern visually evoked potentials (VEP)] were performed. Best-corrected distance visual acuity was 0.5 in the right eye (correction -1.0 Dsph, -1.0 Dcyl, axis 180°) and 0.62 in the left eye (correction -2.0 Dsph). Near visual acuity (Snellen Chart) with the above correction was -0.5 D. A cycloplegic refraction test yielded -1.25 Dsph, -1.25 Dcyl, axis 165° in the right eye, and -2.0 Dsph, -0.25 Dcyl, axis 154° in the left eye. Intraocular pressure was 15 mmHg in both eyes. OCT of the maculae showed no abnormalities. In both eyes, the average ganglion cell layer and inner plexiform layer thickness was 73 μm. OCT of the optic nerve disc showed an average retinal nerve fibre layer thickness of 89 μm in the right eye and 81 μm in the left eye, with symmetry of 90%. The rim area was 1.59 mm^2 and 1.74 mm^2 in the right and left eye, respectively. The disc area was 2.77 mm^2 in the right eye and 2.89 mm^2 in the left. The average cup-to-disc ratio was 0.64 in the right eye and 0.62 in the left eye. Ocular ultrasound depicted single extra echoes inside the vitreous chamber; otherwise, there were no abnormalities. Right and left eyeball lengths were 24.59 mm and 24.51 mm, respectively. Kinetic perimetry revealed no visual field

defects, while static testing showed single relative scotomas. The mean defect was 4.7 dB in the right and 2.6 dB in the left eye. The loss variance values were 4.8 and 3.8 dB for the right and left eye, respectively. Pattern VEP test revealed normal values of P100 Latency. Wave amplitude in the right eye was 50% at a visual angle of 1.0° and 30% at 15'. Due to the rarity of LLS, it seems interesting to present the child ophthalmological examination with changes in the electrophysiological examination.

CONCLUSION

Although eye abnormalities are infrequently described in children with LLS, the patients should undergo eye examinations, especially as they may have central nervous system anomalies that may give rise to visual impairments. Generally, children with genetically determined congenital syndromes should receive regular ophthalmic check-ups for a thorough evaluation of the eyes and prognosis of the development of visual function.

Key Words: Luscan-Lumish syndrome; *SETD2*; Children; Ophthalmology; Case report

©The Author(s) 2025. Published by Baishideng Publishing Group Inc. All rights reserved.

Core Tip: Children with Luscan-Lumish syndrome (LLS) have ocular pathologies, which include strabismus, astigmatism, visual impairment associated with optic nerve hypoplasia or abnormalities in the visual cortex. Retinal vascular telangiectasias, glaucoma or cataracts are also described. This paper aims to present the case of a child with ocular abnormalities associated with LLS.

Citation: Wójcik-Niklewska B, Filipek E. Luscan-Lumish syndrome: A case report. *World J Clin Cases* 2025; 13(18): 101471
URL: https://www.wjgnet.com/2307-8960/full/v13/i18/101471.htm
DOI: https://dx.doi.org/10.12998/wjcc.v13.i18.101471

INTRODUCTION

Luscan-Lumish syndrome (LLS) is a rare, genetically determined congenital syndrome caused by various pathogenic variants in the *SETD2* gene[1-3]. It is characterised by neurodevelopmental disorders featuring delayed psychomotor development, behavioural disorders, primarily autism spectrum disorders, and relative or true macrocephaly. Some children develop tonic-clonic epileptic seizures with onset between 3 and 10 years of age. Brain imaging studies may reveal type I Chiari and/or Dandy-Walker malformations, dilatation of the brain ventricles, and absence or hypoplasia of the corpus callosum. Speech delay is a characteristic feature. Other less common disorders include excessive height and weight[1-3]. Endocrine disorders leading to precocious puberty, hypothyroidism and growth hormone deficiency may also occur. Hearing loss is often found on audiological examination[4]. Children with LLS also suffer from frequent respiratory tract infections, ear infections and sinus infections, but no specific immune disorders have been described. In addition, sleep apnoea, gastrooesophageal reflux, constipation, heart defects, scoliosis and joint hypermobility have been observed[5]. In individual cases, ocular pathologies, which include strabismus, astigmatism, visual impairment associated with optic nerve hypoplasia or abnormalities in the visual cortex are observed. Retinal vascular telangiectasias, glaucoma or cataracts are also described.

This paper aims to present the case of a girl with ocular abnormalities associated with LLS.

CASE PRESENTATION

Chief complaints

A ten-year-old girl diagnosed with LLS was admitted for an eye examination to the Department of Paediatric Ophthalmology, Professor K. Gibiński University Hospital Center, Medical University of Silesia, Katowice, Poland.

History of present illness

The girl remains under the care of a speech therapist due to slurred speech, a psychologist due to autism spectrum disorder and intellectual disability and an ENT specialist due to a slight hearing loss.

History of past illness

Sucking abnormalities were observed in infancy, resulting in poor weight gain up to 4 years of age. Incidents of sleep apnoea and morning hypoglycaemia occurred. Psychomotor retardation was noted in the first year of life. Due to hypotonia, the child required rehabilitation from 4 months of age. She spoke her first words at three years of age and simple sentences at six years of age; autism was diagnosed at that time. Social and intellectual development was delayed. Head magnetic resonance imaging (MRI) performed at six months of age revealed hypoplasia of the corpus callosum.

Encephalography revealed abnormalities resembling epileptic seizures despite the absence of seizure episodes. At four years of age, the child presented for genetic consult for the first time. Physical examination revealed hypertelorism, a prominent forehead with a high frontal hairline, a broad nasal bridge, a short philtrum, a pointed chin, a narrow mouth, low-set ears, broad distal phalanges of the fingers of both hands and hypertrophy of the elbow joints. A wide-based gait and slurred speech were also observed. At four years of age, the child measured 101 cm (10th percentile) and weighed 13.3 kg (below the 3rd percentile). Consultation with specialists did not reveal any heart defects, digestive system or endocrine disorders.

Personal and family history

The patient is the first child of young, healthy, and unrelated parents. The family history was noncontributory. The girl was born at 40 weeks gestation, with a weight of 2820 g, a length of 52 cm and an occipital frontal circumference of 34 cm.

Physical examination

On the day of admission to the Department of Paediatric Ophthalmology, the child was in good general conditio. Physical examination revealed features of facial dysmorphia with hypertelorism. The girl spoke indistinctly and was reluctant to answer questions (Figure 1).

Eye examination revealed convergent strabismus of 11°, simultaneous perception without fusion and stereopsis, and normal pupillary response to light. The best-corrected distance visual acuity was 0.5 in the right eye (correction -1.0 Dsph, -1.0 Dcyl, axis 180°) and 0.62 in the left eye (correction -2.0 Dsph). Near visual acuity (Snellen Chart) with the above correction was -0.5 D. A cycloplegic refraction test yielded -1.25 Dsph, -1.25 Dcyl, axis 165° in the right eye, and -2.0 Dsph, -0.25 Dcyl, axis 154° in the left eye. Slit-lamp examination revealed no abnormalities in the anterior segments. The fundus showed pink optic nerve discs with clear borders and a cup-to-disc ratio of 0.6. Pink maculae with reflexes were observed; no vascular abnormalities were found.

Laboratory examinations

Before hospitalisation in the Paediatric Ophthalmology Unit, the child underwent genetic testing of DNA isolated from peripheral blood. Whole exome sequencing using the SureSelectXT Human All Exon V5 Kit was applied, yielding the following results: Transcript at the cDNA level: C.4860dupA; transcript at the protein level: P.Gly1621ArgfsTer12. *SETD2* gene; reference sequence: LRG_775t1; NM_014159.6; chromosomal position: Hg38 3: 047103402-C > CT.

Frequency in the genome aggregation database (gnomAD): 0. Heterozygous system. Genotype notation according to HGVS: LRG_775t1: c.[4860dupA]; [4860 =]. The selected variant was analysed using ADS in the patient, her parents, and two brothers. The presence of a pathogenic variant in *SETD2* was ruled out in both parents and brothers.

Imaging examinations

The patient's intraocular pressure was 15 mmHg in both eyes. Optical coherence tomography (OCT) of the anterior segment revealed the following findings: A corneal thickness of 506 µm in the right eye and 510 µm in the left eye; an anterior chamber depth of 3.05 mm in the right eye and 3.09 mm in the left eye; and a lens thickness of 3.73 mm in both eyes. No macula abnormalities were found. The average GCL-IPL thickness was 73 µm in both eyes. OCT of the optic nerve disc revealed an average retinal nerve fibre layer thickness of 89 µm in the right eye and 81 µm in the left eye, with symmetry of 90%. The rim area was 1.59 mm^2 and 1.74 mm^2 in the right and left eyes, respectively. The disc area was 2.77 mm^2 in the right eye and 2.89 mm^2 in the left eye. The average cup-to-disc ratio was 0.64 in the right eye and 0.62 in the left eye.

Ocular ultrasound revealed single extra echoes inside the vitreous chamber; otherwise, there were no abnormalities. The right and left eyeball lengths were 24.59 mm and 24.51 mm, respectively. Kinetic perimetry revealed no visual field defects, whereas static testing revealed single relative scotomas. The mean defect was 4.7 dB in the right and 2.6 dB in the left eye. The loss variance values were 4.8 and 3.8 dB for the right and left eyes, respectively. The pattern VEP test revealed normal P100 Latency values. The wave amplitude for the right eye was 50% at a visual angle of 1.0 deg and 30% at 15 min. An abnormal shape of the VEP response, *i.e.*, an extended P100 wave peak, may suggest optic nerve atrophy/underdevelopment or central nervous system abnormalities.

FINAL DIAGNOSIS

The final diagnosis was LLS with an abnormal shape of VEP response.

TREATMENT

No treatment was performed.



Figure 1 Child with Luscan-Lumish syndrome.

OUTCOME AND FOLLOW-UP

Follow-up visits have been scheduled.

DISCUSSION

LLS is a rare, genetically determined congenital syndrome with a variable phenotype. Eye disorders have also been described in patients with LLS. Our patient was found to have speech disorders characteristic of the syndrome, autism, intellectual disability, dysmorphia, hearing loss, ossification disorders and hypoplasia of the corpus callosum on magnetic resonance imaging. Due to problems with distance vision, the child was referred to the Paediatric Ophthalmology Department for a complete ophthalmic examination, which revealed convergent strabismus, myopia in both eyes, astigmatism in the right eye, lack of fusion and stereopsis, reduced levels of the retinal ganglion cell complex, changes in OCT of the optic disc, and an abnormal pattern VEP recording suggesting optic nerve underdevelopment or central nervous system anomalies, possibly related to hypoplasia of the corpus callosum. Fundus images did not show any vascular pathology. The child was prescribed corrective glasses and vision rehabilitation, and a follow-up appointment was scheduled.

Since LLS is a rare condition, ocular abnormalities are sporadically described, especially in paediatric patients.

Van Rij *et al*[2] described two patients with LLS: A 4.5-year-old boy had mild ptosis, whereas a 23-year-old female patient had slightly downslanted palpebral fissures and clear blue eyes. The ophthalmic evaluation was unremarkable in both patients. Wu *et al*[6] identified a novel pathogenic *SETD2* variant in a 3-year-old Chinese boy but reported no eye disorders. Rabin *et al*[7] described 15 children with de novo variants in codon 1740 of *SETD2*. One child had normal eye images at two weeks of life; a repeat examination at 16 months of age revealed leukocoria, exudative detachment and telangiectasia around the periphery of the retina in the right eye, and blood vessels stop and star exudate in the macula of the left eye. Despite the use of a prophylactic laser, retinal detachment was found involving the upper quadrants.

Lumish *et al*[8] reported case of a 17-year-old girl with a de novo c.2028delT (P677 LfsX19) mutation in the SET domain-containing protein 2 (SET Domain Containing 2, Histone Lysine Methyltransferase) *SETD2* gene. She presented with intellectual disabilities and autism spectrum disorder, did not walk until 18 months of age and began speaking at two years of age. Head MRI revealed Arnold-Chiari type I malformation and mild to moderate hydrocephalus of the third and lateral ventricles. However, the authors did not report any eye changes[8]. Suda *et al*[3] also did not mention ocular abnormalities, describing the case of a 20-year-old male with access to the results of an eye examination performed when he was 11 years old.

CONCLUSION

Although eye abnormalities are infrequently described in children with LLS, patients should undergo eye examinations, especially as they may have central nervous system anomalies that may give rise to visual impairments. Generally, children with genetically determined congenital syndromes should receive regular ophthalmic check-ups for a thorough evaluation of the eyes and prognosis of the development of visual function.

FOOTNOTES

Author contributions: Wójcik-Niklewska B was responsible for examination, data collection, text writing; Filipek E was responsible for supervision.

Informed consent statement: Written informed consent has been obtained from parents to publish this paper.

Conflict-of-interest statement: The authors declare no conflict of interest.

CARE Checklist (2016) statement: The authors have read the CARE Checklist (2016), and the manuscript was prepared and revised according to the CARE Checklist (2016).

Open Access: This article is an open-access article that was selected by an in-house editor and fully peer-reviewed by external reviewers. It is distributed in accordance with the Creative Commons Attribution NonCommercial (CC BY-NC 4.0) license, which permits others to distribute, remix, adapt, build upon this work non-commercially, and license their derivative works on different terms, provided the original work is properly cited and the use is non-commercial. See: https://creativecommons.org/Licenses/by-nc/4.0/

Country of origin: Poland

ORCID number: Bogumiła Wójcik-Niklewska 0000-0002-6753-2904; Erita Filipek 0000-0002-4227-1349.

S-Editor: Lin C
L-Editor: A
P-Editor: Zhang L

REFERENCES

1 **Luscan A**, Laurendeau I, Malan V, Francannet C, Odent S, Giuliano F, Lacombe D, Touraine R, Vidaud M, Pasmant E, Cormier-Daire V. Mutations in SETD2 cause a novel overgrowth condition. *J Med Genet* 2014; **51**: 512-517 [PMID: 24852293 DOI: 10.1136/jmedgenet-2014-102402]

2 **van Rij MC**, Hollink IHIM, Terhal PA, Kant SG, Ruivenkamp C, van Haeringen A, Kievit JA, van Belzen MJ. Two novel cases expanding the phenotype of SETD2-related overgrowth syndrome. *Am J Med Genet A* 2018; **176**: 1212-1215 [PMID: 29681085 DOI: 10.1002/ajmg.a.38666]

3 **Suda K**, Fukuoka H, Iguchi G, Kanie K, Fujita Y, Odake Y, Matsumoto R, Bando H, Ito H, Takahashi M, Chihara K, Nagai H, Narumi S, Hasegawa T, Ogawa W, Takahashi Y. A Case of Luscan-Lumish Syndrome: Possible Involvement of Enhanced GH Signaling. *J Clin Endocrinol Metab* 2021; **106**: 718-723 [PMID: 33248444 DOI: 10.1210/clinem/dgaa893]

4 **Zhang Y**, Zhang H, Wu W, Wang D, Lv Y, Zhao D, Wang L, Liu Y, Zhang K. Clinical and genetic features of luscan-lumish syndrome associated with a novel de novo variant of SETD2 gene: Case report and literature review. *Front Genet* 2023; **14**: 1081391 [PMID: 36777730 DOI: 10.3389/fgene.2023.1081391]

5 **Pappas J**, Rabin R. SETD2 Neurodevelopmental Disorders. 2021 Dec 30. In: GeneReviews® [Internet]. Seattle (WA): University of Washington, Seattle; 1993– [PMID: 34978780]

6 **Wu Y**, Liu F, Wan R, Jiao B. A novel SETD2 variant causing global development delay without overgrowth in a Chinese 3-year-old boy. *Front Genet* 2023; **14**: 1153284 [PMID: 37025455 DOI: 10.3389/fgene.2023.1153284]

7 **Rabin R**, Radmanesh A, Glass IA, Dobyns WB, Aldinger KA, Shieh JT, Romoser S, Bombei H, Dowsett L, Trapane P, Bernat JA, Baker J, Mendelsohn NJ, Popp B, Siekmeyer M, Sorge I, Sansbury FH, Watts P, Foulds NC, Burton J, Hoganson G, Hurst JA, Menzies L, Osio D, Kerecuk L, Cobben JM, Jizi K, Jacquemont S, Bélanger SA, Löhner K, Veenstra-Knol HE, Lemmink HH, Keller-Ramey J, Wentzensen IM, Punj S, McWalter K, Lenberg J, Ellsworth KA, Radtke K, Akbarian S, Pappas J. Genotype-phenotype correlation at codon 1740 of SETD2. *Am J Med Genet A* 2020; **182**: 2037-2048 [PMID: 32710489 DOI: 10.1002/ajmg.a.61724]

8 **Lumish HS**, Wynn J, Devinsky O, Chung WK. Brief Report: SETD2 Mutation in a Child with Autism, Intellectual Disabilities and Epilepsy. *J Autism Dev Disord* 2015; **45**: 3764-3770 [PMID: 26084711 DOI: 10.1007/s10803-015-2484-8]

World Journal of Clinical Cases

Submit a Manuscript: https://www.f6publishing.com

World J Clin Cases 2025 June 26; 13(18): 101545

DOI: 10.12998/wjcc.v13.i18.101545

ISSN 2307-8960 (online)

CASE REPORT

Improved superelastic Ni–Ti alloy wire for treating skeletal class III malocclusion combined with anterior crossbite: A case report

Yu-Hsiang Sean Chang, Yuan-Hou Chen, Jian-Hong Yu

Specialty type: Medicine, research and experimental

Provenance and peer review: Unsolicited article; Externally peer reviewed.

Peer-review model: Single blind

Peer-review report's classification

Scientific Quality: Grade B, Grade B, Grade D, Grade D

Novelty: Grade B, Grade B, Grade C, Grade C

Creativity or Innovation: Grade B, Grade B, Grade C, Grade C

Scientific Significance: Grade B, Grade C, Grade C, Grade D

P-Reviewer: Nagamine T; Nguyen VA

Received: September 18, 2024

Revised: January 23, 2025

Accepted: February 17, 2025

Published online: June 26, 2025

Processing time: 161 Days and 17.9 Hours

Yu-Hsiang Sean Chang, Yuan-Hou Chen, Jian-Hong Yu, Department of Orthodontics, China Medical University Hospital, Taichung 404022, Taiwan

Jian-Hong Yu, School of Dentistry, China Medical University, Taichung 40402, Taiwan

Corresponding author: Jian-Hong Yu, Doctor, PhD, Dean, School of Dentistry, China Medical University, No. 91 Xueshi Road, North District, Taichung 404022, Taiwan.
kenkoyu@mail.cmu.edu.tw

Abstract

BACKGROUND

Correcting skeletal class III malocclusion with anterior crossbite in adolescents using only orthodontic treatment poses challenges. This report highlights a novel approach leveraging improved superelastic Ni–Ti alloy wire (ISW) to address these conditions effectively.

CASE SUMMARY

A 17-year-old male patient presented with the chief complaint of an underbite. The patient was given a diagnosis of skeletal class III malocclusion and anterior crossbite. The orthodontic treatment plan was implemented and did not require teeth extractions or orthognathic surgery. Key interventions involved the application of ISW, intermaxillary elastics, and ISW unilateral multi-bend edgewise archwire. The unique combination of these techniques enabled the correction without the need for extractions or surgery. This approach leverages the advanced biomechanical properties of ISW, including its super-elasticity and shape memory, to enhance treatment efficacy. The treatment lasted 17 months, and major improvements in overjet, overbite, and alignment were achieved. The results were favorable, and stability was discovered during follow-up.

CONCLUSION

The application of ISW for treating skeletal class III malocclusion with anterior crossbite in a 17-year-old male patient resulted in exceptional outcomes. The treatment led to a marked improvement in the patient's facial profile and to proper overjet, overbite, and midline alignment. These results were maintained over a one-year follow-up, indicating that a minimally invasive orthodontic approach can effectively address complex skeletal discrepancies in adolescent patients. This case illustrates that with the careful use of advanced orthodontic techniques, major skeletal challenges can be resolved without resorting to surgical procedures.

Key Words: Orthodontics; Skeletal class III malocclusion; Anterior crossbite; Improved superelastic Ni–Ti alloy wire; Multi-bend edgewise archwire; Intermaxillary elastics; Case report

©The Author(s) 2025. Published by Baishideng Publishing Group Inc. All rights reserved.

Core Tip: Correcting skeletal class III malocclusion with anterior crossbite in adolescents can be challenging. In this case, a 17-year-old male with an underbite was successfully treated using improved superelastic Ni–Ti alloy wire (ISW), intermaxillary elastics, and ISW unilateral multi-bend edgewise archwire. These techniques corrected the anterior crossbite, aligned the midline, and achieved proper overjet and overbite. The treatment lasted approximately one year and five months, with a stable outcome observed after one year of follow-up. This case demonstrates that skeletal Class III malocclusion in adolescents can be addressed effectively with minimally invasive orthodontic methods.

Citation: Chang YHS, Chen YH, Yu JH. Improved superelastic Ni–Ti alloy wire for treating skeletal class III malocclusion combined with anterior crossbite: A case report. *World J Clin Cases* 2025; 13(18): 101545
URL: https://www.wjgnet.com/2307-8960/full/v13/i18/101545.htm
DOI: https://dx.doi.org/10.12998/wjcc.v13.i18.101545

INTRODUCTION

Skeletal class III malocclusion, often characterized by a forward-positioned lower jaw leading to an anterior crossbite, presents a major challenge in orthodontic treatment, particularly in adolescent patients. The traditional approaches frequently involve teeth extractions or orthognathic surgery to correct these skeletal discrepancies. Invasive procedures carry risks and have long recovery periods, making them unappealing for some patients and their families.

Less invasive treatments have been developed. For example, aligner-based treatments, intermaxillary elastics (IME) combined with skeletal anchorage, and improved superelastic Ni–Ti alloy wire (ISW) treatments are effective and less invasive alternatives to traditional treatments for skeletal class III malocclusion[1-3]. Biomechanical innovations such as ISW have further enhanced the potential of non-surgical methods by achieving efficient tooth movement with minimal patient discomfort[4]. This report illustrates the successful management of a 17-year-old male adolescent with skeletal class III malocclusion and anterior crossbite, managed without teeth extraction or surgery. The strategic use of ISW, along with IME and a unilateral multi-bend edgewise archwire (ISW MEAW), resulted in substantial improvements in occlusion, facial profile, and dental alignment, highlighting the potential of minimally invasive techniques in addressing complex malocclusions.

CASE PRESENTATION

Chief complaints

A 17-year-old male patient sought orthodontic treatment at our clinic with the chief complaint of an underbite, he also expressed concerns about his dental alignment and overall facial profile. The patient had no notable medical issues or temporomandibular joint symptoms at the time of his visit.

History of present illness

The patient reported no current medical conditions or symptoms at the time of evaluation.

History of past illness

The patient had no significant medical history, nor had undergone any previous orthodontic treatments.

Personal and family history

The patient's family history was unremarkable for any dental or orthodontic conditions.

Physical examination

Initial facial photographs showed a prominent chin without any noticeable deviation when viewed from the front. The maxillary midline was shifted 1.0 mm from the facial midline, while the mandibular midline displayed a slight deviation toward the left side (Figure 1). Intraoral images revealed an anterior crossbite extending from the right lateral incisor to the left canine, alongside a bilateral class III molar relationship. Mild anterior crowding was also observed in both the upper and lower arches (Figure 2).



Figure 1 Pretreatment facial photographs showing a slightly concave profile.



Figure 2 Intraoral photographs illustrating an angle class III malocclusion.

Laboratory examinations

The analysis indicated a skeletal class III discrepancy, characterized by an ANB angle of ≤ 0° and a bilateral class III molar relationship with mesially positioned lower molars relative to the upper molars. No notable facial asymmetry was detected, and other clinical parameters were within normal ranges.

Imaging examinations

Panoramic X-rays confirmed the presence of all teeth, including the third molars in both jaws. Lateral cephalometric analysis (conducted using Romexis 3.2.0, Helsinki, Finland) demonstrated skeletal class III malocclusion with an ANB angle of –2.0°, a mandibular plane angle of 30.0°, and retroclination of the lower incisors at 88.5° relative to the

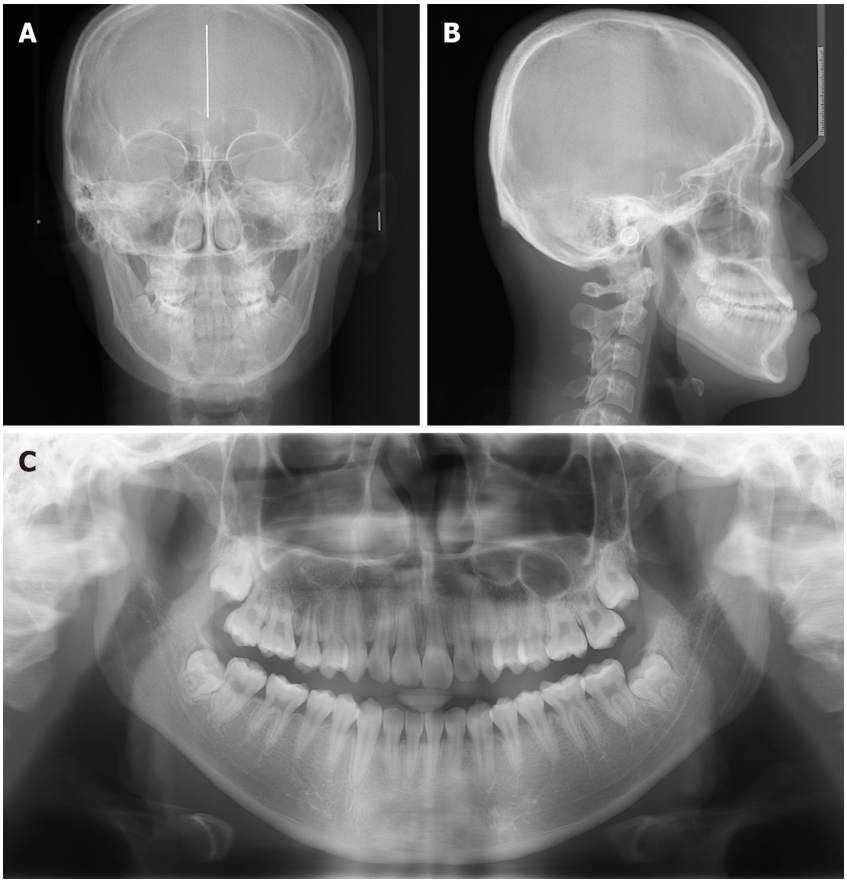


Figure 3 The images confirm a skeletal class III malocclusion. A: Anteroposterior cephalogram; B: Lateral cephalogram; C: Panoramic radiograph.

mandibular plane. Posteroanterior radiographs showed no significant mandibular asymmetry or deviation from the mid-sagittal line (Figure 3).

FINAL DIAGNOSIS

The patient was given a diagnosis of skeletal class III malocclusion, anterior crossbite, mild anterior crowding, and slight leftward mandibular midline deviation, with a balanced vertical facial pattern.

TREATMENT

Treatment objectives

The patient exhibited skeletal class III malocclusion, an anterior crossbite, and mild anterior crowding. The primary goals of treatment were: (1) To correct the anterior crossbite; (2) To relieve the crowding among the anterior teeth; (3) To achieve optimal dental alignment; (4) To establish proper overjet and overbite relationships; and (5) To enhance the patient's facial aesthetics.

Treatment alternatives

Two potential treatment plans were discussed. The first option involved orthognathic surgery to address the skeletal discrepancy. The second, preferred by the patient, was non-surgical orthodontic treatment using ISW and IME to manage the malocclusion.

Treatment progress

The orthodontic treatment commenced with the application of a full-mouth direct bonding system, which refers to the technique of bonding brackets directly onto the tooth surface, followed by leveling with 0.016 × 0.022-inch ISW (Figure 4). ISW MEAW with long class III elastics (16–43 and 26–33) was used to correct the anterior crossbite (Figure 4).

The patient's midline and crowding issues were resolved without surgery (Figure 4). After 13 months of active orthodontic treatment, the fixed appliances were removed, and retainers were provided. The patient was instructed to wear the retainers full-time for the first three months, followed by nighttime-only wear for maintenance.



Figure 4 Teeth movement changes during treatment. Intraoral photographs during initial alignment. Intraoral photographs demonstrating the application of Ni–Ti alloy wire (ISW) multi-bend edgewise archwire (MEAW). Unlike traditional MEAW, which employs L-loops, the ISW MEAW uses step bends tailored to skeletal class III correction. This adaptation leverages the super-elastic properties of ISW to ensure controlled and effective tooth movement without the patient's comfort being compromised. Intraoral photographs after midline correction, showing well-aligned dental midlines.

OUTCOME AND FOLLOW-UP

The patient's anterior crossbite was successfully corrected using the ISW MEAW technique (Figure 4) and wire + aligner (WA) orthodontics (Figure 5); a well-aligned arch and stable occlusion were achieved. The final records (Figures 6, 7, 8, 9, and 10) demonstrated proper alignment of the dental midline, while panoramic radiographs (Figure 10C) confirmed parallel root positioning without any evidence of root resorption. Additionally, the one-year follow-up records (Figure 11) showed that the occlusal corrections remained stable and that proper overjet, overbite, and midline alignment were preserved, confirming the long-term success of the treatment.

Superimposition images (Figure 12) revealed the distal movement of the mandibular molars and the mesial shift of the maxillary molars, which contributed to the establishment of proper overjet and overbite.

The following section discusses the efficacy of ISW MEAW approach for the correction of anterior crossbite and the method of WA orthodontics. Proper arch coordination was achieved in our case. The treatment was a success.

DISCUSSION

In this case, the efficacy of ISW MEAW for the correction of anterior crossbite and midline deviation, along with the method of WA orthodontics, were discussed. Proper arch coordination, midline correction, and profile improvement were achieved, leading to a satisfactory treatment result.

The ISW MEAW technique was employed to correct the patient's anterior crossbite by using step and slope bends for controlled teeth movement, considerably improving dental alignment. Retroclination of the mandibular incisors played a crucial role in establishing an ideal overjet and overbite, improving both the patient's occlusal function and facial aesthetics. In this case, the mandibular anterior teeth were retroclined by 9°, further contributing to the overall outcome. The technique's ability to achieve precise arch coordination made it possible to conservatively treat the skeletal class III malocclusions without the need for surgical intervention[5]. Additionally, the midline correction was achieved through the controlled application of a unilateral ISW MEAW and IME, improving the overall balance of the dentition (Figure 13).

Despite the careful use of anchorage control mechanisms, midline deviation occurred during treatment. To address this, a unilateral ISW MEAW and IME were applied to teeth (13–43 and 23–34) (Figure 14). This combination enabled precise correction of the midline and the simultaneous achievement of the optimal overjet and overbite. Use of the ISW



Figure 5 Wire + aligner orthodontics refers to a treatment approach that integrates wire-based and aligner-based correction methods.



Figure 6 Posttreatment facial photographs. A: Frontal view at rest; B: Frontal view smiling; C: Lateral view at rest, demonstrating improved facial profile.

MEAW facilitated distal tipping of the teeth while minimizing unwanted side effects, making it possible to achieve excellent results without the need for a more invasive anchorage technique, such as miniscrews[6]. One limitation of the approach is the long duration of intermaxillary elastic wear, which can lead to increased proclination of the upper incisors (U1-SN angle) and steepening of the mandibular plane angle. This highlights the need for careful monitoring during treatment to prevent unfavorable side effects. More severe class III cases may require alternative strategies such as the use of mini-screws or molar extraction should be considered. These approaches can provide more effective anchorage control and facilitate the correction of major skeletal discrepancies. For instance, Nguyen *et al*[7] demonstrated the successful application of miniscrew-assisted rapid palatal expansion combined with lingual appliances to address skeletal class III malocclusion in adults. This method is a non-invasive alternative that is suitable for managing severe cases. It improves dental alignment, and maintains esthetics during treatment[7]. Similarly, Ngoc *et al*[8] reported on the effectiveness of asymmetric molar extraction with lingual appliances for treating skeletal class III malocclusion with mandibular deviation. This approach provided sufficient space for retraction and improved the torque control of the lower incisors, leading to favorable facial profile changes and occlusal outcomes[8].

WA orthodontics, a hybrid approach combining wires and aligners, played an essential role in the finishing stages of treatment for our patient. After wire treatment, aligners were used to meet the patient's preference for early debonding. The aligners provided precise control of smaller movements, such as the derotation of tooth (No. 12) (Figure 15), which would have been difficult to achieve with wires alone. Fixed appliances were initially insufficient to fully correct the rotation of tooth (No. 12); therefore clear aligners were introduced after debonding. This approach successfully refined the alignment, as confirmed during follow-up visits (Figure 11), and improved the patient's compliance, oral hygiene, and comfort, contributing to the overall success of the treatment.

Additionally, skeletal class III malocclusion may have a genetic component, which can influence long-term stability. Even after successful correction, there is a potential for relapse because of inherent genetic factors. Thus, long-term retention is essential to maintain treatment outcomes. In this case, retainers were prescribed for full-time wear for the first three months, followed by nighttime wear, ensuring the preservation of overjet, overbite, and midline correction. Addressing genetic predispositions in future treatment planning may provide insights into optimizing long-term stability strategies.

Finally, the combination of the ISW MEAW technique with WA orthodontics produced considerable improvements in the patient's facial profile (Figure 16). The posttreatment ANB angle was 0.5° (Figure 9). This result reflects the increased mandibular plane angle and clockwise rotation of the mandible during treatment, contributing to a more balanced



Figure 7 Photographs illustrating the transition to wire + aligner orthodontics at the debonding stage, facilitating precise finishing and alignment.



Figure 8 Posttreatment intraoral photographs demonstrating the final occlusal outcome.

	Before	After	Mean.	S.D.
Facial angle	93.5	91.0	84.83	3.05
Convexity	-3.0	1.0	7.58	4.95
A-B plane	4.0	-0.5	-4.81	3.50
Mandibular plane	30.0	32.5	28.81	5.23
Y-axis	60.0	62.5	65.38	5.63
Occlusal plane	5.5	6.0	11.42	3.64
Interincisal	119.5	125.0	124.09	7.63
L-1 to Occlusal	23.0	16.0	23.84	5.28
L-1 to Mandibular	88.5	79.5	96.33	5.78
U-1 to A-P plane	5.5	7.5	8.92	1.88
FMIA	61.5	68.0	54.63	6.47
FH to SN plane	9.0	9.0	6.19	2.89
SNA	82.5	82.5	82.32	3.45
SNB	84.5	82.0	78.90	3.45
SNA-SNB diff.	-2.0	0.5	3.39	1.77
U-1 to N-P plane	4.5	7.5	11.74	2.73
U-1 to FH plane	122.0	123.0	111.13	5.54
U-1 to SN plane	112.5	113.5	104.54	5.55
Gonial angle	131.0	131.5	122.23	4.61
Ramus inclination	79.5	81.5	87.07	4.40

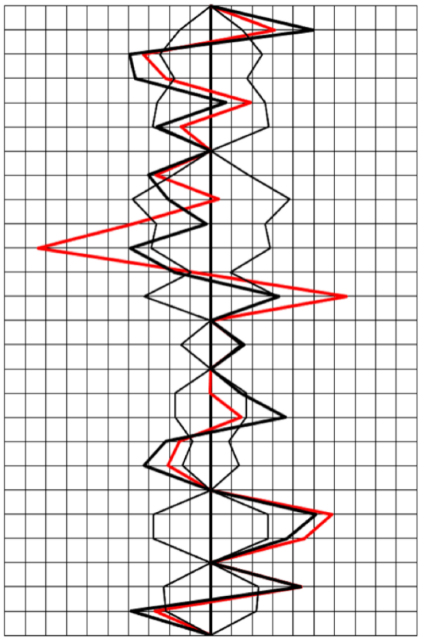


Figure 9 Superimposed cephalometric tracings before and after treatment. The retroclination of the lower incisors compensated for skeletal discrepancies. FH: Frankfort horizontal plane; FMIA: Frankfort mandibular incisor angle; SN: Sella–nasion plane; SNA: Sella–nasion–A point; SNB: Sella–nasion–B point.

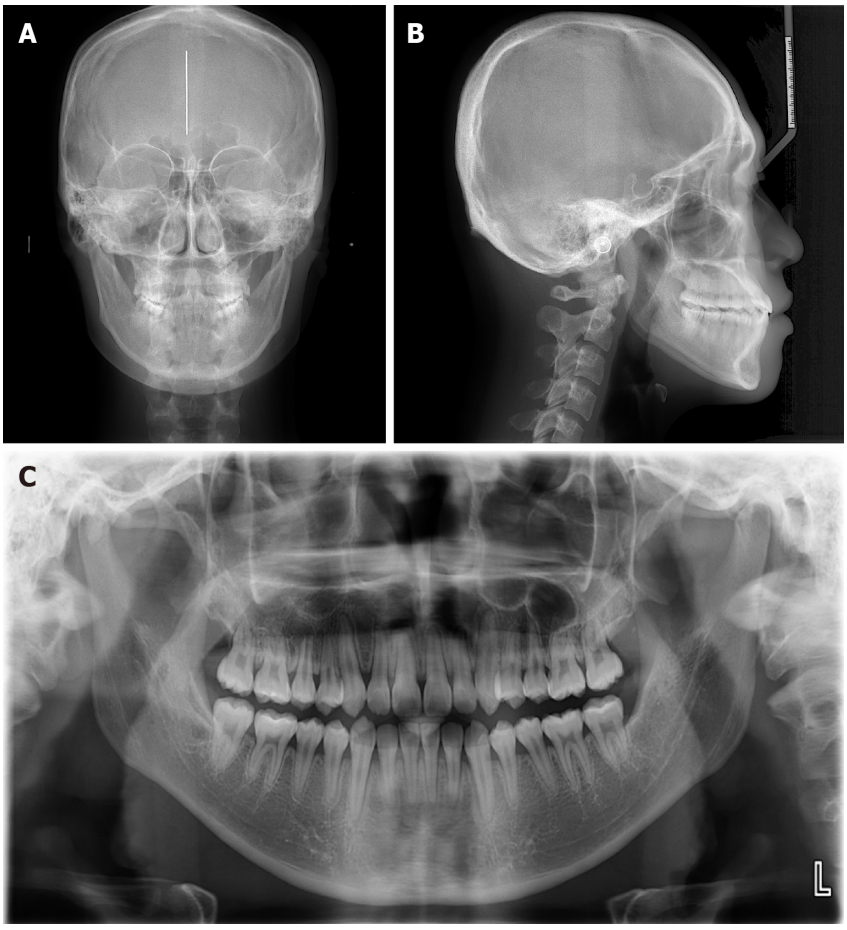


Figure 10 Panoramic radiographs. A: Anteroposterior cephalometric radiograph; B: Lateral cephalometric radiograph; C: Posttreatment panoramic radiograph, confirming proper dental alignment and root parallelism.



Figure 11 Intraoral images taken at the one-year follow-up, confirming the long-term stability of the occlusal corrections and alignment achieved during treatment.

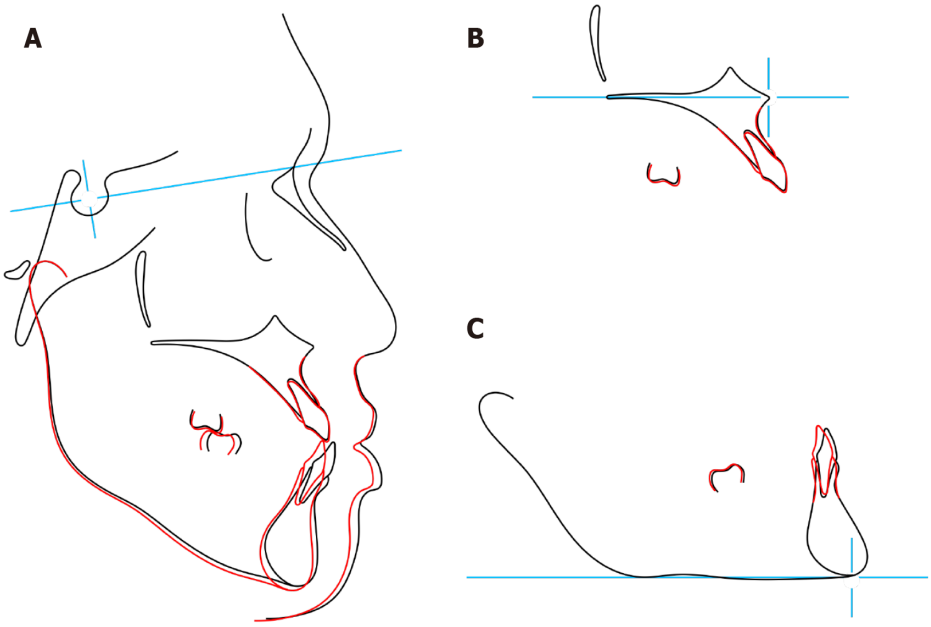


Figure 12 Superimposition images: before (black) and after (red) treatment. A: Superimposed on sella-nasion plane at sella; B: Superimposed on palatal plane at anterior nasal spine; C: Mandibular plane at menton, showing the retroclination of the lower incisors.

skeletal relationship (Figure 12). Controlled retroclination of the lower anterior teeth helped reduce the patient's protrusive lower lip, resulting in a more harmonious and aesthetically balanced profile. Although torque control of the lower incisors resulted in slight root prominence, this was an acceptable compromise because of the patient's preference to avoid extraction and surgical procedures. The patient's periodontal condition was closely monitored and no major issues were discovered during follow-up visits (Figure 11). Retainers were prescribed for full-time wear for the first three

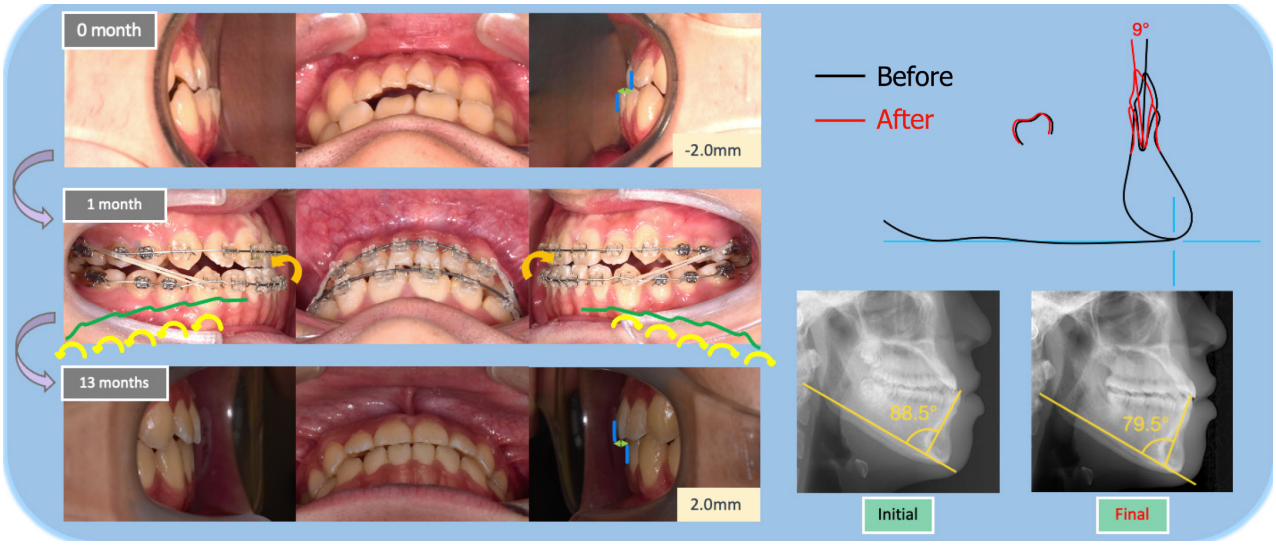


Figure 13 Ni–Ti alloy wire multi-bend edgewise archwire with long class III intermaxillary elastics used for anterior crossbite correction, contributing to controlled retroclination of the lower incisors.

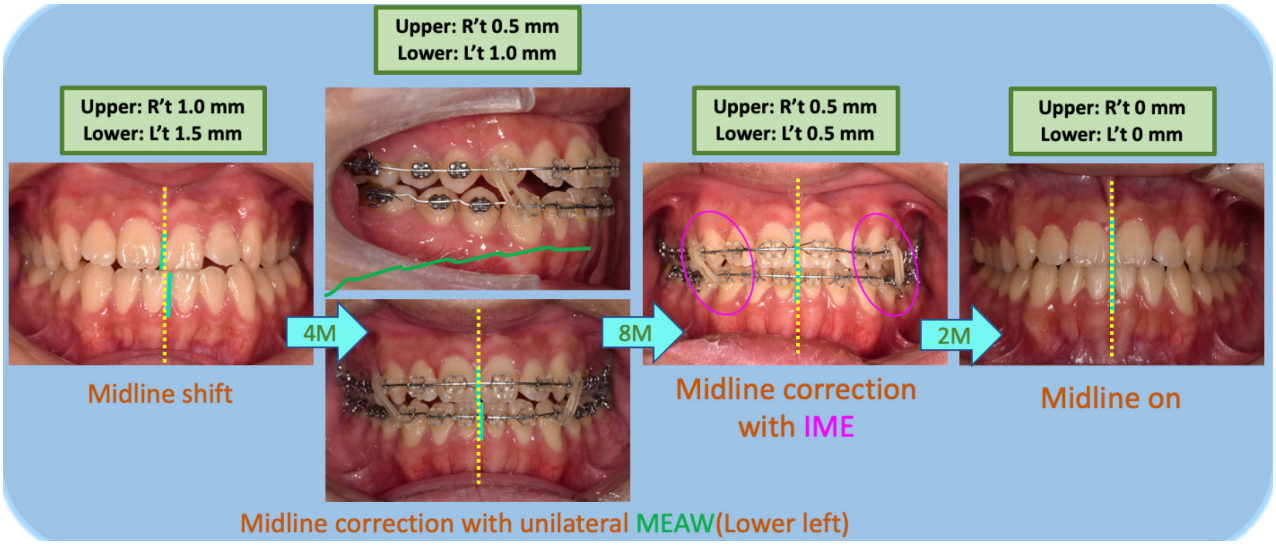


Figure 14 Midline correction achieved through the application of intermaxillary elastics and Ni–Ti alloy wire multi-bend edgewise archwire. IME: intermaxillary elastics; MEAW: Multi-bend edgewise archwire.

months after treatment, which was followed by nighttime wear to maintain the overjet, overbite, and midline correction achieved during active treatment and ensure long-term stability.

CONCLUSION

In the treatment of skeletal class III malocclusion with anterior crossbite, the ISW MEAW technique combined with WA orthodontics proved to be an effective and minimally invasive approach. Through controlled teeth movement and IME, we achieved an improved overjet, overbite, and midline correction. Additionally, the patient's facial aesthetics showed noticeable enhancement, with the nonsurgical approach successfully meeting both functional and cosmetic objectives. While the treatment yielded favorable results, further optimization could be achieved by enhancing the torque control of the lower incisors and considering alternative biomechanical techniques to improve treatment efficiency and accuracy. In this challenging case, a satisfactory result was achieved using a conservative approach.

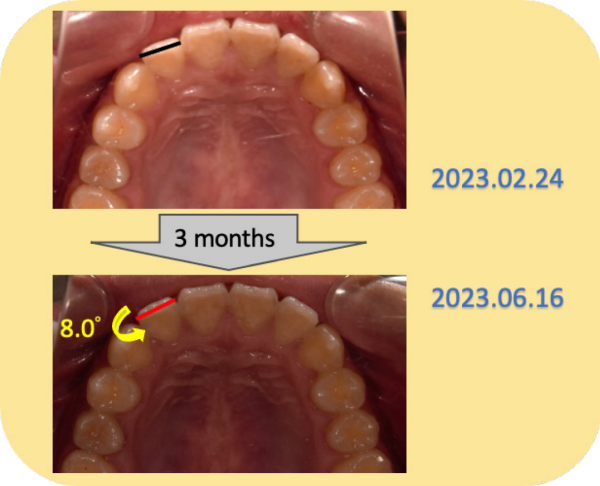
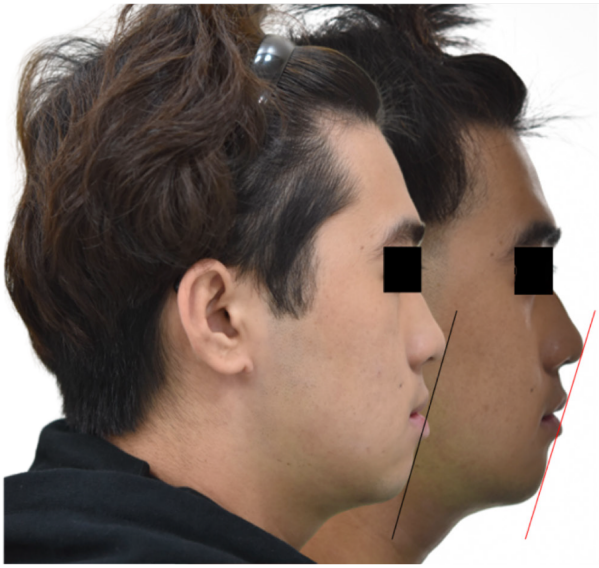


Figure 15 Tooth derotation using wire + aligner orthodontics, demonstrating precise control over individual tooth movement.



	Before	After
Overbite	-2.0 mm	2.0 mm
Overjet	-0.5 mm	2.0 mm
Upper lip to E-line	-1.5 mm	0 mm
Lower lip to E-line	3.5 mm	2.0 mm

Figure 16 Lateral profile change after treatment, showing improved soft tissue harmony as evaluated by the E-line assessment.

FOOTNOTES

Author contributions: Chang YHS was responsible for conception and design of the study, data collection and analysis, drafting and revising the manuscript; Chen YH was responsible for critical revision of the manuscript for important intellectual content and clinical supervision; Yu JH was responsible for study supervision, manuscript review and editing; all of the authors read and approved the final version of the manuscript to be published.

Informed consent statement: Written informed consent was obtained from the patient and/or their legal guardian for the publication of this case report and accompanying images.

Conflict-of-interest statement: The authors declare no conflicts of interest related to this manuscript.

CARE Checklist (2016) statement: The authors have read the CARE Checklist (2016), and the manuscript was prepared and revised according to the CARE Checklist (2016).

Open Access: This article is an open-access article that was selected by an in-house editor and fully peer-reviewed by external reviewers. It is distributed in accordance with the Creative Commons Attribution NonCommercial (CC BY-NC 4.0) license, which permits others to distribute, remix, adapt, build upon this work non-commercially, and license their derivative works on different terms, provided the original work is properly cited and the use is non-commercial. See: https://creativecommons.org/Licenses/by-nc/4.0/

Country of origin: Taiwan

ORCID number: Yu-Hsiang Sean Chang 0009-0002-6464-9178; Jian-Hong Yu 0000-0003-2150-5254.

S-Editor: Luo ML
L-Editor: A
P-Editor: Guo X

REFERENCES

1 **Inchingolo AD**, Patano A, Coloccia G, Ceci S, Inchingolo AM, Marinelli G, Malcangi G, Di Pede C, Garibaldi M, Ciocia AM, Mancini A, Palmieri G, Rapone B, Piras F, Cardarelli F, Nucci L, Bordea IR, Scarano A, Lorusso F, Giovanniello D, Costa S, Tartaglia GM, Di Venere D, Dipalma G, Inchingolo F. Treatment of Class III Malocclusion and Anterior Crossbite with Aligners: A Case Report. *Medicina (Kaunas)* 2022; **58**: 603 [PMID: 35630020 DOI: 10.3390/medicina58050603]

2 **Lim LI**, Choi JY, Ahn HW, Kim SH, Chung KR, Nelson G. Treatment outcomes of various force applications in growing patients with skeletal Class III malocclusion. *Angle Orthod* 2021; **91**: 449-458 [PMID: 33587106 DOI: 10.2319/090320-768.1]

3 **Mehta S**, Chen PJ, Upadhyay M, Yadav S. Intermaxillary elastics on skeletal anchorage and MARPE to treat a class III maxillary retrognathic open bite adolescent: A case report. *Int Orthod* 2021; **19**: 707-715 [PMID: 34452857 DOI: 10.1016/j.ortho.2021.08.001]

4 **Alnefaie M**, Han WJ, Ahn YS, Baik WK, Choi SH. Orthopedic and Nonsurgical Orthodontic Treatment of Adolescent Skeletal Class III Malocclusion Using Bone-Anchored Maxillary Protraction and Temporary Anchorage Devices: A Case Report. *Children (Basel)* 2022; **9**: 683 [PMID: 35626860 DOI: 10.3390/children9050683]

5 **Chen P**, Chen Y, Wang I, Yu J. Improved Super-elastic Ti-Ni alloy wire (ISW) for Treatment of Adult Angle Class III with Anterior Crossbite. *Taiwan J Orthod* 2023; **35** [DOI: 10.38209/2708-2636.1341]

6 **Lo YC**, Chen YH, Chiang HH, Yu JH. Use Improved Super-elastic Ti–Ni Alloy Wire to Correct Class II Division 2 Malocclusion with Unstable Mandibular Position. *Taiwan J Orthod* 2018; **30** [DOI: 10.30036/TJO.201810_31(3).0006]

7 **Nguyen VA**, Nguyen NA, Doan HL, Pham TH, Doan BN. Management of anterior and posterior crossbites with lingual appliances and miniscrew-assisted rapid palatal expansion: A case report. *Medicine (Baltimore)* 2024; **103**: e40832 [PMID: 39654233 DOI: 10.1097/MD.0000000000040832]

8 **Ngoc VTN**, Phuong NTT, Anh NV. Skeletal Class III Malocclusion with Lateral Open Bite and Facial Asymmetry Treated with Asymmetric Lower Molar Extraction and Lingual Appliance: A Case Report. *Int J Environ Res Public Health* 2021; **18**: 5381 [PMID: 34070132 DOI: 10.3390/ijerph18105381]

World Journal of Clinical Cases

Submit a Manuscript: https://www.f6publishing.com

World J Clin Cases 2025 June 26; 13(18): 101612

DOI: 10.12998/wjcc.v13.i18.101612

ISSN 2307-8960 (online)

CASE REPORT

Abdominal tuberculosis with pancreatic head involvement mimicking pancreatic malignancy in a young man: A case report

Lei Ma, Kun-Peng Wang, Chong Jin

Specialty type: Medicine, research and experimental

Provenance and peer review: Unsolicited article; Externally peer reviewed.

Peer-review model: Single blind

Peer-review report's classification

Scientific Quality: Grade A, Grade A, Grade A, Grade B

Novelty: Grade A, Grade A, Grade A, Grade B

Creativity or Innovation: Grade A, Grade B, Grade B, Grade B

Scientific Significance: Grade A, Grade A, Grade B, Grade B

P-Reviewer: Liu KJ; Wu WB; Sun YH

Received: September 20, 2024

Revised: December 15, 2024

Accepted: January 23, 2025

Published online: June 26, 2025

Processing time: 159 Days and 21.4 Hours

Lei Ma, Kun-Peng Wang, Chong Jin, Department of General Surgery, Taizhou Central hospital (Taizhou University Hospital), Taizhou 318000, Zhejiang Province, China

Corresponding author: Chong Jin, MS, Professor, Department of General Surgery, Taizhou Central Hospital (Taizhou University Hospital), No. 999 Donghai Avenue, Jiaojiang District, Taizhou 318000, Zhejiang Province, China. 13757689065@163.com

Abstract

BACKGROUND

Pancreatic tuberculosis (PTB) is a rare disease, even in immunocompetent hosts. Abdominal tuberculosis involving the pancreatic head and peripancreatic areas may simulate pancreatic head carcinoma.

CASE SUMMARY

We present the case of a 32-year-old man who was admitted to our hospital for intermittent epigastric pain and weight loss. A computed tomography scan and magnetic resonance imaging revealed a mass in the head of the pancreas. The lesion was initially diagnosed as pancreatic head carcinoma on abdominal imaging. Laparotomy confirmed the diagnosis of PTB and the patient received anti-tuberculosis therapy.

CONCLUSION

The present case is reported to emphasize the importance of including PTB in the differential diagnosis of pancreatic lesions.

Key Words: Pancreatic tuberculosis; Pancreatic head carcinoma; Computed tomography; Laparotomy; Case report

©The Author(s) 2025. Published by Baishideng Publishing Group Inc. All rights reserved.

Core Tip: Pancreatic tuberculosis (PTB) is a rare and challenging condition, particularly in immunocompetent individuals. It commonly presents with nonspecific symptoms that resemble those of pancreatic malignancies, complicating the diagnosis based solely on clinical and imaging findings. Therefore, a thorough diagnostic approach, including histopathological confirmation, is crucial for accurate identification. Clinicians should maintain a high level of suspicion for PTB, especially in areas with a high prevalence of tuberculosis, and include it in the differential diagnosis of pancreatic lesions to avoid delays in treatment.

Citation: Ma L, Wang KP, Jin C. Abdominal tuberculosis with pancreatic head involvement mimicking pancreatic malignancy in a young man: A case report. *World J Clin Cases* 2025; 13(18): 101612
URL: https://www.wjgnet.com/2307-8960/full/v13/i18/101612.htm
DOI: https://dx.doi.org/10.12998/wjcc.v13.i18.101612

INTRODUCTION

Abdominal tuberculosis involving the pancreas and peripancreatic lymph nodes is an uncommon manifestation within clinical medicine. This form of tuberculosis typically presents insidiously, with nonspecific constitutional symptoms such as abdominal pain, anorexia, weakness, fever, weight loss, and night sweats[1]. Distinguishing pancreatic tuberculosis (PTB) from pancreatic carcinoma presents a substantial challenge due to overlapping clinical presentations. However, a key distinguishing factor is the relatively infrequent occurrence of obstructive jaundice in PTB compared to its more prevalent presence in pancreatic head carcinoma[2-4]. Laboratory assessments, encompassing liver function tests, hematologic parameters, and erythrocyte sedimentation rate, frequently fall short of providing definitive diagnostic insights[5].

The diagnostic process for PTB is notably complex, often necessitating laparotomy for a conclusive diagnosis in the majority of reported cases[6] In this study, we present a compelling case of a male patient displaying a pancreatic head mass on abdominal imaging suggestive of pancreatic head cancer, ultimately diagnosed with PTB through surgical intervention. This case underscores the critical role of surgical exploration in unraveling the intricacies of abdominal tuberculosis involving the pancreas, emphasizing the significance of accurate diagnosis for timely and appropriate management[7].

CASE PRESENTATION

Chief complaints

A 32-year-old man presented with a 1-month history of intermittent epigastric pain, anorexia, and weight loss of 5 kg.

History of present illness

The patient presented with intermittent epigastric pain, described as a dull ache without clear triggers, which began 1 month prior. The pain was mild, with no distinct pattern of exacerbation or relief. It was not associated with nausea, vomiting, chills, fever, diarrhea, or other concomitant symptoms. However, the patient experienced a reduced appetite, and although the intermittent abdominal pain remained stable for 1 month, there was a weight loss of 5 kg.

History of past illness

The patient had a past medical history of chronic erosive gastritis for 1 year, for which he was administered antacid drugs discontinuously.

Personal and family history

The patient denied any history of specific personal illnesses and family history.

Physical examination

The patient's temperature was 37.3 °C; heart rate, 72 beats per minute; respiration rate, 17 breaths per minute; and blood pressure, 114/66 mmHg. The abdomen was flat and soft, with no visible skin abnormalities or other positive signs. There was no friction rub, mild tenderness in the epigastric region, no rebound tenderness, and no palpable enlargement of surface lymph nodes.

Laboratory examinations

Laboratory examination at the time of admission revealed that the complete blood count, liver function tests, bilirubin and amylase levels, serum carbohydrate antigen (CA) 19-9, serum CA 12-5, and carcinoembryonic antigen levels were all within normal limits. The findings on chest radiography were also normal.

Imaging examinations

An abdominal computed tomography (CT) scan revealed an ill-defined 35 mm × 30 mm mass lesion in the head of the pancreas. The mass exhibited inhomogeneous enhancement, with the portal vein encased and compressed by the mass (Figure 1), mimicking a pancreatic head carcinoma. Magnetic resonance imaging (MRI) revealed local stenosis of the portal vein due to compression by the lesion (Figure 2; black arrow). Stricture of the distal common bile duct was observed on magnetic resonance cholangiopancreatography (MRCP) (Figure 2; white arrow), without apparent dilatation of the proximal common bile duct, intrahepatic bile duct, or pancreatic duct. In addition, several enlarged lymph nodes were identified in the retroperitoneum.

FINAL DIAGNOSIS

PTB.

TREATMENT

The appearance of CT and MRI scans indicated a possible diagnosis of a pancreatic malignancy. Therefore, an exploratory laparotomy with pancreaticoduodenectomy as a contingency was planned. Intraoperatively, a mass was identified above the pancreatic head, comprising caseous necrotic tissue (Figure 3). An intraoperative frozen section biopsy confirmed the diagnosis of tuberculous lymphadenitis. Histopathological examination revealed a mass composed of epithelioid cells and occasional multinucleated giant cells, exhibiting caseous necrosis (Figure 4). However, the test for acid-fast bacilli was negative. Antituberculosis therapy was administered to the patient after surgery.

OUTCOME AND FOLLOW-UP

The patient made a full recovery and was subsequently discharged.

DISCUSSION

Tuberculosis is a multisystem infectious disease, primarily affecting the lungs, with abdominal tuberculosis being a common extrapulmonary form. PTB, involving the pancreas and peripancreatic lymph nodes, is rare. Its clinical manifestations typically begin insidiously with nonspecific symptoms, including abdominal pain, anorexia, weakness, fever, weight loss, and night sweats[5]. Obstructive jaundice, common in pancreatic head carcinoma, is uncommon in PTB[7-9]. Laboratory findings often show abnormal liver function, anemia, leukocytosis, or elevated erythrocyte sedimentation rate, but are generally nonspecific[10].

PTB is a rare extrapulmonary manifestation of tuberculosis, with its incidence varying significantly across different regions. PTB is more commonly reported in areas with a high prevalence of tuberculosis, such as Southeast Asia, Africa, and parts of South America. Individuals who are immunocompromised, including those with human immunodeficiency virus/acquired immunodeficiency syndrome, diabetes mellitus, or those receiving immunosuppressive therapy, are at an increased risk of developing PTB. However, the true incidence remains underreported due to its rarity and the diagnostic challenges involved in distinguishing PTB from pancreatic malignancies or other pancreatic disorders[11].

The diagnosis of PTB is challenging in most reported cases, particularly before laparotomy[12]. Since PTB is curable with antituberculosis therapy, obtaining a definitive diagnosis through imaging is critical to avoid unnecessary surgical interventions. However, imaging studies often struggle to reliably distinguish PTB from pancreatic malignancies or other pancreatic conditions. CT is the standard diagnostic imaging modality and is widely employed in clinical practice. Despite its broad application, the CT features of PTB—such as low-density lesions, heterogeneous or peripheral rim enhancement, and calcifications—are nonspecific and can closely resemble those of pancreatic carcinoma[13,14]. Peripheral rim enhancement on CT, often indicative of lymphadenitis, reflects central caseous necrosis surrounded by active inflammation in infected lymph nodes[15].

MRI can provide complementary information to CT in diagnosing PTB. Typical MRI findings include lesions with low intensity on T1-weighted images and high intensity on T2-weighted images, along with peripheral rim enhancement on post-contrast T1-weighted images[16]. Unlike pancreatic malignancies, PTB rarely causes bile duct dilatation on MRCP, even for lesions located in the pancreatic head. Similarly, vascular involvement, a feature commonly associated with advanced pancreatic malignancies, has also been reported in PTB, complicating its differentiation based on imaging alone [6,10,14]. Abdominal imaging of PTB may reveal solid or cystic lesions, typically in the pancreatic head. Therefore, the main differential diagnoses include mucinous/serous cystadenoma, cystic neuroendocrine tumor, and pancreatic adenocarcinoma, whereas PTB mimicking pancreatic abscess has also been reported[13].

Given these limitations of imaging, histological or bacteriological confirmation is essential for a definitive diagnosis. Cytological examination of PTB typically reveals caseous necrosis, granulomatous inflammation, epithelioid histiocytes, multinucleated giant cells, and lymphocytes; however, acid-fast bacilli are rarely observed[17]. Biopsy techniques,

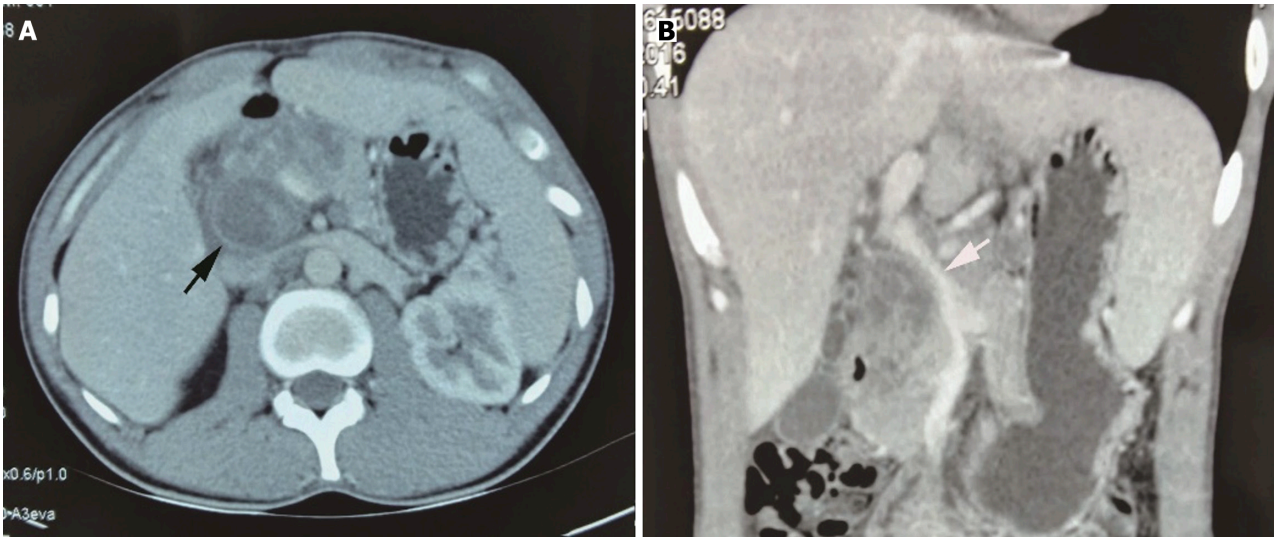


Figure 1 Contrast-enhanced computed tomography scan. A: An ill-defined mass with peripheral rim enhancement and internal low density in the head of the pancreas (left panel, black arrow); B: A coronal computed tomography scan revealing that the portal vein was partially encased by the lesion (right panel, white arrow).

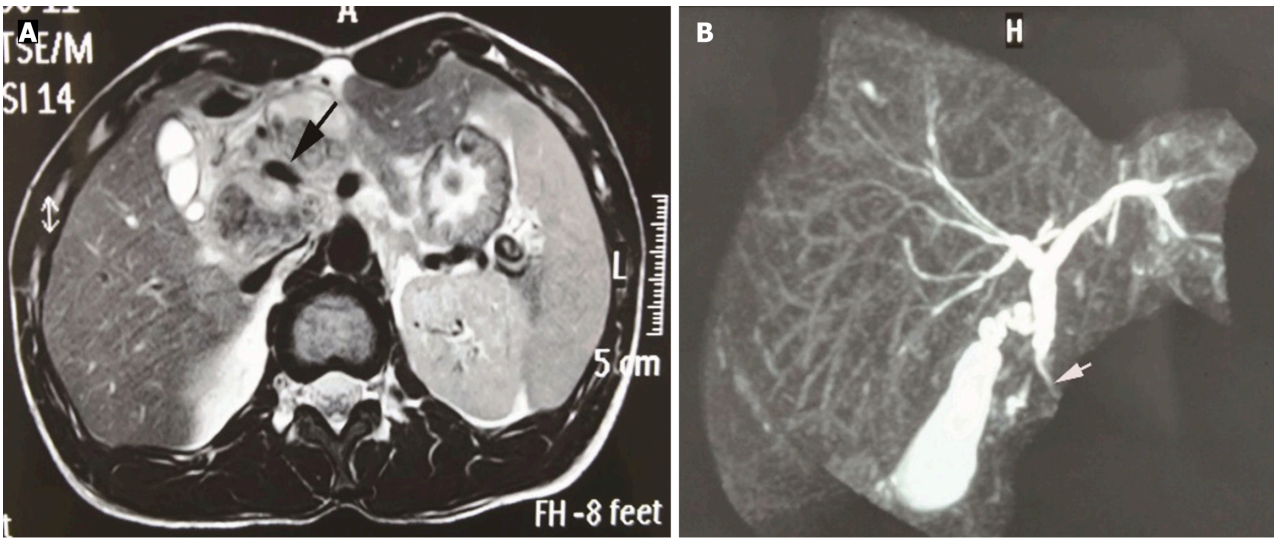


Figure 2 Magnetic resonance imaging result. A: The portal vein is locally narrowed due to compression by the mass (left panel, black arrow); B: Magnetic resonance cholangiopancreatography revealing a stricture of the distal common bile duct (right panel, white arrow).

including percutaneous ultrasound- or CT-guided biopsy and endoscopic ultrasound-guided fine needle aspiration (EUS-FNA), play a crucial role in confirming PTB. While EUS-FNA is widely recognized as safe and effective, it carries risks such as insufficient sample retrieval and complications in suspected malignancy cases[3,9,10,18] To enhance the early recognition of PTB, several strategies can be implemented. First, increasing clinical awareness of PTB, particularly in regions with a high prevalence of tuberculosis, is vital. Second, integrating advanced imaging modalities such as diffusion-weighted MRI with histological and microbiological diagnostics can significantly improve diagnostic accuracy. Finally, adopting a multidisciplinary approach involving radiologists, gastroenterologists, and pathologists can accelerate diagnosis and treatment, ultimately improving patient outcomes.

The hallmark histological features of PTB include granulomatous inflammation with caseous necrosis. These granulomas are typically composed of epithelioid histiocytes, multinucleated Langhans-type giant cells, and a peripheral lymphocytic rim. The presence of caseous necrosis is a key distinguishing feature of PTB, as it is absent in other granulomatous diseases, such as sarcoidosis. Special staining methods, such as Ziehl-Neelsen staining for acid-fast bacilli, can detect mycobacterial organisms, although their sensitivity varies. Diagnostic accuracy can be further enhanced using immunohistochemical staining for mycobacterial antigens or molecular techniques such as PCR, particularly in paucibacillary cases[2,19].

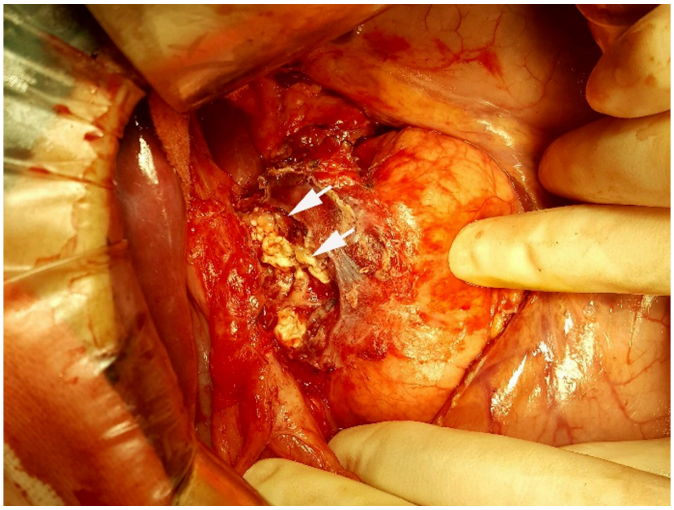


Figure 3 On laparotomy, tissue with caseous necrosis is identified above the pancreatic head (arrows).

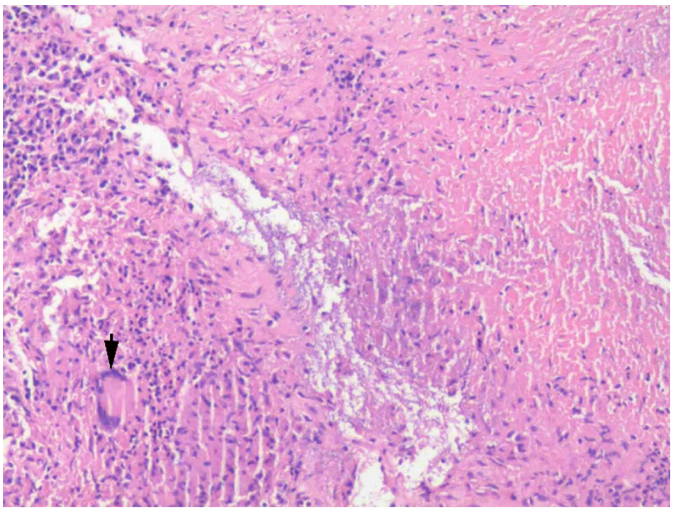


Figure 4 Pathological examination showing epithelioid granulomatous inflammation with caseous necrosis, composed of epitheloid cells and occasional multinucleated giant cells (arrow). Hematoxylin and eosin staining; magnification, × 100.

CONCLUSION

This case underscores the importance of considering PTB as a differential diagnosis, even in immunocompetent individuals, where clinical and imaging findings may resemble those of malignancy. It emphasizes the progress in understanding PTB, particularly the necessity of a thorough diagnostic approach, which includes histopathological confirmation. The study also highlights the critical role of imaging in clinical decision-making, although these techniques have limitations in distinguishing PTB from pancreatic malignancies. Future research should aim to develop more accurate, non-invasive diagnostic tools, such as advanced imaging technologies or biomarkers, to facilitate early detection of PTB. Additionally, optimizing treatment regimens for PTB, especially in cases with atypical presentations or complications, warrants further investigation. It is crucial to emphasize the significance of PTB in younger, immunocompetent individuals, as this group is often overlooked in the differential diagnosis, which may delay appropriate treatment.

ACKNOWLEDGEMENTS

We are very grateful to our colleagues from the Department of Imaging for providing the computed tomography pictures.

FOOTNOTES

Author contributions: Ma L and Wang KP designed this study, reviewed the literature, and wrote the manuscript; Ma L and Jin C collected the patient's clinical data; Ma L, Wang KP, and Jin C revised the manuscript. All authors read and approved the final manuscript.

Informed consent statement: Informed written consent was obtained from the patient and legal guardian for publication of this report and any accompanying images.

Conflict-of-interest statement: The authors declare that they have no conflict of interest to report.

CARE Checklist (2016) statement: The authors have read the CARE Checklist (2016), and the manuscript was prepared and revised according to the CARE Checklist (2016).

Open Access: This article is an open-access article that was selected by an in-house editor and fully peer-reviewed by external reviewers. It is distributed in accordance with the Creative Commons Attribution NonCommercial (CC BY-NC 4.0) license, which permits others to distribute, remix, adapt, build upon this work non-commercially, and license their derivative works on different terms, provided the original work is properly cited and the use is non-commercial. See: https://creativecommons.org/Licenses/by-nc/4.0/

Country of origin: China

ORCID number: Kun-Peng Wang 0000-0001-5088-2548; Chong Jin 0000-0002-2103-2226.

S-Editor: Liu H
L-Editor: Filipodia
P-Editor: Zhang XD

REFERENCES

1 **Mao XB**, Li N, Huang ZS, Ding CM, Bao WJ, Fan J, Li HL. (18)F-FDG PET-CT Diagnosis of Tuberculosis in Celiac Lymph Nodes. *Int J Gen Med* 2020; **13**: 1335-1339 [PMID: 33293851 DOI: 10.2147/IJGM.S287115]
2 **Ben Hammouda S**, Chaka A, Njima M, Korbi I, Zenati H, Zakhama A, Hadhri R, Zouari K. Primary pancreatic tuberculosis mimicking pancreatic body cancer. A case report and review of the literature. *Ann Med Surg (Lond)* 2020; **58**: 80-83 [PMID: 32953104 DOI: 10.1016/j.amsu.2020.08.040]
3 **Yu D**, Li X, Gong J, Li J, Xie F, Hu J. Left-sided portal hypertension caused by peripancreatic lymph node tuberculosis misdiagnosed as pancreatic cancer: a case report and literature review. *BMC Gastroenterol* 2020; **20**: 276 [PMID: 32811429 DOI: 10.1186/s12876-020-01420-x]
4 **Jemni I**, Akkari I, Mrabet S, Jazia EB. Isolated pancreatic tuberculosis mimicking pancreatic cancer in an immunocompetent host: An elusive diagnosis. *Radiol Case Rep* 2020; **15**: 1575-1578 [PMID: 32685072 DOI: 10.1016/j.radcr.2020.06.041]
5 **Soni A**, Tyagi R, Selhi PK, Sood A, Sood N. Pancreatic tuberculosis: A close mimicker of malignancy. *Turk J Gastroenterol* 2019; **30**: 1001-1003 [PMID: 31767560 DOI: 10.5152/tjg.2019.18832]
6 **Kaur M**, Dalal V, Bhatnagar A, Siraj F. Pancreatic Tuberculosis with Markedly Elevated CA 19-9 Levels: A Diagnostic Pitfall. *Oman Med J* 2016; **31**: 446-449 [PMID: 27974961 DOI: 10.5001/omj.2016.89]
7 **García Del Olmo N**, Boscà Robledo A, Penalba Palmí R, Añón Iranzo E, Aguiló Lucía J. Primary peripancreatic lymph node tuberculosis as a differential diagnosis of pancreatic neoplasia. *Rev Esp Enferm Dig* 2017; **109**: 528-530 [PMID: 28506074 DOI: 10.17235/reed.2017.4811/2016]
8 **Sun PJ**, Lin Y, Cui XJ. Isolated pancreatic tuberculosis with elevated CA 19-9 levels masquerading as a malignancy: A rare case report and literature review. *Medicine (Baltimore)* 2018; **97**: e13858 [PMID: 30593188 DOI: 10.1097/MD.0000000000013858]
9 **ForȚofoiu MC**, Popescu DM, Pădureanu V, Dobrinescu AC, Dobrinescu AG, Mită A, Foarfă MC, Bălă VS, Muşetescu AE, Ionovici N, ForȚofoiu M. Difficulty in positive diagnosis of ascites and in differential diagnosis of a pulmonary tumor. *Rom J Morphol Embryol* 2017; **58**: 1057-1064 [PMID: 29250690]
10 **Yamada R**, Inoue H, Yoshizawa N, Kitade T, Tano S, Sakuno T, Harada T, Nakamura M, Katsurahara M, Hamada Y, Tanaka K, Horiki N, Takei Y. Peripancreatic Tuberculous Lymphadenitis with Biliary Obstruction Diagnosed by Endoscopic Ultrasound-guided Fine-needle Aspiration Biopsy. *Intern Med* 2016; **55**: 919-923 [PMID: 27086805 DOI: 10.2169/internalmedicine.55.6123]
11 **Machicado JD**, Papachristou GI. Pancreatogenic diabetes, acute pancreatitis management, and pancreatic tuberculosis: Appraising the present and setting goals for the future. *United European Gastroenterol J* 2020; **8**: 365-368 [PMID: 32364055 DOI: 10.1177/2050640620917017]
12 **Lee YJ**, Hwang JY, Park SE, Kim YW, Lee JW. Abdominal tuberculosis with periportal lymph node involvement mimicking pancreatic malignancy in an immunocompetent adolescent. *Pediatr Radiol* 2014; **44**: 1450-1453 [PMID: 24801816 DOI: 10.1007/s00247-014-2997-x]
13 **Naisbitt CJ**, Filobbos R, Bonington A, O'Reilly D. A space occupying lesion masquerading as pancreatic carcinoma. *BMJ Case Rep* 2013; **2013** [PMID: 23704465 DOI: 10.1136/bcr-2013-009933]
14 **Khaniya S**, Koirala R, Shakya VC, Adhikary S, Regmi R, Pandey SR, Agrawal CS. Isolated pancreatic tuberculosis mimicking as carcinoma: a case report and review of the literature. *Cases J* 2010; **3**: 18 [PMID: 20205859 DOI: 10.1186/1757-1626-3-18]
15 **Cho SB**. Pancreatic tuberculosis presenting with pancreatic cystic tumor: a case report and review of the literature. *Korean J Gastroenterol* 2009; **53**: 324-328 [PMID: 19458471 DOI: 10.4166/kjg.2009.53.5.324]
16 **Kim JB**, Lee SS, Kim SH, Byun JH, Park DH, Lee TY, Lee BU, Jeong SU, Seo DW, Lee SK, Kim MH. Peripancreatic tuberculous lymphadenopathy masquerading as pancreatic malignancy: a single-center experience. *J Gastroenterol Hepatol* 2014; **29**: 409-416 [PMID:

24303923 DOI: 10.1111/jgh.12410]
17 **Mansoor J**, Umair B. Primary pancreatic tuberculosis: a rare and elusive diagnosis. *J Coll Physicians Surg Pak* 2013; **23**: 226-228 [PMID: 23458052]
18 **Iglesias García J**, Ferreiro R, Lariño Noia J, Abdulkader I, Alvarez Del Castillo M, Cigarrán B, Forteza Vila J, Domínguez Muñoz JE. Pancreatic fusocellular sarcoma. The importance of endoscopic ultrasound-guided fine needle aspiration in the differential diagnosis of solid pancreatic tumors. *Rev Esp Enferm Dig* 2009; **101**: 498-504 [PMID: 19642843 DOI: 10.4321/s1130-01082009000700009]
19 **Liu X**, Li F, Xu J, Ma J, Duan X, Mao R, Chen M, Chen Z, Huang Y, Jiang J, Huang B, Ye Z. Deep learning model to differentiate Crohn's disease from intestinal tuberculosis using histopathological whole slide images from intestinal specimens. *Virchows Arch* 2024; **484**: 965-976 [PMID: 38332051 DOI: 10.1007/s00428-024-03740-9]

World Journal of Clinical Cases

Submit a Manuscript: https://www.f6publishing.com

World J Clin Cases 2025 June 26; 13(18): 101882

DOI: 10.12998/wjcc.v13.i18.101882

ISSN 2307-8960 (online)

CASE REPORT

Concurrent invasive ductal carcinoma and ductal carcinoma *in situ* arising inside and outside a breast hamartoma: A case report

Lai Wei, Zhe Tian, Zhi-Yong Wang, Wei-Jia Liu, Hong-Bo Li, Ying Zhang

Specialty type: Medicine, research and experimental

Provenance and peer review: Unsolicited article; Externally peer reviewed.

Peer-review model: Single blind

Peer-review report's classification

Scientific Quality: Grade A
Novelty: Grade A
Creativity or Innovation: Grade A
Scientific Significance: Grade A

P-Reviewer: Losanoff JE

Received: September 29, 2024
Revised: January 28, 2025
Accepted: February 12, 2025
Published online: June 26, 2025
Processing time: 150 Days and 17.2 Hours

Lai Wei, Zhe Tian, Zhi-Yong Wang, Wei-Jia Liu, Department of Surgery, Affiliated Hospital of Beihua University, Jilin 132011, Jilin Province, China

Hong-Bo Li, Department of Breast and Thyroid Surgery, Jinhua People's Hospital, Jinhua 321000, Zhejiang Province, China

Ying Zhang, Department of Pathology, Affiliated Hospital of Beihua University, Jilin 132011, Jilin Province, China

Co-first authors: Lai Wei and Zhe Tian.

Corresponding author: Zhi-Yong Wang, Associate Chief Physician, Associate Professor, Department of Surgery, Affiliated Hospital of Beihua University, No. 12 Jiefang Middle Road, Jilin 132011, Jilin Province, China. 2166715675@qq.com

Abstract

BACKGROUND

Breast hamartomas are rare benign breast tumors, with an incidence rate of 0.8%-4.8%. Further, the coexistence of hamartomas and carcinoma is also uncommon. Our case report presents a unique instance where invasive ductal carcinoma (IDC) and ductal carcinoma *in situ* were found both inside and outside a breast hamartoma. This is the second case reported in the literature.

CASE SUMMARY

A 51-year-old woman presented with a 6.0 cm breast tumor on mammography and ultrasound, with suspicious areas indicative of malignant transformation. Biopsy of the suspicious area confirmed IDC with intraductal carcinoma. Breast magnetic resonance imaging showed typical hamartoma changes with irregular areas of abnormal enhancement both inside and outside. A breast-conserving surgery was performed, and postoperative pathology confirmed mammary hamartoma, concurrent with IDC and intraductal carcinoma occurring both inside and outside the hamartoma. Subsequently, appropriate adjuvant therapy was initiated. Currently, the patient is in good condition. Breast cancer may be located both inside and outside the ipsilateral mammary hamartoma, which is difficult to detect preoperatively, especially when there is a focus of intraductal carcinoma, requiring accurate assessment of the tumor extent by modern imaging techniques. Early detection of the coexistence of cancer is clinically important as it can alter patient management.

CONCLUSION
This case emphasizes the importance of modern imaging techniques in accurately evaluating mammary hamartomas associated with malignancies prior to surgery.

Key Words: Breast; Hamartoma; Ductal carcinoma *in situ*; Invasive ductal carcinoma; Case report

©The Author(s) 2025. Published by Baishideng Publishing Group Inc. All rights reserved.

Core Tip: This case reports a rare instance of concurrent invasive ductal carcinoma and ductal carcinoma *in situ* inside and outside a breast hamartoma in a 51-year-old woman. Imaging suggested suspicious malignancy within the hamartoma, confirmed by postoperative pathology. It highlights the importance of modern imaging in preoperative evaluation of breast hamartomas associated with malignancies. Thorough assessment is crucial for determining safe margins in breast-conserving surgery and reducing postoperative recurrence risk.

Citation: Wei L, Tian Z, Wang ZY, Liu WJ, Li HB, Zhang Y. Concurrent invasive ductal carcinoma and ductal carcinoma *in situ* arising inside and outside a breast hamartoma: A case report. *World J Clin Cases* 2025; 13(18): 101882
URL: https://www.wjgnet.com/2307-8960/full/v13/i18/101882.htm
DOI: https://dx.doi.org/10.12998/wjcc.v13.i18.101882

INTRODUCTION

Breast hamartomas are rare, benign lesions resulting from the abnormal development of residual mammary ductal buds, fibrous tissue, and adipose tissue, typically encapsulated Hogeman and Osbterg[1] first described this lesion in 1968, with the term "hamartoma" introduced by Arrigoni *et al*[2]. in 1971. Breast hamartomas account for 0.8%-4.8% of benign breast tumors[3,4]. Clinically, they present as slow-growing, localized tumors with clear margins, often misdiagnosed as fibroadenomas or lipomas. The most common subtypes are adenolipomas and chondrolipomas. Although generally benign and not increasing breast cancer risk, there is a possibility of associated malignancies. Over ten cases of breast cancer associated with breast hamartomas have been reported, with most cancer lesions occurring within the hamartoma [5-9]. This report details a rare case of invasive ductal carcinoma (IDC) with ductal carcinoma *in situ* occurring both inside and outside a breast hamartoma.

CASE PRESENTATION

Chief complaints

A 51-year-old woman was admitted to our hospital due to the discovery of a mass in the right breast for 2 days.

History of present illness

Two days ago, during a physical examination at another hospital, the patient was found to have an abnormal hypoechoic nodule in the right breast through ultrasound examination. The nodule measured approximately 1.11 cm × 0.81 cm × 1.44 cm, with unclear borders and an irregular shape, classified as Breast Imaging Reporting and Data System 4B. She was referred to our breast clinic for further evaluation.

History of past illness

There was no history of past illness.

Personal and family history

There was no personal and family history.

Physical examination upon admission

Physical examination revealed a palpable, oval mass in the outer right breast, approximately 6.0 cm × 5.0 cm × 5.0 cm, firm with smooth surfaces and good mobility. However, near the nipple, the mass was hard with unclear borders and poor mobility.

Laboratory examinations

Not applicable.

Imaging examinations

Mammography showed an irregular density increase in the outer right breast, measuring approximately 8.3 cm × 5.7 cm (Figure 1A). Due to discrepancies between the ultrasound findings and physical examination, a repeat ultrasound was performed. It revealed an irregular hypoechoic structure in the outer right breast, measuring approximately 1.02 cm × 1.26 cm, with unclear borders and blood flow signals, suggesting a suspicious malignancy. Additionally, an uneven hypoechoic structure with a suspected capsule, measuring approximately 5.5 cm × 3.5 cm × 3.0 cm, was observed in the outer right breast near the suspicious hypoechoic structure (Figure 1B). Chest computed tomography showed an oval mass in the outer right breast with uneven density (Figure 1C). Magnetic resonance imaging (MRI) clearly showed a 5.4 cm hamartoma with an IDC and ductal carcinoma *in situ* lesion within it. Additionally, a suspicious lesion outside the hamartoma exhibiting a type 2 enhancement curve suggestive of malignancy was detected (Figure 1D).

FINAL DIAGNOSIS

Ultrasound-guided biopsy of the irregular hypoechoic structure revealed IDC with low-grade ductal carcinoma *in situ*.

Postoperatively, pathology showed IDC (grades I-II) with two cancer foci, both being IDC. One focus was within the hamartoma, measuring approximately 1.0 cm × 0.5 cm, and the other was outside the hamartoma, with a maximum microscopic diameter of approximately 0.7 cm. Both foci contained abundant low-grade to intermediate-grade ductal carcinoma *in situ* with comedo-type necrosis (Figure 2). Immunohistochemistry revealed: (1) Estrogen receptor (100% 3+); (2) Progesterone receptor (90% 2+); (3) Human epidermal growth factor receptor 2 (1+); (4) Ki67 (10%+); (5) Calponin (-); (6) P63 (-); (7) Cytokeratin (CK) 5/6 (-); and (8) CK8 (+).

TREATMENT

The patient expressed a desire for breast-conserving surgery and therefore underwent breast-conserving surgery and sentinel lymph node biopsy. Postoperatively, she received adjuvant radiotherapy and is currently undergoing letrozole treatment.

OUTCOME AND FOLLOW-UP

During the 19-month follow-up, no recurrence or metastasis has been detected.

DISCUSSION

The incidence of breast cancer associated with hamartomas is very low. The first case was reported by Mendiola *et al*[5] in 1982. To date, 19 cases have been reported in the literature[6,10-12]. In previous reports, the median age of patients was 59 years (range: 25-78 years)[6,13,14]. The patient in this case is 51 years old, younger than the median age.

In this case, a palpable mass was found in the lateral right breast, characterized by clear boundaries and good mobility, consistent with benign hamartoma features as reported in the literature. However, the periphery of the mass near the nipple was hardened, with unclear boundaries and poor mobility, more indicative of malignancy, distinguishing this case from others.

Mammography in this case revealed typical benign hamartoma features, such as uneven glandular density, with no signs of malignancy like calcification. In previous reports, mammography was performed in 10 cases, and in addition to the typical appearance of hamartomas, suspicious malignant features such as clustered microcalcifications, polymorphic microcalcifications, spiculated masses, and twisted amorphous calcifications were observed[6,15-17]. In contrast, no such features were found in this case.

Breast MRI performed in this case indicated not only the typical lobulated abnormal signal of a mammary hamartoma but also an irregular abnormal enhancement signal within the hamartoma, confirmed by biopsy as an IDC with ductal carcinoma *in situ*. Additionally, a local abnormal enhancement signal below the hamartoma was detected, with a dynamic enhancement curve (TICmax) showing a plateau (type II), suggesting malignancy. The pathological diagnosis from the surgically removed lesion confirmed the biopsy results. This lesion was not detected in the physical examination, ultrasound, or mammography, suggesting that breast MRI may be a valuable imaging tool for detecting malignant lesions associated with mammary hamartomas.

In previously reported cases, 14 were diagnosed as IDC or ductal carcinoma *in situ*, 4 as lobular carcinoma, and 1 as mixed ductal and lobular carcinoma[6,18-20]. Our case was diagnosed as IDC with a significant component of low-grade ductal carcinoma *in situ*, consistent with the majority of reported cases. Among the three cases with reported molecular subtypes, estrogen and progesterone receptors were either negative or weakly positive[7,9,12]. In our case, both the invasive lesion within the hamartoma and the one outside it were strongly positive for estrogen and progesterone receptors, with a molecular subtype of Luminal A, differing from previous reports.

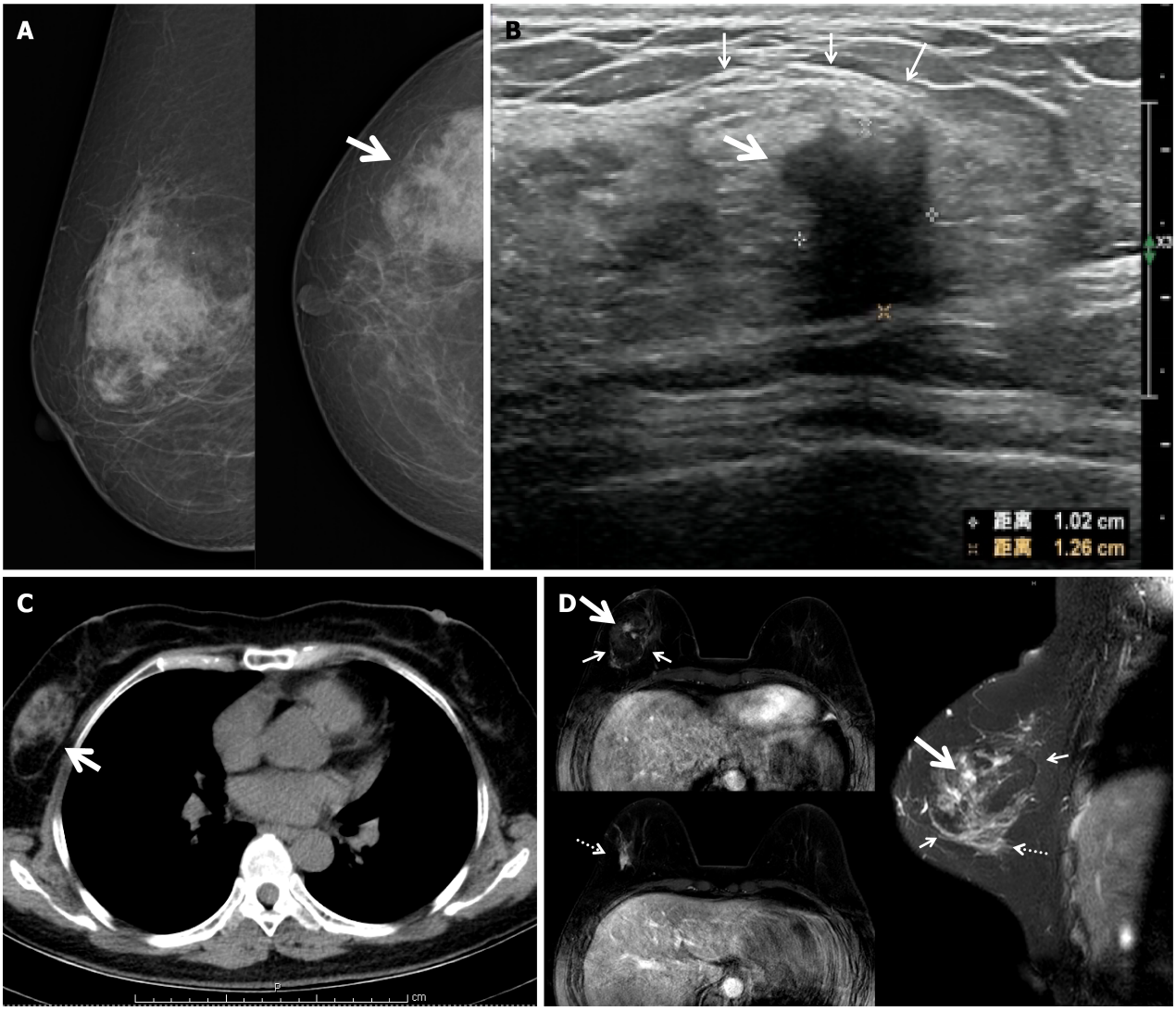


Figure 1 Mammography. A: Mammography revealed a circumscribed mass including fat and glands with suspicious local architectural distortion; B: Ultrasonography revealed a heterogeneous tumor with a smooth capsule (hamartoma; thin arrow) and an irregular, hypoechoictumor with posterior decrescence and an indistinct boundary (invasion; thick arrows); C: Computed tomography revealed a well-defined elliptical mass with uneven density; D: Magnetic resonance imaging showing the circumscribed mammary hamartomaswith dense fibroglandular tissue and fat (hamartoma; thin arrow). Note the marked irregular enhancement region with type 2 enhancement curves within hamartoma(thick arrows) , and the concerning area of architectural distortion with type 2 enhancement curves at the lower margin of the hamartoma (white dot arrows).

In our case, the foci of invasive carcinoma and ductal carcinoma *in situ* were located both within and outside the hamartoma. Despite the distance between the two foci, their molecular subtypes were similar, suggesting that they may have originated as a single central lesion within the hamartoma, similar to the case reported by Anani and Hessler[7] in 2012. The mechanism by which the ductal carcinoma *in situ* component migrated outside the hamartoma remains unclear. We propose the following potential mechanisms: (1) There may be an anastomosis between the ductal systems of the hamartoma and the surrounding gland. Ohtake *et al*[21] found multiple anastomoses between different mammary ductal systems. There is no true fibrous capsule between normal breast tissue and hamartomas, only compressed adjacent breast tissue. It is possible that anastomoses between the lobules could allow ductal carcinoma *in situ* within the hamartoma to spread outside *via* ductal anastomoses. However, apart from Ohtake *et al*'s study[21], other studies have not found such connections[22], suggesting that these anastomoses may not be common and further research is needed; and (2) Ductal carcinoma *in situ* may spread within the breast ducts toward the nipple and then to adjacent mammary ductal lobular systems, which we consider the most likely mechanism of dissemination. Studies have found that different ductal systems connect together behind the areola, forming 5-8 common collectors[23]. Ductal carcinoma *in situ* may spread to adjacent ductal lobular units *via* these common collectors and then retrogradely spread peripherally, forming extensive ductal spread. Epigenetic events such as telomere crisis[24] could then allow the tumor cells to break through the basement membrane and migrate into adjacent tissues[25], forming invasive lesions. The pathology and MRI findings of our reported case further support this possibility.

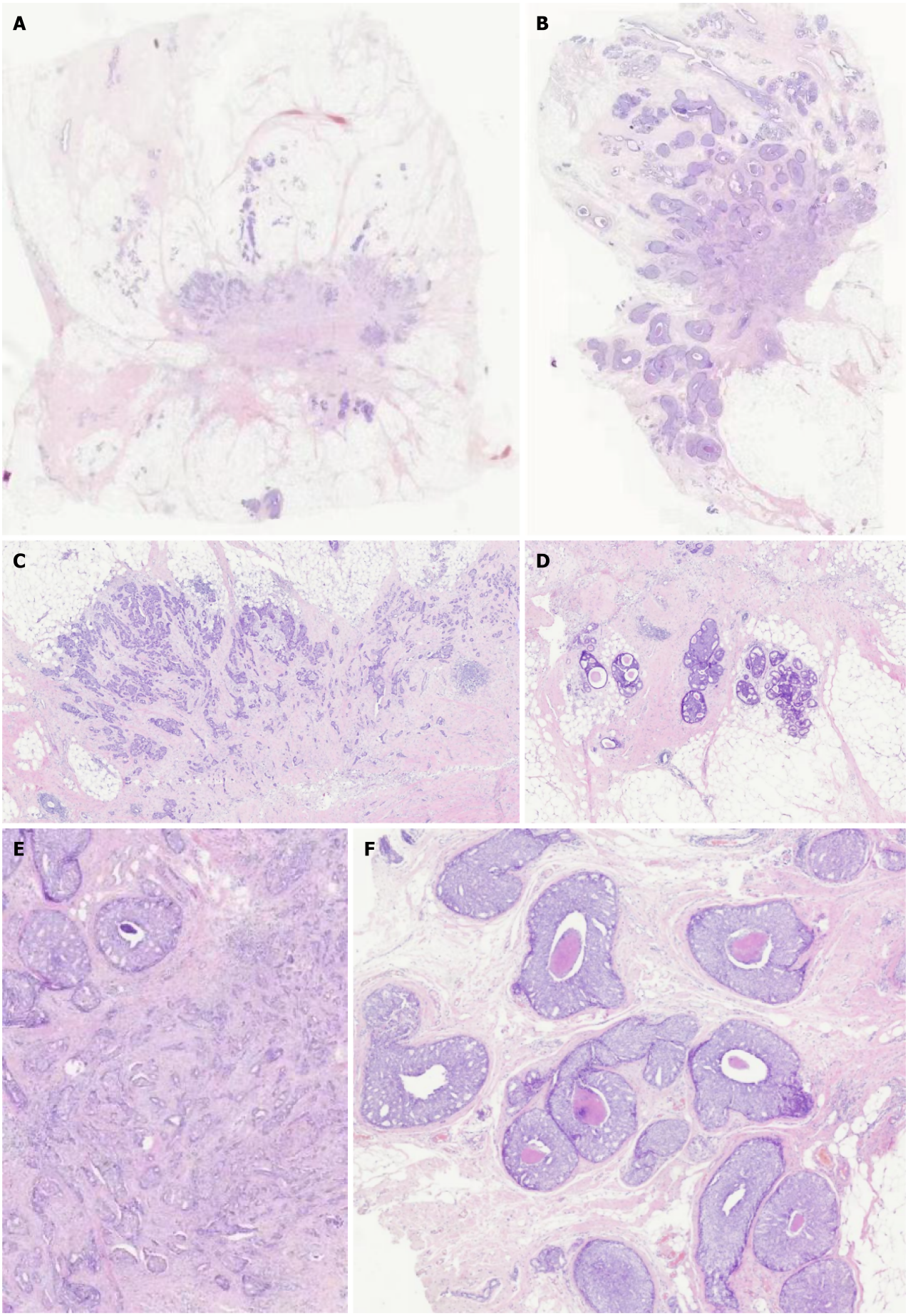


Figure 2 Pathology. A: Low power magnification [haematoxylin and eosin (HE) staining, 12.5 ×]: Mass including invasive ductal carcinoma and ductal carcinoma

in situ inside was encapsulated by delicate fibrous tissue; B: Low power magnification (HE staining, 12.5 ×): Invasive ductal carcinoma and ductal carcinoma *in situ* involved normal breast tissue external to hamartoma; C: High power field of invasive ductal carcinoma lesion of Figure 2A (HE staining, 100 ×); D: High power field of ductal carcinoma in situ lesion of Figure 2A (HE staining, 100 ×); E: High power field of invasive ductal carcinoma lesion of Figure 2B (HE staining, 200 ×); F: High power field of ductal carcinoma in situ lesion of Figure 2B (HE staining, 200 ×).

CONCLUSION

This case demonstrates that although most mammary hamartomas are benign, there is a potential for malignancy. Breast MRI serves as a useful tool in detecting malignant lesions associated with mammary hamartomas. The ductal carcinoma arising from a mammary hamartoma can also cause metastasis, whereby cancer cells spread to adjacent or distant ductal lobular units. Therefore, a thorough evaluation of the lesion's nature and defined margins is necessary before proceeding with surgical treatment.

FOOTNOTES

Author contributions: Wei L drafted the manuscript; Wei L and Tian Z contributed equally to this study as co-first authors, both of two authors have made equally significant contributions to the work and share equal responsibility and accountability for it; Wei L, Tian Z and Wang ZY contributed to conception and design of the study; Tian Z and Li HB organized the database; Liu WJ and Zhang Y collected histopathological data; all authors contributed to manuscript revision, and have read and approved the submitted version.

Supported by Jilin City Science and Technology Innovation Development Plan Project, China, No. 20230406201; and Jilin Province Traditional Chinese Medicine Technology Project, China, No. 2024159.

Informed consent statement: The study participant's legal guardian, provided informed written consent prior to study enrollment.

Conflict-of-interest statement: The authors declare that they have no conflicts of interest.

CARE Checklist (2016) statement: The authors have read the CARE Checklist (2016), and the manuscript was prepared and revised according to the CARE Checklist (2016).

Open Access: This article is an open-access article that was selected by an in-house editor and fully peer-reviewed by external reviewers. It is distributed in accordance with the Creative Commons Attribution NonCommercial (CC BY-NC 4.0) license, which permits others to distribute, remix, adapt, build upon this work non-commercially, and license their derivative works on different terms, provided the original work is properly cited and the use is non-commercial. See: https://creativecommons.org/Licenses/by-nc/4.0/

Country of origin: China

ORCID number: Zhi-Yong Wang 0009-0009-4234-7268.

S-Editor: Luo ML
L-Editor: A
P-Editor: Zhang L

REFERENCES

1 **Hogeman KE**, Ostberg G. Three cases of postlactational breast tumour of a peculiar type. *Acta Pathol Microbiol Scand* 1968; **73**: 169-176 [PMID: 5662493 DOI: 10.1111/j.1699-0463.1968.tb00489.x]
2 **Arrigoni MG**, Dockerty MB, Judd ES. The identification and treatment of mammary hamartoma. *Surg Gynecol Obstet* 1971; **133**: 577-582 [PMID: 5096305]
3 **Fisher CJ**, Hanby AM, Robinson L, Millis RR. Mammary hamartoma--a review of 35 cases. *Histopathology* 1992; **20**: 99-106 [PMID: 1559675 DOI: 10.1111/j.1365-2559.1992.tb00938.x]
4 **Sevim Y**, Kocaay AF, Eker T, Celasin H, Karabork A, Erden E, Genc V. Breast hamartoma: a clinicopathologic analysis of 27 cases and a literature review. *Clinics (Sao Paulo)* 2014; **69**: 515-523 [PMID: 25141109 DOI: 10.6061/clinics/2014(08)03]
5 **Mendiola H**, Henrik-Nielsen R, Dyreborg U, Blichert-Toft M, Al-Hariri JA. Lobular carcinoma in situ occurring in adenolipoma of the breast. Report of a case. *Acta Radiol Diagn (Stockh)* 1982; **23**: 503-505 [PMID: 7158415 DOI: 10.1177/028418518202300511]
6 **Choi N**, Ko ES. Invasive ductal carcinoma in a mammary hamartoma: case report and review of the literature. *Korean J Radiol* 2010; **11**: 687-691 [PMID: 21076596 DOI: 10.3348/kjr.2010.11.6.687]
7 **Kai M**, Tada K, Tamura M, Gomi N, Horii R, Akiyama F, Iwase T. Breast cancer associated with mammary hamartoma. *Breast Cancer* 2012; **19**: 183-186 [PMID: 19657714 DOI: 10.1007/s12282-009-0147-3]
8 **Lambert J**, Jerjir N, Casselman J, Steyaert L. Invasive lobular carcinoma arising in a hamartoma of the breast: a case report. *Clin Breast Cancer* 2015; **15**: e63-e66 [PMID: 25240620 DOI: 10.1016/j.clbc.2014.07.011]
9 **Komaki K**, Funagayama M, Saitoh T, Maeda Y, Hayashi T, Kanematsu M, Tangoku A. Ductal carcinoma in situ of the breast arising in

encapsulated mammary hamartoma ; A case report. *J Med Invest* 2020; **67**: 368-371 [PMID: 33148919 DOI: 10.2152/jmi.67.368]

10 **Pervatikar SK**, Rao R, Dinesh US, Parameswaraiah S. Large mammary hamartoma with focal invasive ductal carcinoma. *Indian J Pathol Microbiol* 2009; **52**: 249-251 [PMID: 19332930 DOI: 10.4103/0377-4929.48935]

11 **Kemp TL**, Kilgore MR, Javid SH. Invasive ductal carcinoma arising within a large mammary hamartoma. *Breast J* 2015; **21**: 196-197 [PMID: 25613435 DOI: 10.1111/tbj.12378]

12 **Fukai S**, Yoshida A, Akiyama F, Tsunoda H, Lefor AK, Kimura J, Sakamoto T, Suzuki K, Mizokami K. Ductal Carcinoma in situ of the breast in sclerosing adenosis encapsulated by a hamartoma: A case report. *Int J Surg Case Rep* 2018; **45**: 9-12 [PMID: 29554537 DOI: 10.1016/j.ijscr.2018.03.002]

13 **Coyne J**, Hobbs FM, Boggis C, Harland R. Lobular carcinoma in a mammary hamartoma. *J Clin Pathol* 1992; **45**: 936-937 [PMID: 1430271 DOI: 10.1136/jcp.45.10.936]

14 **Anani PA**, Hessler C. Breast hamartoma with invasive ductal carcinoma. Report of two cases and review of the literature. *Pathol Res Pract* 1996; **192**: 1187-1194 [PMID: 9182287 DOI: 10.1016/S0344-0338(96)80149-X]

15 **Baron M**, Ladonne JM, Gravier A, Picquenot JM, Berry M. Invasive lobular carcinoma in a breast hamartoma. *Breast J* 2003; **9**: 246-248 [PMID: 12752637 DOI: 10.1046/j.1524-4741.2003.09313.x]

16 **Lee EH**, Wylie EJ, Bourke AG, Bastiaan De Boer W. Invasive ductal carcinoma arising in a breast hamartoma: two case reports and a review of the literature. *Clin Radiol* 2003; **58**: 80-83 [PMID: 12565210 DOI: 10.1053/crad.2003.1133]

17 **Ruiz-Tovar J**, Reguero-Callejas ME, Aláez AB, Ramiro C, Rojo R, Collado MV, González-Palacios F, Muñoz J, García-Villanueva A. Infiltrating ductal carcinoma and ductal carcinoma in situ associated with mammary hamartoma. *Breast J* 2006; **12**: 368-370 [PMID: 16848850 DOI: 10.1111/j.1075-122X.2006.00279.x]

18 **Mester J**, Simmons RM, Vazquez MF, Rosenblatt R. In situ and infiltrating ductal carcinoma arising in a breast hamartoma. *AJR Am J Roentgenol* 2000; **175**: 64-66 [PMID: 10882247 DOI: 10.2214/ajr.175.1.1750064]

19 **Tse GM**, Law BK, Pang LM, Cheung HS. Ductal carcinoma in situ arising in mammary hamartoma. *J Clin Pathol* 2002; **55**: 541-542 [PMID: 12101205 DOI: 10.1136/jcp.55.7.541]

20 **Kuroda N**, Sugimoto T, Numoto S, Enzan H. Microinvasive lobular carcinoma associated with intraductal spread arising in a mammary hamartoma. *J Clin Pathol* 2002; **55**: 76-77 [PMID: 11825932 DOI: 10.1136/jcp.55.1.76]

21 **Ohtake T**, Kimijima I, Fukushima T, Yasuda M, Sekikawa K, Takenoshita S, Abe R. Computer-assisted complete three-dimensional reconstruction of the mammary ductal/lobular systems: implications of ductal anastomoses for breast-conserving surgery. *Cancer* 2001; **91**: 2263-2272 [PMID: 11413514 DOI: 10.1002/1097-0142(20010615)91:12<2263::aid-cncr1257>3.0.co;2-5]

22 **Going JJ**, Moffat DF. Escaping from Flatland: clinical and biological aspects of human mammary duct anatomy in three dimensions. *J Pathol* 2004; **203**: 538-544 [PMID: 15095476 DOI: 10.1002/path.1556]

23 **Halliwell TM**. Atlas of Ultrasound and Ductal Echography of the Breast (1995) Blackwell Science,Germany. *Clin Radiol* 1996

24 **Chin K**, de Solorzano CO, Knowles D, Jones A, Chou W, Rodriguez EG, Kuo WL, Ljung BM, Chew K, Myambo K, Miranda M, Krig S, Garbe J, Stampfer M, Yaswen P, Gray JW, Lockett SJ. In situ analyses of genome instability in breast cancer. *Nat Genet* 2004; **36**: 984-988 [PMID: 15300252 DOI: 10.1038/ng1409]

25 **Casasent AK**, Schalck A, Gao R, Sei E, Long A, Pangburn W, Casasent T, Meric-Bernstam F, Edgerton ME, Navin NE. Multiclonal Invasion in Breast Tumors Identified by Topographic Single Cell Sequencing. *Cell* 2018; **172**: 205-217 [PMID: 29307488 DOI: 10.1016/j.cell.2017.12.007]

World Journal of Clinical Cases

Submit a Manuscript: https://www.f6publishing.com

World J Clin Cases 2025 June 26; 13(18): 102194

DOI: 10.12998/wjcc.v13.i18.102194

ISSN 2307-8960 (online)

CASE REPORT

Misdiagnosis of psoriatic arthritis in a patient with paronychia confirmed by dermatological examination: A case report

Angelo Nigro

Specialty type: Medicine, research and experimental

Provenance and peer review: Unsolicited article; Externally peer reviewed.

Peer-review model: Single blind

Peer-review report's classification

Scientific Quality: Grade D

Novelty: Grade C

Creativity or Innovation: Grade C

Scientific Significance: Grade C

P-Reviewer: Zhou C

Received: October 11, 2024

Revised: December 11, 2024

Accepted: February 18, 2025

Published online: June 26, 2025

Processing time: 138 Days and 22.5 Hours

Angelo Nigro, Department of Rheumatology of Lucania, UOSD of Rheumatology, "Madonna delle Grazie" Hospital, Matera 75100, Basilicata, Italy

Corresponding author: Angelo Nigro, MD, Chief Physician, Department of Rheumatology of Lucania, UOSD of Rheumatology, "Madonna delle Grazie" Hospital, Via Cattedra Ambulante, Matera 75100, Basilicata, Italy. angelonigro13@gmail.com

Abstract

BACKGROUND

This case highlights the importance of a multidisciplinary approach in differentiating localized infections from systemic inflammatory diseases like psoriatic arthritis. Nail psoriasis can mimic conditions like paronychia, complicating diagnosis. We wrote this report to emphasize the need for clinical vigilance when interpreting imaging findings, especially in patients with a family history of psoriasis. Misdiagnosis can lead to unnecessary systemic treatments, underscoring the significance of dermatological input in achieving accurate diagnoses.

CASE SUMMARY

A 56-year-old woman presented with redness and swelling of multiple fingertips. Her family history of psoriasis raised suspicion of psoriatic arthritis. Two rheumatologists diagnosed psoriatic arthritis based on ultrasound findings of enthesitis with a positive Doppler signal and recommended methotrexate. However, she was reluctant to initiate therapy due to potential side effects. At our Rheumatology Center, paronychia was suspected, and laboratory tests excluded systemic inflammatory arthritis. Dermatological examination confirmed paronychia, and treatment with fluconazole and ceftriaxone was initiated to address suspected mixed bacterial and fungal infections. Imaging studies, including hand and wrist X-rays, showed no erosions or other signs of psoriatic arthritis. The patient responded well to antimicrobial therapy, with resolution of symptoms. This case highlights the need for thorough clinical evaluation, careful interpretation of imaging findings, and collaboration between rheumatologists and dermatologists to avoid misdiagnosis and inappropriate treatment.

CONCLUSION

This case underscores the need for thorough clinical evaluation and caution in interpreting nonspecific imaging findings, especially in patients with a family history of psoriasis. While familial predisposition may raise suspicion for psoriatic arthritis, it is essential to integrate laboratory data, imaging studies, and clinical

presentation, including response to targeted antimicrobial therapy. A multidisciplinary approach, involving both rheumatologists and dermatologists, is crucial to preventing misdiagnosis, ensuring appropriate treatment, and avoiding the potential harms of unwarranted therapies.

Key Words: Psoriatic arthritis; Paronychia; Misdiagnosis; Multidisciplinary approach; Case report

©The Author(s) 2025. Published by Baishideng Publishing Group Inc. All rights reserved.

Core Tip: This case report emphasizes the importance of a multidisciplinary approach in distinguishing localized conditions, such as paronychia, from systemic inflammatory diseases like psoriatic arthritis. Misdiagnosis based on imaging findings, such as enthesitis with positive Doppler signal, can lead to unnecessary systemic treatments with potential adverse effects. A comprehensive clinical evaluation, including dermatological expertise, revealed paronychia as the underlying condition in a patient initially misdiagnosed with psoriatic arthritis. Timely antimicrobial therapy resolved the symptoms, highlighting the critical role of integrating clinical, imaging, and laboratory findings to avoid diagnostic errors and optimize patient outcomes.

Citation: Nigro A. Misdiagnosis of psoriatic arthritis in a patient with paronychia confirmed by dermatological examination: A case report. *World J Clin Cases* 2025; 13(18): 102194
URL: https://www.wjgnet.com/2307-8960/full/v13/i18/102194.htm
DOI: https://dx.doi.org/10.12998/wjcc.v13.i18.102194

INTRODUCTION

Accurate diagnosis is essential for appropriate treatment, especially when systemic diseases like psoriatic arthritis are suspected[1]. Psoriasis can involve the nails and, in some cases, present features that resemble paronychia. Recent literature suggests that nail psoriasis may mimic inflammatory conditions of the nail bed[2]. Moreover, paronychia can occur as an isolated condition or as a manifestation of underlying systemic diseases, adverse drug reactions, or chemical irritation[3]. We present the case of a 56-year-old woman with a family history of psoriasis, who was initially misdiagnosed with psoriatic arthritis. This case emphasizes the complexity of the differential diagnosis when familial predisposition to psoriasis is present.

CASE PRESENTATION

Chief complaints

The patient, a 56-year-old woman, presented with redness and swelling of multiple fingertips involving several digits (Figure 1).

History of present illness

The symptoms had been present for weeks, prompting consultations with two rheumatologists. Based on her family history of psoriasis and ultrasound findings suggestive of enthesitis with positive Doppler signals, she was diagnosed with psoriatic arthritis and prescribed methotrexate, which she declined due to concerns about side effects.

History of past illness

Her medical history was unremarkable, with no prior systemic inflammatory diseases, significant infections, or chronic illnesses.

Personal and family history

Her father had a history of psoriasis, raising suspicion for psoriatic arthritis.

Physical examination

Examination revealed erythema and swelling localized to the fingertips, with no other psoriatic skin lesions or arthritic signs beyond the digital involvement.

Laboratory examinations

Blood tests, including inflammatory markers, were normal, excluding systemic inflammatory arthritis. HLA-B27 testing was not performed.



Figure 1 The photos show redness, nail alterations and swelling in the periungual region, particularly of the left hand's first finger and the right hand's third and fourth fingers.

Imaging examinations

Hand and wrist X-rays showed no erosions or features typical of psoriatic arthritis. However, an ultrasound examination reported enthesitis with positive Doppler signals (Figure 2), a finding commonly associated with psoriatic arthritis but also seen in other conditions[3,4].

FINAL DIAGNOSIS

The final diagnosis is paronychia, confirmed by dermatological examination.

TREATMENT

The patient was treated with fluconazole and ceftriaxone to address suspected bacterial and fungal pathogens.

OUTCOME AND FOLLOW-UP

The patient showed significant improvement, with resolution of symptoms after antimicrobial therapy.

DISCUSSION

This case highlights the importance of a cautious and comprehensive diagnostic approach. While a family history of psoriasis increases the index of suspicion for psoriatic arthritis, it is crucial to consider other diagnostic elements such as the CASPAR criteria for psoriatic arthritis, laboratory findings, and the presence or absence of characteristic skin or nail psoriatic lesions. The absence of radiographic changes, systemic inflammatory markers, and progression of joint involvement helped rule out psoriatic arthritis.

Paronychia can be due to bacterial, fungal, or mixed infections and may also result from underlying conditions such as diabetes, adverse drug reactions, or psoriasis. In cases of multifinger involvement, as seen here, one should carefully consider systemic factors. Despite the family history of psoriasis, our patient's presentation and laboratory findings did not support psoriatic arthritis. Instead, the clinical and therapeutic response strongly pointed towards an infectious etiology.

The empirical use of fluconazole alongside ceftriaxone was guided by dermatological consultation. Some cases of persistent paronychia may involve fungal colonization, especially when multiple digits are affected and the response to standard antibacterial treatment is uncertain. While fluconazole is typically reserved for confirmed fungal infections, it was chosen here to address the possibility of a fungal component. This approach led to rapid improvement, reinforcing the diagnosis of an infectious rather than inflammatory arthritic process.

Ultimately, a multidisciplinary approach involving rheumatologists and dermatologists is key to distinguishing between psoriatic arthritis and mimickers like paronychia[5] By carefully evaluating clinical, laboratory, and imaging findings, and considering underlying conditions that could lead to multifocal paronychia, clinicians can avoid misdiagnosis and unnecessary exposure to immunosuppressive therapy.

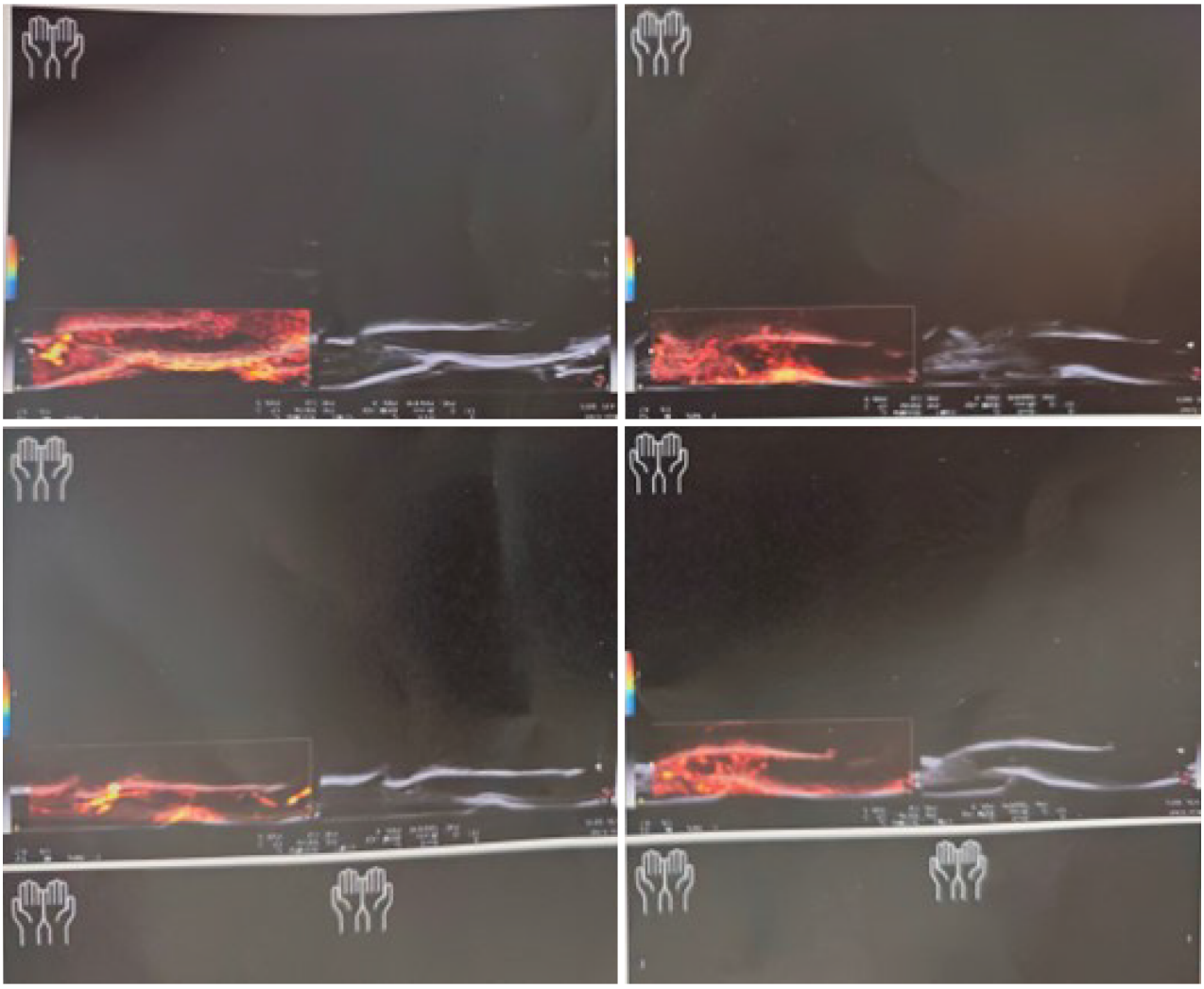


Figure 2 Ultrasound image with positive Doppler signal at the nail entheses of the left hand's third and fourth fingers.

CONCLUSION

This case underscores the need for thorough clinical evaluation and caution in interpreting nonspecific imaging findings, especially in patients with a family history of psoriasis. While familial predisposition may raise suspicion for psoriatic arthritis, it is essential to integrate laboratory data, imaging studies, and clinical presentation, including response to targeted antimicrobial therapy. A multidisciplinary approach, involving both rheumatologists and dermatologists, is crucial to preventing misdiagnosis, ensuring appropriate treatment, and avoiding the potential harms of unwarranted therapies.

FOOTNOTES

Author contributions: Nigro A is the sole author of this manuscript. He was responsible for the conception, design, analysis, and interpretation of the data. He also drafted and critically revised the manuscript, ensuring the accuracy and integrity of all aspects of the work.

Informed consent statement: Written informed consent was obtained from the patient (or their legal guardian, if applicable) for the publication of this case report, including all accompanying images and clinical information. Every effort was made to ensure the patient's anonymity and confidentiality.

Conflict-of-interest statement: The author, Angelo Nigro, declares no conflicts of interest related to the publication of this manuscript. No financial, personal, or professional relationships that could be perceived to influence the content of this work exist.

CARE Checklist (2016) statement: The authors have read the CARE Checklist (2016), and the manuscript was prepared and revised according to the CARE Checklist (2016).

Open Access: This article is an open-access article that was selected by an in-house editor and fully peer-reviewed by external reviewers. It is distributed in accordance with the Creative Commons Attribution NonCommercial (CC BY-NC 4.0) license, which permits others to distribute, remix, adapt, build upon this work non-commercially, and license their derivative works on different terms, provided the original work is properly cited and the use is non-commercial. See: https://creativecommons.org/Licenses/by-nc/4.0/

Country of origin: Italy

ORCID number: Angelo Nigro 0009-0001-0802-6825.

S-Editor: Lin C
L-Editor: A
P-Editor: Zhang L

REFERENCES

1 **van de Kerkhof PC**. From Empirical to Pathogenesis-Based Treatments for Psoriasis. *J Invest Dermatol* 2022; **142**: 1778-1785 [PMID: 35249726 DOI: 10.1016/j.jid.2022.01.014]
2 **Lee DK**, Lipner SR. Optimal diagnosis and management of common nail disorders. *Ann Med* 2022; **54**: 694-712 [PMID: 35238267 DOI: 10.1080/07853890.2022.2044511]
3 **Kehl AS**, Corr M, Weisman MH. Review: Enthesitis: New Insights Into Pathogenesis, Diagnostic Modalities, and Treatment. *Arthritis Rheumatol* 2016; **68**: 312-322 [PMID: 26473401 DOI: 10.1002/art.39458]
4 **Visalli E**, Crispino N, Foti R. Multidisciplinary Management of Psoriatic Arthritis: The Benefits of a Comprehensive Approach. *Adv Ther* 2019; **36**: 806-816 [PMID: 30805821 DOI: 10.1007/s12325-019-00901-0]
5 **Zhou C**, Yu G, Wang Q, Yang Z, Wang H, Zhao Y. Global trends and hotspots in research of paronychia: A bibliometric analysis. *Medicine (Baltimore)* 2024; **103**: e39838 [PMID: 39331909 DOI: 10.1097/MD.0000000000039838]

World Journal of Clinical Cases

Submit a Manuscript: https://www.f6publishing.com

World J Clin Cases 2025 June 26; 13(18): 103055

DOI: 10.12998/wjcc.v13.i18.103055

ISSN 2307-8960 (online)

CASE REPORT

Primary mucosa associated lymphoid tissue lymphoma of the gallbladder: A case report and review of literature

Mi-Rin Lee, Kyu-Yun Jang, Jae-Do Yang

Specialty type: Medicine, research and experimental

Provenance and peer review: Unsolicited article; Externally peer reviewed.

Peer-review model: Single blind

Peer-review report's classification
Scientific Quality: Grade B, Grade C
Novelty: Grade B, Grade B
Creativity or Innovation: Grade A, Grade C
Scientific Significance: Grade A, Grade C

P-Reviewer: Regmi P; Wang ZS

Received: November 12, 2024
Revised: December 21, 2024
Accepted: January 27, 2025
Published online: June 26, 2025
Processing time: 107 Days and 23.8 Hours

Mi-Rin Lee, Jae-Do Yang, Department of Surgery, Jeonbuk National University Hospital, Jeonju 54907, Jeollabuk-do, South Korea

Mi-Rin Lee, Kyu-Yun Jang, Jae-Do Yang, Research Institute of Clinical Medicine, Jeonbuk National University, Jeonju 54907, Jeollabuk-do, South Korea

Mi-Rin Lee, Kyu-Yun Jang, Jae-Do Yang, Biomedical Research Institute, Jeonbuk National University Hospital, Jeonju 54907, Jeollabuk-do, South Korea

Kyu-Yun Jang, Department of Pathology, Jeonbuk National University Hospital, Jeonju 54907, Jeollabuk-do, South Korea

Corresponding author: Jae-Do Yang, MD, PhD, Professor, Department of Surgery, Jeonbuk National University Hospital, No. 20 Geonjiro Deokjin-gu, Jeonju 54907, Jeollabuk-do, South Korea. yjd@jbnu.ac.kr

Abstract

BACKGROUND

The primary lymphomas of mucosa associated lymphoid tissue (MALT) of the gallbladder (GB) is an extremely rare of non-Hodgkin lymphoma. Many patients exhibit symptoms like gallstone disease, and in some cases, the lymphoma may be detected through imaging even without apparent symptoms. Only 19 cases of primary MALT lymphoma in the GB have been previously reported. Differential diagnosis from typical GB carcinoma based solely on imaging findings can be challenging, and definitive diagnosis often requires surgical intervention.

CASE SUMMARY

We present a patient in an 82-year-old man who was initially diagnosed with prostate cancer but incidentally detected GB wall thickening from magnetic resonance imaging conducted for prostatic surgery and subsequent radical cholecystectomy revealed primary MALT lymphoma of the GB. The patient was followed up by a medical oncologist, and after discussion, the decision was made to continue observation with close monitoring without systemic chemotherapy given the asymptomatic presentation. The patient has been free of recurrence for 16 months after the surgery. Although precise diagnosis before the surgery was difficult in this case, preoperative examinations revealed a submucosal tumor-like lesion.

CONCLUSION
MALT lymphoma of GB remains little known in many previous studies. It is really difficult to preoperatively diagnose. The combination of clinical presentation, postoperative histology and immunohistochemistry contribute to diagnosis and carry out appropriate management.

Key Words: Mucosa-associated lymphoid tissue lymphoma; Gallbladder; Cholecystectomy; Literature review; Case report

©The Author(s) 2025. Published by Baishideng Publishing Group Inc. All rights reserved.

Core Tip: Mucosa-associated lymphoid tissue lymphoma of the gallbladder (GB) often presents symptoms similar to cholecystitis. In addition, diagnosis and treatment through surgical resection should not be delayed, as distinguishing it from GB cancer on imaging is difficult. The prognosis is favorable after surgical resection, allowing monitoring with appropriate follow-up.

Citation: Lee MR, Jang KY, Yang JD. Primary mucosa associated lymphoid tissue lymphoma of the gallbladder: A case report and review of literature. *World J Clin Cases* 2025; 13(18): 103055
URL: https://www.wjgnet.com/2307-8960/full/v13/i18/103055.htm
DOI: https://dx.doi.org/10.12998/wjcc.v13.i18.103055

INTRODUCTION

Mucosa-associated lymphoid tissue (MALT) lymphoma is characterized by the neoplastic proliferation of B-cells within the marginal zone of lymphoid tissue, classifying it as a marginal zone B-cell lymphoma. MALT lymphoma can manifest in various extranodal sites, including the stomach, gastrointestinal tract, thyroid, salivary glands, lungs, and skin[1]. In contrast to nodal lymphomas, MALT lymphomas pose diagnostic challenges owing to their diverse organ involvement and nonspecific symptoms.

The incidence of primary MALT lymphoma in the gallbladder (GB) is exceptionally rare, making it challenging to determine, with few documented cases[1-3]. Here, we present a case of MALT lymphoma of the GB and provide a review of the pertinent literature.

CASE PRESENTATION

Chief complaints

An 82-year-old male with a history of prostate cancer was found incidentally to have thickening of the GB wall (9 mm) involving the liver parenchyma on prostate magnetic resonance imaging (MRI) (Figure 1).

History of present illness

The patient had no specific symptoms of chronic or acute cholecystitis, such as abdominal pain, fever, nausea, vomiting, or indigestion. He was hospitalized for further examination because of suspected GB cancer or adenoma.

History of past illness

The patient was diagnosed with hepatitis B virus (HBV) infection and liver cirrhosis 30 years ago. Twenty years prior, he underwent left lateral hepatic sectionectomy for hepatocellular carcinoma (HCC) and was followed-up for five years, with no HCC recurrence.

Personal and family history

The patient's family history had no notable findings.

Physical examination

Physical examination revealed a soft and non-tender abdomen without rebound tenderness or Murphy's sign.

Laboratory examinations

Laboratory tests revealed the following results: White blood cell count, 6710/μL; red blood cell count, 427 × 10^4/μL; platelet count, 286 × 10^3/μL; total protein, 7.6 g/dL; albumin, 4.8 g/dL; aspartate aminotransferase, 22 IU/L; alanine aminotransferase, 16 IU/L; alkaline phosphatase, 79 IU/L; gamma-glutamyl transferase, 38 IU/L; lactate dehydrogenase, 165 IU/L; total bilirubin, 0.60 mg/dL; direct bilirubin, 0.21 mg/dL; and C-reactive protein, 0.02 mg/dL.

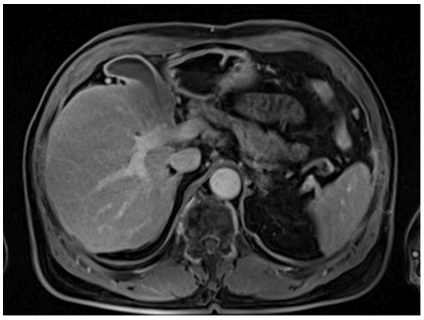


Figure 1 Magnetic resonance imaging of gallbladder. Prostate magnetic resonance imaging depicted the gallbladder wall thickening (10 mm) with a low-intensity relative to the liver parenchyma on the T1-weighted.

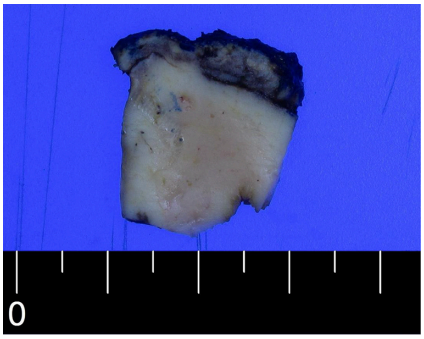


Figure 2 Macroscopic image of gallbladder. The gallbladder wall appeared to be broadly thickened by approximately 1 cm.

The HBV markers were HBsAg-negative, Anti-HBe-positive, and HBsAb-positive, with an HBV DNA titer of 695 IU/mL. Tumor markers were all normal: carcinoembryonic antigen 2.68 ng/mL; carbohydrate antigen 19-9 9.27 U/mL; total prostate-specific antigen 3.2 ng/mL; alpha-fetoprotein 2.30 ng/mL; and prothrombin induced by vitamin K absence-II 27 mAU/mL.

Macroscopically, the GB wall appeared broadly thickened by approximately 1 cm (Figure 2). Microscopic examination revealed the infiltration of lymphoid tumor cells throughout all layers of the GB wall (Figure 3A). These tumor cells also infiltrated the GB mucosa and liver parenchyma (Figure 3B and C), exhibiting a diffuse pattern with small and inconspicuous nucleoli (Figure 3D). The cells infiltrated the cytokeratin-positive GB mucosa; however, no lymphoepithelial lesions were observed (Figure 3E).

Immunohistochemical staining showed that the tumor cells were positive for CD20, BCL2, and κ light chain (Figure 3F–H). However, they were negative for TdT, CD3, CD5, CD10, BCL6, CD23, cyclin D1, and λ light chain (Figure 3I–P). The tumor cells had a Ki-67 index of 10%.

Imaging examinations

MRI revealed GB wall thickening (10 mm) with low intensity relative to the liver parenchyma on T1-weighted MRI (Figure 1).

A thickened GB wall (10 mm) was also observed on contrast-enhanced computed tomography (CECT) with homogeneous enhancement in the arterial, portal, and delayed phases (Figure 4). CECT also showed laminar enhancement in the liver bed, indicating hepatic invasion. These imaging findings did not conclusively distinguish the lesion as malignant. There were no specific findings, such as metastasis, on chest CT.

FINAL DIAGNOSIS

Based on these findings, the patient received a diagnosis of GB MALT lymphoma.

TREATMENT

The patient underwent an open cholecystectomy with a sleeve resection of the liver and surrounding lymph nodes dissection. During surgery, a frozen biopsy of the cystic duct confirmed a diagnosis of lymphoma. However, additional bile duct resection was not considered, and surgery was performed.

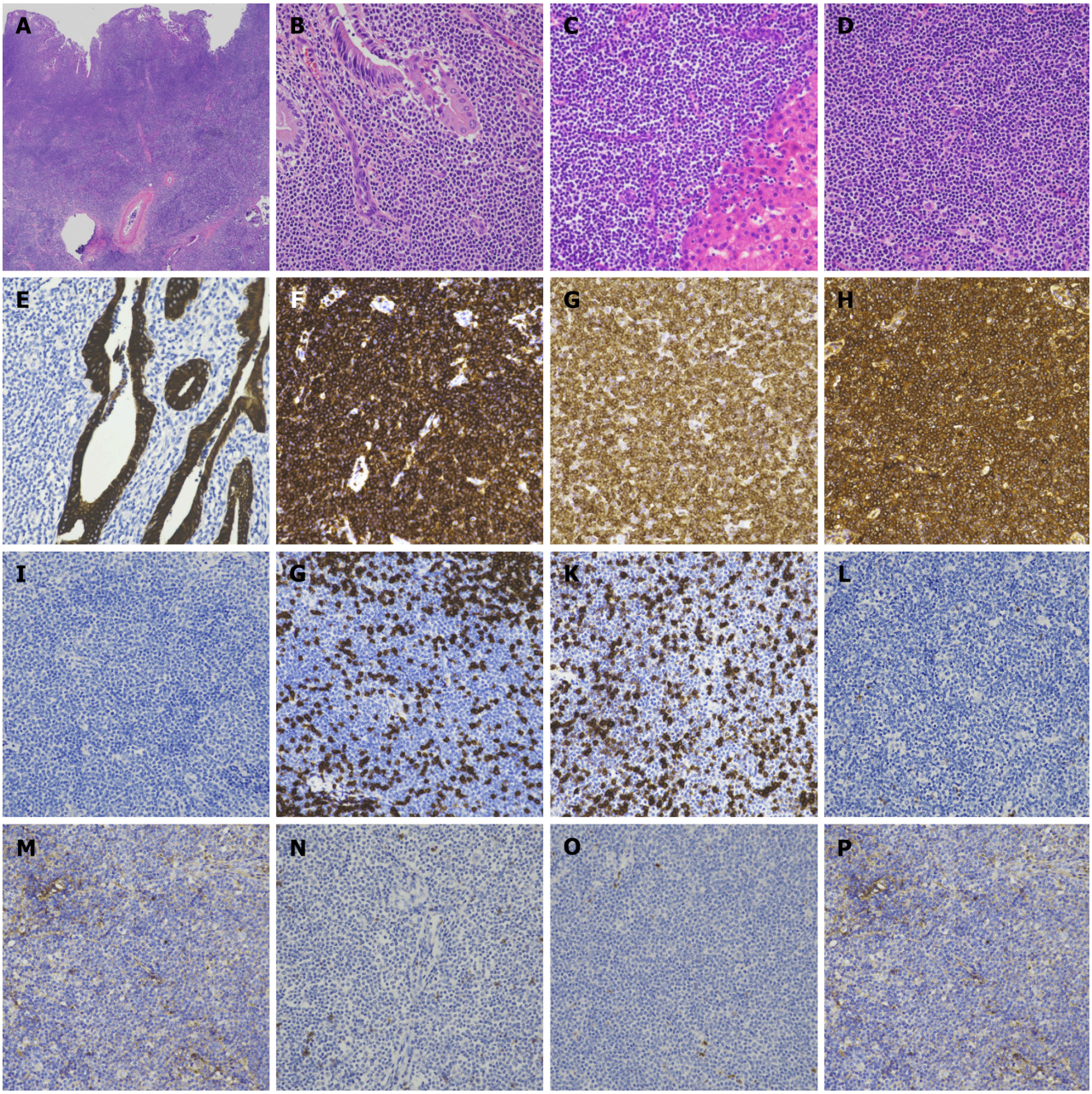


Figure 3 Histologic findings of mucosa associated lymphoid tissue lymphoma of the gallbladder. A: Lymphoid tumor cells infiltrate whole layers of the gallbladder wall; B-C: Tumor cells infiltrate around the gallbladder mucosa (B) and liver parenchyma (C); D: Diffusely infiltrating tumor cells are small sized with inconspicuous nucleoli; E: Tumor cells infiltrate between cytokeratin-positive gallbladder mucosa, but do not form a lymphoepithelial lesion; F-H: Tumor cells are positive for CD20 (F), BCL2 (G), and Kappa light chain (H); I-P: Tumor cells are negative for TdT (I), CD3 (J), CD5 (K), CD10 (L), BCL6 (M), CD23 (N), cyclin D1 (O), and Lambda light chain (P). Original magnification: A: × 40; B-P: × 400.

OUTCOME AND FOLLOW-UP

Postoperatively, positron emission tomography/CT, bone marrow biopsy, and endoscopy were performed, revealing stage I disease. Testing for *Helicobacter pylori* (*H. pylori*) and HCV infections, which are known causes of MALT lymphoma, was negative. Given the patient's advanced age, systemic chemotherapy and radiation therapy were not pursued. Instead, the patient is monitored in the outpatient setting, with follow-up visits scheduled every 3–6 months for five years, followed by annual checkups. The patient remained recurrence-free for 16 months postoperatively.

DISCUSSION

Malignant lymphoma of GB accounts for only 0.1 to 0.2% of all GB cancer patients. The most common subtype is the MALT lymphoma account for 40%, followed by diffuse large B-cell lymphoma[1,4]. MALT lymphoma accounts for approximately 8% of all non-Hodgkin lymphomas, predominantly affecting middle-aged and older individuals (ranging

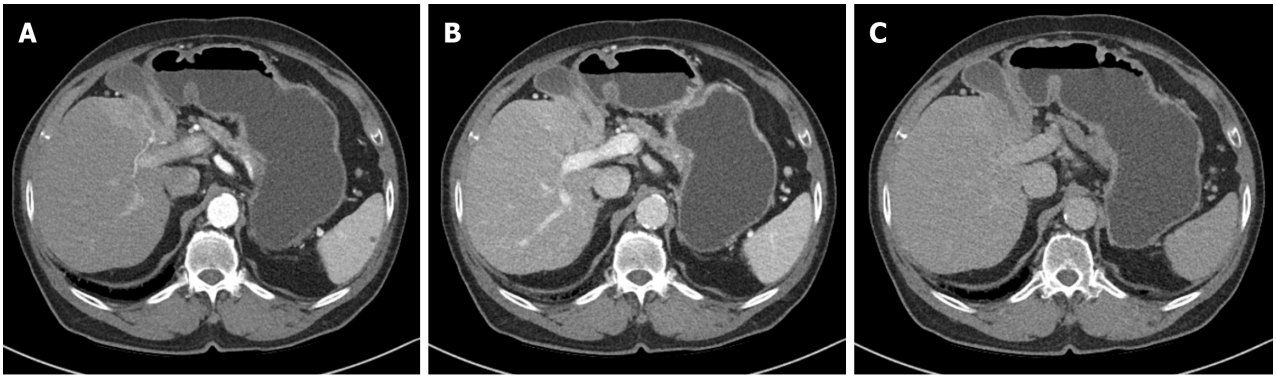


Figure 4 Abdomen contrast-enhanced computed tomography imaging. A: Thickened gallbladder wall (10 mm) was observed with homogeneous enhancement shown on the arterial; B: Thickened gallbladder wall (10 mm) was observed with homogeneous enhancement shown on the portal; C: Thickened gallbladder wall (10 mm) was observed with homogeneous enhancement shown on the delayed phases. Also, contrast-enhanced computed tomography showed laminar enhancement on the liver bed, which indicated invasion of the hepatic bed.

from 31 to 84 years), especially women (65%)[4]. MALT lymphoma arises in mucosal tissues and can manifest in various organs. They are divided into gastric (50%) and non-gastric lymphomas [salivary glands (13%), skin (6%), orbits (5%), thyroid gland, lungs and mammary gland] depending on its location[4]. However, involvement of the GB is rare, with only approximately 19 cases reported in the English literature[1-3].

Primary MALT lymphoma of the GB has an unclear pathogenesis due to the absence of lymphoid tissue in the GB wall. One hypothesized suggests that lymphocyte migration may occur as a result of bacterial infections, such as chronic cholecystitis or cholelithiasis. In addition, antigenic stimulation may lead to the formation of a fusion protein called API2-MALT1, which induces antigen-independent cell proliferation and inhibits apoptosis through NF-κB-mediated upregulation of anti-apoptotic genes, ultimately contributes to the development of MALT lymphoma[5]. Another possible mechanism is that consistent chronic inflammation results in irreversible genetic rearrangements, which inactivate the cell's response to IL-2 regulation, eventually helping to develop MALT lymphoma[6].

In most cases, surgical resection is performed to distinguish between cholecystitis, GB cancer, and lymphoma, with final diagnosis confirmed by immunostaining. In chronic cholecystitis, immunohistochemistry (IHC) reveals a mononuclear cell infiltrate composed of both T and B lymphocytes, and macrophages[7]. GB cancer exhibits specific markers associated with prognosis and tumor behavior. The IHC in GB cancer shows overexpression of *PLA2GA*, particularly in early-stage GB cancer and positive staining for MRP2, CXCR4 and PD-L1, which is associated with better prognosis in late-stage tumor[8]. MALT lymphoma displays characteristic B-cell markers and lymphoepithelial lesions that atypical lymphocytes infiltrating all layers of the GB wall. The IHC in MALT lymphoma of GB demonstrates positive staining for CD 20 and BCL-237, otherwise negative staining for CD3, CD5, BCL-6, CD43, and cyclin D13. It has Ki67 proliferation index (PI) of approximately 5%[1,3]. These distinct immunostaining profiles aid in accurate diagnosis and guide appropriate treatment strategies for each condition.

Ki-67 is a nuclear protein that plays a crucial role in assessing tumor proliferation characteristics in gastric MALT lymphoma. The majority (85%) of gastric MALT lymphomas have a Ki-67 index ≤ 20%[9]. Also, The Ki-67 PI is used to determine the growth fraction of tumors and has significant implications for prognosis and treatment decisions. The Ki-67 PI is particularly useful in differentiating low-grade MALT lymphomas from high-grade lymphomas. A cut-off value of 45% can help differentiate indolent (low-grade) from aggressive (high-grade) lymphomas[10]. The assessment of Ki-67 in gastric MALT lymphoma can provide valuable information for monitoring patients at risk. But, in non-gastric MALT lymphoma, there are no studies on the roles.

As imaging alone does not reliably distinguish among these diagnoses, regular checkups are necessary for asymptomatic GB wall thickening. The common United States features of primary GB lymphoma present as thickening of the GB wall or a soft tissue mass located in GB with or without gallstone, which has lower echo compared to GB carcinoma[11]. According to reports from several cases, MRI findings for GB MALT lymphoma typically shown low intensity on T1-weighted sequences and high intensity on T2-weighted sequences compared to the liver parenchyma. The difference between GB cancer and MALT lymphoma in MRI is that the T2-weighted sequence signal intensity of GB MALT lymphoma is lower and more uniform compared to GB cancer[11,12].

The treatment strategy for MALT lymphoma depends on the location of the primary lesions. The most common type of MALT lymphoma, gastric MALT lymphoma, is caused by *H. pylori* infection, and can be successful resolved with *H. pylori* eradication therapy, leading to complete remission in 100% of cases[13]. In contrast, for MALT lymphoma originating in the GB, no treatment policy has been established, and surgery is the only diagnosis and treatment. With surgical treatment, prognosis is better, and only one of the 20 cases documented cases showed recurrence in the stomach five years after surgical resection, requiring chemotherapy[14]. The targeted approaches could potentially be applicable to GB MALT lymphoma, especially in cases where molecular profiling identifies relevant mutations or overexpression of these targets, such as EGFR inhibitors, FGFR inhibitors, HER2-targeted therapies, and PD-1/PD-L1 inhibitors[15]. Given the slow-growing nature of MALT lymphoma and its favorable prognosis following cholecystectomy, watchful waiting may be appropriate in asymptomatic cases; however, cholecystectomy is recommended for cases with symptomatic or significant GB wall thickening due to its good prognosis and difficulty distinguishing it from GB cancer.

Only 19 cases of MALT lymphoma of the GB have been reported in the English literature (Table 1). Including the present case, MALT lymphoma of the GB is more prevalent in women (60%), and the age of occurrence is widely diverse, ranging from 31 to 84 years (median, 74 years). Most patients present with symptoms resembling acute cholecystitis, right upper quadrant pain, nausea, and vomiting. In addition, 65% of cases are associated with cholelithiasis. However, in this case, it was accidentally detected as asymptomatic. It was confirmed as GB MALT lymphoma after surgical treatment because it was difficult to differentiate it from GB cancer radiologically. With the exception of one, they underwent cholecystectomy and there was no recurrence during the observation period.

Table 1 Published cases and radiological findings of mucosa associated lymphoid tissue lymphoma of the gallbladder

No	Age	Sex	Symptoms	Gallbladder stone	Radiological findings	Treatment	Recurrence	Ref.
1	80	M	-	N	Fairly nodular proliferation	-	Death from other causes	Honda *et al*[1]
2	60	F	RUQ pain, fever, nausea and vomiting	Y	Distended and thin	Cholecystectomy	No at 6 months	
3	75	F	RUQ pain, nausea and vomiting	Y	Mass	Cholecystectomy	No at 12 months	
4	82	M	Jaundice and abdominal pain	Y	Wall thickening	Cholecystectomy	Death from other causes	
5	74	F	RUQ pain and nausea	Y	-	-	-	
6	58	F	Abdominal pain	N	Polypoid lesions	Cholecystectomy	No at 24 months	
7	65	F	RUQ pain	N	-	Cholecystectomy (Chemotherapy)	Recurrence at 96 months in stomach	
8	31	F	RUQ pain	N	Wall thickening	Cholecystectomy	-	
9	60	F	Abnormal liver function tests	Y	-	Cholecystectomy	No at 3 months	
10	51	F	RUQ pain	Y	-	Cholecystectomy	No at 2 months	
11	75	F	RUQ pain	Y	Wall thickening	Cholecystectomy	No at 16 months	
12	78	M	Nothing	N	Polypoid lesions	Cholecystectomy	No at 3 months	
13	74	M	-	Y	-	-	-	
14	84	F	-	N	-	-	-	
15	65	F	RUQ pain and nausea	Y	Polypoid lesions	Cholecystectomy	No at 3 months	
16	73	M	Abdominal pain and distension	Y	Wall thickening	Laparoscopic cholecystectomy	No at 12 months	
17	80	M	RUQ pain	Y	Mass	Cholecystectomy	No at 39 months	
18	39	M	RUQ pain, fever, weight loss and fatigue	N	Mass	Laparoscopic cholecystectomy	-	Papamichail *et al*[3]
19	73	F	RUQ pain	Y	-	Laparoscopic cholecystectomy	No at 1 months	Farmah *et al*[2]
20	82	M	Nothing	N	Wall thickening	Radical cholecystectomy	No at 16 months	Present case

F: Female; M: Male; RUQ: Right upper quadrant.

CONCLUSION

MALT lymphoma originating from the GB is a rare disease with no established diagnostic tools. Given its clinical similarity to GB cancer and favorable prognosis following surgical resection, timely surgical intervention is recommended for both diagnosis and treatment.

FOOTNOTES

Author contributions: Yang JD and Lee MR designed the study and contributed to the manuscript writing; Jang KY contributed to

writing and reviewing the pathology, findings; all of the authors read and approved the final version of the manuscript to be published.

Supported by Biomedical Research Institute, Jeonbuk National University Hospital.

Informed consent statement: All study participants, or their legal guardian, provided informed written consent prior to study enrollment.

Conflict-of-interest statement: We have no conflicts of interest to disclose. All authors declare that they have no conflicts of interest.

CARE Checklist (2016) statement: The authors have read the CARE Checklist (2016), and the manuscript was prepared and revised according to the CARE Checklist (2016).

Open Access: This article is an open-access article that was selected by an in-house editor and fully peer-reviewed by external reviewers. It is distributed in accordance with the Creative Commons Attribution NonCommercial (CC BY-NC 4.0) license, which permits others to distribute, remix, adapt, build upon this work non-commercially, and license their derivative works on different terms, provided the original work is properly cited and the use is non-commercial. See: https://creativecommons.org/Licenses/by-nc/4.0/

Country of origin: South Korea

ORCID number: Mi-Rin Lee 0000-0001-7032-0390; Kyu-Yun Jang 0000-0002-5276-4446; Jae-Do Yang 0000-0001-9701-7666.

S-Editor: Liu H
L-Editor: A
P-Editor: Zhang XD

REFERENCES

1 **Honda M M D**, Furuta Y M D Ph D, Naoe H M D Ph D, Sasaki Y M D Ph D. Primary mucosa-associated lymphoid tissue (MALT) lymphoma of the gallbladder and review of the literature. *BMJ Case Rep* 2017; **2017** [PMID: 28551602 DOI: 10.1136/bcr-2017-220161]
2 **Farmah P**, Mehta AH, Vu AH, Tchokouani LS, Nazir S. Extranodal Marginal Zone Mucosa-Associated Lymphoid Tissue Lymphoma of the Gallbladder: A Case Report and Literature Review. *Cureus* 2023; **15**: e35825 [PMID: 37033512 DOI: 10.7759/cureus.35825]
3 **Papamichail M**, Dimitrokallis N, Gogoulou I, Nomikos A, Ioannides C. Primary Large Mucosa-Associated Lymphoid Tissue (MALT) Lymphoma of the Gallbladder. *Cureus* 2022; **14**: e23799 [PMID: 35518540 DOI: 10.7759/cureus.23799]
4 **Zucca E**, Conconi A, Pedrinis E, Cortelazzo S, Motta T, Gospodarowicz MK, Patterson BJ, Ferreri AJ, Ponzoni M, Devizzi L, Giardini R, Pinotti G, Capella C, Zinzani PL, Pileri S, López-Guillermo A, Campo E, Ambrosetti A, Baldini L, Cavalli F; International Extranodal Lymphoma Study Group. Nongastric marginal zone B-cell lymphoma of mucosa-associated lymphoid tissue. *Blood* 2003; **101**: 2489-2495 [PMID: 12456507 DOI: 10.1182/blood-2002-04-1279]
5 **Bagwan IN**, Ping B, Lavender L, de Sanctis S. Incidental presentation of gall bladder MALT lymphoma. *J Gastrointest Cancer* 2011; **42**: 61-64 [PMID: 20509055 DOI: 10.1007/s12029-010-9162-z]
6 **Cho YH**, Byun JH, Kim JH, Lee SS, Kim HJ, Lee MG. Primary malt lymphoma of the common bile duct. *Korean J Radiol* 2013; **14**: 764-768 [PMID: 24043969 DOI: 10.3348/kjr.2013.14.5.764]
7 **Jeffrey GP**, Reed WD, Carrello S, Shilkin KB. Histological and immunohistochemical study of the gall bladder lesion in primary sclerosing cholangitis. *Gut* 1991; **32**: 424-429 [PMID: 2026342 DOI: 10.1136/gut.32.4.424]
8 **Tittarelli A**, Barría O, Sanders E, Bergqvist A, Brange DU, Vidal M, Gleisner MA, Vergara JR, Niechi I, Flores I, Pereda C, Carrasco C, Quezada-Monrás C, Salazar-Onfray F. Co-Expression of Immunohistochemical Markers MRP2, CXCR4, and PD-L1 in Gallbladder Tumors Is Associated with Prolonged Patient Survival. *Cancers (Basel)* 2023; **15** [PMID: 37444550 DOI: 10.3390/cancers15133440]
9 **Zeggai S**, Harir N, Tou A, Sellam F, Mrabent MN, Salah R. Immunohistochemistry and scoring of Ki-67 proliferative index and p53 expression in gastric B cell lymphoma from Northern African population: a pilot study. *J Gastrointest Oncol* 2016; **7**: 462-468 [PMID: 27284480 DOI: 10.21037/jgo.2016.01.01]
10 **Broyde A**, Boycov O, Strenov Y, Okon E, Shpilberg O, Bairey O. Role and prognostic significance of the Ki-67 index in non-Hodgkin's lymphoma. *Am J Hematol* 2009; **84**: 338-343 [PMID: 19384938 DOI: 10.1002/ajh.21406]
11 **Ono A**, Tanoue S, Yamada Y, Takaji Y, Okada F, Matsumoto S, Mori H. Primary malignant lymphoma of the gallbladder: a case report and literature review. *Br J Radiol* 2009; **82**: e15-e19 [PMID: 19095809 DOI: 10.1259/bjr/30768802]
12 **Yamamoto T**, Kawanishi M, Yoshiba H, Kanehira E, Itoh H. Primary non-Hodgkin's lymphoma of the gallbladder. *AJR Am J Roentgenol* 2005; **184**: S86-S87 [PMID: 15728033 DOI: 10.2214/ajr.184.3_supplement.01840s86]
13 **Violeta Filip P**, Cuciureanu D, Sorina Diaconu L, Maria Vladareanu A, Silvia Pop C. MALT lymphoma: epidemiology, clinical diagnosis and treatment. *J Med Life* 2018; **11**: 187-193 [PMID: 30364585 DOI: 10.25122/jml-2018-0035]
14 **Chim CS**, Liang R, Loong F, Chung LP. Primary mucosa-associated lymphoid tissue lymphoma of the gallbladder. *Am J Med* 2002; **112**: 505-507 [PMID: 11959069 DOI: 10.1016/s0002-9343(01)01132-9]
15 **Zhou Y**, Yuan K, Yang Y, Ji Z, Zhou D, Ouyang J, Wang Z, Wang F, Liu C, Li Q, Zhang Q, Li Q, Shan X, Zhou J. Gallbladder cancer: current and future treatment options. *Front Pharmacol* 2023; **14**: 1183619 [PMID: 37251319 DOI: 10.3389/fphar.2023.1183619]

World Journal of Clinical Cases

Submit a Manuscript: https://www.f6publishing.com

World J Clin Cases 2025 June 26; 13(18): 103426

DOI: 10.12998/wjcc.v13.i18.103426

ISSN 2307-8960 (online)

CASE REPORT

Temporal changes in computed tomography findings of a persimmon bezoar: A case report

Masaya Iwamuro, Tomoki Yoshikawa, Tomohiro Kamio, Shoichiro Hirata, Katsunori Matsueda, Daisuke Kametaka, Motoyuki Otsuka

Specialty type: Medicine, research and experimental

Provenance and peer review: Invited article; Externally peer reviewed.

Peer-review model: Single blind

Peer-review report's classification

Scientific Quality: Grade C, Grade C, Grade D, Grade D

Novelty: Grade B, Grade C, Grade C, Grade C

Creativity or Innovation: Grade B, Grade C, Grade C, Grade C

Scientific Significance: Grade B, Grade B, Grade C, Grade C

P-Reviewer: Chaemsupaphan T, Lim KT, Namata TT,

Received: November 26, 2024

Revised: January 18, 2025

Accepted: February 6, 2025

Published online: June 26, 2025

Processing time: 93 Days and 16.2 Hours

Masaya Iwamuro, Tomoki Yoshikawa, Tomohiro Kamio, Shoichiro Hirata, Katsunori Matsueda, Daisuke Kametaka, Motoyuki Otsuka, Department of Gastroenterology and Hepatology, Okayama University Graduate School of Medicine, Dentistry and Pharmaceutical Sciences, Okayama 700-8558, Japan

Corresponding author: Masaya Iwamuro, MD, PhD, Assistant Professor, Department of Gastroenterology and Hepatology, Okayama University Graduate School of Medicine, Dentistry and Pharmaceutical Sciences, 2-5-1 Shikata-Cho, Kita-Ku, Okayama 700-8558, Japan. pr145h2k@okayama-u.ac.jp

Abstract

BACKGROUND

Gastric bezoars are masses of indigestible material that accumulate in the stomach, causing nausea, abdominal pain, and vomiting. Persimmon bezoars (diospyrobezoars), which comprise tannins and fibers from persimmons, are relatively rare but may cause significant gastric complications, including gastric outlet obstruction or ileus. Although computed tomography (CT) is a useful imaging tool, diagnosing bezoars can be challenging because their density is similar to that of food debris and gastric content.

CASE SUMMARY

Here, we report the case of a 72-year-old woman with a persimmon bezoar that was diagnosed using serial CT imaging and confirmed by endoscopy. CT performed over several months revealed changes in the internal structure and density of the bezoar, suggesting progressive hardening. The patient had a history of a partial gastrectomy and excessive persimmon consumption, both of which are risk factors for bezoar formation. Endoscopic fragmentation of the bezoar successfully resolved symptoms.

CONCLUSION

Gastric bezoars, particularly persimmon bezoars, present diagnostic challenges because of their variable imaging characteristics. Serial CT can document temporal changes in bezoar density, potentially reflecting changes in hardness. Early diagnosis and endoscopic treatment are essential for effective management, particularly in patients with predisposing factors. This case underscores the importance of considering bezoars in the differential diagnosis of gastric masses, and highlights the value of CT for monitoring changes in bezoar characteristics over

time.

Key Words: Computed tomography; Endoscopic treatment; Gastric bezoar; Persimmon bezoar; Temporal changes; Case report

©The Author(s) 2025. Published by Baishideng Publishing Group Inc. All rights reserved.

Core Tip: Gastric bezoars, particularly persimmon bezoars, are rare but significant clinical entities that can lead to complications such as gastric outlet obstruction and ileus. Diagnosis can be challenging because they often appear similar to food debris on imaging. Serial computed tomography can be used to document temporal changes in the internal structure and density of bezoars, reflecting their progressive hardening over time. Early recognition and endoscopic fragmentation remain the most effective management strategies, particularly in patients with predisposing factors such as prior gastric surgery or excessive persimmon consumption.

Citation: Iwamuro M, Yoshikawa T, Kamio T, Hirata S, Matsueda K, Kametaka D, Otsuka M. Temporal changes in computed tomography findings of a persimmon bezoar: A case report. *World J Clin Cases* 2025; 13(18): 103426
URL: https://www.wjgnet.com/2307-8960/full/v13/i18/103426.htm
DOI: https://dx.doi.org/10.12998/wjcc.v13.i18.103426

INTRODUCTION

Gastric bezoars are conglomerates of indigestible materials that accumulate in the stomach, leading to abdominal pain, bloating, nausea, and vomiting. Among the various types of bezoars, persimmon bezoars, or diospyrobezoars, are relatively rare and primarily comprise tannins and fibers found in persimmons. These substances can polymerize into a solid mass in the acidic gastric environment, particularly in individuals with predisposing factors, such as prior gastric surgery, delayed gastric emptying, and excessive persimmon consumption[1-5]. Diospyrobezoars are more prevalent in regions where persimmons are widely consumed, and pose a unique diagnostic challenge because of their nonspecific presentation[5].

Computed tomography (CT) plays a significant role in identifying gastric bezoars; however, the density of bezoars often resembles that of food debris or gastric contents, making them difficult to detect[6-10]. Misinterpretation of CT findings can delay the diagnosis and treatment of gastric bezoars, leading to complications, such as obstruction of the gastric outlet or migration to the small intestine, thereby causing ileus[11-13]. Serial imaging studies are rarely performed in the case of bezoars; as such, there is a limited understanding of the temporal changes in their physical properties over time, such as density and internal structure.

This report presents a unique case of a persimmon bezoar, focusing on serial CT findings that documented changes in the internal structure and density of the bezoar over time. These findings provide insights into the natural history of bezoars and suggest potential correlations between their imaging characteristics and physical properties. Additionally, this report emphasizes the importance of clinical context and dietary history in diagnosing and managing bezoars effectively.

CASE PRESENTATION

Chief complaints

A 72-year-old Japanese woman presenting with intermittent abdominal bloating and vomiting was referred to our hospital.

History of present illness

The patient had undergone a pylorus-preserving gastrectomy for gastric cancer and right oophorectomy at 43 years of age. At the age of 66 years, the patient was diagnosed with advanced colon cancer. Chemotherapy was initiated but discontinued after four courses because of adverse effects, and the patient subsequently declined further chemotherapy. As tumor shrinkage was achieved with treatment, the patient underwent right hemicolectomy for the ascending colon cancer, which included resection of the small intestine, ovary, and peritoneum, owing to tumor invasion. Due to intolerance to preoperative chemotherapy, the patient refused postoperative chemotherapy. The patient requested CT scans every three months, and no recurrence was noted after surgery.

The patient experienced abdominal fullness after meals and occasional vomiting from ingested food. However, because the symptoms were intermittent, the patient refused to take any medication. Seven months after symptom onset, she developed gastric obstruction, which made eating difficult, and she passed black stools for approximately 10 days. Following the onset of abdominal symptoms, the patient continued to undergo CT scans every three months to monitor for colorectal cancer recurrence, and the radiologist reported no notable abnormalities or signs of recurrence at the time of

imaging. She visited her primary care physician, who prescribed mosapride, famotidine, and *Clostridium butyricum* tablets, which partially relieved the symptoms. Nine months after the onset of the abdominal symptoms, the patient visited our hospital upon request. No endoscopic examinations were performed between abdominal symptom onset and her visit to our hospital.

At the time of her visit to our hospital, she was taking mosapride, famotidine, and *Clostridium butyricum* tablets. The patient was 150 cm tall and weighed 41 kg, resulting in a body mass index of approximately 18.2.

History of past illness

As previously described, the patient underwent a pylorus-preserving gastrectomy for gastric cancer and right oophorectomy at the age of 43 years. At 66 years of age, the patient underwent right hemicolectomy, including resection of the small intestine, ovary, and peritoneum, for advanced ascending colon cancer.

Personal and family history

The patient had no history of alcohol consumption or smoking, and no family history of malignancies or gastrointestinal diseases.

Physical examination

Physical examination revealed multiple scars on her abdomen from previous surgeries for gastric and colon cancers. Her abdomen was soft and flat without palpable masses or signs of peripheral lymphadenopathy.

Laboratory examinations

Laboratory tests at her initial visit showed anemia, with a red blood cell count of $3.3 \times 10^6/\mu L$, hemoglobin concentration of 10.7 g/dL, and hematocrit of 34.8%. Decreased levels of total protein (6.2 g/dL) and albumin (3.9 g/dL) were observed, along with increased levels of aspartate aminotransferase (45 U/L), alanine aminotransferase (43 U/L), gamma-glutamyl transpeptidase (66 U/L), lactate dehydrogenase [267 U/L (normal range: 124-222 U/L)], blood urea nitrogen (22.6 mg/dL), and creatinine (1.24 mg/dL). We considered her anemia, hypoalbuminemia, mild elevation of liver enzyme levels, and impaired renal function to be primarily attributable to malnutrition and dehydration resulting from insufficient oral intake. The carcinoembryonic antigen level was elevated to 9.76 ng/mL (normal range: 0-5 ng/mL), although it had fluctuated within this range over the past year. Cancer antigen 19-9 and other biochemical parameters were within normal limits.

Imaging examinations

Although medication from the patient's primary care physician partially relieved her symptoms, we performed esophagogastroduodenoscopy to further evaluate gastric obstruction and the passage of black stools. Esophagogastroduodenoscopy revealed an elongated black gastric bezoar, approximately 10 cm in length, within the stomach (Figure 1A). A review of the patient's dietary history revealed that she had consumed 4-5 persimmons daily for two weeks, approximately 10 months before presentation. Infrared spectrometry of the bezoar fragments showed a > 98% similarity to the spectra of the persimmon extracts (Figure 1B). Therefore, a definitive diagnosis of persimmon bezoar was established.

The gastric bezoar was not identified on previous CT scans, even according to the radiologist's interpretation. Upon reviewing the CT images obtained 12 months previously, no abnormalities were observed in the stomach (Figure 2A). However, a spherical lesion was observed within the stomach on CT performed nine months previously (Figure 2B, arrow). This lesion persisted on CT for six months, with changes observed in its internal structure (Figure 2C, arrows).

FINAL DIAGNOSIS

Based on the findings of esophagogastroduodenoscopy and infrared spectrometry of the bezoar fragments, the patient was diagnosed with a persimmon bezoar.

TREATMENT

Endoscopic fragmentation of the gastric bezoar was performed using alligator forceps (Figure 1C). The procedure was completed in 2.5 hours, during which the bezoar was fragmented into as many small pieces as possible (Figure 1D). Because the patient requested no sedation, an overtube was not used; therefore, repeated insertion and withdrawal of the endoscope were avoided, and bezoar fragment retrieval was not performed using a net device.

OUTCOME AND FOLLOW-UP

On the following day, follow-up esophagogastroduodenoscopy confirmed complete clearance of the bezoar fragments. The patient's symptoms resolved completely and no recurrence was observed during subsequent monitoring.

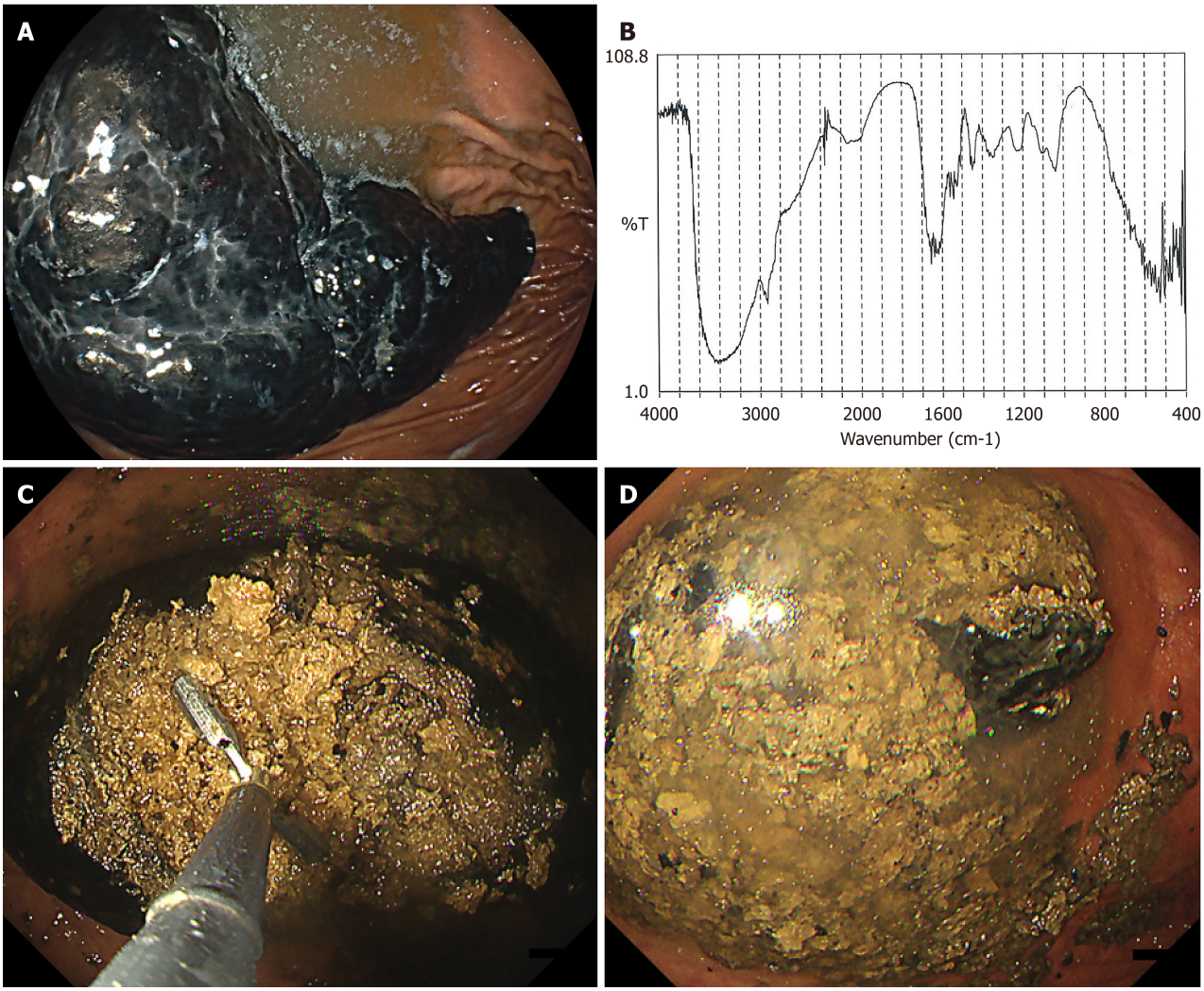


Figure 1 Endoscopic findings and treatment of persimmon bezoar. A: Esophagogastroduodenoscopy showing an elongated, black gastric bezoar approximately 10 cm in length; B: Infrared spectrometry of the bezoar fragments revealing a > 98% similarity to the spectra of persimmon extracts, confirming the diagnosis of persimmon bezoar; C: Endoscopic fragmentation of the bezoar using alligator forceps; D: Bezoar fragments after successful fragmentation. The procedure was completed in 2.5 hours.

DISCUSSION

When a mass lesion is detected in the stomach, differential diagnoses typically include neoplastic lesions such as gastric cancer, lymphoma, metastatic tumors, and gastrointestinal stromal tumors, as well as other conditions such as hyperplastic polyps and inflammatory pseudotumors[14-16]. In the present case, a spherical mass-like lesion suddenly appeared in the stomach. Initial CT revealed that the lesion contained air (Figure 1B); however, after three months, the lesion had changed to a homogeneous isodensity (Figure 1C). This finding was inconsistent with those mentioned above and suggested the possibility of a gastric bezoar[1,10].

The patient consumed 4-5 persimmons daily for two weeks, after which a gastric bezoar was detected on CT. Persimmon bezoars, also known as diospyrobezoars, are phytobezoars formed by the ingestion of persimmons[2-4]. Predisposing risk factors include prior gastric surgery such as partial gastrectomy, vagotomy, and pyloroplasty, as well as being an older adult or having diabetes[6,7,17,18]. These conditions result in reduced gastric acidity and delayed gastric emptying, which increase the likelihood of bezoar formation. Bezoars can cause abdominal pain, nausea, and vomiting, and obstruct the gastric outlets[19-21]. In some cases, mechanical irritation of the gastric mucosa by bezoars led to the formation of gastric ulcers[5,10], and in other cases, bezoars migrated to the small intestine, causing ileus[11-13]. The patient had a history of excessive persimmon consumption and partial gastrectomy, both of which are risk factors for gastric bezoar formation. Esophagogastroduodenoscopy revealed no gastric ulcers; however, an episode of black stool occurred two months earlier, possibly due to mucosal injury caused by the bezoar.

Infrared spectroscopy is a valuable tool for identifying the components of gastric bezoars[5]. It has been widely used to analyze urinary stones and to provide detailed information on their composition. Similarly, infrared spectroscopy can be applied to gastric bezoars to determine their constituent substances. By identifying the components of gastric bezoars, this technique aids in understanding their formation and contributes to the development of preventive strategies. Early identification and analysis of bezoar composition can lead to better management and potentially reduce the recurrence of

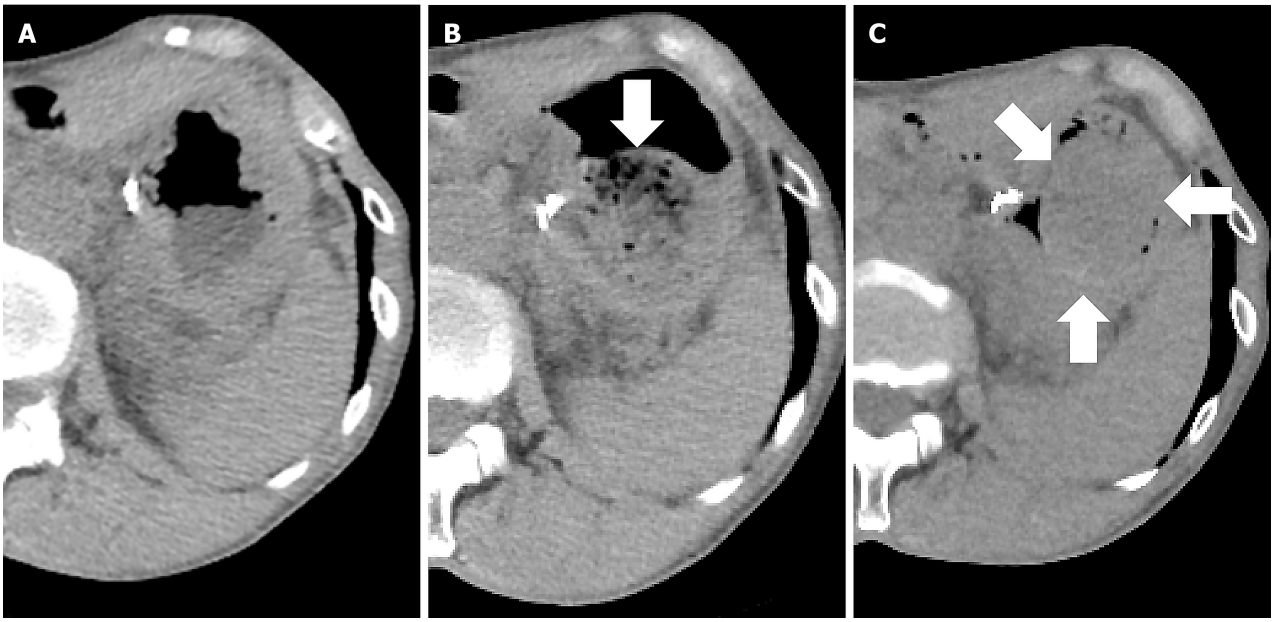


Figure 2 Computed tomography imaging of persimmon bezoar over time. A: Computed tomography (CT) image obtained 12 months prior to presentation showing no visible abnormality in the stomach; B: CT image obtained nine months prior showing a spherical lesion (arrow) within the stomach, suggestive of a gastric bezoar; C: CT image obtained six months prior showing the bezoar's internal structure and density changes, with the lesion becoming more homogeneous (arrows).

bezoars in at-risk patients. In the present case, infrared spectroscopy led to a definitive diagnosis of a persimmon bezoar. We believe that the recurrence of gastric bezoars can be prevented by advising patients to avoid persimmon consumption.

Bezoars can be difficult to detect using CT because their density is often similar to that of the surrounding gastric contents and soft tissues[6-10]. This is particularly true for phytobezoars, which have a density similar to that of food residue and gastric fluid, making them challenging to identify using imaging techniques. Therefore, additional diagnostic methods, such as endoscopy, are required. A previous study revealed that although eight of nine patients underwent CT before endoscopy, the bezoars were mistaken for food debris on CT findings and were overlooked[10]. The bezoar in this patient appeared on CT imaging but was not recognized as an abnormal finding. An interesting aspect of this case is that CT was performed every few months before and after the gastric bezoar formed. A CT scan performed after bezoar formation revealed a spherical mass containing air. However, three months later, the air within the bezoar was no longer visible, and the density became uniform. This suggests that the internal structure of gastric bezoars changes over time. Although there is no method for assessing changes in bezoar hardness over time, bezoars can become harder as time passes after their initial formation.

CONCLUSION

This case illustrates the temporal changes in gastric bezoars observed on CT and highlights the importance of correlating imaging findings with clinical history and dietary habits. Early recognition and timely endoscopic treatment are crucial for successful management of gastric bezoars, particularly in patients with predisposing risk factors. Notably, changes in the internal density of the bezoar observed on serial CT scans may reflect progressive hardening of the bezoar over time, providing valuable insights into its natural course.

FOOTNOTES

Author contributions: Iwamuro M wrote the manuscript; Yoshikawa T, Kamio T, Hirata S, Matsueda K, and Kametaka D contributed to the endoscopic diagnosis and treatment; Otsuka M revised the manuscript for important intellectual content; all the authors have read and approved the final manuscript.

Informed consent statement: Written informed consent was obtained from the patient before writing this manuscript.

Conflict-of-interest statement: The authors declare no conflict of interest related to this manuscript.

CARE Checklist (2016) statement: The authors have read the CARE Checklist (2016), and the manuscript was prepared and revised according to the CARE Checklist (2016).

Open Access: This is an open-access article selected by an in-house editor and fully peer-reviewed by external reviewers. It is distributed in accordance with the Creative Commons Attribution NonCommercial (CC BY-NC 4.0) license, which permits others to distribute, remix, adapt, build upon this work noncommercially and license their derivative works on different terms, provided that the original work is properly cited and the use is noncommercial. See: https://creativecommons.org/Licenses/by-nc/4.0/

Country of origin: Japan

ORCID number: Masaya Iwamuro 0000-0002-1757-5754; Tomohiro Kamio 0009-0004-5471-1753; Shoichiro Hirata 0009-0001-7814-9353; Katsunori Matsueda 0000-0002-6497-730X; Motoyuki Otsuka 0000-0003-2869-2881.

S-Editor: Luo ML
L-Editor: Wang TQ
P-Editor: Zhang L

REFERENCES

1 **Zhang RL**, Yang ZL, Fan BG. Huge gastric disopyrobezoar: a case report and review of literatures. *World J Gastroenterol* 2008; **14**: 152-154 [PMID: 18176981 DOI: 10.3748/wjg.14.152]
2 **Paschos KA**, Chatzigeorgiadis A. Pathophysiological and clinical aspects of the diagnosis and treatment of bezoars. *Ann Gastroenterol* 2019; **32**: 224-232 [PMID: 31040619 DOI: 10.20524/aog.2019.0370]
3 **Liu LN**, Wang L, Jia SJ, Wang P. Clinical Features, Risk Factors, and Endoscopic Treatment of Bezoars: A Retrospective Analysis from a Single Center in Northern China. *Med Sci Monit* 2020; **26**: e926539 [PMID: 33027245 DOI: 10.12659/MSM.926539]
4 **Ben-Porat T**, Sherf Dagan S, Goldenshluger A, Yuval JB, Elazary R. Gastrointestinal phytobezoar following bariatric surgery: Systematic review. *Surg Obes Relat Dis* 2016; **12**: 1747-1754 [PMID: 27989523 DOI: 10.1016/j.soard.2016.09.003]
5 **Iwamuro M**, Okada H, Matsueda K, Inaba T, Kusumoto C, Imagawa A, Yamamoto K. Review of the diagnosis and management of gastrointestinal bezoars. *World J Gastrointest Endosc* 2015; **7**: 336-345 [PMID: 25901212 DOI: 10.4253/wjge.v7.i4.336]
6 **Wang N**, Wu X, Lin X, Zhang S, Shen W. Computed tomography with clinical scoring to differentiate phytobezoar from feces in childhood small bowel obstruction. *Turk J Pediatr* 2023; **65**: 1002-1011 [PMID: 38204315 DOI: 10.24953/turkjped.2023.338]
7 **Sugimori H**, Masaki S, Honjo H, Kudo M, Watanabe T. Visualization of Gastrointestinal Bezoar Movement Causing and Releasing Small Bowel Obstruction on Computed Tomography in a Patient With Diabetes Mellitus. *Cureus* 2023; **15**: e49133 [PMID: 38130514 DOI: 10.7759/cureus.49133]
8 **Wiener BG**, Burton RL, Smith SW, Su MK, Biary R, Tay ET. A "madd"-ening confounding: fruit seeds mimicking enteral drug concealment by computed tomography. *Clin Toxicol (Phila)* 2023; **61**: 559-560 [PMID: 37403697 DOI: 10.1080/15563650.2023.2227760]
9 **Parker Cote JL**, Gerber BT, Lee H, Miller SN, Meggs WJ. Failure of Computed Tomography (CT) in Detecting an Aspirin Pharmacobezoar: A Case Report. *Am J Case Rep* 2022; **23**: e936752 [PMID: 36536587 DOI: 10.12659/AJCR.936752]
10 **Iwamuro M**, Tanaka S, Moritou Y, Inaba T, Higashi R, Kusumoto C, Yunoki N, Ishikawa S, Okamoto Y, Kawai Y, Kitada KI, Takenaka R, Toyokawa T, Okada H. Importance of Second-look Endoscopy on an Empty Stomach for Finding Gastric Bezoars in Patients with Gastric Ulcers. *Acta Med Okayama* 2017; **71**: 241-247 [PMID: 28655944 DOI: 10.18926/AMO/55207]
11 **Dikicier E**, Altintoprak F, Ozkan OV, Yagmurkaya O, Uzunoglu MY. Intestinal obstruction due to phytobezoars: An update. *World J Clin Cases* 2015; **3**: 721-726 [PMID: 26301232 DOI: 10.12998/wjcc.v3.i8.721]
12 **Kosmidis CS**, Mystakidou CM, Varsamis N, Koulouris C, Sevva C, Papadopoulou K, Michael C, Katsios NI, Theodorou V, Miltiadous P, Papadopoulos K, Vlassopoulos K, Zarampouka K, Mantalovas S. Phytobezoar-Induced Mechanical Ileus and Incipient Intussusception: A Case Report. *Medicina (Kaunas)* 2023; **59**: 1227 [PMID: 37512039 DOI: 10.3390/medicina59071227]
13 **Pal NL**, Panandiker SD, Katiyar G, Vernekar JA. Unusual causes of Small bowel obstruction: a review of the literature and revisited cross-sectional imaging checklist. *Emerg Radiol* 2024; **31**: 733-748 [PMID: 38926239 DOI: 10.1007/s10140-024-02256-8]
14 **Schulz C**, Schütte K, Malfertheiner P. Rare Neoplasia of the Stomach. *Gastrointest Tumors* 2015; **2**: 52-60 [PMID: 26674659 DOI: 10.1159/000435899]
15 **Humphris JL**, Jones DB. Subepithelial mass lesions in the upper gastrointestinal tract. *J Gastroenterol Hepatol* 2008; **23**: 556-566 [PMID: 18086121 DOI: 10.1111/j.1440-1746.2007.05232.x]
16 **Oda**, Kondo H, Yamao T, Saito D, Ono H, Gotoda T, Yamaguchi H, Yoshida S, Shimoda T. Metastatic tumors to the stomach: analysis of 54 patients diagnosed at endoscopy and 347 autopsy cases. *Endoscopy* 2001; **33**: 507-510 [PMID: 11437044 DOI: 10.1055/s-2001-14960]
17 **Riaz M**, Akbar I, Hassan RE, Ahmad W, Khan H, Khan AU, Khan MH, Shah SS, Tahir A, Tanveer S. Effect of Coca-Cola on the Dissolution of Persimmon-Related Phytobezoar in a Tertiary Care Hospital. *Cureus* 2024; **16**: e54420 [PMID: 38510864 DOI: 10.7759/cureus.54420]
18 **Gentile M**, Illario M, De Luca V, Cestaro G, Velotti N, Sivero S, Musella M. Gastrointestinal bezoars: Review of the literature and report of a rare case of pumpkin seed rectal impaction. *Asian J Surg* 2023; **46**: 3432-3436 [PMID: 37225563 DOI: 10.1016/j.asjsur.2023.05.030]
19 **Leung E**, Barnes R, Wong L. Bezoar in gastro-jejunostomy presenting with symptoms of gastric outlet obstruction: a case report and review of the literature. *J Med Case Rep* 2008; **2**: 323 [PMID: 18831730 DOI: 10.1186/1752-1947-2-323]
20 **Sulaiman Ambusaidi FM**, Al-Yaqoubi M. Gastric bezoar. *Int J Pediatr Adolesc Med* 2020; **7**: 199-200 [PMID: 33319020 DOI: 10.1016/j.ijpam.2020.05.002]
21 **Mahir S**, Salih AM, Ahmed OF, Kakamad FH, Salih RQ, Mohammed SH, Usf DC, Hassan HA, Abdulla F. Giant phytobezoar; an unusual cause of gastric outlet obstruction: A case report with literature review. *Int J Surg Case Rep* 2020; **67**: 154-156 [PMID: 32062123 DOI: 10.1016/j.ijscr.2020.02.012]

World Journal of Clinical Cases

Submit a Manuscript: https://www.f6publishing.com

World J Clin Cases 2025 June 26; 13(18): 103438

DOI: 10.12998/wjcc.v13.i18.103438

ISSN 2307-8960 (online)

CASE REPORT

Rectal abscess secondary to foreign body insertion: A case report

Cristina Isabel Martínez-Hincapie, Daniel González-Arroyave, Carlos M Ardila

Specialty type: Medicine, research and experimental

Provenance and peer review: Invited article; Externally peer reviewed.

Peer-review model: Single blind

Peer-review report's classification

Scientific Quality: Grade B, Grade B, Grade B, Grade B, Grade B

Novelty: Grade A, Grade B, Grade B, Grade B, Grade B

Creativity or Innovation: Grade A, Grade A, Grade B, Grade B, Grade C

Scientific Significance: Grade B, Grade B, Grade B, Grade B, Grade B

P-Reviewer: Alsuliman RM; Suarez Matias M; Zhang L

Received: November 19, 2024

Revised: January 16, 2025

Accepted: February 12, 2025

Published online: June 26, 2025

Processing time: 100 Days and 4.9 Hours

Cristina Isabel Martínez-Hincapie, Daniel González-Arroyave, Department of Surgery, Pontificia Universidad Bolivariana, Medellín 050031, Antioquia, Colombia

Carlos M Ardila, Department of Basic Sciences, Faculty of Dentistry Universidad de Antioquia, Medellin 0057, Antioquia, Colombia

Carlos M Ardila, Department of Periodontics, Saveetha Dental College, and Hospitals, Saveetha Institute of Medical and Technical Sciences, Saveetha University, Saveetha, Saveetha 600077, India

Corresponding author: Carlos M Ardila, Department of Basic Sciences, Faculty of Dentistry Universidad de Antioquia, Calle 70 No. 52-21, Medellín 0057, Antioquia, Colombia.
martin.ardila@udea.edu.co

Abstract

BACKGROUND

Rectal foreign bodies, though uncommon, present diagnostic and therapeutic challenges, particularly when they result from accidental ingestion. The non-specific symptoms and the potential for serious complications necessitate a thorough and methodical approach to diagnosis and treatment. This case report aims to highlight the diagnostic complexities and management strategies involved in treating a patient with a rectal foreign body, focusing on the use of advanced imaging techniques and the importance of a multidisciplinary approach.

CASE SUMMARY

A 48-year-old male with a history of hypertension presented with a one-year history of post-defecation anorectal pain and mild post-defecation rectorrhagia. Initial evaluation revealed hemodynamic stability and a tender, non-mucosal lesion in the anterior left rectal region. Imaging studies, including colonoscopy, magnetic resonance imaging, and endosonography, identified an erythematous, exophytic lesion and a perirectal abscess containing a foreign body. Surgical intervention revealed necrotic tissue and purulent material, along with two solid foreign body fragments (bone or plant matter). Postoperative follow-up showed the patient in good condition, and pathology confirmed the fragments as mature bone.

CONCLUSION

This case underscores the diagnostic challenges posed by rectal foreign bodies with nonspecific symptoms and no clear history of ingestion.

Key Words: Rectal foreign bodies; Abscess; Endosonography; Colonoscopic polypectomy;

Chronic inflammation; Case report

©The Author(s) 2025. Published by Baishideng Publishing Group Inc. All rights reserved.

Core Tip: This case report highlights the diagnostic and therapeutic challenges of rectal foreign bodies, emphasizing the crucial role of advanced imaging techniques, including colonoscopy, magnetic resonance imaging, and endosonography, in accurate diagnosis. A multidisciplinary approach combining endoscopic and surgical expertise is essential for successful management. Comprehensive physical examination and regular postoperative follow-up are vital to ensure recovery and monitor for complications. Patient education on the risks of ingesting foreign objects, particularly in high-risk groups, is imperative for prevention. This report underscores the importance of a thorough and methodical approach in managing rectal foreign bodies with nonspecific symptoms and no clear history of ingestion.

Citation: Martínez-Hincapie CI, González-Arroyave D, Ardila CM. Rectal abscess secondary to foreign body insertion: A case report. *World J Clin Cases* 2025; 13(18): 103438
URL: https://www.wjgnet.com/2307-8960/full/v13/i18/103438.htm
DOI: https://dx.doi.org/10.12998/wjcc.v13.i18.103438

INTRODUCTION

Rectal foreign bodies are infrequent when they occur accidentally secondary to ingestion[1-3]. Most foreign bodies in the rectum are inserted through the anal canal because of sexual practices; however, a small proportion of these foreign bodies are due to the ingestion of foreign objects, most commonly animal bones[4-6]. Approximately 10% to 20% of foreign bodies fail to be eliminated from the gastrointestinal tract. When these advance through the digestive tract, it has been described that they can potentially lodge in the pylorus, the ileocecal valve, and the rectum, with less than 1% resulting in perforation[7-9].

A growing body of literature highlights the increasing prevalence of rectal foreign bodies, with cases ranging from accidental ingestion to intentional insertion. A U.S.-based study estimated 38948 emergency visits for rectal foreign bodies from 2012 to 2021, with an annual incidence rising from 1.2 to 1.9 per 100000 people[10]. Most cases are associated with sexual practices involving foreign objects, while a smaller percentage result from accidental ingestion[11,12]. In our case, detailed history-taking after pathology findings revealed that the foreign body—a chicken bone—was accidentally ingested during a meal. This highlights the diagnostic challenge posed by accidental ingestion, especially when patients fail to recall relevant historical events.

Complications of rectal foreign bodies include anal incontinence, perforation, fistulas, and the formation of perirectal abscesses. The symptoms presented by patients are very nonspecific and have a wide spectrum, ranging from mild lower abdominal pain, constipation, rectal pain, and pelvic pain to rectal bleeding with signs of perforation in complicated cases [2]. The presentation of patients with accidental unconscious ingestion can be a true diagnostic challenge as these patients may not recall any historical trigger for their symptoms, making an accurate diagnosis a real challenge. We present the case of an adult patient who accidentally ingested bone material, which led to a significant inflammatory process with the formation of a secondary perirectal abscess.

CASE PRESENTATION

Chief complaints

A 48-year-old patient with a history of hypertension consulted the coloproctology service due to a one-year history of post-defecation anorectal pain, associated with mild post-defecation rectorrhagia.

History of present illness

The patient denied weight loss, alterations in bowel habits, or stool consistency.

History of past illness

Notably, within the patient's medical history, only the presence of arterial hypertension was mentioned. However, retrospectively, it was identified that more than a year ago, the patient had suffered a choking episode due to accidentally ingesting a chicken bone. At that time, the patient did not mention this incident, as he did not believe it had any relation to his current clinical picture.

Personal and family history

Arterial hypertension.

Physical examination

During the initial evaluation, the patient was hemodynamically stable and afebrile. On physical examination, the patient was alert, oriented in all three mental spheres, with a soft abdomen, no tenderness on palpation, and no masses or hepatomegaly. A digital rectal examination revealed no anal fissures or polyps. However, a non-mucosal lesion was palpated in the anterior left region above the left puborectalis muscle, which was tender to touch but without active bleeding. Based on these findings, imaging studies were requested for a more objective characterization of the lesion.

Laboratory examinations

Biopsies reported granulation tissue.

Imaging examinations

Various imaging studies were utilized to comprehensively address the patient's clinical picture. A colonoscopy was performed as an initial study. Given the patient's age (48 years) and his chronic symptoms of one year, which included post-defecatory anorectal pain and mild rectal bleeding, and since he had not undergone prior screening studies for colorectal cancer, this was deemed necessary. The colonoscopy revealed an erythematous, exophytic lesion in the distal rectum, proximal to the dentate line, measuring 13 mm × 10 mm with an inflammatory, lobulated, villous appearance, involving less than 20% of the circumference and not causing rectal lumen stenosis (Figure 1).

Following this study, an endoscopic polypectomy was successfully performed using a hot snare technique, leaving the bed without bleeding (Figure 2). Samples were sent to pathology, which reported a hyperplastic polyp.

In addition, a magnetic resonance imaging (MRI) was performed to evaluate the soft tissues in greater detail, assessing the depth of the lesion, the volume of the collection, and its precise location relative to adjacent structures. The MRI revealed a fistulous tract with an internal opening extending from 1 to 43 mm from the anal verge, with an intramural abscess and a collection between the left iliococcygeal muscle and the left prostatic lobe. The lesion had a thick wall with peripheral enhancement after contrast administration, containing a 34 mm hypodense linear lesion within the abscess (foreign body) (Figure 3).

MULTIDISCIPLINARY EXPERT CONSULTATION

For the appropriate management of the case, interdisciplinary collaboration was carried out, involving specialties such as gastroenterology and general surgery. However, the coloproctology department led the process and performed the surgical intervention.

FINAL DIAGNOSIS

The MRI revealed a fistulous tract with an internal opening.

TREATMENT

Based on these imaging study results, an anorectal endosonography was decided upon to better characterize the abscess and the foreign body. During the physical evaluation, the presence of external fistulous tracts was ruled out.

Anorectal endosonography reported a collection originating at the periphery of the left prostatic lobe and descending to the external anal sphincter without involving the internal anal sphincter. There was no external opening, suggesting it was located above the dentate line, on the left lateral wall.

With the analysis of these results, a decision was made in conjunction with the patient to proceed with surgical intervention. During surgery, a mucosal lesion measuring 15 mm × 15 mm was identified on the anterior left rectal wall just above the left puborectalis muscle at the lower boundary of the prostate, with the release of abundant fetid purulent material. A nodular mucosal lesion was resected, finding a necrotic-bordered orifice measuring 8 mm × 10 mm in the rectal wall. An explorer was introduced, revealing a cavity measuring 30 mm × 40 mm, which was debrided, releasing abundant necrotic material with pus and fetid tissue. Additionally, two fragments of a solid foreign body (bone *vs* vegetal fragments) were identified and removed (Figure 4).

Following the pathology report identifying mature bone tissue, the patient was reinterviewed. He recalled ingesting a chicken bone during a meal of fried chicken months earlier but had not considered it relevant at the time.

OUTCOME AND FOLLOW-UP

Due to the supra-elevator abscess, it was decided to debride and marsupialize the edges of the large rectal defect to ensure continuous drainage. Samples were sent for pathological study. The patient was discharged with a prescription for analgesics and antibiotics for continued outpatient management and follow-up.

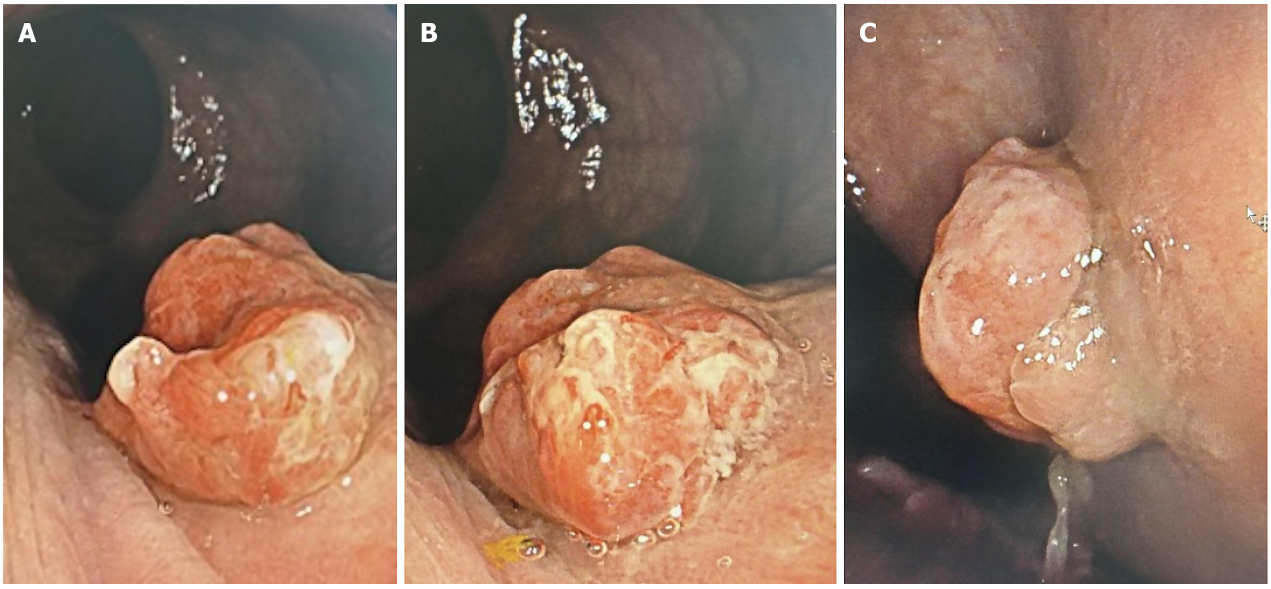


Figure 1 Erythematous, exophytic lesion in the distal rectum below the distal valve of Houston, proximal to the dentate line, measuring 13 mm × 10 mm, with an inflammatory, lobulated, and villous appearance, not involving more than 20% of the circumference or causing stenosis of the rectal lumen. A: Frontal view of the polyp; B: Lateral view of the polyp; C: Medial view of the polyp.

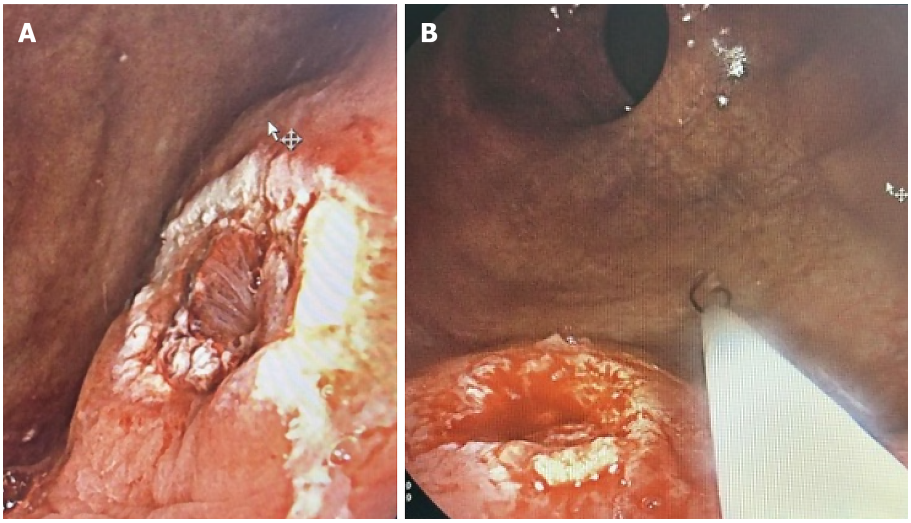


Figure 2 Successful endoscopic polypectomy using hot snare technique, with no bleeding observed at the resection site. A: Lateral view of the polyp resection; B: Frontal view of the polyp resection.

Two weeks later, the patient attended a postoperative follow-up appointment, where he was found to be in very good general condition, stable, afebrile, calm, with controlled pain, and without signs of postoperative complications. The pathology results indicated that the fragments extracted from the rectal region were consistent with mature bone tissue. Therefore, the antibiotic treatment was continued for an additional two weeks, along with dietary and care recommendations.

DISCUSSION

Rectal foreign bodies are relatively rare, especially those resulting from accidental ingestion. However, voluntary insertions for sexual purposes or iatrogenic causes represent more frequent occurrences. Although the exact incidence of rectal foreign bodies due to accidental ingestion remains poorly documented, the rate is considered low. The most commonly ingested foreign objects include toothpicks, chicken bones, and plastic objects such as erasers or small toys. These objects may cause significant complications if left undiagnosed or untreated, including perforation, anal incontinence, fistulas, and abscess formation. Misdiagnosis or delayed diagnosis of rectal foreign bodies can lead to these potentially severe consequences, underscoring the clinical importance of timely identification and appropriate

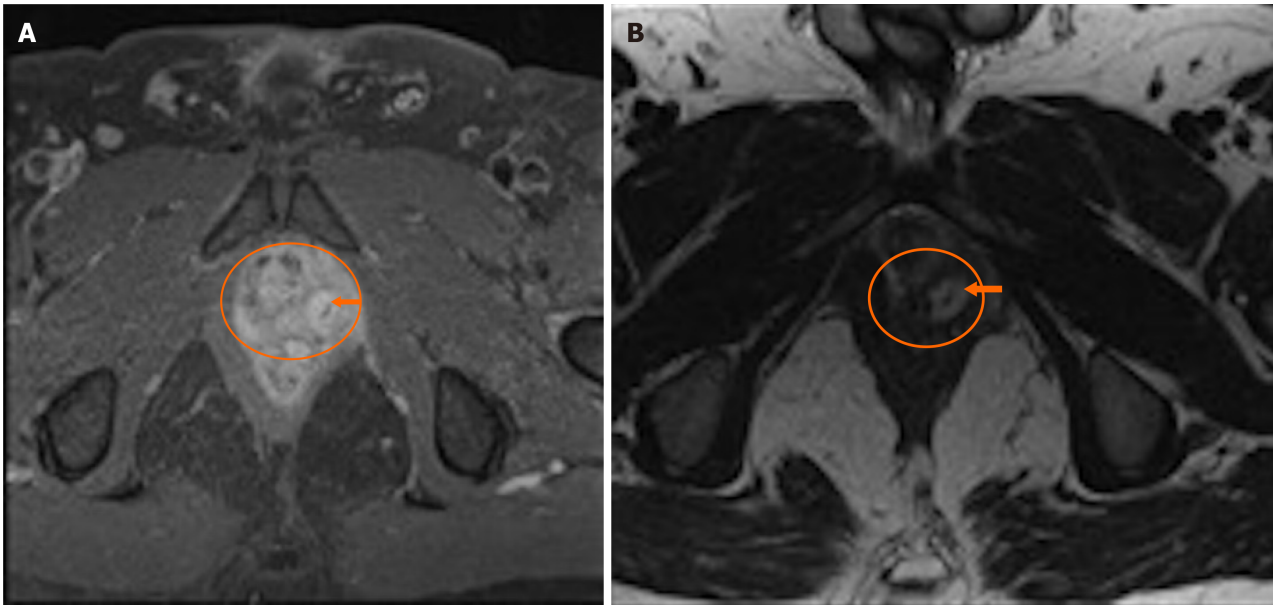


Figure 3 Intramural abscess and collection between the left iliococcygeal muscle and left prostatic lobe with thickened wall and peripheral enhancement post-contrast, along with a 34 mm linear hypodense lesion within the abscess (Foreign body). A: T1 sequence of magnetic resonance imaging; B: T2 sequence of magnetic resonance imaging.



Figure 4 Bone fragments extracted during surgical resection.

management[1,8,13].

Studies indicate that between 10% to 20% of foreign bodies fail to pass through the gastrointestinal tract and may become lodged in various sites, including the rectum. Though these cases are rare, complications such as perforation can occur in less than 1% of patients. This underscores the need for early and precise intervention to avoid life-threatening outcomes[1].

During the initial evaluation of the case, the patient reported nonspecific symptoms, including a one-year history of post-defecation anorectal pain associated with mild post-defecation rectorrhagia. The patient did not recall any specific trigger or the ingestion of any type of foreign body that could have caused these symptoms. Therefore, it was indeed a significant diagnostic challenge to elucidate the cause of these symptoms.

Table 1 Key clinical features, diagnostic aids, and diagnostic results

Key clinical features	Diagnostic aids	Diagnostic results
Post-defecatory anorectal pain	Total colonoscopy	Erythematous, exophytic lesion in the distal rectum at the distal valve of Houston, proximal to the dentate line, measuring 13 x 10 mm with an inflammatory, lobulated, villous appearance, involving less than 20% of the circumference and not causing rectal lumen stenosis
Scant post-defecatory rectorrhagia	Contrast-enhanced pelvic magnetic resonance imaging	Fistulous tract with internal opening ranging from 1 to 43 mm from the anal verge, with an intramural abscess and a collection between the left iliococcygeal muscle and left prostatic lobe, with thick walls and peripheral enhancement post-contrast, containing a 34 mm hypodense linear lesion (foreign body)
Clinical presentation lasting 1 year	Anorectal endosonography	Collection originating from the periphery of the left prostatic lobe descending to the external anal sphincter without involving the internal anal sphincter. No external opening, seemingly located above the dentate line on the left lateral wall
Non-mucosal lesion, painful on palpation, no active bleeding	Not applicable	Not applicable

The first step in the evaluation and treatment of a patient with a rectal foreign body is to determine whether perforation has occurred. When perforation is suspected, it is crucial to determine as soon as possible if the patient is stable or unstable. Hypotension, tachycardia, severe abdominal pain, and fever are indicative of perforation. The physical examination should be detailed, looking for abnormalities that help identify the etiology, and a rectal examination should not be omitted[7,13]. In our patient, a lesion of non-mucosal origin was identified, which was tender to touch, without active bleeding, in the anterior left region above the left puborectalis muscle, requiring imaging studies to further characterize the lesion.

Given the patient's age (48 years), lack of prior colorectal cancer screening, and symptoms of one-year duration, a colonoscopy was prioritized to rule out neoplastic lesions. Retrospectively, a targeted rectoscopy might have been a more focused approach for identifying rectal lesions. The MRI findings suggested a fistulous tract extending from 1 to 43 mm from the anal verge; however, the lesion's location and inflammatory surroundings likely obscured its detection during colonoscopy, highlighting a limitation of this modality in such scenarios. When a foreign body is removed or absent in the rectal vault, rigid proctoscopy or endoscopic evaluation may reveal the rectal lesion or the foreign body located higher up in the rectosigmoid[3]. Computed tomography, ultrasound, and magnetic resonance imaging can further enhance the diagnostic ability to visualize smaller objects. In our patient, these imaging studies were necessary as the initial images showed that the duration of the retained bone had triggered a chronic inflammatory state, precluding any possibility of endoscopic recovery.

In clinically stable patients without evidence of perforation or peritonitis, the rectal foreign body should be removed in the emergency department or operating room. Depending on the size and shape of the object, various methods can be used. Most objects can be removed transanally, as was the case with our patient. If this is not possible or if safe extraction cannot be achieved, a transabdominal approach is used.

While rectal foreign bodies are a known clinical entity, reports of cases involving non-digestible objects, such as bone fragments, are rare. Existing literature provides limited case series, which often describe similar presentations but without a consistent approach to diagnosis and management. The variability in treatment strategies reflects the lack of standardized guidelines for managing these cases. As such, treatment often depends on the specifics of the case, including the location of the foreign body, the presence of complications such as abscesses, and the patient's overall health. The case presented here further underscores the need for a tailored approach to treatment, as no one-size-fits-all strategy has yet emerged in the literature.

Table 1 summarizes the key clinical features, diagnostic aids, and the results obtained from various diagnostic techniques used to evaluate a patient with anorectal pain and suspected foreign body ingestion. The diagnostic process, including imaging studies such as colonoscopy, MRI, and anorectal endosonography, contributed to identifying the lesion and the foreign body, ultimately guiding treatment decisions.

CONCLUSION

This case underscores the importance of selecting appropriate diagnostic modalities based on patient history and clinical findings. While colonoscopy is valuable for screening, it may miss lesions outside the rectal lumen. Targeted rectoscopy, in combination with advanced imaging techniques like anorectal endosonography, can enhance diagnostic accuracy. Reassessing the patient's history after pathology results can provide crucial insights into the etiology of rare presentations, such as rectal foreign bodies. Comprehensive evaluation, including detailed physical examinations and advanced imaging methods like magnetic resonance imaging and endosonography, is essential for accurate lesion characterization. The successful transanal removal and subsequent surgical debridement highlight the significance of personalized management strategies tailored to the patient's clinical condition and the foreign body's characteristics. Regular postoperative follow-up is key for ensuring recovery and monitoring for complications. This case also emphasizes the need for patient education regarding the risks of ingesting foreign objects, especially in high-risk populations, and the value of a multidisciplinary approach for achieving optimal outcomes.

FOOTNOTES

Author contributions: Martínez-Hincapie CI, González-Arroyave D, and Ardila CM performed the conceptualization, data curation, data analysis, manuscript writing, and revision of the manuscript.

Informed consent statement: The participant provided informed written consent prior to study enrollment.

Conflict-of-interest statement: The authors declare having no conflicts of interest.

CARE Checklist (2016) statement: The authors have read the CARE Checklist (2016), and the manuscript was prepared and revised according to the CARE Checklist (2016).

Open Access: This article is an open-access article that was selected by an in-house editor and fully peer-reviewed by external reviewers. It is distributed in accordance with the Creative Commons Attribution NonCommercial (CC BY-NC 4.0) license, which permits others to distribute, remix, adapt, build upon this work non-commercially, and license their derivative works on different terms, provided the original work is properly cited and the use is non-commercial. See: https://creativecommons.org/Licenses/by-nc/4.0/

Country of origin: Colombia

ORCID number: Daniel González-Arroyave 0000-0002-2162-8484; Carlos M Ardila 0000-0002-3663-1416.

S-Editor: Liu H
L-Editor: A
P-Editor: Zhang L

REFERENCES

1 **Elmoghrabi A**, Mohamed M, Wong K, McCann M. Proctalgia and colorectal stricture as the result of a 2-year transit of a retained rectal chicken bone: a case presentation and review of the literature. *BMJ Case Rep* 2016; **2016**: bcr-2016 [PMID: 27325671 DOI: 10.1136/bcr-2016-215913]
2 **Coskun A**, Erkan N, Yakan S, Yıldirim M, Cengiz F. Management of rectal foreign bodies. *World J Emerg Surg* 2013; **8**: 11 [PMID: 23497492 DOI: 10.1186/1749-7922-8-11]
3 **Singaporewalla RM**, Tan DE, Tan TK. Use of endoscopic snare to extract a large rectosigmoid foreign body with review of literature. *Surg Laparosc Endosc Percutan Tech* 2007; **17**: 145-148 [PMID: 17450100 DOI: 10.1097/SLE.0b013e318045bf1a]
4 **Goh BK**, Chow PK, Quah HM, Ong HS, Eu KW, Ooi LL, Wong WK. Perforation of the gastrointestinal tract secondary to ingestion of foreign bodies. *World J Surg* 2006; **30**: 372-377 [PMID: 16479337 DOI: 10.1007/s00268-005-0490-2]
5 **Alkandari AF**, Alsarraf HM, Alkandari MF. Ingested Chicken Bone (Xiphoid Process) in the Anal Canal: A Case Report and Literature Review. *Cureus* 2023; **15**: e35060 [PMID: 36942189 DOI: 10.7759/cureus.35060]
6 **Hong KH**, Kim YJ, Kim JH, Chun SW, Kim HM, Cho JH. Risk factors for complications associated with upper gastrointestinal foreign bodies. *World J Gastroenterol* 2015; **21**: 8125-8131 [PMID: 26185385 DOI: 10.3748/wjg.v21.i26.8125]
7 **Cash DJ**, Sadat MM, Abu-Own AS. Anorectal abscess and fistula caused by an ingested chicken bone. *Am J Gastroenterol* 2004; **99**: 1617-1618 [PMID: 15307883 DOI: 10.1111/j.1572-0241.2004.40259.x]
8 **Emir S**, Ozkan Z, Altınsoy HB, Yazar FM, Sözen S, Bali I. Ingested bone fragment in the bowel: Two cases and a review of the literature. *World J Clin Cases* 2013; **1**: 212-216 [PMID: 24340269 DOI: 10.12998/wjcc.v1.i7.212]
9 **Tokunaga Y**, Hata K, Nishitai R, Kaganoi J, Nanbu H, Ohsumi K. Spontaneous perforation of the rectum with possible stercoral etiology: report of a case and review of the literature. *Surg Today* 1998; **28**: 937-939 [PMID: 9744404 DOI: 10.1007/s005950050256]
10 **Loria A**, Marianetti I, Cook CA, Melucci AD, Ghaffar A, Juviler P, Temple LK, Jones CMC, Fleming FJ. Epidemiology and healthcare utilization for rectal foreign bodies in United States adults, 2012-2021. *Am J Emerg Med* 2023; **69**: 76-82 [PMID: 37060632 DOI: 10.1016/j.ajem.2023.03.041]
11 **Bhasin S**, Williams JG. Rectal foreign body removal: increasing incidence and cost to the NHS. *Ann R Coll Surg Engl* 2021; **103**: 734-737 [PMID: 34719960 DOI: 10.1308/rcsann.2020.7129]
12 **Fischer J**, Krishnamurthy J, Hansen S, Reeves PT. Austere Foreign Body Injuries in Children and Adolescents: A Characterization of Penile, Rectal, and Vaginal Injuries Presenting to Emergency Departments in the United States From 2008 to 2017. *Pediatr Emerg Care* 2021; **37**: e805-e811 [PMID: 30870345 DOI: 10.1097/PEC.0000000000001803]
13 **Cologne KG**, Ault GT. Rectal foreign bodies: what is the current standard? *Clin Colon Rectal Surg* 2012; **25**: 214-218 [PMID: 24294123 DOI: 10.1055/s-0032-1329392]

World Journal of Clinical Cases

Submit a Manuscript: https://www.f6publishing.com

World J Clin Cases 2025 June 26; 13(18): 103571

DOI: 10.12998/wjcc.v13.i18.103571

ISSN 2307-8960 (online)

CASE REPORT

Unexpected contralateral axillary lymph node metastasis without ipsilateral involvement in triple-negative breast cancer: A case report and review of literature

Yun-Ting Lin, Zhi-Jie Hong, Guo-Shiou Liao, Ming-Shen Dai, Tai-Kuang Chao, Wen-Chiuan Tsai, Yu-Kai Sung, Chuang-Hsin Chiu, Cheng-Kuang Chang, Jyh-Cherng Yu

Specialty type: Medicine, research and experimental

Provenance and peer review: Unsolicited article; Externally peer reviewed.

Peer-review model: Single blind

Peer-review report's classification

Scientific Quality: Grade B, Grade B

Novelty: Grade B, Grade B

Creativity or Innovation: Grade B, Grade C

Scientific Significance: Grade B, Grade C

P-Reviewer: Cruz Diaz WE; Wang N

Received: December 9, 2024

Revised: January 15, 2025

Accepted: January 24, 2025

Published online: June 26, 2025

Processing time: 82 Days and 18.8 Hours

Yun-Ting Lin, Department of General Medicine, Tri Service General Hospital, National Defense Medical Center, Taipei 114, Taiwan

Zhi-Jie Hong, Division of Traumatology, Department of Surgery, Tri-Service General Hospital, National Defense Medical Center, Taipei 114, Taiwan

Guo-Shiou Liao, Jyh-Cherng Yu, Division of General Surgery, Department of Surgery, Tri Service General Hospital, National Defense Medical Center, Taipei 114, Taiwan

Ming-Shen Dai, Division of Hematology/Oncology, Department of Internal Medicine, National Defense Medical Center, Taipei 114, Taiwan

Tai-Kuang Chao, Yu-Kai Sung, Department of Pathology and Parasitology, Tri-Service General Hospital, National Defense Medical Center, Taipei 114, Taiwan

Wen-Chiuan Tsai, Department of Pathology, National Defense Medical Center, Taipei 114, Taiwan

Chuang-Hsin Chiu, Department of Nuclear Medicine, Tri-Service General Hospital, National Defense Medical Center, Taipei 114, Taiwan

Cheng-Kuang Chang, Department of Radiology, Tri-Service General Hospital, National Defense Medical Center, Taipei 114, Taiwan

Co-corresponding authors: Zhi-Jie Hong and Jyh-Cherng Yu.

Corresponding author: Zhi-Jie Hong, MD, PhD, Assistant Professor, Chief Physician, Division of Traumatology, Department of Surgery, Tri-Service General Hospital, National Defense Medical Center, No. 325 Section 2, Chenggong Road, Neihu District, Taipei 114, Taiwan. lgf670822@mail.ndmctsgh.edu.tw

Abstract

BACKGROUND

Breast cancer is a leading cause of cancer-related mortality among women worldwide, with invasive ductal carcinoma (IDC) being the most prevalent subtype. Lymph node metastasis is the primary prognostic indicator, typically

evaluated *via* biopsy of the ipsilateral sentinel or axillary lymph nodes. Contralateral axillary metastasis (CAM) without ipsilateral involvement is exceedingly rare, particularly in early-stage breast cancer. This report presents a case of CAM in a patient with triple-negative breast cancer (TNBC), underscoring diagnostic and therapeutic complexities.

CASE SUMMARY

A 73-year-old female presented with left-sided early-stage IDC in February 2023. Despite a modified radical mastectomy and pathologically negative ipsilateral lymph nodes, a postoperative positron emission tomography (PET) scan detected fluorodeoxyglucose-avid nodes in the contralateral axilla. Biopsy confirmed metastatic ductal carcinoma with triple-negative status, resulting in an upstaged diagnosis of metastatic breast cancer, stage IV, M1. The patient underwent six cycles of adjuvant chemotherapy, with follow-up PET imaging showing regression of the contralateral lesion. This case highlights the importance of advanced imaging in TNBC for precise staging and treatment optimization.

CONCLUSION

This case highlights the aggressive nature of TNBC and the need for advanced imaging to ensure accurate staging and effective management.

Key Words: Triple negative breast neoplasms; Invasive ductal carcinoma; Lymphatic metastasis; Contralateral axillary metastasis; Positron-emission tomography; Case report

©The Author(s) 2025. Published by Baishideng Publishing Group Inc. All rights reserved.

Core Tip: We present a 73-year-old female with triple-negative breast cancer (TNBC) exhibiting contralateral axillary lymph node metastasis without ipsilateral involvement. Despite early-stage diagnosis and modified radical mastectomy, positron emission tomography (PET) imaging and biopsy later upstaged the disease to metastatic stage IV. This case highlights the aggressive nature of TNBC, its complex lymphatic spread, the potential utility of PET scans for accurate staging in high-risk early breast cancers and treatment for contralateral axillary metastasis. These findings suggest reconsidering mandatory PET imaging for early TNBC or other high-risk cases to ensure accurate staging and optimal systemic therapy for improved outcomes.

Citation: Lin YT, Hong ZJ, Liao GS, Dai MS, Chao TK, Tsai WC, Sung YK, Chiu CH, Chang CK, Yu JC. Unexpected contralateral axillary lymph node metastasis without ipsilateral involvement in triple-negative breast cancer: A case report and review of literature. *World J Clin Cases* 2025; 13(18): 103571

URL: https://www.wjgnet.com/2307-8960/full/v13/i18/103571.htm

DOI: https://dx.doi.org/10.12998/wjcc.v13.i18.103571

INTRODUCTION

Breast cancer is one of the most common malignancies affecting women worldwide and remains a primary cause of cancer-related deaths[1]. The management of breast cancer is complex and requires a multimodal approach. Treatment strategies are guided by factors such as lymph node status, which is typically evaluated *via* biopsy of the ipsilateral sentinel or axillary lymph nodes, tumor size, biology, disease stage, patient age, and underlying conditions, particularly in older individuals[2,3].

Among the various subtypes of breast cancer, invasive ductal carcinoma (IDC) is the most prevalent. IDC originates in the milk ducts and subsequently invades the surrounding breast tissues[4]. A particularly challenging subtype of IDC is triple-negative breast cancer (TNBC), which lacks the expression of estrogen receptor (ER), progesterone receptor (PR), and human epidermal growth factor receptor 2 (HER2/Neu)[5]. TNBC is associated with poorer prognosis, higher recurrence rates, and limited treatment options because it does not respond to hormonal or HER2-targeted therapies[6]. Nevertheless, recent studies have demonstrated that adding pembrolizumab to standard neoadjuvant chemotherapy improved prognosis in patients with early-stage TNBC[7,8]. These data emphasize the evolving landscape of TNBC treatment and highlight the importance of a precise stage to improve outcomes.

Considering the aggressive behavior and limited treatment options for TNBC, comprehensive diagnostic imaging and careful monitoring are critical for guiding treatment decisions and improving outcomes[9]. According to the National Comprehensive Cancer Network Guidelines, version 6, 2024, positron emission tomography (PET) or computed tomography (CT) is most beneficial and accurate for advanced disease, such as stage III or higher with invasive ductal histology. Nevertheless, these modalities may also be beneficial in selected circumstances for earlier stage disease, such as equivocal CT or bone scan results, suspicion of undetected nodal or distant disease, and treatment response assessment. Therefore, preoperative PET is currently not routinely performed in patients with early-stage breast cancer[10].

In addition to whether PET should be routinely performed for early-stage breast cancer, contralateral axillary metastasis (CAM) is another novel topic for breast cancer. CAM refers to the spread of cancer to the axillary lymph nodes on the side opposite to the primary breast tumor without the involvement of ipsilateral axillary lymph nodes[11]. CAM is a rare clinical presentation in breast cancer, with an incidence rate reported approximately 1.9%-6% in various studies[12, 13]. Classifying CAM as synchronous or metachronous is essential for understanding its clinical implications and guiding management strategies. Synchronous CAM exhibits better outcomes in terms of overall survival than other metastatic diseases[13]. Nonetheless, patients with metachronous CAM exhibit survival similar to that of patients with distant metastasis[14].

Here, we describe a rare case of a 73-year-old woman diagnosed with TNBC who exhibited an unusual metastasis pattern, involving the contralateral axillary lymph node without the involvement of the ipsilateral or internal mammary lymph node. This case underscores the diagnostic challenges and complexities in managing advanced TNBC. It also emphasizes the potential role of advanced imaging techniques, such as whole-body PET, in achieving more accurate staging before adjuvant chemotherapy, whether for early detection or staging of metastatic disease.

CASE PRESENTATION

Chief complaints

A 73-year-old female presented with a palpable left breast mass for 4 months.

History of present illness

The patient reported a palpable mass in her left breast for 4 months. Mammography and ultrasonography categorized the mass as highly suspicious for neoplasm with breast imaging-reporting and data system (BI-RADS) category 4c in February 2023. A subsequent core needle biopsy revealed IDC, grade II, with triple-negative status (ER-, PR-, HER2-, Ki-67: 10%, Nottingham histological score 7). After additional evaluations, including abdominal sonography and chest X-ray, the clinical stage was determined as cT2N0M0, with the largest tumor measuring 22.6 mm × 12.6 mm. The patient was a candidate for neoadjuvant chemotherapy, and based on guidelines, we strongly recommended that she undergo neoadjuvant chemotherapy. Nevertheless, considering the relatively small tumor size in T2, her age, and frailty, she ultimately refused neoadjuvant chemotherapy and opted to proceed directly with surgery.

History of past illness

In 2018, the patient experienced a microvascular rupture and underwent brain surgery.

Personal and family history

She had no relevant family history of breast cancer or other malignancies. However, she had some relevant personal histories related to breast cancer, including first childbirth after the age of 35 years and a breastfeeding duration of < 2 years.

Physical examination

Physical examination revealed a fixed mass in the left breast without palpable lymph nodes in the bilateral axillary or supraclavicular regions.

Laboratory examinations

Preoperative CEA and CA153 Levels were 0.77 ng/mL and 7.8 U/mL, respectively, whereas postoperative levels were 1.52 ng/mL and 9.57 U/mL, respectively.

Histopathological analysis

Core needle biopsy of the left tumor revealed IDC, grade II, with triple-negative status (ER-, PR-, HER2-, Ki-67: 10%, Nottingham histological score 7).

Pathology of modified radical mastectomy, left IDCs, grade III with triple-negative status (ER-, PR-, HER2-, Ki-67: 40%, Nottingham histological score 9) and free of tumor invasion in the surgical margin, lymph nodes (0/11), including sentinel node (0/3), level I (0/7), level II (0/1). No lymphovascular space or perineural invasion was identified.

Core needle biopsy of the right axillary lymph node revealed metastatic ductal carcinoma with triple-negative status (ER-, PR-, HER2-, Ki-67: 30%, GATA3+).

Imaging examinations

Mammography (Figure 1) revealed well-circumscribed lobular masses with pleomorphic calcifications in the left breast, classified as BI-RADS category 4c.

Breast sonography performed on February 6, 2023 (Figure 2), revealed multiple masses with poorly defined margins and a dilated duct. The largest mass, located at the 12 o'clock position of the left breast, measured 22.6 mm × 12.6 mm and was classified as BI-RADS category 4c. Enlarged lymph nodes were also detected in the left axillary fossa, which might be adenopathy. No obvious enlarged lymph nodes were detected in the right axillary fossa.

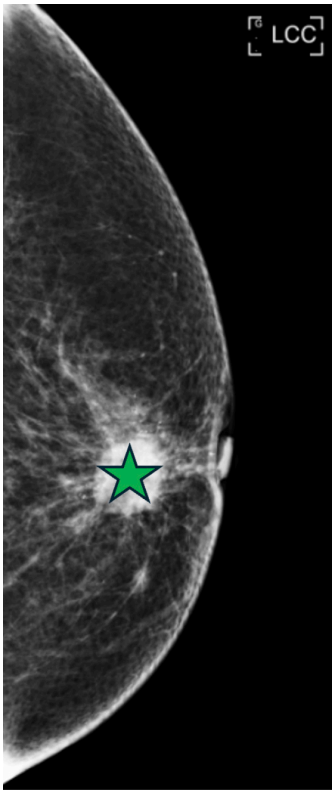


Figure 1 Mammography on February 6, 2023. Well circumscribed lobular masses with pleomorphic calcifications in the left breast (green star, size: Up to about 1.78 cm, in the 12 o'clock, M/3, about 1.05 cm away from the nipple on the craniocaudal view view), probably neoplasms.

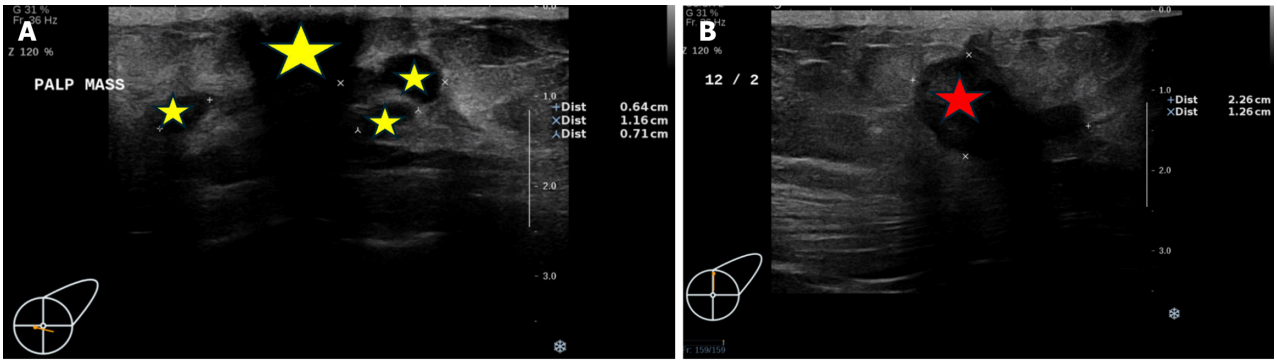


Figure 2 Breast sonography on February 6, 2023. Multiple masses (yellow star at the left picture) with poorly defined margin and dilated duct in left breast, the biggest one (red star at the right picture) is at 12 o'clock position of left breast, (12/2 cm), 22.6 mm × 12.6 mm in size, might be neo-growth. Breast imaging reporting and data system category 4c: Moderate suspicious abnormality.

Abdominal sonography revealed a 0.8-cm hepatic cyst in segment 4 of the liver.

Modified radical mastectomy was performed on the left breast on February 17, 2023, which revealed two major tumors, with the larger tumor measuring 2.1 mm × 1.3 cm and the smaller one measuring 1.3 mm × 0.6 cm.

Whole-body PET performed in March 2023 (Figure 3) revealed mild fluorodeoxyglucose (FDG) avidity in the right axilla and right lobe of the liver. The FDG-avid nodule in the right axilla was confirmed as metastatic ductal carcinoma in the right axillary lymph node by needle biopsy. The FDG-avid lesion in the right lobe of the liver was suspicious for a cyst upon further evaluation by abdominal CT with contrast.

Abdominal CT with contrast performed in April 2023 identified that the liver lesion exhibited no significant enhancement after contrast administration, supporting the diagnosis of a cyst, consistent with the previous mild FDG avidity observed on PET.

Sono-guided core needle biopsy for mild FDG avidity over the right axillary region was performed on April 19, 2023, which revealed an enlarged lymph node in the right axillary fossa.

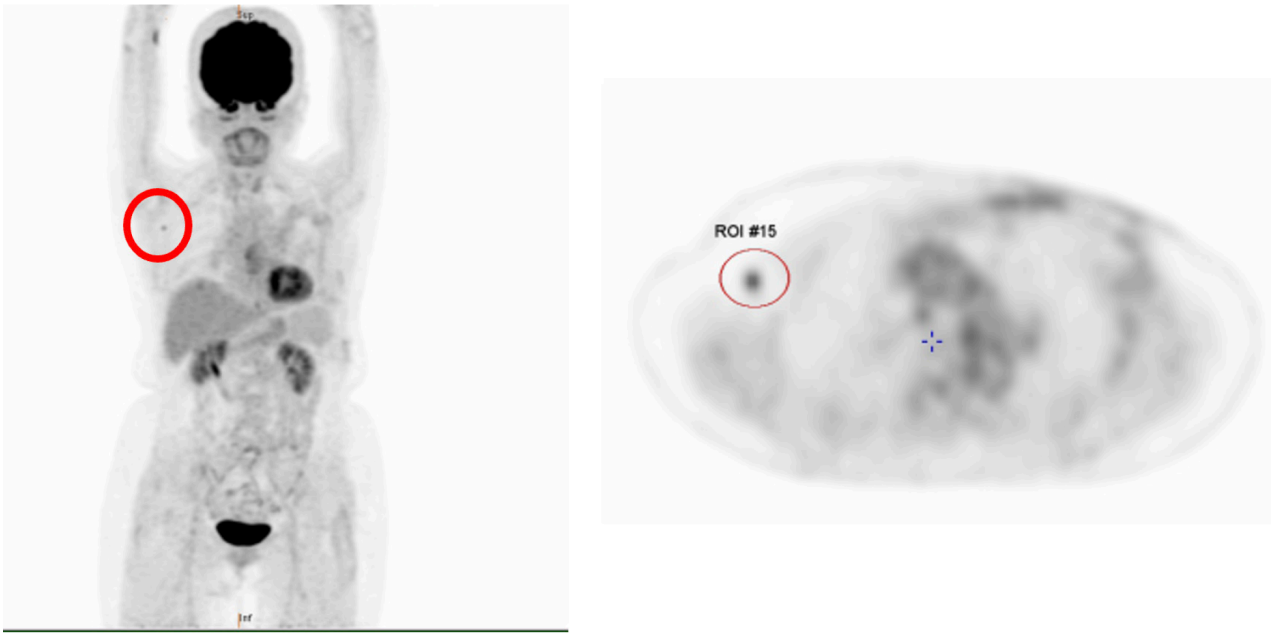


Figure 3 Fluorodeoxyglucose- positron emission tomography whole body scan on March 21, 2023 (coronal view and axial view). One mild fluorodeoxyglucose-avidity over the right axillary region (red circle, maximal standard uptake value = 3.0, size > 0.4 cm) favoring reactive node. Based on clinical history [pT2(m)N0] and the imaging findings, the current PET finding suggesting no metabolic evidence of malignancy (left breast cancer), cT2(m)N0M0[35].

FINAL DIAGNOSIS

IDC, grade III, triple-negative (ER-, PR-, HER2-, Ki-67: 40%, Nottingham histological score 9), with metastatic involvement of the right axillary lymph node. Final staging: PT2N0M1, stage IV (Figure 4).

TREATMENT

The patient underwent a modified radical mastectomy, followed by adjuvant chemotherapy with six cycles of docetaxel and cyclophosphamide, with dose reductions due to age and intolerable side effects, such as skin rash, pitting edema, hand-foot syndrome, myalgia, and nausea.

OUTCOME AND FOLLOW-UP

A PET scan performed in August 2023 demonstrated regression of the FDG-avid nodule in the right axilla (Figure 3) and no evidence of distant organ involvement. Radiotherapy to the right axillary region was planned; however, the patient and her family declined the treatment due to her age and underlying conditions. She experienced no significant complications following the course of treatment and surveillance.

DISCUSSION

TNBC is a distinct and challenging subtype of breast cancer characterized by the absence of targeted therapies[6]. It is associated with aggressive behavior, higher recurrence rates, and poorer prognosis compared with other subtypes of breast cancer[15]. In the present case, the patient exhibited a high Ki-67 index, which increased from 10% preoperatively to 40% in the final pathological analysis, signifying a highly proliferative tumor and further complicating the prognosis [16]. Hence, although this patient did not meet the criteria for preoperative PET, due to her strong refusal to undergo neoadjuvant chemotherapy and even her initial refusal to accept adjuvant chemotherapy and radiotherapy, err on the side of caution, we still arranged a postoperative PET after achieving pathologically free margins. Unexpectedly, the PET scan revealed CAM, resulting in the disease being reclassified as stage IV. Consequently, the patient agreed to proceed with adjuvant chemotherapy. Therefore, PET should be considered routinely in high-risk breast cancer, including TNBC.

The rare occurrence of CAM presents significant diagnostic and therapeutic challenges. This atypical presentation may necessitate modifications to postoperative adjuvant systemic therapy and radiotherapy. The observed pattern suggests that the lymphatic spread pathways in TNBC differ from those of other subtypes of breast cancer, potentially bypassing the conventional routes of local dissemination and resulting in unexpected metastatic sites. The absence of internal

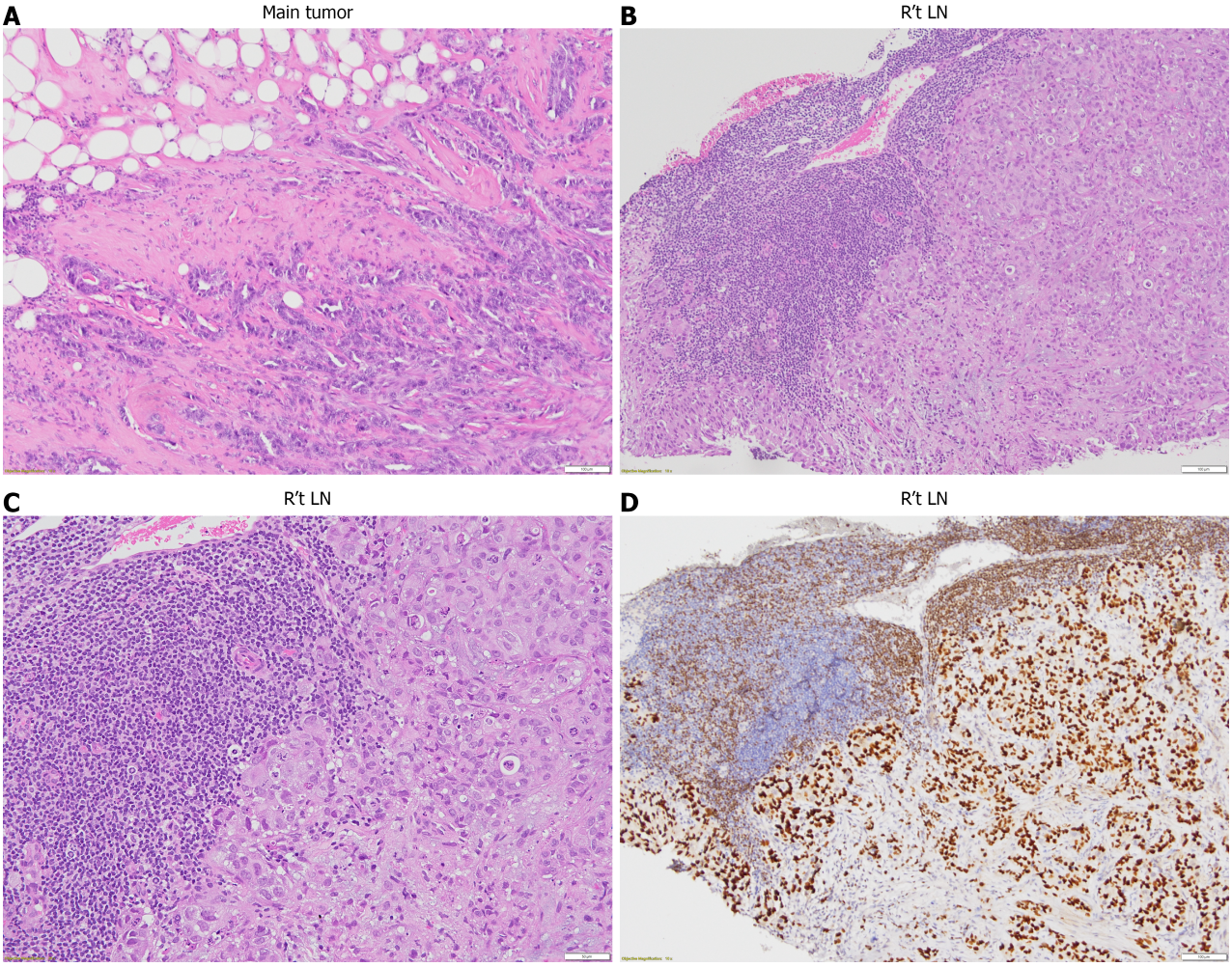


Figure 4 H&E stain of the main tumor and the right axillary lymph node and immunohistochemical stain of the right axillary lymph node. A: H&E stain of the main tumor with magnification 100 ×. An invasive carcinoma consists of tumor cells with nuclear pleomorphism and high N/C ratio, arranged in distorted glandular to solid nested patterns, infiltrating to the fibrous stroma and adipose tissue; B and C: H&E stain of the right axillary lymph node with magnification 100 × (B) and 200 × (C). Follicular structure of normal lymphoid tissue is effaced by solid nested tumor cells with nuclear pleomorphism; D: Immunohistochemical stain of the right axillary lymph node with magnification 100 ×. Mammary origin of metastatic tumor is identified with positive GATA3. R't LN: Right lymph node.

mammary and mediastinal lymph node involvement raises intriguing questions concerning the selective nature of metastatic spread in TNBC. In our case, we used an individualized strategy rather than a standard-of-care protocol because of the general conditions, including the patient's comorbidities, preference, and the rare condition of CAM with TNBC.

The prognosis associated with CAM warrants further discussion. Although distant metastasis in breast cancer is typically associated with poorer prognosis, CAM may represent a distinct entity with unique clinical implications[17]. Emerging evidence suggests that synchronous CAM differs prognostically from metachronous CAM; therefore, an individualized strategy rather than a standard-of-care protocol should be used for each patient.

The concept of oligometastasis is relevant to isolated CAM as well as this case. Oligometastatic disease, characterized by limited metastatic burden, has been associated with better survival rates than polymetastatic disease[18]. A critical debate in the management of metastatic breast cancer lies in the choice between systemic therapy alone and a combination of systemic and localized therapies. Systemic therapy remains the standard of care for metastatic disease, due to its ability to address disseminated cancer cells[19,20]. Nevertheless, in cases of limited metastatic burden, combining systemic therapy with localized interventions, such as surgery and stereotactic body radiotherapy, has shown promise in improving outcomes[21,22].

Another consideration was whether contralateral axillary surgery was suitable for this patient. Although the role of contralateral axillary surgery in CAM is not well-established, it could provide several potential benefits, including local disease control and improved staging accuracy. Nonetheless, it is essential to carefully weigh its limitations, including the risk of surgical morbidity and uncertain survival benefits[23,24]. Further studies are required to elucidate the indications for contralateral axillary surgery in CAM, particularly in the context of TNBC.

Especially considering the complexities of TNBC, comprehensive imaging plays a vital role in its management. A previous study emphasized that preoperative PET scans significantly affect early-stage breast cancer cases with tumors ≥ 2 cm[25], demonstrating superior performance in detecting axillary lymph node metastases than other diagnostic imaging methods, although SLNB remains the gold standard technique[26,27]. The use of whole-body PET scans, although not

routinely performed for early-stage breast cancer, may facilitate the early detection of distant metastases not evident on other imaging modalities such as abdominal sonography, chest X-ray, and even CT scans[10]. In our case, the identification of FDG-avid lesions in the right axilla emphasizes the importance of PET scans in achieving early and accurate staging of TNBC, which is essential for accurately guiding treatment decisions and improving prognostication[25,28].

The findings from this case prompt a discussion on whether whole-body PET scans should be routinely incorporated into the diagnostic workup for early-stage breast cancer. Although whole-body PET scans are not currently standard for early-stage breast cancer, concerns regarding cost, radiation exposure, and risk of false positives leading to overtreatment remain inadequately addressed[29]. Nevertheless, in aggressive subtypes such as TNBC and HER2-positive breast cancer, PET scans may provide significantly improved staging accuracy[28]. The detection of asymptomatic metastatic disease can lead to changes in staging and enable more precise adjuvant therapies, including chemotherapy and radiotherapy. This case presents such a scenario, where the patient's disease was upgraded from stage IIA to stage IV based on PET findings and subsequent tissue diagnosis.

Therefore, further investigations are necessary to establish clear guidelines and identify which patients with early-stage breast cancer might benefit from routine whole-body PET scans and further treatment of CAM. This is particularly applicable for those with high-risk features such as aggressive pathology, a high Ki-67 index, large tumors, and immunocompromised status[30].

CONCLUSION

This case underscores the aggressive nature of TNBC and the importance of detailed diagnostic evaluation and follow-up, particularly considering the unusual patterns of metastasis[31,32]. The isolated CAM emphasizes the need for tailored treatment strategies and vigilant monitoring. The management of CAM must consider the patient's clinical context, input from a multidisciplinary team, and the potential role of advanced imaging techniques, such as whole-body PET scans. Therapeutic decision-making should also consider factors such as the extent of the metastatic disease, the potential for localized treatments, and the patient's overall prognosis and preferences. Although whole-body PET scans are not yet the standard for early-stage breast cancer, they may provide significant benefits in accurately staging aggressive subtypes such as TNBC[33]. Further studies are required to develop guidelines for the selective use of whole-body PET scans in early-stage TNBC, particularly for patients with high-risk features[34]. Moreover, studies focusing on optimizing the management of CAM through a combination of systemic and localized therapies, guided by multidisciplinary input and tailored to the individual patient, are necessary to optimize treatment strategies and improve outcomes.

ACKNOWLEDGEMENTS

The authors wish to acknowledge the assistance of the people in the Department of Surgery, Hematology and Oncology, Pathology, Nuclear Medicine and Radiology, Tri Service General Hospital, National Defense Medical Center. This report would not have been possible without their efforts in data collection and interprofessional collaboration in treating this patient.

FOOTNOTES

Author contributions: Hong ZJ and Yu JC contribute equally to this stud as co-corresponding author; Lin YT reviewed the literature and contributed to manuscript as first author; Hong ZJ contributed to this study as corresponding authors and reviewed the article; Liao GS reviewed the article; Dai MS is an oncologist and drew up chemotherapy for the patient; Chao TK, Tsai WC and Sung YK are the pathologists and interpreted the pathological reports; Chiu CH is a nuclear medicine radiologist and interpreted the positron emission tomography computed tomography scan; Chang CK is a radiologist and interpreted the images; Yu JC is the patient's surgeon; Yu JC conceptualized and designed the manuscript, critically revised the manuscript, and approved the final version for submission.

Informed consent statement: Informed written consent was obtained from the patient for publication of this report and any accompanying images. This study was approved by the Institutional Review Board (IRB) of Tri-Service General Hospital, National Defense Medical Center, Taipei, Taiwan, and complied with relevant guidelines (IRB: B202415203, date of approval 19 November 2024).

Conflict-of-interest statement: The authors declare no conflicts of interest or competing interests.

CARE Checklist (2016) statement: The authors have read the CARE Checklist (2016), and the manuscript was prepared and revised according to the CARE Checklist (2016).

Open Access: This article is an open-access article that was selected by an in-house editor and fully peer-reviewed by external reviewers. It is distributed in accordance with the Creative Commons Attribution NonCommercial (CC BY-NC 4.0) license, which permits others to distribute, remix, adapt, build upon this work non-commercially, and license their derivative works on different terms, provided the original work is properly cited and the use is non-commercial. See: https://creativecommons.org/Licenses/by-nc/4.0/

Country of origin: Taiwan

ORCID number: Yun-Ting Lin 0009-0001-1302-5261; Zhi-Jie Hong 0000-0002-8414-2297; Guo-Shiou Liao 0000-0003-1082-679X; Wen-Chiuan Tsai 0000-0003-1085-9014; Chuang-Hsin Chiu 0000-0002-7275-6558; Jyh-Cherng Yu 0000-0002-1791-5333.

S-Editor: Lin C
L-Editor: A
P-Editor: Zhang XD

REFERENCES

1 **Łukasiewicz S**, Czeczelewski M, Forma A, Baj J, Sitarz R, Stanisławek A. Breast Cancer-Epidemiology, Risk Factors, Classification, Prognostic Markers, and Current Treatment Strategies-An Updated Review. *Cancers (Basel)* 2021; **13** [PMID: 34503097 DOI: 10.3390/cancers13174287]
2 **DeSantis CE**, Ma J, Gaudet MM, Newman LA, Miller KD, Goding Sauer A, Jemal A, Siegel RL. Breast cancer statistics, 2019. *CA Cancer J Clin* 2019; **69**: 438-451 [PMID: 31577379 DOI: 10.3322/caac.21583]
3 **Mamounas EP**, Kuehn T, Rutgers EJT, von Minckwitz G. Current approach of the axilla in patients with early-stage breast cancer. *Lancet* 2017 [PMID: 28818521 DOI: 10.1016/S0140-6736(17)31451-4]
4 **Makki J**. Diversity of Breast Carcinoma: Histological Subtypes and Clinical Relevance. *Clin Med Insights Pathol* 2015; **8**: 23-31 [PMID: 26740749 DOI: 10.4137/CPath.S31563]
5 **Bianchini G**, Balko JM, Mayer IA, Sanders ME, Gianni L. Triple-negative breast cancer: challenges and opportunities of a heterogeneous disease. *Nat Rev Clin Oncol* 2016; **13**: 674-690 [PMID: 27184417 DOI: 10.1038/nrclinonc.2016.66]
6 **Lehmann BD**, Bauer JA, Chen X, Sanders ME, Chakravarthy AB, Shyr Y, Pietenpol JA. Identification of human triple-negative breast cancer subtypes and preclinical models for selection of targeted therapies. *J Clin Invest* 2011; **121**: 2750-2767 [PMID: 21633166 DOI: 10.1172/JCI45014]
7 **Schmid P**, Cortes J, Dent R, McArthur H, Pusztai L, Kümmel S, Denkert C, Park YH, Hui R, Harbeck N, Takahashi M, Im SA, Untch M, Fasching PA, Mouret-Reynier MA, Foukakis T, Ferreira M, Cardoso F, Zhou X, Karantza V, Tryfonidis K, Aktan G, O'Shaughnessy J; KEYNOTE-522 Investigators. Overall Survival with Pembrolizumab in Early-Stage Triple-Negative Breast Cancer. *N Engl J Med* 2024; **391**: 1981-1991 [PMID: 39282906 DOI: 10.1056/NEJMoa2409932]
8 **Ali MA**, Aiman W, Shah SS, Hussain M, Kashyap R. Efficacy and safety of pembrolizumab based therapies in triple-negative breast cancer: A systematic review of clinical trials. *Crit Rev Oncol Hematol* 2021; **157**: 103197 [PMID: 33309890 DOI: 10.1016/j.critrevonc.2020.103197]
9 **Dent R**, Trudeau M, Pritchard KI, Hanna WM, Kahn HK, Sawka CA, Lickley LA, Rawlinson E, Sun P, Narod SA. Triple-negative breast cancer: clinical features and patterns of recurrence. *Clin Cancer Res* 2007; **13**: 4429-4434 [PMID: 17671126 DOI: 10.1158/1078-0432.CCR-06-3045]
10 **Groheux D**, Hindie E. Breast cancer: initial workup and staging with FDG PET/CT. *Clin Transl Imaging* 2021; **9**: 221-231 [PMID: 33937141 DOI: 10.1007/s40336-021-00426-z]
11 **Zhao Q**, Yang F, Wu HL, Mo M, Ling YX, Liu GY. Contralateral axillary lymph node metastasis in breast cancer: An oligometastatic-like disease. *Breast* 2023; **72**: 103589 [PMID: 37839139 DOI: 10.1016/j.breast.2023.103589]
12 **Strazzanti A**, Gangi S, Trovato C, Pacini N, Basile F. Contralateral lymph node metastasis in a woman with new primary breast cancer: Systemic desease or locoregional diffusion? *Int J Surg Case Rep* 2018; **53**: 400-402 [PMID: 30567054 DOI: 10.1016/j.ijscr.2018.11.001]
13 **Díaz-Roldán J**, Eguía-Larrea M, Rubio-Sánchez T, Muñoz-Bellvís L. Systematic review of synchronous contralateral axillary metastases in breast cancer: really M1 disease? *Breast Cancer* 2022; **29**: 9-18 [PMID: 34652689 DOI: 10.1007/s12282-021-01293-2]
14 **Jung JJ**, Cheun JH, Kang E, Shin I, Byeon J, Lee H, Kim HK, Lee HB, Han W, Moon HG. Survival After Contralateral Axillary Metastasis in Breast Cancer. *Ann Surg Oncol* 2024; **31**: 5189-5196 [PMID: 38695982 DOI: 10.1245/s10434-024-15370-1]
15 **Foulkes WD**, Smith IE, Reis-Filho JS. Triple-negative breast cancer. *N Engl J Med* 2010; **363**: 1938-1948 [PMID: 21067385 DOI: 10.1056/NEJMra1001389]
16 **Lee J**, Lee YJ, Bae SJ, Baek SH, Kook Y, Cha YJ, Lee JW, Son BH, Ahn SH, Lee HJ, Gong G, Jeong J, Lee SB, Ahn SG. Ki-67, 21-Gene Recurrence Score, Endocrine Resistance, and Survival in Patients With Breast Cancer. *JAMA Netw Open* 2023; **6**: e2330961 [PMID: 37647069 DOI: 10.1001/jamanetworkopen.2023.30961]
17 **Huston TL**, Pressman PI, Moore A, Vahdat L, Hoda SA, Kato M, Weinstein D, Tousimis E. The presentation of contralateral axillary lymph node metastases from breast carcinoma: a clinical management dilemma. *Breast J* 2007; **13**: 158-164 [PMID: 17319857 DOI: 10.1111/j.1524-4741.2007.00390.x]
18 **Terao M**, Niikura N. Diagnosis of oligometastasis. *Transl Cancer Res* 2020; **9**: 5032-5037 [PMID: 35117868 DOI: 10.21037/tcr.2020.01.04]
19 **Liang Y**, Zhang H, Song X, Yang Q. Metastatic heterogeneity of breast cancer: Molecular mechanism and potential therapeutic targets. *Semin Cancer Biol* 2020; **60**: 14-27 [PMID: 31421262 DOI: 10.1016/j.semcancer.2019.08.012]
20 **Loibl S**, Poortmans P, Morrow M, Denkert C, Curigliano G. Breast cancer. *Lancet* 2021; **397**: 1750-1769 [PMID: 33812473 DOI: 10.1016/S0140-6736(20)32381-3]
21 **Yoon SM**, Bazan JG. Navigating Breast Cancer Oligometastasis and Oligoprogression: Current Landscape and Future Directions. *Curr Oncol Rep* 2024; **26**: 647-664 [PMID: 38652425 DOI: 10.1007/s11912-024-01529-2]
22 **Burgaleta AM**, Burguete AB, Gutiérrez LR, Nuín EB, Felipe GA, de la Vega FA. Local treatment in oligometastasis from breast cancer: an overview. *Clin Transl Oncol* 2023; **25**: 2861-2867 [PMID: 37106239 DOI: 10.1007/s12094-023-03170-0]
23 **Zwimpfer TA**, Schwab FD, Steffens D, Kaul F, Schmidt N, Geiger J, Geissler F, Heinzelmann-Schwarz V, Weber WP, Kurzeder C. Contralateral lymph node metastasis in recurrent ipsilateral breast cancer with Lynch syndrome: a locoregional event. *World J Surg Oncol* 2023; **21**: 40 [PMID: 36755294 DOI: 10.1186/s12957-023-02918-w]
24 **Zhang Z**, Zhang Y, Sun X. Therapeutic options for contralateral axillary lymph node metastasis in breast cancer. *Curr Probl Cancer* 2021; **45**: 100706 [PMID: 33468335 DOI: 10.1016/j.currproblcancer.2020.100706]
25 **Bernsdorf M**, Berthelsen AK, Wielenga VT, Kroman N, Teilum D, Binderup T, Tange UB, Andersson M, Kjær A, Loft A, Graff J. Preoperative PET/CT in early-stage breast cancer. *Ann Oncol* 2012; **23**: 2277-2282 [PMID: 22357250 DOI: 10.1093/annonc/mds002]

26 **Ferahman S**, Velidedeoglu M, Tosun Y, Albeniz G, Ulusan K, Celik V, Ferahman M, Gazioglu E. The effect of preoperative (18)F-FDG PET on the surgical decision in early breast cancer: 5-Year follow-up. *Hell J Nucl Med* 2020; **23**: 256-263 [PMID: 33306756 DOI: 10.1967/s002449912205]

27 **Bove S**, Fragomeni SM, Romito A, DI Giorgio D, Rinaldi P, Pagliara D, Verri D, Romito I, Paris I, Tagliaferri L, Marazzi F, Visconti G, Franceschini G, Masetti R, Garganese G. Techniques for sentinel node biopsy in breast cancer. *Minerva Surg* 2021; **76**: 550-563 [PMID: 34338468 DOI: 10.23736/S2724-5691.21.09002-X]

28 **Hadebe B**, Harry L, Ebrahim T, Pillay V, Vorster M. The Role of PET/CT in Breast Cancer. *Diagnostics (Basel)* 2023; **13** [PMID: 36832085 DOI: 10.3390/diagnostics13040597]

29 **Katal S**, Eibschutz LS, Saboury B, Gholamrezanezhad A, Alavi A. Advantages and Applications of Total-Body PET Scanning. *Diagnostics (Basel)* 2022; **12** [PMID: 35204517 DOI: 10.3390/diagnostics12020426]

30 **Martei YM**, Matro JM. Identifying patients at high risk of breast cancer recurrence: strategies to improve patient outcomes. *Breast Cancer (Dove Med Press)* 2015; **7**: 337-343 [PMID: 26504408 DOI: 10.2147/BCTT.S91981]

31 **Cadoo KA**, Fornier MN, Morris PG. Biological subtypes of breast cancer: current concepts and implications for recurrence patterns. *Q J Nucl Med Mol Imaging* 2013; **57**: 312-321 [PMID: 24322788]

32 **Gündoğdu R**, Gemici K, Kaya M, Turgut S. The effect of preoperative 18f Fdg-Pet on staging and treatment protocols in breast cancer patients. *Ann Ital Chir* 2021; **92**: 346-352 [PMID: 34728590]

33 **Ko H**, Baghdadi Y, Love C, Sparano JA. Clinical Utility of 18F-FDG PET/CT in Staging Localized Breast Cancer Before Initiating Preoperative Systemic Therapy. *J Natl Compr Canc Netw* 2020; **18**: 1240-1246 [PMID: 32886897 DOI: 10.6004/jnccn.2020.7592]

34 **Won KA**, Spruck C. Triple-negative breast cancer therapy: Current and future perspectives (Review). *Int J Oncol* 2020; **57**: 1245-1261 [PMID: 33174058 DOI: 10.3892/ijo.2020.5135]

35 **Amin MB**, Gress DM, Meyer Vega LR, Edge SB, Greene FL, Byrd DR, Brookland RK, Washington MK, Compton CC. AJCC Cancer Staging Manual, Eighth Edition. Cham: Springer, 2018

World Journal of Clinical Cases

Submit a Manuscript: https://www.f6publishing.com

World J Clin Cases 2025 June 26; 13(18): 103618

DOI: 10.12998/wjcc.v13.i18.103618

ISSN 2307-8960 (online)

CASE REPORT

Refractory Crohn's disease complicated with Guillain-Barré syndrome: A case report

A-Niu Liu, Jia-Yi Yang, Xing-Yu Chen, Shan-Shan Wu, Se-Niu Ji Zhi, Shu-Mei Zheng

Specialty type: Medicine, research and experimental

Provenance and peer review: Unsolicited article; Externally peer reviewed.

Peer-review model: Single blind

Peer-review report's classification
Scientific Quality: Grade C
Novelty: Grade B
Creativity or Innovation: Grade C
Scientific Significance: Grade B

P-Reviewer: Tang Y

Received: November 26, 2024
Revised: January 24, 2025
Accepted: February 17, 2025
Published online: June 26, 2025
Processing time: 94 Days and 2.2 Hours

A-Niu Liu, Department of Gastroenterology and Hepatology, Chengdu Medical College, Chengdu 610500, Sichuan Province, China

A-Niu Liu, Xing-Yu Chen, Shan-Shan Wu, Se-Niu Ji Zhi, Shu-Mei Zheng, Department of Gastroenterology and Hepatology, The General Hospital of Western Theater Command, Chengdu 610083, Sichuan Province, China

Jia-Yi Yang, Department of Radiology, Wuxi People's Hospital, Nanjing Medical University, Nanjing 214023, Jiangsu Province, China

Corresponding author: Shu-Mei Zheng, MD, Chief Physician, Department of Gastroenterology and Hepatology, The General Hospital of Western Theater Command, No. 270 Rongdu Road, Chengdu 610083, Sichuan Province, China. zhengsm@163.com

Abstract

BACKGROUND

Inflammatory bowel disease (IBD) comprises a group of chronic inflammatory gastrointestinal disorders, including Crohn's disease (CD) and ulcerative colitis, with uncertain etiologies. The natural course of IBD can be accompanied by extraintestinal manifestations involving the skin, mucous membranes, musculoskeletal structures, eyes, cardiovascular system and nervous system. Guillain-Barré syndrome (GBS) is a type of peripheral neuropathy. However, the etiology and pathogenesis of IBD combined with GBS are unclear, and only a few clinical cases have been reported. Here, we report a case of refractory CD complicated by GBS and review the previous literature to improve the understanding of these diseases.

CASE SUMMARY

A 34-year-old man had a 9-year history of refractory CD. He became unresponsive to multiple drugs and experienced recurrent intestinal fistulas. After several abdominal surgeries and treatment with ustekinumab, he achieved clinical remission. Unfortunately, he developed GBS during maintenance treatment with ustekinumab. According to previous reports, in some patients with IBD combined with GBS, GBS may be a comorbidity, an extraintestinal manifestation of IBD, or an adverse reaction to IBD therapeutic drugs. After a comprehensive evaluation, we suspected that GBS might have been a comorbidity in this patient. To avoid fatal disease relapse after medication discontinuation, we concluded that ustekinumab should not be withdrawn. On the basis of a joint decision between doctors and the patient, we decided to continue maintenance treatment with

ustekinumab along with intravenous immunoglobulin, dexamethasone and traditional Chinese medicine acupuncture, which resulted in a steady improvement in his GBS symptoms and sustained remission of CD.

CONCLUSION
When IBD is complicated by a neurological disease, it is first necessary to analyze the patient's condition and then choose the corresponding treatment strategy. If the neurological disease is a specific comorbidity, treatment of both IBD and the comorbid disease should be considered. For IBD patients with extraintestinal manifestations involving the nervous system, neurological manifestations tend to resolve when the active IBD is controlled. When an adverse drug reaction is suspected, the medication should be discontinued, and symptomatic treatment should be administered.

Key Words: Inflammatory bowel disease; Crohn's disease; Ulcerative colitis; Guillain-Barré syndrome; Biological agents; Case report

©The Author(s) 2025. Published by Baishideng Publishing Group Inc. All rights reserved.

Core Tip: Inflammatory bowel disease (IBD) comprises a group of chronic inflammatory gastrointestinal disorders, including Crohn's disease (CD) and ulcerative colitis. The natural course of IBD can be accompanied by several extraintestinal manifestations. IBD combined with Guillain-Barré syndrome (GBS) has rarely been reported. Here, we describe a patient with refractory CD who stopped responding to multiple drugs and experienced recurrent complicated intestinal fistulas. After several abdominal surgeries and treatment with ustekinumab, he achieved clinical remission. Unfortunately, he developed GBS during maintenance therapy. In patients with IBD combined with GBS, GBS may be a comorbidity, an extraintestinal manifestation of IBD, or an adverse reaction to IBD therapeutic drugs. We suspected that GBS might have been a comorbidity in this patient; therefore, we decided to continue maintenance treatment with ustekinumab along with intravenous immunoglobulin, dexamethasone and traditional Chinese medicine acupuncture, which resulted in a steady improvement in his GBS symptoms and sustained remission of CD.

Citation: Liu AN, Yang JY, Chen XY, Wu SS, Ji Zhi SN, Zheng SM. Refractory Crohn's disease complicated with Guillain-Barré syndrome: A case report. *World J Clin Cases* 2025; 13(18): 103618
URL: https://www.wjgnet.com/2307-8960/full/v13/i18/103618.htm
DOI: https://dx.doi.org/10.12998/wjcc.v13.i18.103618

INTRODUCTION

In recent years, the prevalence of inflammatory bowel disease (IBD) has increased in China[1]. IBD is often accompanied by extraintestinal manifestations, and these extraintestinal disorders can influence the diagnosis of and treatment strategy for IBD. Extraintestinal involvement in IBD frequently affects organs and tissues such as the skin and mucous membranes, the musculoskeletal system, the eyes, the liver and bile ducts, and the cardiovascular and nervous systems. IBD complicated by neurological diseases, including central nervous and peripheral nervous system diseases, may have a poor prognosis, as evidenced by limited neurological function recovery, which has a harmful effect on quality of life[2]. The prevalence of neurological manifestations or complications of IBD is heterogeneous and varies between 0.2% and 36%, with peripheral neuropathy being especially frequent[3]. Guillain-Barré syndrome (GBS) is an immune-mediated acute inflammatory peripheral neuropathy with an annual incidence of 0.81-1.89 per 100000 people and a male-to-female incidence ratio of approximately 3:2[4]. GBS is characterized mainly by symmetric weakness of the limbs, weakened or absent tendon reflexes, decreased or abnormal sensation of the distal limbs, and albuminocytologic dissociation in cerebrospinal fluid (CSF) in some patients. Furthermore, GBS can be life-threatening in some severe cases[5-7]; thus, early diagnosis and appropriate treatment are extremely important.

CASE PRESENTATION

Chief complaints

A 34-year-old male presented with intermittent abdominal pain and diarrhea for more than 9 years and weakness of the limbs for 3 days.

History of present illness

The patient was clinically diagnosed with acute appendicitis and underwent appendectomy at his local hospital in June 2014. In July 2015, the patient experienced recurrent right lower abdominal pain with diarrhea. An abdominal computed

tomography (CT) scan revealed irregular thickening and swelling of the transverse and hepatic flexure of the colon and ileocecal region. Colonoscopy revealed a cobblestone-like appearance with ulceration and polypoid hyperplasia in the transverse colon and ileocecal region. Single-balloon enteroscopy revealed a longitudinal ulcer in the distal ileum. The subsequent esophagogastroduodenoscopy examination revealed normal findings. Histological analysis of the colon and ileal biopsy samples revealed chronic active inflammation with ulceration in the transverse colon and ileocecal and terminal ileum. Zeihel-Nelson staining was negative for acid-fast bacilli, and the results of skin testing for pure protein derivatives of tuberculin were negative. On the basis of the above clinical, imaging, endoscopic and histological findings, the final diagnosis of the patient was active Crohn's disease (CD) (A2 L3B3). Oral prednisone at 40 mg/day was then administered for 10 days. All of his symptoms were ameliorated one month later. Oral prednisone was maintained for 5 months with 5 mg tapering at 2-week intervals and combined with 75 mg/day azathioprine. The patient's clinical symptoms were relieved, and his C-reactive protein (CRP) level and erythrocyte sedimentation rate returned to normal. In January 2019, the patient underwent intestinal adhesion relaxation; partial resection of the transverse colon, ileum and duodenum; ileal valve repair; and duodenum-ileo-transverse colon lateral anastomosis due to recurrent intestinal obstruction and ileal transverse colon anastomosis-duodenal fistula. After the operation, the patient experienced recurrent abdominal pain, fever, an incision fistula and a right lower abdominal intestinal fistula. Treatment, such as anti-infection and nutritional therapies, was provided. In October 2019, intravenous infusion of infliximab was initiated (250 mg at 0, 2 and 6 weeks during the induction period and every 8 weeks during the maintenance period). In July 2020, the treatment was switched to ustekinumab (first 260 mg IV and subsequently 90 mg injected subcutaneously every 8 weeks) because the patient was unresponsive to infliximab. In July 2022, he underwent duodenal and jejunal fistula repair, partial colectomy, partial ileectomy, ileum–ileum anastomosis and ileum–descending colon anastomosis. At this point, a continuous digestive tract was finally achieved, and the patient gradually transitioned to a normal diet. With regular postoperative ustekinumab treatment, the patient remained in clinical remission. Unfortunately, he subsequently experienced limb weakness, unstable holding of objects, and difficulty standing and walking for no apparent reason in December 2022.

History of past illness

The patient had a 10-year history of hepatitis B virus infection and had taken the oral antiviral drug entecavir for 7 years.

Personal and family history

The patient had no related personal or family history.

Physical examination

On examination, several scars were found on the skin of the patient's abdominal wall and right lower limb. He was clear and mentally alert, his advanced cognitive function and cranial nerve examination results were normal, and he had normal superficial sensation and limb muscular tension. The patient's limb muscle strength was weak, with upper and lower limb muscle strengths of level 3 and 2, respectively. Limb tendon reflexes were weak, physiological reflexes were normal, and pathological reflexes were negative.

Laboratory examinations

Blood cell analysis revealed increased white blood cell and neutrophilic granulocyte counts of 10.78 × 10^9/L (normal range 3.5 × 10^9-9.5 × 10^9/L) and 8.25 × 10^9/L (normal range 1.8 × 10^9-6.3 × 10^9/L), respectively. The CRP level was 5.23 mg/L (normal range 0-3 mg/L). A hepatitis panel was positive for hepatitis B surface antigen and hepatitis B core antibody. Hepatitis B viral DNA test results were negative. CSF routine and biochemical test results and tuberculosis smear results were negative. The results of routine stool tests, occult blood analysis, and bacterial cultures were negative.

Imaging examination

Head magnetic resonance imaging (MRI) and CT findings were normal. Abdominal X-ray revealed some gas and fecal shadows in the intestine, a small amount of liquid and gas in the middle and lower abdomen and chain-shaped dense shadows on both sides of the middle and lower abdomen.

Nerve conduction velocity

Nerve conduction velocity revealed demyelination in the motor nerve axons of the limbs. No F waves were observed in either upper limb, indicating demyelination changes in the proximal portion of both upper limbs. The H-reflexes of both upper limbs were normal.

Electromyography

When the right gastrocnemius and quadriceps muscles contracted, the average wave amplitude increased, indicating the presence of neurogenic damage in these muscles.

FINAL DIAGNOSIS

(1) CD (A2 L3 + L4B3) complicated by duodenal fistula, jejunal fistula, colonic fistula, ileostomy closure, partial resection of the small intestine and partial resection of the colon; (2) GBS; and (3) Chronic hepatitis B.

TREATMENT

Dexamethasone sodium phosphate (10 mg/day) and immunoglobulin (17.5 g/day) were intravenously administered for 7 days in combination with traditional Chinese medicine acupuncture and rehabilitation training.

OUTCOME AND FOLLOW-UP

The patient's limb muscle strength gradually recovered. His limb muscle strength returned to normal, and he was able to hold objects, move, and walk independently at the 16-month follow-up. During this period, subcutaneous injections of ustekinumab 90 mg/8 weeks were administered regularly, and the patient achieved clinical remission. On April 2, 2024, a repeat colonoscopy revealed an anastomosis 35 cm away from the anus and a 0.6 cm × 0.3 cm longitudinal ulcer in the proximal intestine 60 cm away from the anastomosis.

DISCUSSION

The etiology and pathogenesis of GBS are not fully understood, and GBS is currently believed to be related to factors such as genetic susceptibility, infection and immune abnormalities. GBS is a typical postinfection disease. At onset, approximately two-thirds of GBS patients have a history of respiratory or gastrointestinal infections. Eighty-five percent of patients with diarrhea as a precursor symptom were previously infected with *Campylobacter jejuni*. Other related pathogens include cytomegalovirus, EB virus, *Mycoplasma pneumoniae*, hepatitis B virus, human immunodeficiency virus and Zika virus[8-10]. Vaccination may also be associated with the onset of GBS, but controversies regarding this association still exist. Furthermore, polymorphisms in immune-related genes lead to differences in the recognition of specific antigen substances and the intensity of immune responses among individuals, thereby affecting their susceptibility to diseases. However, the genes associated with susceptibility to GBS have not yet been identified. Other studies have revealed that leukemia, lymphoma, the use of immunosuppressants after organ transplantation, and autoimmune disorders such as systemic lupus erythematosus and rheumatoid arthritis are frequently associated with GBS, suggesting that immunological disorders are associated with the pathogenesis of GBS[11-14]. IBD is caused by the interaction of various factors, such as environmental, genetic, infection and immune factors. Up to 50% of IBD patients have extraintestinal manifestations[3], whereas the combination of IBD and GBS is uncommon, with only a few cases reported.

It may be difficult to determine whether GBS is due to medications used to treat IBD, IBD itself, or both. We searched recent English literature and found 10 case reports of IBD combined with GBS (6 patients with CD and 4 patients ulcerative colitis (UC), as shown in Table 1). Among these ten patients with IBD complicated by GBS, one first presented with GBS symptoms. After intravenous immunoglobulin (IVIG) therapy, his GBS symptoms gradually ameliorated. Two weeks after the onset of GBS, the patient developed abdominal pain, diarrhea and bloody stools. Subsequent colonoscopy and histological changes suggested UC. In this case, UC and GBS were difficult to distinguish between primary and secondary cases, and each disease course did not influence the other, suggesting that when GBS occurs in combination with IBD, it is a special comorbidity[15]. Three of the 10 patients were diagnosed with UC and were treated with 5-ASA, prednisolone or azathioprine. All three patients presented with symptoms of GBS during the course of UC[16-18]. Furthermore, a study revealed that, in 33% of CD patients and 40% of UC patients, peripheral neuropathy was related to the exacerbation of IBD, suggesting that the development of peripheral neuropathy is mediated by immune factors. Therefore, GBS may be an extraintestinal manifestation of IBD[19]. Another 5/10 patients were diagnosed with CD; three of them received adalimumab[20-22], and the other two received vedolizumab[23] and ustekinumab[24]. GBS symptoms appeared during biological treatment in these 5 patients. The authors suspected that the presence of GBS during the course of CD may be related to these biologics. Therefore, biologics were discontinued, and IVIG was administered upon GBS symptom onset. In addition to IBD, GBS has also been related to other immune-related disorders and treatment with biologics. Cases of psoriasis and ankylosing spondylitis combined with GBS were reported by Natividade *et al*[25] and Bouchra *et al*[26]. The 2 patients in these reports were treated with adalimumab and infliximab. After the onset of GBS symptoms, the biologics were discontinued, IVIG and other treatments were administered, and the GBS symptoms were relieved. Therefore, in these patients, GBS may have been an adverse reaction to IBD therapeutic drugs. The remaining 1/10 patients developed GBS after treatment with adalimumab[27]. Because the patient had active CD and was willing, adalimumab injection was continued along with IVIG therapy, and the GBS symptoms were gradually alleviated. On the basis of the above reports, there may be several possibilities for the occurrence of neurological manifestations in patients with IBD: (1) Special neurological comorbidities occur along with IBD; (2) Extraintestinal manifestations of IBD involving the nervous system occur; and (3) Neurological manifestations occur as a complication of IBD or as adverse nervous system reactions to IBD therapeutic drugs.

In this study, our patient had a 9-year history of refractory CD and discontinued the use of multiple drugs because of poor treatment efficacy or secondary unresponsiveness. After several surgeries and treatment with ustekinumab, he achieved clinical remission. Unfortunately, he developed GBS during maintenance treatment with ustekinumab. Considering that GBS may be a comorbidity in this patient, we continued maintenance treatment with ustekinumab along with IVIG, dexamethasone and traditional Chinese medicine acupuncture, which resulted in a steady improvement in his GBS symptoms and sustained remission of CD.

Table 1 Treatment and prognosis of inflammatory bowel disease combined with Guillain-Barré syndrome

Ref.	Age/sex	Diagnosis	Drug	Medication and symptoms interval	Treatment	Prognosis
Tominaga *et al*[15]	39/M	UC	None	None	IVIG	CR
Jayasundara *et al*[16]	24/M	UC	AZA + prednisolone	Not mentioned	IVIG	PR
Krystallis *et al*[17]	59/M	UC	Prednisolone + 5-ASA	Not mentioned	IVIG + prednisolone	CR
Liu *et al*[18]	31/F	UC	5-ASA	Not mentioned	Methylprednisolone	CR
Cesarini *et al*[20]	72/M	CD	Adalimumab	1 month	IVIG + methylpred-nisolone	PR
Cançado *et al*[21]	64/M	CD	Adalimumab	2 weeks	Prednisone	CR
Patwala *et al*[22]	37/M	CD	Adalimumab	9 months	IVIG	PR
De Azevedo *et al*[23]	31/M	CD	Vedolizumab	2 weeks	IVIG	Not mentioned
Fukushima *et al*[24]	32/M	CD	Ustekinumab	1 year	IVIG	PR
Natividade *et al*[25]	45/M	Psoriasis	Adalimumab	1 year	IVIG	PR
Bouchra *et al*[26]	47/F	AS	Infliximab	2 months	IVIG	CR
Lee *et al*[27]	33/F	CD	Adalimumab	2 months	Adalimumab + IVIG	CR

CD: Crohn's disease; UC: Ulcerative colitis; IVIG: Intravenous immunoglobulin; AS: Ankylosing spondylitis; 5-ASA: 5-aminosalicylate; AZA: Azathioprine; CR: Complete remission; PR: Partial remission.

CONCLUSION

With the increasing prevalence of IBD in China, the number of patients with IBD combined with extraintestinal manifestations, such as neurological diseases, may gradually increase. When an IBD case is complicated by a neurological disease, it is first necessary to analyze the patient's condition and then choose the corresponding treatment strategy. If the neurological disease is a specific comorbidity, treatment of both IBD and the comorbidity should be considered. For IBD patients with extraintestinal manifestations involving the nervous system, neurological manifestations tend to resolve when the active IBD is controlled. When an adverse drug reaction is suspected, the medication should be discontinued, and symptomatic treatment should be administered. The underlying mechanism of IBD combined with neurological diseases is still not fully understood, and some neurological diseases can lead to poor outcomes or even death. Therefore, it is necessary to identify IBD and neurological diseases as early as possible and provide reasonable treatments to improve the prognosis.

FOOTNOTES

Author contributions: Zheng SM designed the report; Liu AN and Chen XY collected the patient's clinical data; Yang JY and Liu AN analyzed the magnetic resonance imaging and computed tomography images; Wu SS and Ji Zhi SN analyzed the microscopy images; Liu AN and Zheng SM wrote the paper; Yang JY edited the English language version of the manuscript; and all authors have read and approved the final version to be published.

Informed consent statement: Informed written consent was obtained from the patient for publication of this report.

Conflict-of-interest statement: The authors declare that they have no conflict of interest to disclose.

CARE Checklist (2016) statement: The authors have read the CARE Checklist (2016), and the manuscript was prepared and revised according to the CARE Checklist (2016).

Open Access: This article is an open-access article that was selected by an in-house editor and fully peer-reviewed by external reviewers. It is distributed in accordance with the Creative Commons Attribution NonCommercial (CC BY-NC 4.0) license, which permits others to distribute, remix, adapt, build upon this work non-commercially, and license their derivative works on different terms, provided the original work is properly cited and the use is non-commercial. See: https://creativecommons.org/Licenses/by-nc/4.0/

Country of origin: China

ORCID number: A-Niu Liu 0009-0004-8997-6356; Jia-Yi Yang 0000-0002-5282-1092; Xing-Yu Chen 0009-0001-4251-7804; Shan-Shan Wu 0009-0001-4215-6690; Se-Niu Ji Zhi 0009-0003-6008-1631; Shu-Mei Zheng 0000-0002-4463-9784.

S-Editor: Qu XL
L-Editor: A
P-Editor: Guo X

REFERENCES

1 **Kaplan GG**, Ng SC. Understanding and Preventing the Global Increase of Inflammatory Bowel Disease. *Gastroenterology* 2017; **152**: 313-321.e2 [PMID: 27793607 DOI: 10.1053/j.gastro.2016.10.020]
2 **Katsanos AH**, Katsanos KH, Kosmidou M, Giannopoulos S, Kyritsis AP, Tsianos EV. Cerebral sinus venous thrombosis in inflammatory bowel diseases. *QJM* 2013; **106**: 401-413 [PMID: 23243293 DOI: 10.1093/qjmed/hcs229]
3 **Gordon H**, Burisch J, Ellul P, Karmiris K, Katsanos K, Allocca M, Bamias G, Barreiro-de Acosta M, Braithwaite T, Greuter T, Harwood C, Juillerat P, Lobaton T, Müller-Ladner U, Noor N, Pellino G, Savarino E, Schramm C, Soriano A, Michael Stein J, Uzzan M, van Rheenen PF, Vavricka SR, Vecchi M, Zuily S, Kucharzik T. ECCO Guidelines on Extraintestinal Manifestations in Inflammatory Bowel Disease. *J Crohns Colitis* 2024; **18**: 1-37 [PMID: 37351850 DOI: 10.1093/ecco-jcc/jjad108]
4 **Sejvar JJ**, Baughman AL, Wise M, Morgan OW. Population incidence of Guillain-Barré syndrome: a systematic review and meta-analysis. *Neuroepidemiology* 2011; **36**: 123-133 [PMID: 21422765 DOI: 10.1159/000324710]
5 **Yuki N**, Hartung HP. Guillain-Barré syndrome. *N Engl J Med* 2012; **366**: 2294-2304 [PMID: 22694000 DOI: 10.1056/NEJMra1114525]
6 **van den Berg B**, Walgaard C, Drenthen J, Fokke C, Jacobs BC, van Doorn PA. Guillain-Barré syndrome: pathogenesis, diagnosis, treatment and prognosis. *Nat Rev Neurol* 2014; **10**: 469-482 [PMID: 25023340 DOI: 10.1038/nrneurol.2014.121]
7 **Goodfellow JA**, Willison HJ. Guillain-Barré syndrome: a century of progress. *Nat Rev Neurol* 2016; **12**: 723-731 [PMID: 27857121 DOI: 10.1038/nrneurol.2016.172]
8 **Cao-Lormeau VM**, Blake A, Mons S, Lastère S, Roche C, Vanhomwegen J, Dub T, Baudouin L, Teissier A, Larre P, Vial AL, Decam C, Choumet V, Halstead SK, Willison HJ, Musset L, Manuguerra JC, Despres P, Fournier E, Mallet HP, Musso D, Fontanet A, Neil J, Ghawché F. Guillain-Barré Syndrome outbreak associated with Zika virus infection in French Polynesia: a case-control study. *Lancet* 2016; **387**: 1531-1539 [PMID: 26948433 DOI: 10.1016/S0140-6736(16)00562-6]
9 **Jacobs BC**, Rothbarth PH, van der Meché FG, Herbrink P, Schmitz PI, de Klerk MA, van Doorn PA. The spectrum of antecedent infections in Guillain-Barré syndrome: a case-control study. *Neurology* 1998; **51**: 1110-1115 [PMID: 9781538 DOI: 10.1212/wnl.51.4.1110]
10 **van den Berg B**, van der Eijk AA, Pas SD, Hunter JG, Madden RG, Tio-Gillen AP, Dalton HR, Jacobs BC. Guillain-Barré syndrome associated with preceding hepatitis E virus infection. *Neurology* 2014; **82**: 491-497 [PMID: 24415572 DOI: 10.1212/WNL.0000000000000111]
11 **Zhang L**, Arrington S, Keung YK. Guillain-Barré syndrome after transplantation. *Leuk Lymphoma* 2008; **49**: 291-297 [PMID: 18231916 DOI: 10.1080/10428190701760003]
12 **Javadi Parvaneh V**, Jari M, Qhasemi S, Nasehi MM, Rahmani K, Shiari R. Guillain-Barre syndrome as the first manifestation of juvenile systemic lupus erythematosus: a case report. *Open Access Rheumatol* 2019; **11**: 97-101 [PMID: 31114404 DOI: 10.2147/OARRR.S204109]
13 **Nazir Z**, Habib A, Ali T, Shafiq Khan K, Abbas Jaffri S, Haque MA. Co-occurrence of Guillain-Barre syndrome and rheumatoid arthritis in a young female: A case report from a low middle-income country. *Clin Case Rep* 2024; **12**: e8481 [PMID: 38333652 DOI: 10.1002/ccr3.8481]
14 **Grisold W**, Grisold A, Marosi C, Meng S, Briani C. Neuropathies associated with lymphoma(†). *Neurooncol Pract* 2015; **2**: 167-178 [PMID: 31386037 DOI: 10.1093/nop/npv025]
15 **Tominaga K**, Tsuchiya A, Sato H, Kimura A, Oda C, Hosaka K, Kawata Y, Kimura N, Hayashi K, Yokoyama J, Terai S. Co-existent ulcerative colitis and Guillain-Barré syndrome: a case report and literature review. *Clin J Gastroenterol* 2019; **12**: 243-246 [PMID: 30778832 DOI: 10.1007/s12328-019-00939-1]
16 **Jayasundara JMHD**, Samarawickrama VT, Peiris R, Aponso T, Abeynayake D. Concomitant Guillain-Barré Syndrome in a young Sri Lankan male with severe ulcerative colitis. *BMC Gastroenterol* 2022; **22**: 411 [PMID: 36064313 DOI: 10.1186/s12876-022-02455-y]
17 **Krystallis CS**, Kamberoglou DK, Cheilakos GB, Maltezou MN, Tzias VD. Guillain-Barré syndrome during a relapse of ulcerative colitis: a case report. *Inflamm Bowel Dis* 2010; **16**: 555-556 [PMID: 19714764 DOI: 10.1002/ibd.21071]
18 **Liu Z**, Zhou K, Tian S, Dong W. Ulcerative colitis with Guillain-Barré syndrome: A case report. *Medicine (Baltimore)* 2018; **97**: e11013 [PMID: 29923987 DOI: 10.1097/MD.0000000000011013]
19 **Casella G**, Tontini GE, Bassotti G, Pastorelli L, Villanacci V, Spina L, Baldini V, Vecchi M. Neurological disorders and inflammatory bowel diseases. *World J Gastroenterol* 2014; **20**: 8764-8782 [PMID: 25083051 DOI: 10.3748/wjg.v20.i27.8764]
20 **Cesarini M**, Angelucci E, Foglietta T, Vernia P. Guillain-Barrè syndrome after treatment with human anti-tumor necrosis factorα (adalimumab) in a Crohn's disease patient: case report and literature review. *J Crohns Colitis* 2011; **5**: 619-622 [PMID: 22115384 DOI: 10.1016/j.crohns.2011.06.010]
21 **Cançado GG**, Vilela EG. Guillain-Barré syndrome during adalimumab therapy for Crohn´s disease: coincidence or consequence? *Scand J Gastroenterol* 2017; **52**: 473-476 [PMID: 27931132 DOI: 10.1080/00365521.2016.1263682]
22 **Patwala K**, Crump N, De Cruz P. Guillain-Barré syndrome in association with antitumour necrosis factor therapy: a case of mistaken identity. *BMJ Case Rep* 2017; **2017**: bcr2017219481 [PMID: 28679512 DOI: 10.1136/bcr-2017-219481]
23 **de Azevedo MFC**, Queiroz NSF, Damião AOMC. Guillain-Barré Syndrome in a Crohn`s Disease Patient Treated With Vedolizumab. *J Crohns Colitis* 2020; **14**: 1788-1789 [PMID: 32417923 DOI: 10.1093/ecco-jcc/jjaa101]
24 **Fukushima T**, Nakajima K, Nozawa H, Nishino H, Sugita A, Koganei K, Futatsuki R, Yamaguchi S, Asano S, Matsushima M. [A case of Crohn's disease complicated by Guillain-Barrè syndrome during ustekinumab therapy]. *Nihon Shokakibyo Gakkai Zasshi* 2019; **116**: 324-329 [PMID: 30971669 DOI: 10.11405/nisshoshi.116.324]
25 **Natividade NB**, Felix PAO, Lerer C. Guillain-Barré syndrome in a patient on adalimumab for the treatment of psoriasis. *An Bras Dermatol*

2017; **92**: 85-87 [PMID: 29267456 DOI: 10.1590/abd1806-4841.20175871]

26 **Bouchra A**, Benbouazza K, Hajjaj-Hassouni N. Guillain-Barre in a patient with ankylosing spondylitis secondary to ulcerative colitis on infliximab therapy. *Clin Rheumatol* 2009; **28** Suppl 1: S53-S55 [PMID: 19277812 DOI: 10.1007/s10067-009-1154-7]

27 **Lee JH**, Park JS, Park D. Successful IVIG treatment without discontinuation of TNF-α blocker in Guillain-Barre syndrome induced by adalimumab in patient with Crohn's disease. *Neurol Sci* 2018; **39**: 595-598 [PMID: 29101591 DOI: 10.1007/s10072-017-3179-z]

World Journal of Clinical Cases

Submit a Manuscript: https://www.f6publishing.com

World J Clin Cases 2025 June 26; 13(18): 103777

DOI: 10.12998/wjcc.v13.i18.103777

ISSN 2307-8960 (online)

CASE REPORT

New surgical approach for distal clavicle fractures: A case report

Wen-Tao Hu, Zi-Yan Zhang, Ji Qu, Cheng-Dong Piao

Specialty type: Orthopedics

Provenance and peer review: Unsolicited article; Externally peer reviewed.

Peer-review model: Single blind

Peer-review report's classification

Scientific Quality: Grade B, Grade C

Novelty: Grade B, Grade B

Creativity or Innovation: Grade B, Grade B

Scientific Significance: Grade B, Grade B

P-Reviewer: Bonk MN

Received: December 2, 2024

Revised: December 29, 2024

Accepted: February 6, 2025

Published online: June 26, 2025

Processing time: 89 Days and 1.1 Hours

Wen-Tao Hu, Zi-Yan Zhang, Ji Qu, Cheng-Dong Piao, Department of Orthopedics, The Second Hospital of Jilin University, Changchun 130041, Jilin Province, China

Corresponding author: Cheng-Dong Piao, Department of Orthopedics, The Second Hospital of Jilin University, No. 218 Ziqiang Road, Nanguan Street, Changchun 130041, Jilin Province, China. pucd@jlu.edu.cn

Abstract

BACKGROUND

Clavicle fractures are a common type of fracture that often occurs after high-energy trauma. The treatment methods for clavicle fractures remain controversial. Both locking compression and hook plates are recommended.

CASE SUMMARY

A 44-year-old male suffered an injury during skiing. Radiography revealed a right-sided distal clavicular fracture. The fracture was treated using a hook plate due to its small size. During the surgical procedure, Kirschner wires were used to drill holes in the acromion. The end of the hook plate was inserted into the hole rather than below the edge of the acromion.

CONCLUSION

One year later, imaging revealed complete healing of the fracture, and the hook plate was removed. The patient was satisfied with the course and treatment results. Additionally, a new classification system was proposed based on the degree of injury to the distal clavicle joint surface. The incidence of postoperative complications associated with the use of hook plates for clavicular fracture treatment is relatively high. Complications can be reduced by changing the hook plate placement.

Key Words: Clavicle; Distal clavicle fracture; Hook plate; Complications; Classification; Classification system; Case report

©The Author(s) 2025. Published by Baishideng Publishing Group Inc. All rights reserved.

Core Tip: Based on the original Operation Method, the new operation method drilled the acromion to reduce the complications of hook plate. We present a classification of distal clavicular fractures based on the distal clavicular articular surface.

Citation: Hu WT, Zhang ZY, Qu J, Piao CD. New surgical approach for distal clavicle fractures: A case report. *World J Clin Cases* 2025; 13(18): 103777
URL: https://www.wjgnet.com/2307-8960/full/v13/i18/103777.htm
DOI: https://dx.doi.org/10.12998/wjcc.v13.i18.103777

INTRODUCTION

Clavicle fracture is a common type of fracture, accounting for 2.6%–4% of fractures in adults[1]. Robert William Smith studied this injury as early as 1847; however, it was considered trivial at that time[2]. It was not until the 1960s that they gradually gained attention. In 1963, Neer proposed the Neer classification of clavicle fractures, further systematizing their treatment. This classification has been used since then[3]. Neer type I and III fractures are more stable, and nonsurgical treatment can produce ideal results. Neer type II distal clavicle fractures occur when the distal fracture fragment moves downwards under muscle traction due to injury of the conoid ligament with a large distance between the fracture ends. The rate of delayed healing after conservative treatment can reach up to 45%, and the incidence of non-union can reach 20%–30%[4]. Therefore, surgical treatment is usually required for Neer type II distal clavicular fractures. Common fixation methods include clavicular hook plates, distal locking plates, Kirschner wires, suture anchors, and band plates. To date, there is no consensus on the best treatment method for distal clavicle fractures, and their treatment remains challenging[5]. Herein, we report the case of a patient with Neer type II clavicle fracture who underwent surgical treatment. The patient achieved a good prognosis by changing the placement of the hook plate.

CASE PRESENTATION

Chief complaints

A 44-year-old man presented with right-sided shoulder pain and a deformity secondary to skiing.

History of present illness

Case report and new operation: Shoulder joint movement was difficult, and no signs of vascular or nerve injury were observed. Plain radiographs and computed tomography (CT) scans revealed a distal clavicle fracture on the right side (Figure 1). The clavicle was split into three fragments, and the fracture was classified as Neer Type II.

History of past illness

No past medical history.

Personal and family history

Smoking history; no family history.

Physical examination

Shoulder joint movement was difficult, and no signs of vascular or nerve injury were observed.

Laboratory examinations

There was no obvious abnormality in laboratory examination.

Imaging examinations

Plain radiographs and CT scans revealed a distal clavicle fracture on the right side (Figure 1). The clavicle was split into three fragments, and the fracture was classified as Neer Type II.

FINAL DIAGNOSIS

Distal clavicle fracture.

TREATMENT

After a detailed explanation of the surgical plan, the patient agreed to undergo surgery and actively cooperated. Surgery was performed under general anesthesia, with the patient in the supine position. The right shoulder was elevated, and an anterolateral clavicular approach was used to make an incision from the clavicle to the acromion, stripping the periosteum to expose the lateral aspect of the clavicle and acromion. The acromioclavicular ligament was intact, and the subacromial soft tissue was gently stripped. A 2.5 mm Kirschner wire was predrilled vertically into the acromion. After

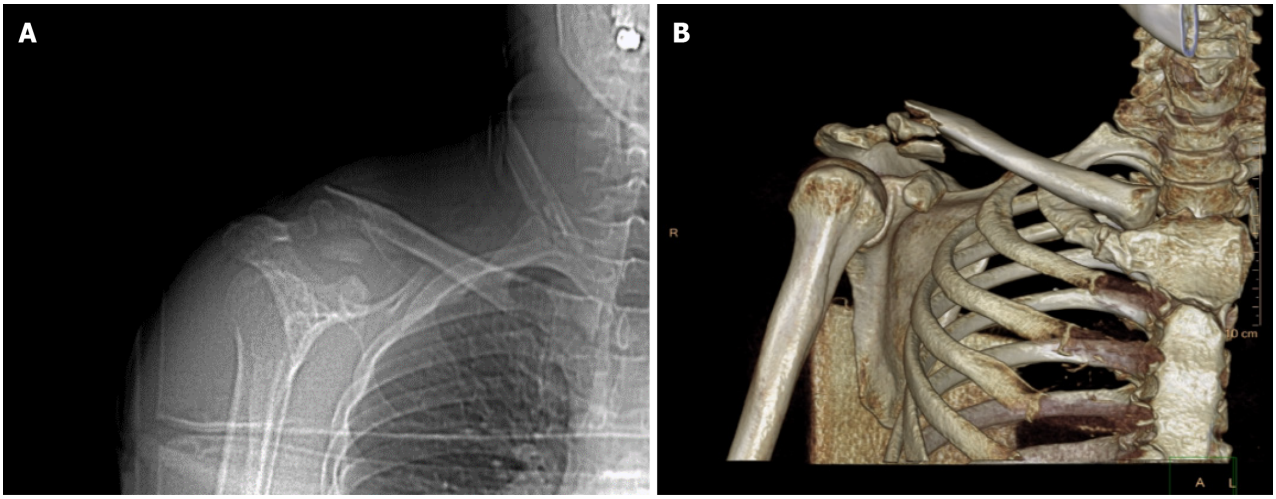


Figure 1 The preoperative images of the patient. A: X-ray image; B: 3D computed tomography image.

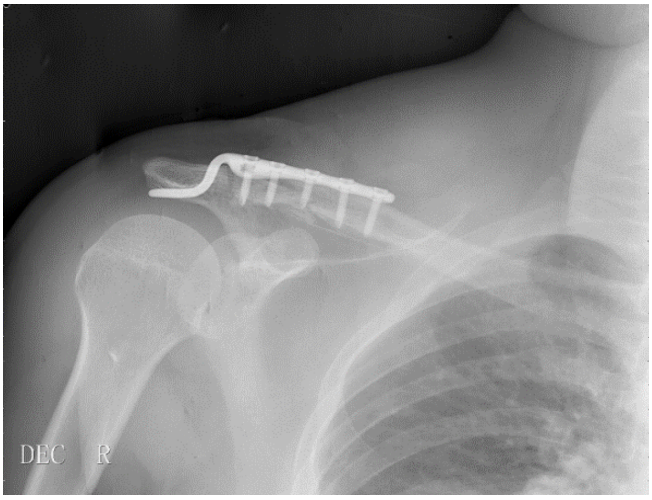


Figure 2 The postoperative X-ray of the patient.

reducing the fracture, the surgeon attempted to insert a hook plate suitable for the three fragments into the acromion. Distal pull and proximal compression of the hook plates were tested, and the most suitable plate was selected. The hook end of the plate was inserted through the hole into the acromial bone rather than below the acromion, and the proximal end was attached to the upper clavicle (Figure 2). The incision was sutured after fixation. The patient awoke without discomfort except for pain.

OUTCOME AND FOLLOW-UP

The patient began active and passive range-of-motion training on the third postoperative day. The patient returned to the hospital after 14 months. The patient received no treatment at any other hospital during this period, and the only discomfort experienced was limited movement of the shoulder joint. At this time, the range of motion of the shoulder joint was as follows: Elevation 120° forward (Figure 3A), horizontal abduction 90° (Figure 3B), and elevation 30° posteriorly (Figure 3C). The patient was not a manual laborer or athlete, and the DASH score was approximately 8.4. Plain radiographs and CT scans revealed complete healing of the fracture, without any hyperdense shadows and the plate hook ends having not penetrated the acromion, as well as no osteolysis (Figure 4). The plate was then removed (Figure 5), thereby increasing the range of motion of the shoulder joint.

New classification system

The injury simultaneously involves the joint surface of the distal clavicle. No studies have investigated the relationship between the degree of injury to the distal clavicle joint surface and the long-term prognosis. Veeger and van der Helm demonstrated that the clavicle bears horizontal forces to support the thorax[6], and Flatow *et al*[7]. discovered that there is a 5°–8° rotational micromotion between the clavicle and acromion. Consequently, we believe that the patient may

Table 1 Patient demographic characteristics, *n* (%)/mean ± SD

Characteristics	Patient (*n* = 29)
Sex ratio (Male/Female)	15/14
	(1: 0.93)
Age (year)	46.6 ± 13.3
Age (male/female)	44.0 ± 13.6/49.3 ± 12.9
Shoulder	15 (51.7)
Left	15 (51.7)
Right	14 (48.3)



Figure 3 Photograph of the patient before surgery to remove the plate. A and B: Shoulder abduction; C: Shoulder extension.

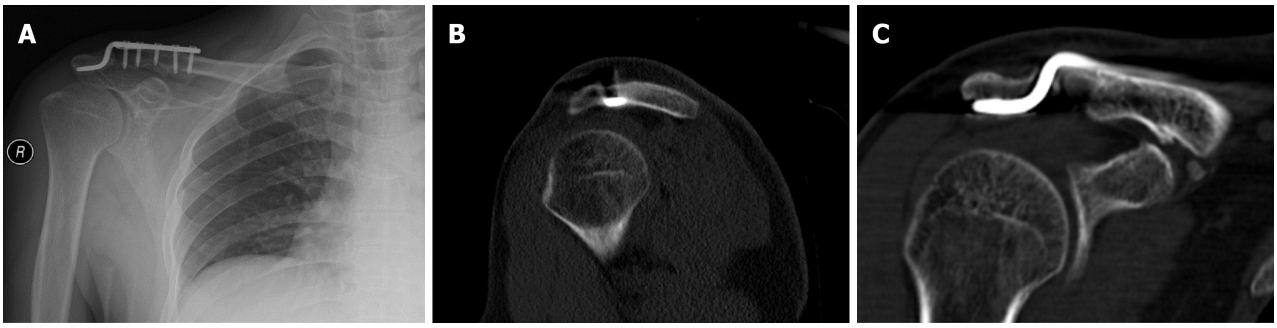


Figure 4 X-ray of the patient reviewed one year later. A: X-ray image; B: and C: CT image.

experience discomfort due to the irregularity of the distal clavicular joint surface and the long-term effects of these forces. The stability and flatness of fractures involving the clavicular joint surface must be restored.

Currently, Neer, Rockwood, and Robinson classifications are widely used and include inclusive classifications. However, there are few detailed descriptions of joint surface injuries, and treatment approaches vary among physicians, each with its own rationale.

Therefore, we searched for patients with clavicular fractures who were treated surgically at our hospital between July 2022 and July 2024. Based on the inclusion criteria, 29 patients were included in this study. Demographic data of the included patients are listed in Table 1. A new classification was proposed based on the statistical analysis of the fracture morphology of these patients (Figure 6).

Due to the small sample size, this article only tentatively presents this classification and provides data for scholars who intend to continue in-depth studies. More importantly, the purpose of this classification is to communicate that it should be refined rather than generalized. Besides, the operator's dependence on surgical experience should be reduced.

The inclusion criteria were as follows: (1) Surgery was performed during hospitalization; (2) Age > 18 years; (3) At least one end of the fracture line was located at or beyond the middle third of the clavicle; and (4) Postoperative imaging revealed a good reduction, flat joint surfaces, and no significant displacement.

Four observers, two experts, and two attending physicians were included in this study. The two experts had an average experience of 20 (± 3) years, and the two attending physicians had an average experience of 11 (± 1) years.

We identified 168 patients with clavicular fractures at our institution between July 2022 and July 2024. A total of 29 patients met the inclusion criteria, of which 15 (51.7%) were male and 14 (48.3%) were female. Left-sided fractures were

Table 2 Fleiss kappa test results (total)[1]

	Fleiss Kappa	Standard error	*Z* value	*P* value	95%CI
First Round	0.912	0.070	13.056	0.000	0.907-0.917
Second Round	1.000	0.068	14.720	0.000	0.995-1.005
First treat	0.701	0.076	9.251	0.000	0.696-0.706
Second treat	0.826	0.076	10.890	0.000	0.820-0.831

[1]The data contains 4 reviewers and 29 evaluators.

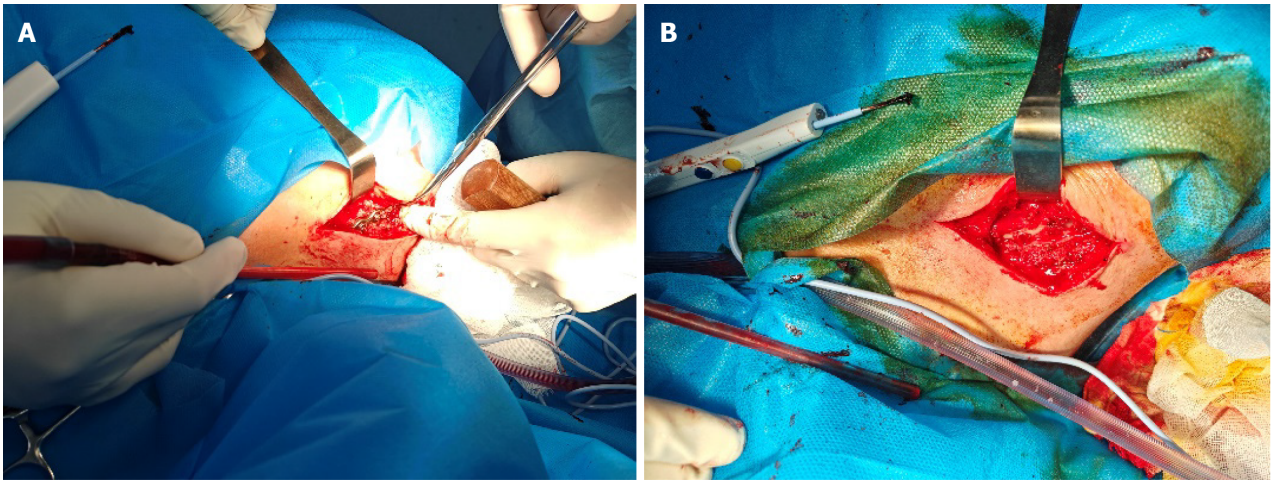


Figure 5 Plate being removed. A and B: Photo of the plate being removed.

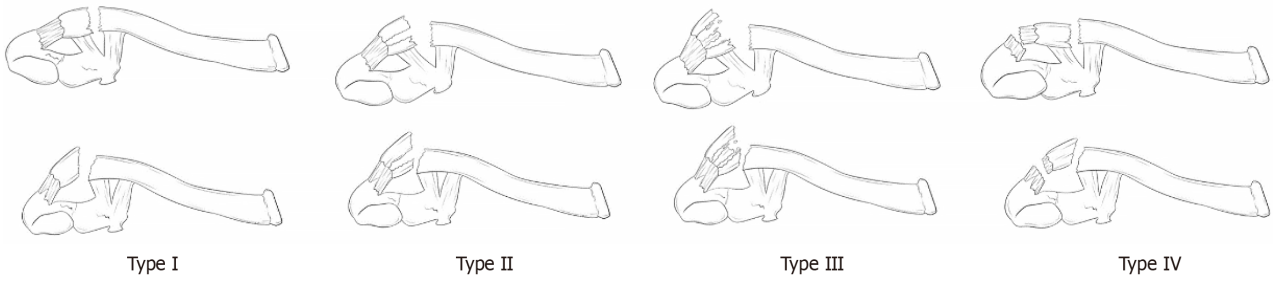


Figure 6 Schematic diagram of the new classification.

present in 15 patients (51.7%), while right-sided fractures were present in 14 patients (48.3%). The imaging data, age, and gender of each participant were recorded. The physicians were asked to classify the fractures according to the new classification system and propose the best surgical approach. Four weeks later, four observers were invited to reevaluate the patients.

According to the proposed new classification scheme, Type I fractures are pure distal clavicle fractures that do not involve the joint surface, regardless of the number of fracture lines. Type II fractures have only one fracture line involving the joint surface. Type III fractures have at least two fracture lines involving the joint surface. Type IV fractures with at least one fracture line involving the joint surface and an acromioclavicular joint separation (Figure 6).

Evaluation of the reliability of the new classification and treatment plan: Consistency among evaluators was assessed using Fleiss' kappa. The reliability of the evaluators was assessed by comparing the results of the two evaluations.

Statistical analysis was performed using Statistical Package for the Social Sciences software (version 27.0; IBM, Armonk). Both classifications by observers with different years of experience resulted in perfect agreement ($\kappa = 0.912$, $\kappa = 1.000$). Treatment plans demonstrated significant agreement ($\kappa = 0.701$) and perfect agreement ($\kappa = 0.826$) (Table 2)[8].

Some controversial cases, such as patients 1 and 2, were also observed. Two attending physicians classified patient 1 as Type II, while two experts classified it as Type I. Compared to the experts, the two attending physicians were more inclined to use 3D CT reconstruction to diagnose the fracture rather than the original images. The 3D CT reconstruction image could blur some details of the fracture, leading to misdiagnosis of the disease. In the second round of testing, the

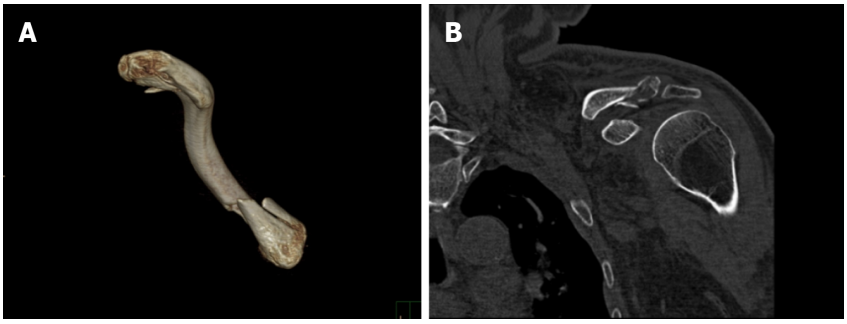


Figure 7 Images of patient 1. A: 3D computed tomography (CT) image; B: CT images.

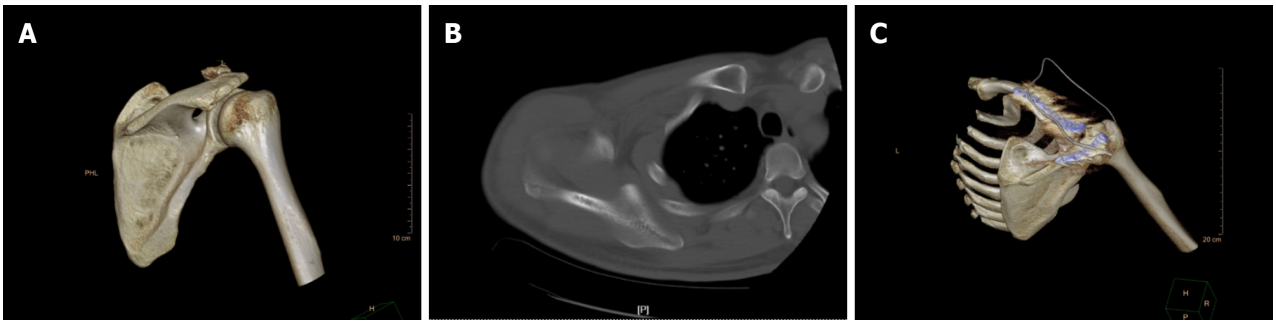


Figure 8 Images of patient 2. A and B: 3D computed tomography (CT) images of patient 2; C: CT images of patient 2.

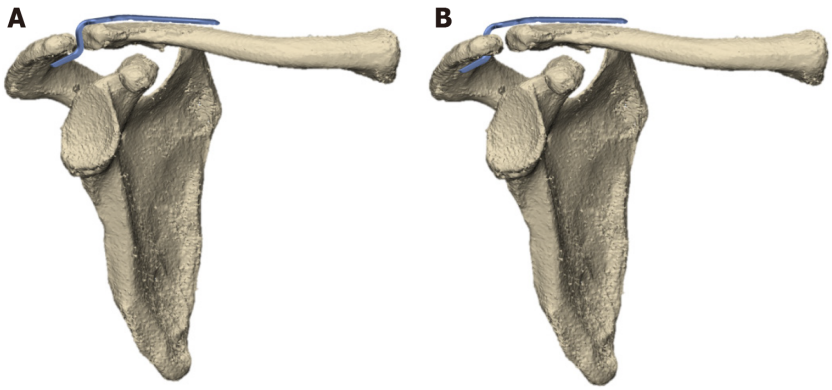


Figure 9 Comparison between new and old techniques. A: The conventional hook plate technique; B: The modified hook plate technique.

two attending physicians classified patient 1 as Type I after reviewing the original images (Figure 7).

Another controversial case was that of patient 2. In the first round of testing, one expert believed that a locking plate should be used, whereas the other three assessors believed that a hook plate should be used. Ultimately, the patient 2 was treated with a locking plate because of an associated acromial fracture (Figure 8), which precluded the use of a hook plate.

These two cases demonstrate that this classification has some limitations. These include the difficulty in defining the extent of the distal clavicular articular surface and the single factor of extensive focus on it. Besides, although we wanted to reduce the influence of inexperience on fracture treatment by classifying fractures, the classification of fractures depends on experience.

DISCUSSION

Section 1: Case report and new operation

Surgical treatment is often necessary for distal-clavicular fractures. When the distal fragment is too small, the hook plate is considered superior to the locking plate[9]. However, complications associated with the hook plates are difficult to

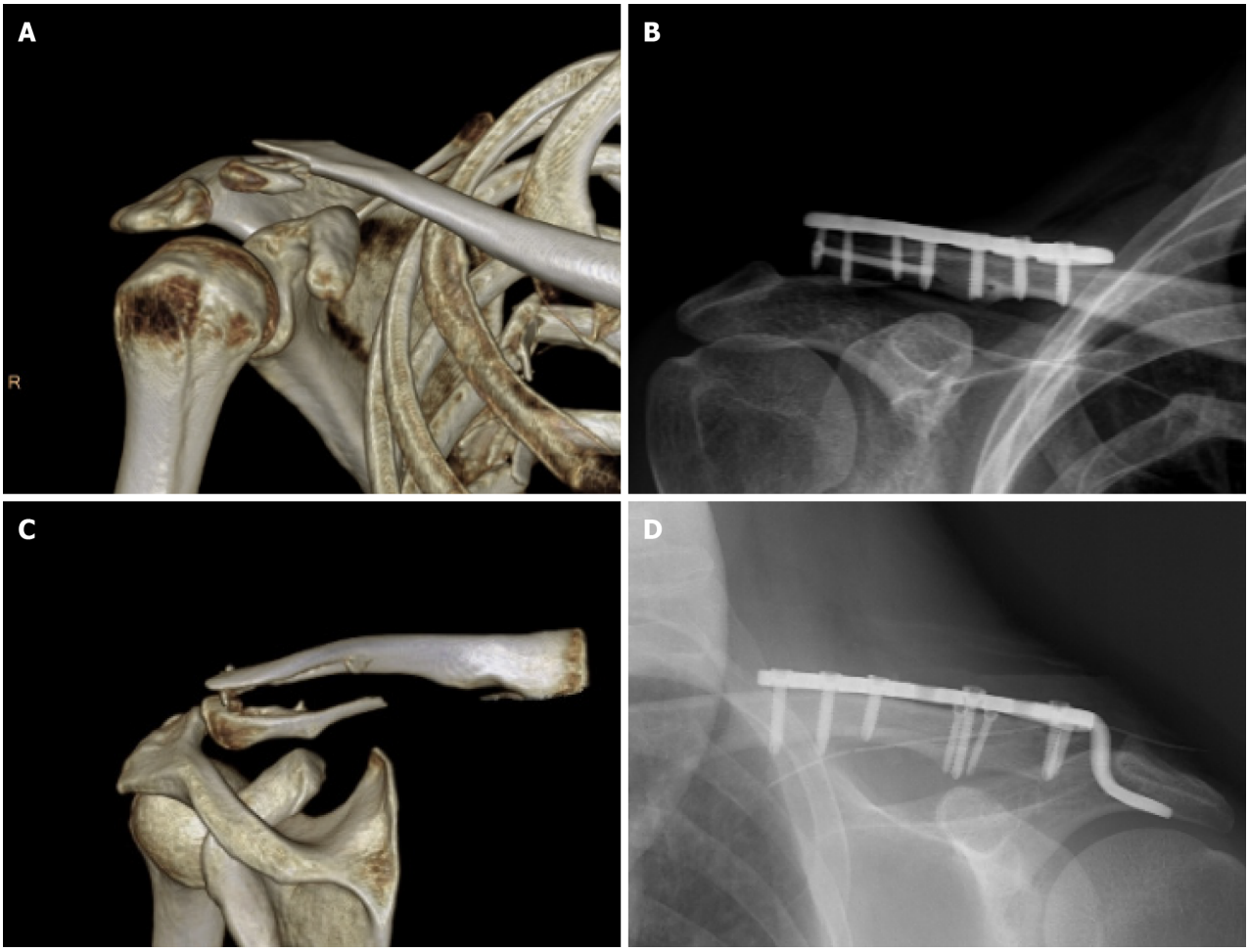


Figure 10 The images of patients classified as Type II. A: Preoperative computed tomography (CT) image of the patient classified as Type II; B: Postoperative X-ray of the patient classified as Type II; C: Preoperative CT images of another patients classified as Type II; D: Postoperative X-ray of another patient classified as Type II.

resolve[10,11]. ElMaraghy *et al*[12] demonstrated through cadaver studies that excessive elevation or rotation of the clavicle could cause micro-motion at the tip of the hook, causing bone erosion or resorption at the point of contact. Li *et al*[13] developed and used a shoulder height measurement device to control the length of the hook plate hook, thereby reducing complications, including shoulder osteolysis and impingement.

Our approach involved externally rotating the hook plate and inserting the hook tip into the shoulder acromion rather than beneath it (Figure 9). This technique inhibits clavicle rotation and micromotion, thereby reducing friction between the hook tip and acromion, which reduces the occurrence of bone resorption. However, this also temporarily reduced the range of motion of the shoulder joint until the plate was removed. Most scholars believe that the hook plates should be removed. Consequently, we consider the reduction in the shoulder joint range of motion to be temporary and acceptable.

As the hook tip is inserted within the acromion, the length of the hook tip is determined by the thickness of the acromion. If the hook tip is too long, the plate can easily be lifted; if it is too short, the plate cannot adhere to the clavicle. As a consequence, the surgeon can select the optimal hook tip length without requiring any measuring tool, thereby significantly reducing the occurrence of shoulder impingement. However, this implies that the surgical procedure requires a higher level of expertise.

Drilling the acromion can destroy its structure, increasing the risk of acromial fractures. As a result, it is unsuitable for the treatment of patients with osteoporosis.

Herein, we report the case of a patient who underwent this procedure. At the 14-month follow-up, the patient made a satisfactory recovery. Consequently, we believe that surgery is feasible. However, more cases are required to confirm its efficacy.

Section 2: New classification system

In this study, the novel classification scheme for distal clavicular fractures achieved significant or perfect agreement with physicians with different years of experience regarding classification and choice of treatment.

Neer classification has been used since the 1960s, but its inclusiveness and practicality are uncontested. The Neer classification systematically categorizes fractures according to their location and the relationship between the ligaments. However, it can only be used for injuries involving the acromioclavicular joint in Neer Type III and does not provide further subclassification. When surgeons develop surgical plans, they provide limited information. In our clinical

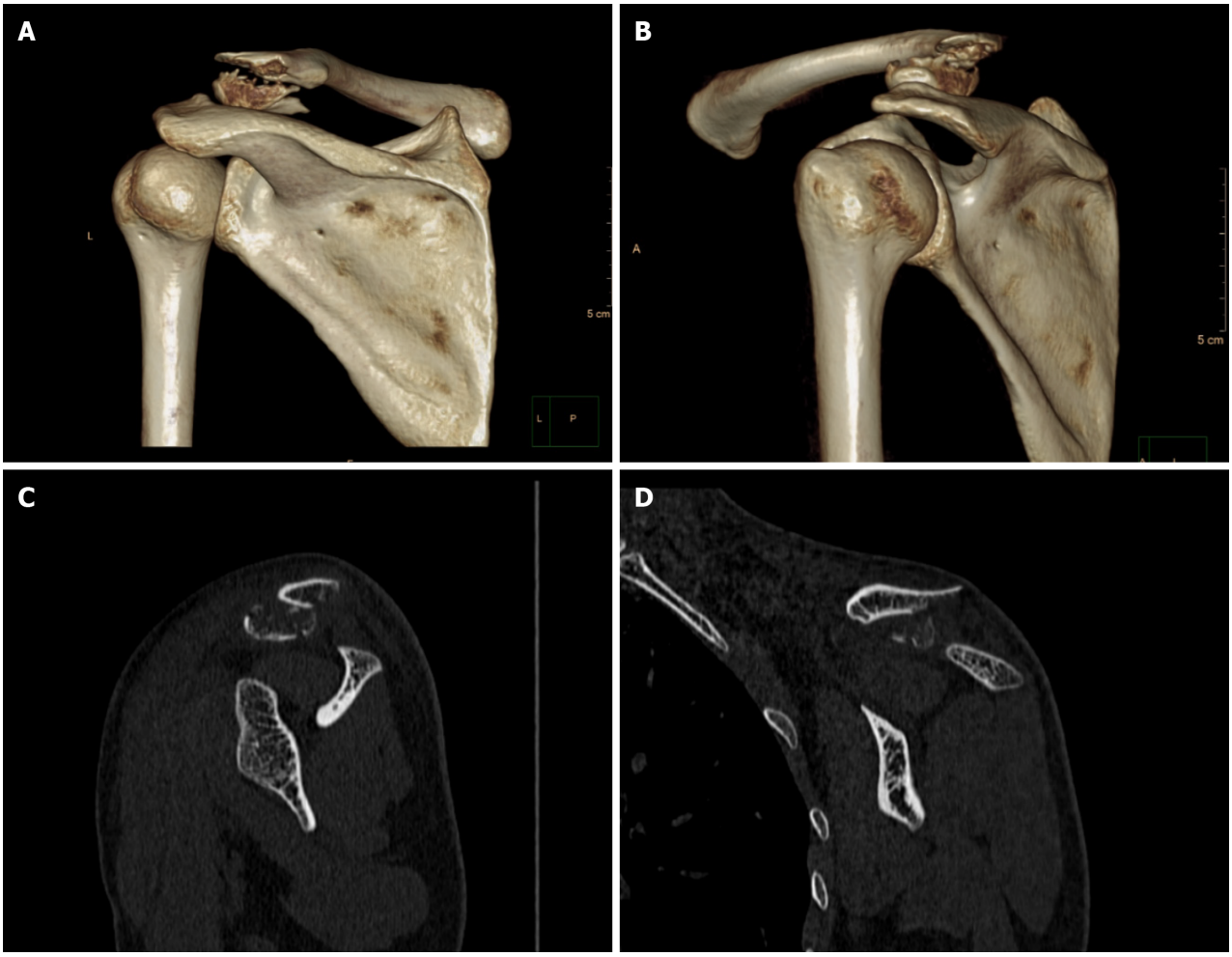


Figure 11 Computed tomography images of patient 3. A and B: 3D computed tomography (CT) images of patient 3; C and D: CT images of patient 3.

practice, we discovered that fracture morphology is the most influential factor in the treatment of clavicular fractures. Cases of associated ligament injury are relatively rare. An ideal fracture classification should be comprehensive, simple, and operational while also achieving a high degree of consistency among physicians with different years of experience. However, it was difficult for all three qualities to coexist in the actual classification. Typically, only two of these conditions are satisfied.

The Neer classification is highly inclusive. However, it fails to resolve the controversies surrounding the treatment of distal-clavicular fractures. Therefore, we believe that a classification scheme with a guiding meaning should be developed in a more refined direction, and this classification system has been proposed.

In the new classification system, the use of hook plates for Type I fractures is almost non-controversial. However, Type II fractures are significantly more difficult to treat than Type I fractures, and this classification requires a certain level of surgical experience to begin surgery.

Type II fractures typically require the use of hook plates in combination with additional free-locking screws (Figure 10). These screws have the following functions: 1. The distal fracture fragment was temporarily fixed before the plate was installed to ensure that the joint surface was flat. 2. When the fracture surface was too vertical, screws were applied horizontally to compensate for the functional shortcomings of vertical screws on the plate.

Type III fractures often contain small fragments, for example, patient 3 (Figure 11). Most of these small fragments are unmanageable and must be discarded. However, the absence of small fragments can lead to instability following fracture reduction. As a result, ligation with sutures is recommended before installing the plate in Type III fractures, and free screws and screws on the plate should be used cautiously, as the fragments are small, and too many screws may exacerbate the comminution of the fracture.

Type IV fractures are relatively rare, and no Type IV fractures were found in 29 patients in this study. Consequently, a treatment plan for this type of fracture was not proposed.

This new classification system can serve as a reference for surgeons, facilitating the formulation of surgical plans. However, the treatment plan for fractures is influenced by various factors, and the classification system and treatment plan proposed in this study remain controversial, such as patient 2. Research on classification has verified the reliability of the new system and proven its credibility among different doctors. Due to the limitations of the research conditions, we anticipate enlarging the sample size, particularly by including those with shoulder ligament injuries.

CONCLUSION

The optimal treatment for distal clavicular fractures remains controversial and challenging. In this study, a patient with a Neer type II clavicle fracture was treated by inserting a hook plate into the acromion, thereby achieving satisfactory prognostic effects. It is possible to move the hook plate outward after drilling holes in the clavicle for insertion into the acromion, thereby reducing complications. Bone resorption and acromion impingement can be reduced by sacrificing mobility in exchange for more stable fixation and shorter hook length. This serves as a reference for treating distal-clavicular fractures. Only one case was included in this study, and the new classification system for distal clavicle fractures requires more samples to determine its reliability. We have listed various situations of distal clavicle fractures and proposed corresponding treatment plans. This study can act as a reference for doctors, especially for those with fewer years of experience.

FOOTNOTES

Author contributions: Hu WT collect cases and write papers; Zhang ZY, Qu J, Piao CD performed the research.

Informed consent statement: Consent was obtained by all participants in this study. Informed consent was obtained from the patient for publication of this case report details.

Conflict-of-interest statement: The authors declare that they have no affiliations with or involvement in any organization or entity with any financial interest in the subject matter or materials discussed in this manuscript.

CARE Checklist (2016) statement: The authors have read the CARE Checklist (2016), and the manuscript was prepared and revised according to the CARE Checklist (2016).

Open Access: This article is an open-access article that was selected by an in-house editor and fully peer-reviewed by external reviewers. It is distributed in accordance with the Creative Commons Attribution NonCommercial (CC BY-NC 4.0) license, which permits others to distribute, remix, adapt, build upon this work non-commercially, and license their derivative works on different terms, provided the original work is properly cited and the use is non-commercial. See: https://creativecommons.org/Licenses/by-nc/4.0/

Country of origin: China

ORCID number: Wen-Tao Hu 0009-0000-2978-4054; Cheng-Dong Piao 0000-0003-1024-5733.

S-Editor: Liu H
L-Editor: A
P-Editor: Zheng XM

REFERENCES

1 **Kihlström C**, Möller M, Lönn K, Wolf O. Clavicle fractures: epidemiology, classification and treatment of 2 422 fractures in the Swedish Fracture Register; an observational study. *BMC Musculoskelet Disord* 2017; **18**: 82 [PMID: 28202071 DOI: 10.1186/s12891-017-1444-1]
2 A Treatise on Fractures in the Vicinity of Joints, and on Certain Forms of Accidental and Congenital Dislocations. *Med Chir Rev* 1847; **6**: 137-152 [PMID: 29919181]
3 **Neer CS**. 5 Fractures of the Distal Third of the Clavicle. *Clin Orthop Relat Res* 1968; **58**: 43-50 [DOI: 10.1097/00003086-196805000-00007]
4 **Choi S**, Kim SR, Kang H, Kim D, Park YG. Modified tension band fixation and coracoclavicular stabilisation for unstable distal clavicle fracture. *Injury* 2015; **46**: 259-264 [PMID: 25458056 DOI: 10.1016/j.injury.2014.09.025]
5 **Kim DW**, Kim DH, Kim BS, Cho CH. Current Concepts for Classification and Treatment of Distal Clavicle Fractures. *Clin Orthop Surg* 2020; **12**: 135-144 [PMID: 32489533 DOI: 10.4055/cios20010]
6 **Veeger HE**, van der Helm FC. Shoulder function: the perfect compromise between mobility and stability. *J Biomech* 2007; **40**: 2119-2129 [PMID: 17222853 DOI: 10.1016/j.jbiomech.2006.10.016]
7 **Flatow EL**. The biomechanics of the acromioclavicular, sternoclavicular, and scapulothoracic joints. *Instr Course Lect* 1993; **42**: 237-245 [PMID: 8463672]
8 **Landis JR**, Koch GG. The Measurement of Observer Agreement for Categorical Data. *Biometrics* 1977; **33**: 159-174 [DOI: 10.2307/2529310]
9 **Sim E**, Schwarz N, Höcker K, Berzlanovich A. Repair of complete acromioclavicular separations using the acromioclavicular-hook plate. *Clin Orthop Relat Res* 1995; 134-142 [PMID: 7634626 DOI: 10.1097/00003086-199505000-00017]
10 **Erdle B**, Izadpanah K, Jaeger M, Jensen P, Konstantinidis L, Zwingmann J, Südkamp NP, Maier D. Comparative analysis of locking plate versus hook plate osteosynthesis of Neer type IIB lateral clavicle fractures. *Arch Orthop Trauma Surg* 2017; **137**: 651-662 [PMID: 28321570 DOI: 10.1007/s00402-017-2645-7]
11 **Kirsch JM**, Blum L, Hake ME. Distal Clavicle Fractures: Open Reduction and Internal Fixation With a Hook Plate. *J Orthop Trauma* 2018; **32** Suppl 1: S2-S3 [PMID: 29985889 DOI: 10.1097/BOT.0000000000001214]
12 **ElMaraghy AW**, Devereaux MW, Ravichandiran K, Agur AM. Subacromial morphometric assessment of the clavicle hook plate. *Injury* 2010; **41**: 613-619 [PMID: 20116056 DOI: 10.1016/j.injury.2009.12.012]
13 **Li D**, Qiao R, Yang N, Zhang K, Zhu Y, Song Z. Clinical analysis of the acromial height-measuring device combined with new-type clavicular

hook plate and standard clavicular hook plate in the treatment of Neer type II distal clavicle fractures. *J Orthop Surg Res* 2022; **17**: 448 [PMID: 36224636 DOI: 10.1186/s13018-022-03338-4]

Published by **Baishideng Publishing Group Inc**
7041 Koll Center Parkway, Suite 160, Pleasanton, CA 94566, USA
Telephone: +1-925-3991568
E-mail: office@baishideng.com
Help Desk: https://www.f6publishing.com/helpdesk
https://www.wjgnet.com

© 2025 Baishideng Publishing Group Inc. All rights reserved.